Supplementary Information

Hydroxy Acid Conjugation to Lipids Increases Structural and Hydrolytic Stability

R. Edri[1], S. Fisher[1], Y. Levi-Kalisman[2], and M. Frenkel-Pinter[1,2]*

[1] Institute of Chemistry, The Hebrew University of Jerusalem, Israel 9190401

[2] The Center for Nanoscience and Nanotechnology, The Hebrew University of Jerusalem, Israel 9190401

*Corresponding author:

Dr. Moran Frenkel-Pinter
The Center for Nanoscience and Nanotechnology
Institute of Chemistry
The Hebrew University of Jerusalem
Edmond J. Safra Campus
Jerusalem 9190401, Israel
Ph: (+972)-2-6584171
moran.fp@mail.huji.ac.il

Contents

Materials

Decanoic acid (C1875), Dodecanoic acid (L4250), Octanoic acid (O3907), Glycolic acid (124737), L-Lactic acid (199257, purity 85%), L-Malic acid (M1000), and 3-L-Phenyllactic acid (113069) were purchased from Merck. Chloroform-D_3 (99.8%, 300816) and D_2O (99.9%, 301496) were purchased from ZEOtope. Hydrochloric acid 37% (320331), sodium hydroxide (S8045), sodium dihydrogen phosphate monohydrate (1.06346), and citric acid (27109) were purchased from Sigma-Merck. Tris(hydroxymethyl)aminomethane (17-1321-01) was purchased from Cativa., merocyanine 450, dye content 90%, 323756), and rhodamine 6G (dye content 99%, 252433) were purchased from Sigma-Merck. Solvents used for LC-MS analyses were of LC-MS grade. Double-distilled water (conductivity ≤20μS/cm) was used for structural characterization.

Methods

Single-step dry reactions.

Binary mixtures of decanoic acid (DA) and hydroxy acids (HAs) at 1:1, 1:2, and 1:4 molar ratios were prepared in 7mL scintillation vials. DA's amount was fixed at 200 μmol and HAs's amount was adjusted accordingly. All components were weighed except for lactic acid (LA) which was added volumetrically. The mixtures were placed at 85 °C for seven days. Samples of either DA (200 μmol) alone or hydroxy acids (400 μmol) alone were prepared as control. An aliquot of 1M HCl (1 μmol) was added to the DA control. All samples were prepared in triplicates. For binary mixtures of octanoic acid (OcA) and LA, 600μmol OcA and 2400μmol LA were used. For binary mixtures of dodecanoic acid (dDA) and LA, 100μmol dDA and 400μmol LA were used. For ternary mixtures of DA, glycolic acid (GA) and LA, 200μmol DA, 400μmol GA, and 400μmol LA were used.

High-Performance Liquid Chromatography / LC-MS.

HPLC analyses were conducted using an Agilent 1260 quaternary pump and autosampler (Agilent Technologies, Santa Clara, CA, USA) with a DAD UV-vis detector at 210nm and 259nm. LC-MS data were collected using an Agilent G6135C single quadrupole mass spectrometer with a capillary voltage of 4.0 kV and a source fragmentation voltage of 70

V. Scan range: 50-1500 m/z. Chromatographic separation was achieved using InfinityLab Poroshell 120 EC-C18 column (150 x 3.0 mm, 2.7µm, with a SecurityGuard™ C18 4x2.0mm), at a constant 0.3 mL/min flow rate. Column cell temperature was maintained at 20 °C. Gradient elution was carried out using (A) 0.1% formic acid in water and (B) acetonitrile as follow: 5min 100% A, 20min ramp to 20% A, 10min 100% B.

For the identification of the reaction products obtained with phenyllactic acid (PLA), gradient elution was carried out using (A) 0.1% formic acid in water and (B) 0.1% formic acid in acetonitrile as follow: 5min 100% A, 20min ramp to 20% A, 10min 100% B.

For the identification of the reaction products obtained with decanoic acid and lactic acid, chromatographic separation was achieved using InfinityLab Poroshell 120 EC-C18 column (150 x 3.0 mm, 2.7µm, with a SecurityGuard™ C18 4x2.0mm), at constant 0.5 mL/min flow rate. Column cell temperature was maintained at 30 °C. Gradient elution was carried out using (A) 0.1% formic acid in water and (B) acetonitrile as follows: 3min 90% A, 3min ramp to 20% A, 1.5min 20% A, 7.5min ramp to 100% B, 5min 100% B.

For the identification and qualitative analyses of the reaction products obtained with dodecanoic acid, chromatographic separation was achieved using InfinityLab Poroshell 120 EC-C18 column (150 x 3.0 mm, 2.7µm, with a SecurityGuard™ C18 4x2.0mm), at a constant 0.4 mL/min flow rate. Column cell temperature was maintained at 20 °C. Gradient elution was carried out using (A) 0.1% formic acid in water and (B) acetonitrile as follows: 5min 95% A, 7min ramp to 30% A, 10min ramp to 100% B, 8min 100% B.

For the identification and qualitative analyses of the reaction products obtained with octanoic acid, chromatographic separation was achieved using InfinityLab Poroshell 120 EC-C18 column (150 x 3.0 mm, 2.7µm, with a SecurityGuard™ C18 4x2.0mm), at a constant 0.3 mL/min flow rate. Column cell temperature was maintained at 20 °C. Gradient elution was carried out using (A) 0.1% formic acid in water and (B) acetonitrile as follows: 5min 90% A, 5min ramp to 55% A, 20min ramp to 100% B.

For the identification and qualitative analyses of the reaction products obtained with decanoic acid and α-leucic acid, chromatographic separation was achieved using InfinityLab Poroshell 120 EC-C18 column (150 x 3.0 mm, 2.7µm, with a SecurityGuard™ C18 4x2.0mm), at a constant 0.4 mL/min flow rate. Column cell temperature was maintained at 20 °C. Gradient elution was carried out using (A) 0.1% formic acid in water and (B) acetonitrile as follows: 3min 90% A, 5min ramp to 50% A, 6min ramp to 30% A, 10min ramp to 5% A, 11 min 5%A.

For the hydrolysis study analyses of the reaction products obtained with decanoic acid and phenyllactic acid, chromatographic separation was achieved using InfinityLab Poroshell 120 EC-C18 column (150 x 3.0 mm, 2.7µm, with a SecurityGuard™ C18 4x2.0mm), at a constant 0.5 mL/min flow rate. Column cell temperature was maintained at 20 °C. Gradient elution was carried out using (A) 0.1% formic acid in water and (B) acetonitrile as follows: 3min 40% A, 4min ramp to 100% B, 10min 100% B.

Critical aggregation concentration (CAC) determination.

The critical aggregation concentration of DA in fresh controls and reaction products was determined using the Merocyanine 540 assay. To that end, dilution lines were prepared by diluting stocks of fresh monomers or reaction products (see sample rehydration) with 50 mM phosphate buffer (final concentration) at pH 6.8. The dilution lines were constructed to cover a range of DA concentrations that are below and above the CAC. The resulting dilutions were mixed with Merocyanine 540 stock of 1mg/mL, resulting in a final Merocyanine 540 concentration of 20µg/mL. 150µL sample were placed in 96-wells black plate. Spectra were recorded on a Synergy H1 plate reader (BioTek Instruments, VT, USA) between 400 nm to 620 nm. The ratio between the absorption at 570 nm and 530 nm was calculated and plotted against DA concentration. The point at which the ratio increases significantly was considered as the CAC. The determined values were extracted from the intersection between the fitting lines at the first two regions of the curves.
The critical aggregation concentration of OcA and dDA was determined in a similar way with one exception of pH and buffer concentration. For OcA, CAC was determined at pH 6.6 and 200mM phosphate buffer and for dDA at pH 7.4 and 50mM phosphate buffer.
For DA:PLA fresh monomers and reaction product at 1:1 molar ratio, CAC was determined at pH 6.8 and 50mM phosphate buffer.

Hydrolysis and degradation experiments.

The hydrolysis and degradation profile of the dried products obtained in the drying reactions was evaluated for the products of DA:LA binary mixture at 1:4 molar ratio and for LA control reaction products. Crude reaction products were rehydrated in water and with either 1M solutions of tris, phosphate monobasic, or citric acid, and the pH of the samples was further adjusted to 8.0, 6.8, or 5.5, respectively. DA and LA concentrations

were 50 mM and 200 mM, respectively, referring to initial amounts prior to the reaction. The buffer concentration was 50 mM. The resulting rehydrated samples were dispensed into eight 500 µL aliquots in 1.5 mL microtubes. Each sample was withdrawn at different time points. Samples were stored at various temperatures for different periods of time as follows: at room temperature (23 °C ±3 °C) for 7, 14, 21, 28, 35, 42, and 49 days. At 40 °C for 4, 8, 12, 16, 20, 24, and 28 days. At 60 °C for 2, 4, 6, 8, 10, 12, and 14 days. In addition, t0 samples were withdrawn immediately after sample preparation. All withdrawn samples were stored at -80 °C until being analyzed by HPLC/ LC-MS. Prior to HPLC analyses, the pH of each sample was roughly measured using a pH Indicator Strip, universal Specification (0 - 14.0) (Millipore, Merck). For HPLC analyses, samples were diluted ten times fold in ACN:water 50:50. To confirm that no degradation occurred during the analysis itself, representative samples were injected several times during the course of the analysis.

An additional hydrolysis experiment was conducted by rehydrating the reaction product of DA:LA at a 1:4 molar ratio in water and phosphate buffer at pH 6.8. The resulting rehydrated product was divided into thirteen 300 µL aliquots in 1.5 mL microtube. Microtubes were placed at 40 °C and samples were withdrawn immediately after preparation and after 1, 2, 3, 4, 6, 8, 12, 16, 20, 24, 48, and 72hr. The withdrawn samples were treated as described above.

Control samples of LA reaction products using the initial amount of either 400 µmol or 800 µmol were tested for hydrolysis as well. The dry reaction products were rehydrated in water and phosphate buffer and the pH was adjusted to 6.8. The final concentration of LA was either 100 mM or 200 mM, referring to initial amounts prior to the reaction. The rehydrated products were stored at RT and samples of 800 µL were withdrawn immediately after preparation and after 12hr and 4 days. The withdrawn samples were treated as described above.

The hydrolysis of additional fatty acids and hydroxy acids was carried out as well. Reaction products of OcA:LA, at 1:4 molar ratio were rehydrated in water and phosphate buffer (200mM) at pH 6.6. The concentration of OcA and LA was 150mM and 600mM, respectively, referring to the initial quantity prior to reaction initiation. Reaction products of dDA:LA, at 1:4 molar ratio, were rehydrated in water and phosphate buffer (50mM) at pH 7.4. The concentration of dDA and LA was 20mM and 80mM, respectively, referring to the initial quantity prior to reaction initiation. Reaction products of DA:LA:GA

at 1:2:2 molar ratio were rehydrated in water and phosphate buffer (50mM) at pH 6.8. The concentration of DA, LA and GA was 50mM, 100mM and 100mM respectively, referring to initial quantity prior to reaction initiation. The rehydrated products were divided into eleven 350 µL aliquots in 1.5 mL microtube. Microtubes were placed at 40 °C and samples were withdrawn immediately after preparation and after 1, 2, 3, 4, 6, 8, 12, 24, 48, and either 72hr or 96hr. The withdrawn samples were treated as described above. Reaction products of DA:PLA at 1:1 molar ratio were rehydrated in water containing tris buffer (50mM) at pH 8.0. The concentrations of DA and PLA were 50mM, referring to the initial quantity prior to reaction initiation. The rehydrated products were divided into eleven 350 µL aliquots in 1.5 mL microtube. Microtubes were placed at 40 °C and samples were withdrawn immediately after preparation and after 1, 2, 4, 8, 12, 24, 48, 72hr, 120 and 192 hr. The withdrawn samples were treated as described above.

Supplementary Figures

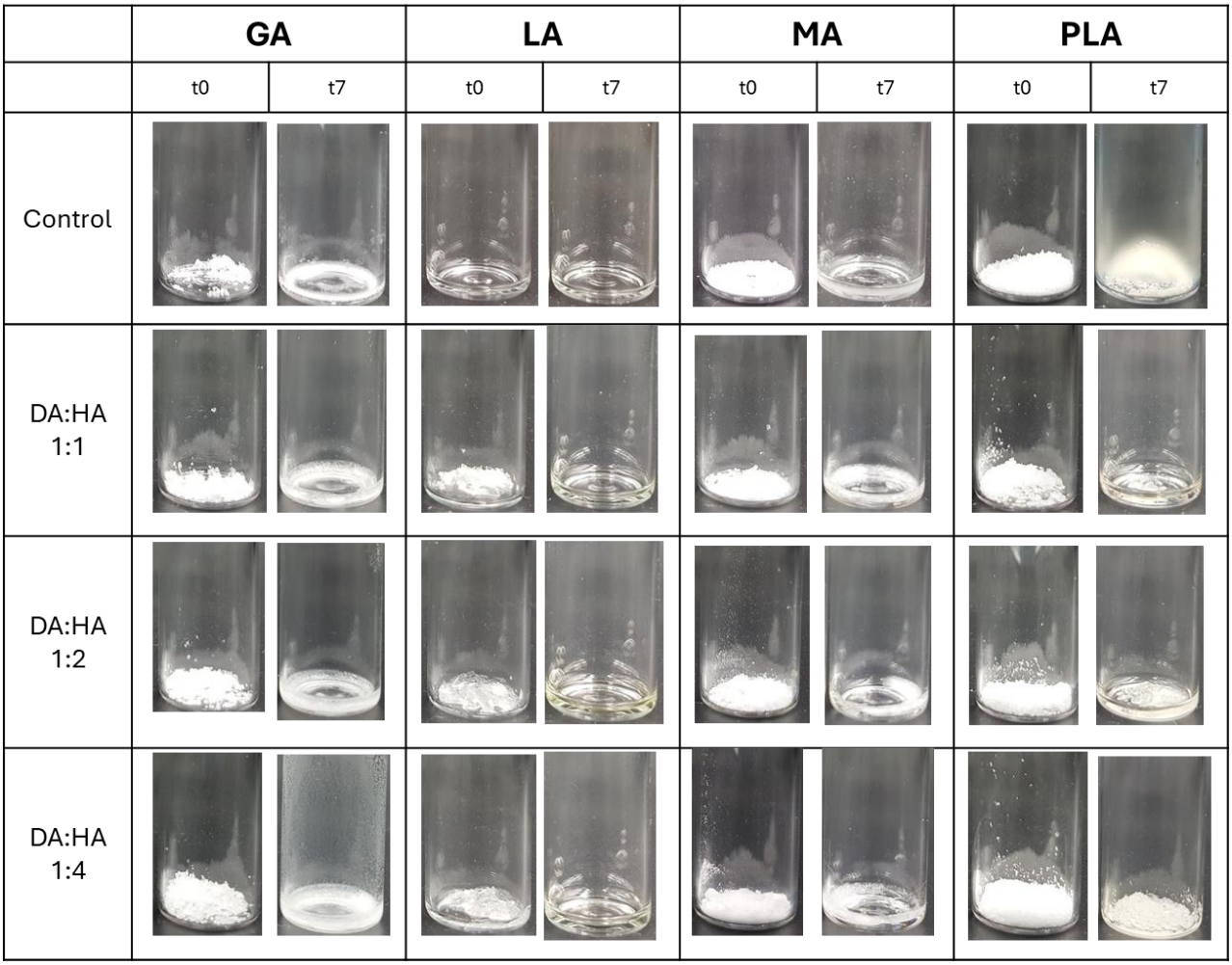

Figure S1. Visual appearance of the binary mixtures of DA and the tested HAs at 1:1, 1:2, and 1:4 molar ratios and HAs control samples. The images on the left and right represent the sample prior to reaction initiation and after reaction termination respectively (t7 – seven days).

A

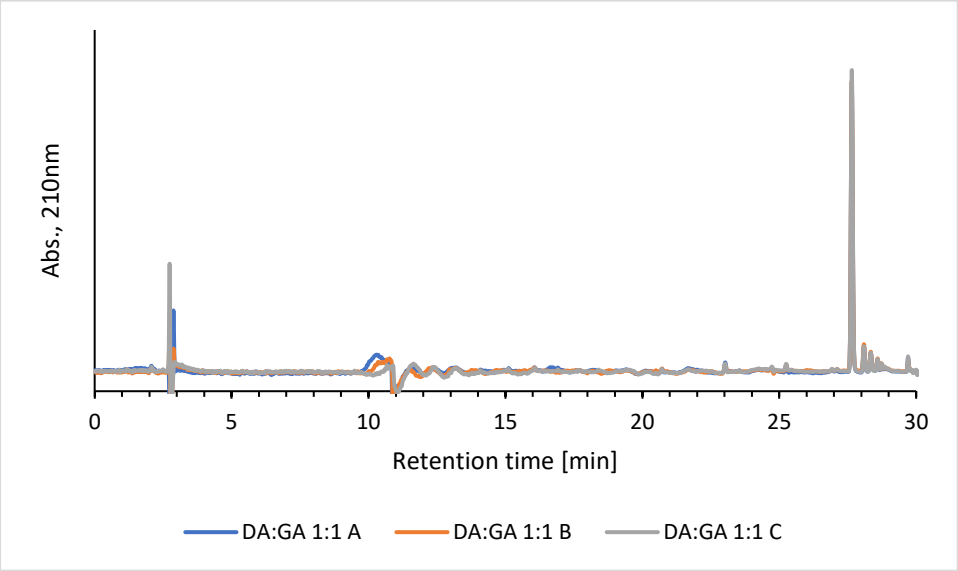

B

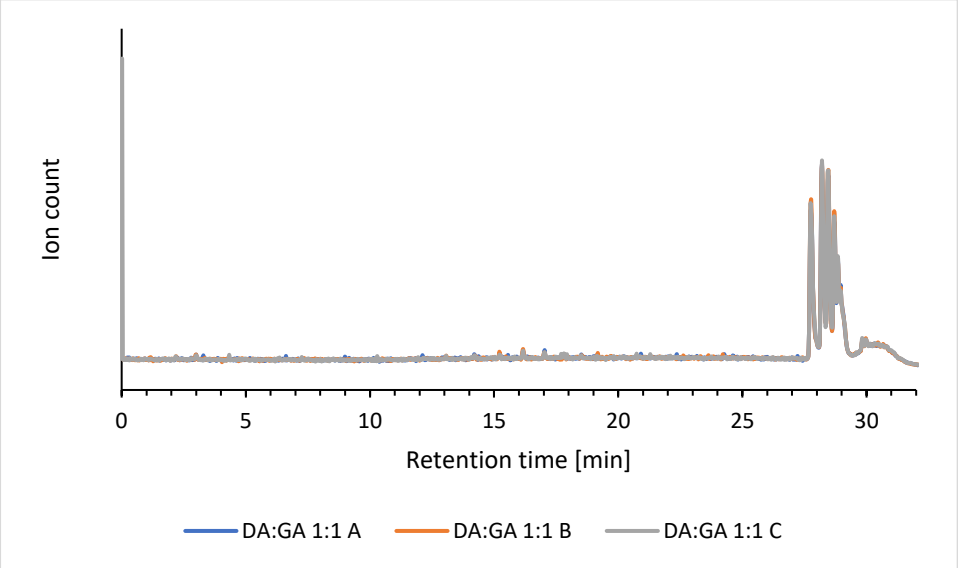

Figure S2. LC-MS analysis confirms the formation of products obtained by the reaction of DA and GA at a 1:1 molar ratio. DA and GA reacted under dry conditions at 85 °C for 7 days and the reaction products were analyzed by HPLC at 210nm (A) and LC-MS operating at negative mode (B). Chromatograms were obtained for three individual preparations.

A

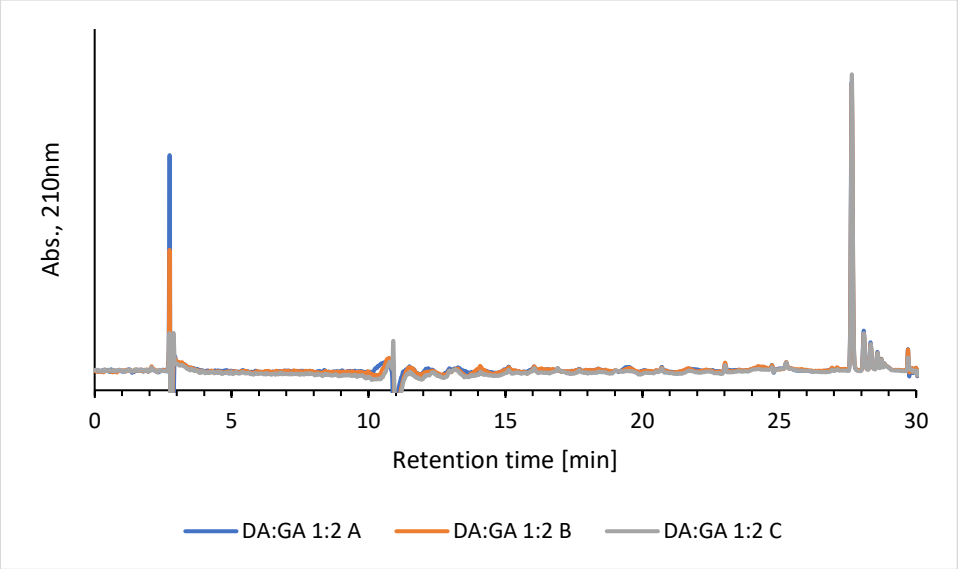

B

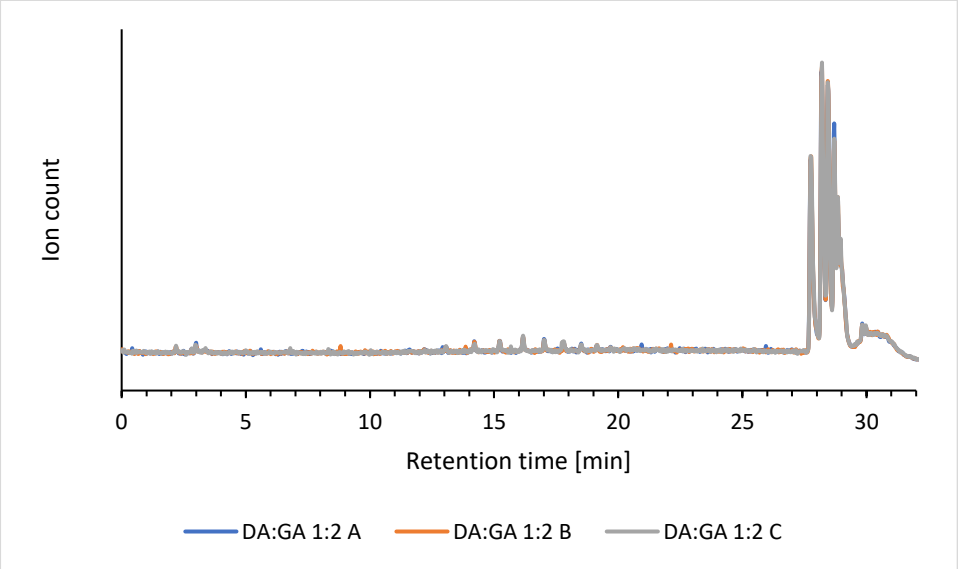

Figure S3. LC-MS analysis confirms the formation of products obtained by the reaction of DA and GA at a 1:2 molar ratio. DA and GA reacted under dry conditions at 85 °C for 7 days and the reaction products were analyzed by HPLC at 210nm (A) and LC-MS operating at negative mode (B). Chromatograms were obtained for three individual preparations.

A

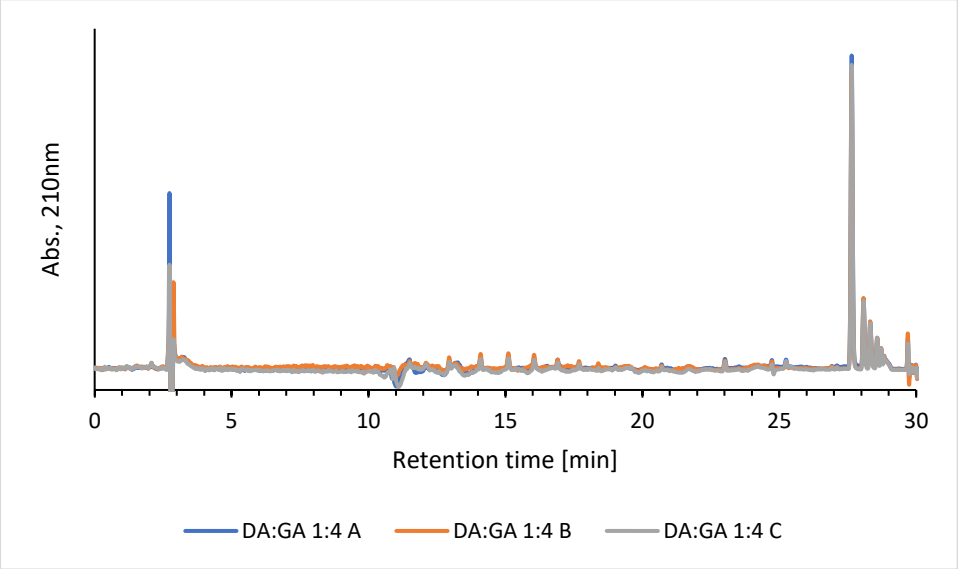

B

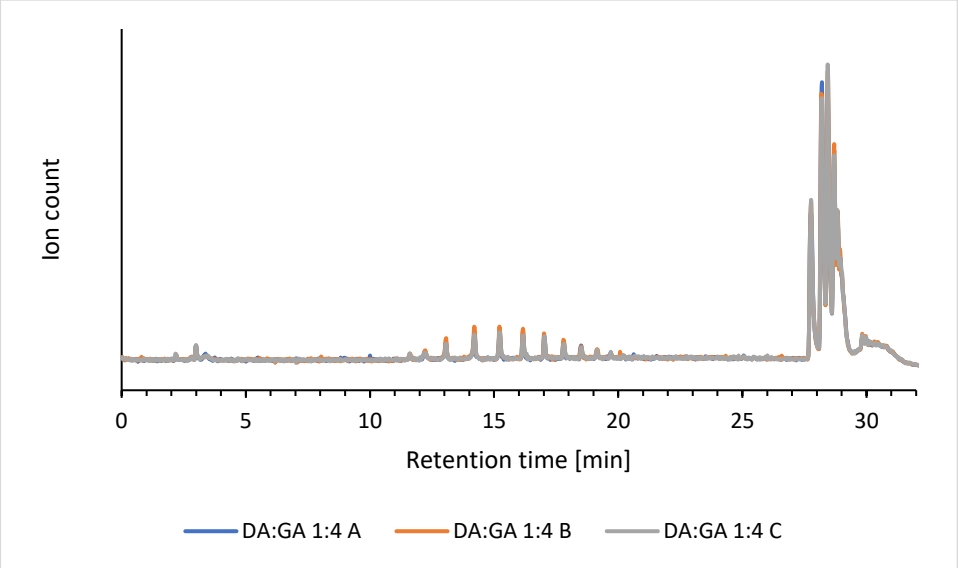

Figure S4. LC-MS analysis confirms the formation of products obtained by the reaction of DA and GA at a 1:4 molar ratio. DA and GA reacted under dry conditions at 85 °C for 7 days and the reaction products were analyzed by HPLC at 210nm (A) and LC-MS operating at negative mode (B). Chromatograms were obtained for three individual preparations.

A

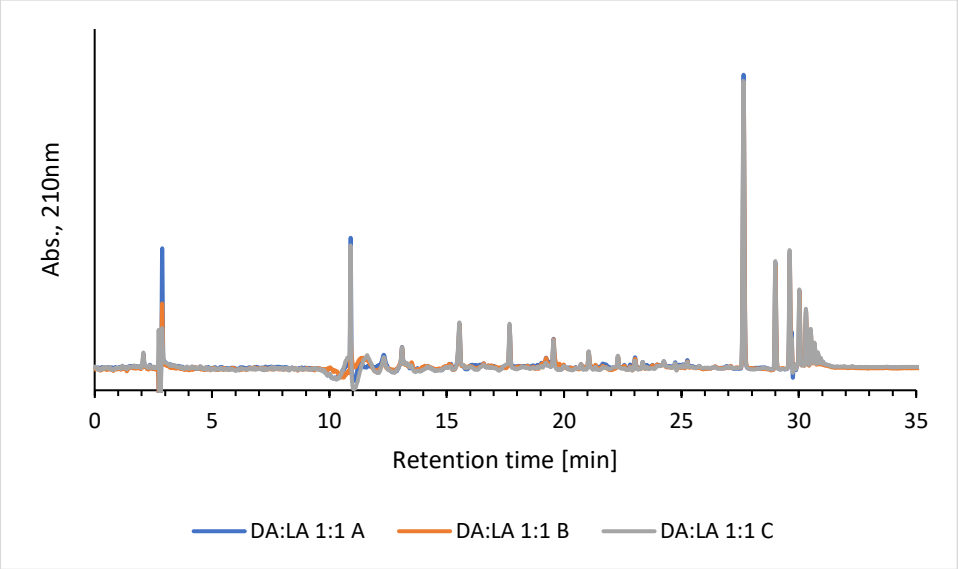

B

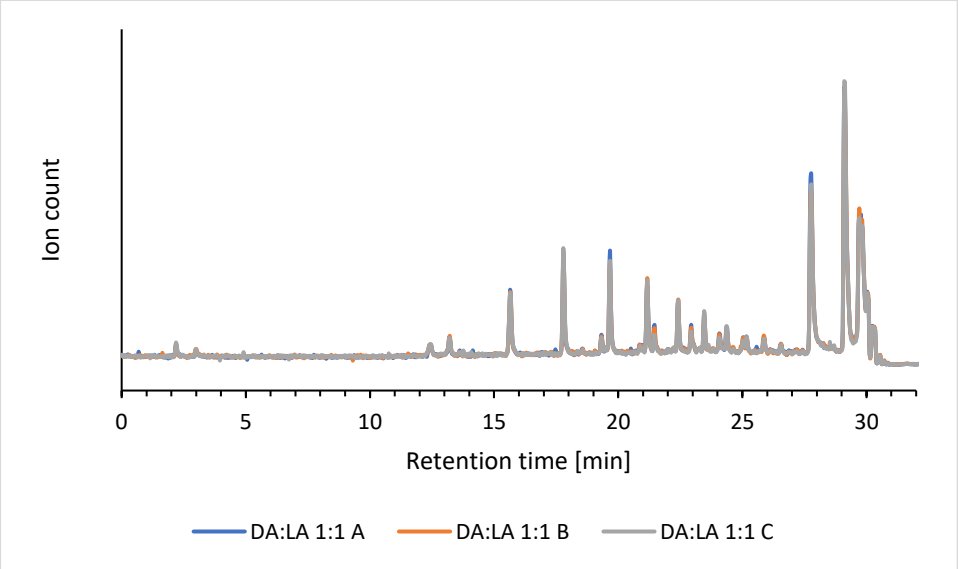

Figure S5. LC-MS analysis confirms the formation of products obtained by the reaction of DA and LA at a 1:1 molar ratio. DA and LA reacted under dry conditions at 85 °C for 7 days and the reaction products were analyzed by HPLC at 210nm (A) and LC-MS operating at negative mode (B). Chromatograms were obtained for three individual preparations.

A

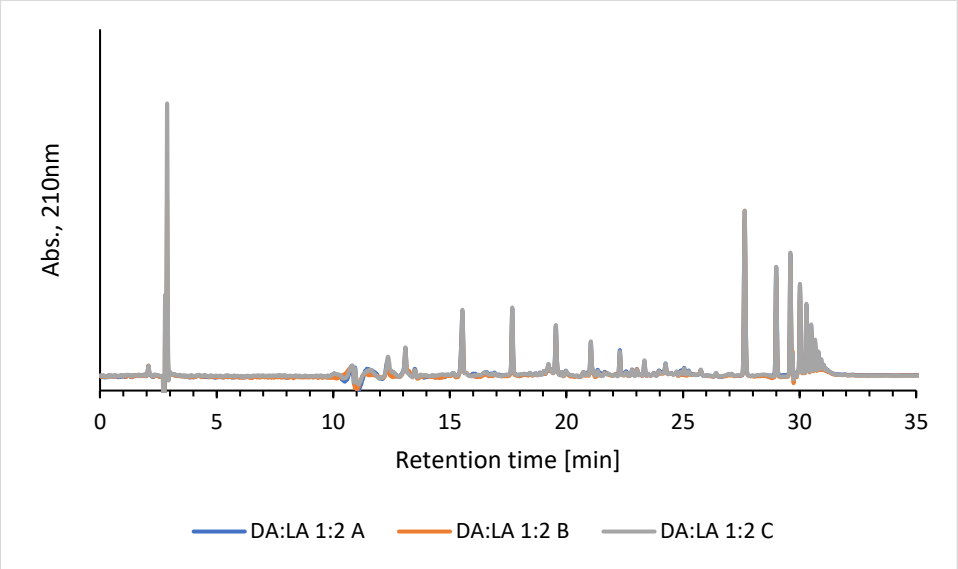

B

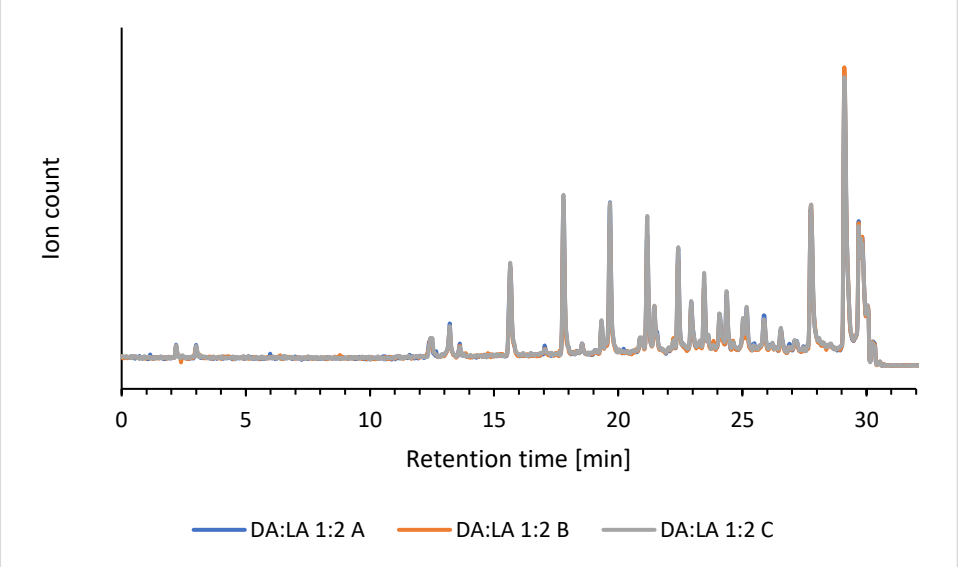

Figure S6. LC-MS analysis confirms the formation of products obtained by the reaction of DA and LA at a 1:2 molar ratio. DA and LA reacted under dry conditions at 85 °C for 7 days and the reaction products were analyzed by HPLC at 210nm (A) and LC-MS operating at negative mode (B). Chromatograms were obtained for three individual preparations.

A

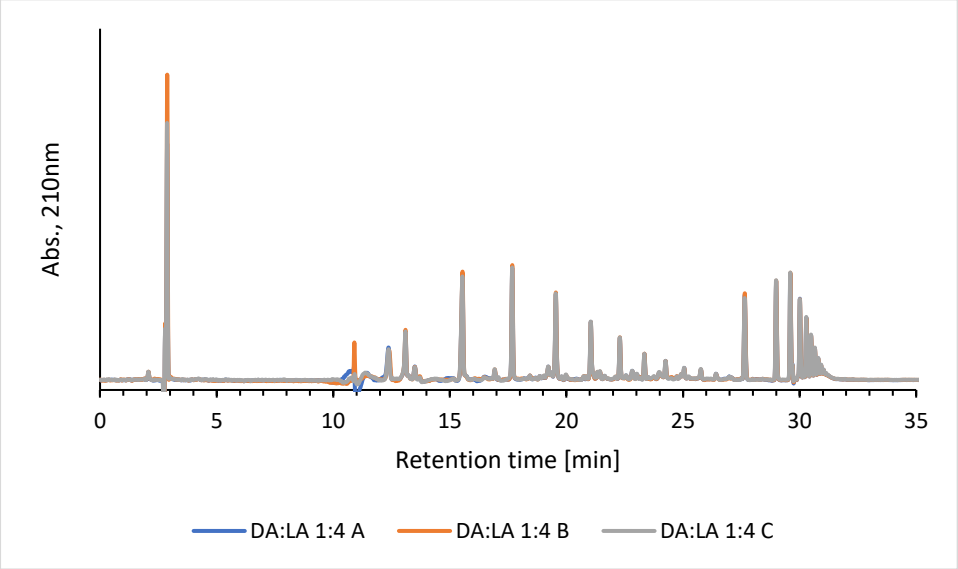

B

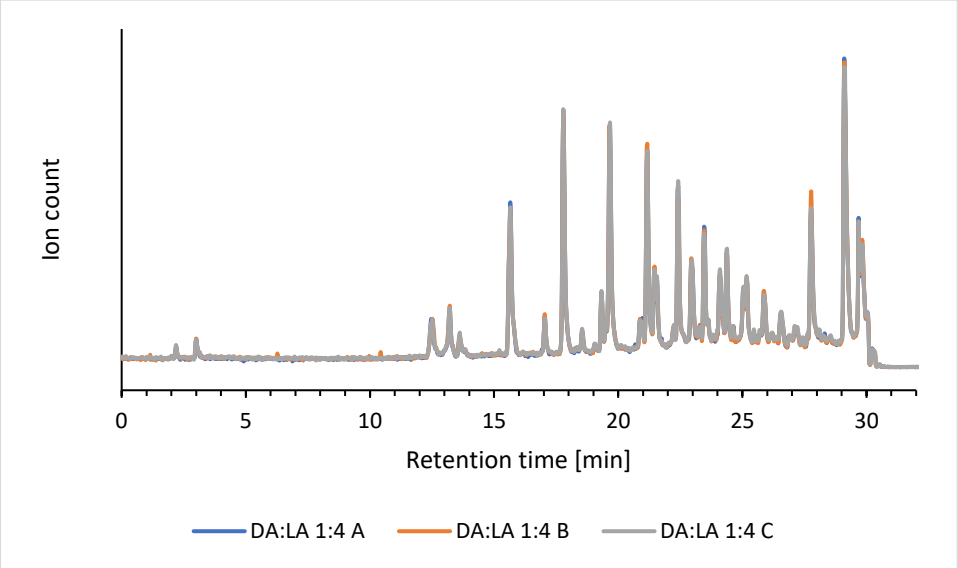

Figure S7. LC-MS analysis confirms the formation of products obtained by the reaction of DA and LA at a 1:4 molar ratio. DA and LA reacted under dry conditions at 85 °C for 7 days and the reaction products were analyzed by HPLC at 210nm (A) and LC-MS operating at negative mode (B). Chromatograms were obtained for three individual preparations.

A

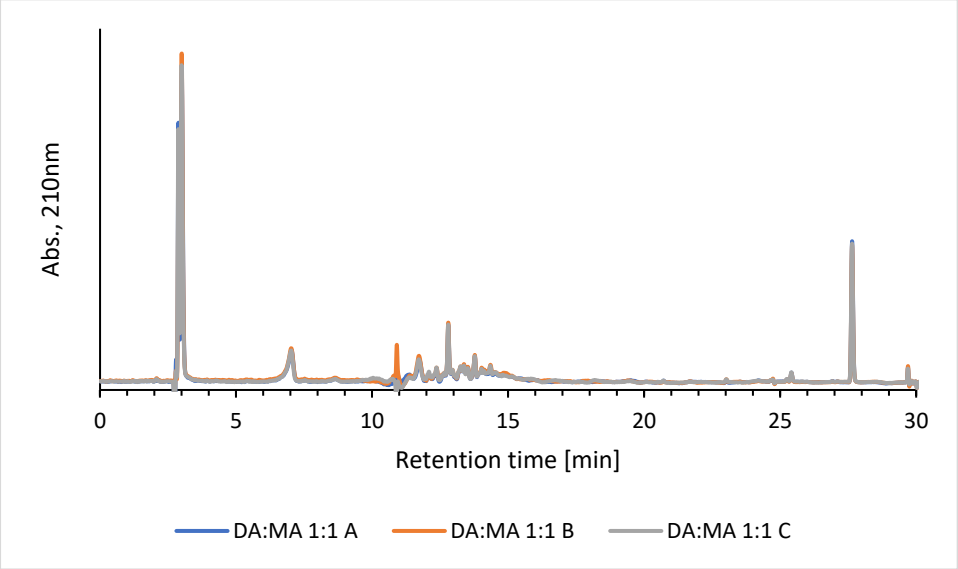

B

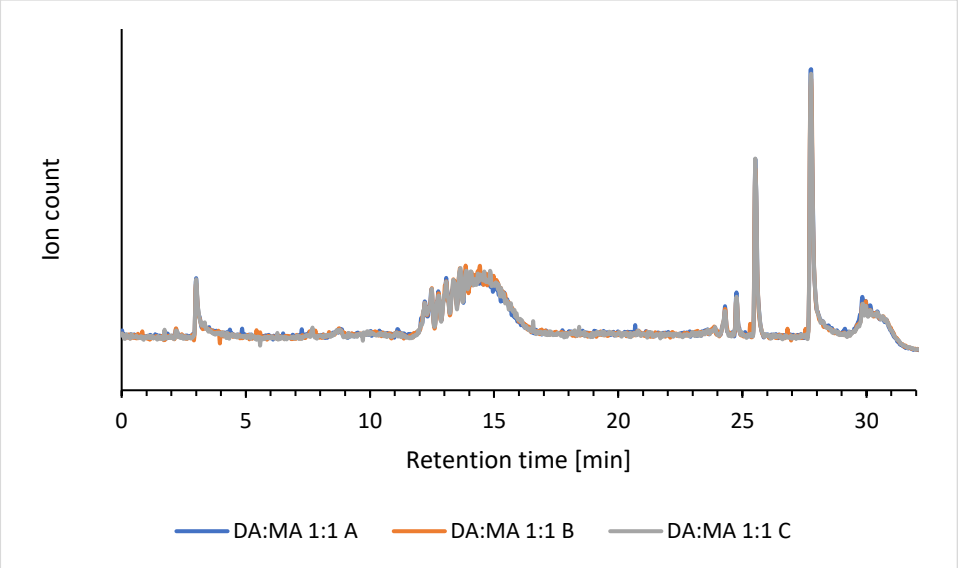

Figure S8. LC-MS analysis confirms the formation of products obtained by the reaction of DA and MA at a 1:1 molar ratio. DA and MA reacted under dry conditions at 85 °C for 7 days and the reaction products were analyzed by HPLC at 210nm (A) and LC-MS operating at negative mode (B). Chromatograms were obtained for three individual preparations.

A

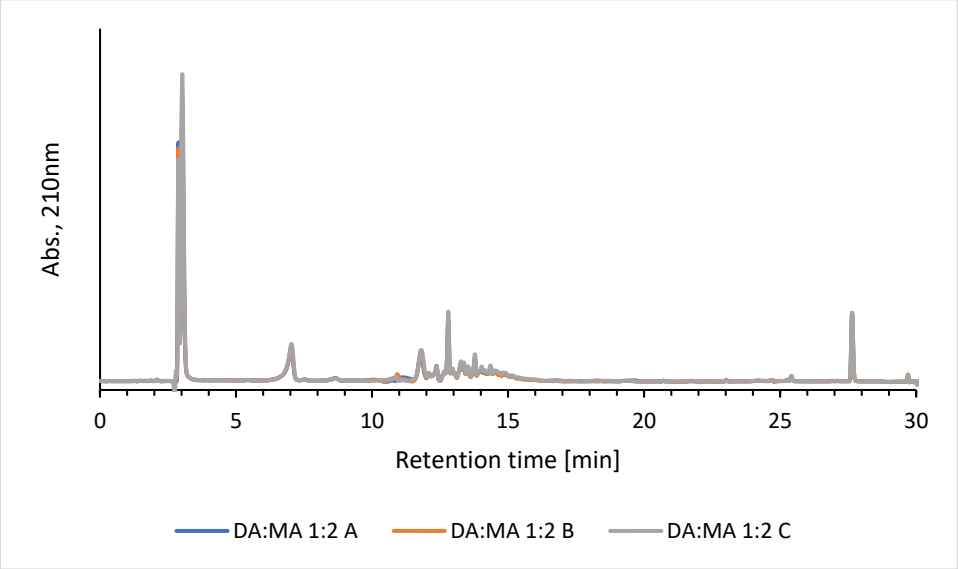

B

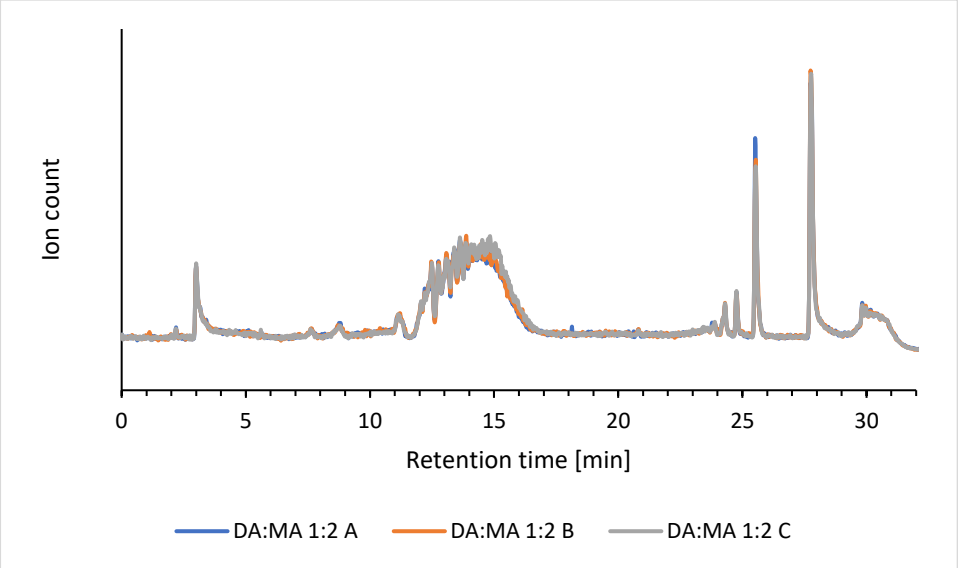

Figure S9. LC-MS analysis confirms the formation of products obtained by the reaction of DA and MA at a 1:2 molar ratio. DA and MA reacted under dry conditions at 85 °C for 7 days and the reaction products were analyzed by HPLC at 210nm (A) and LC-MS operating at negative mode (B). Chromatograms were obtained for three individual preparations.

A

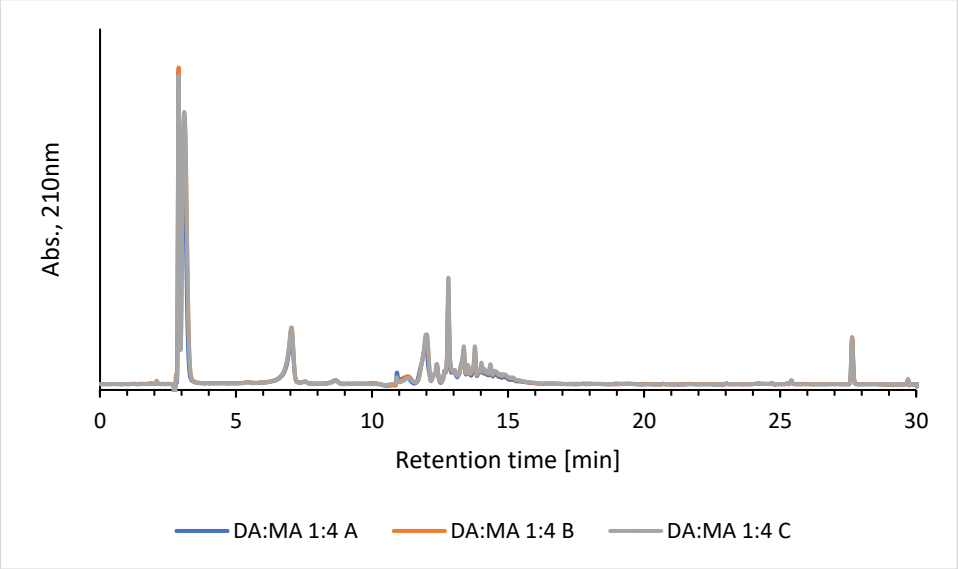

B

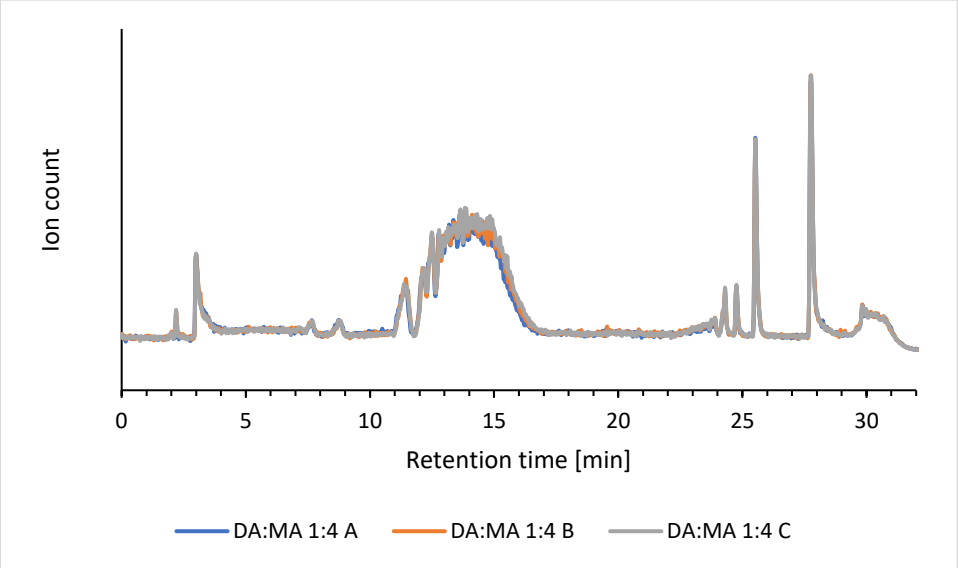

Figure S10. LC-MS analysis confirms the formation of products obtained by the reaction of DA and MA at a 1:4 molar ratio. DA and MA reacted under dry conditions at 85 °C for 7 days and the reaction products were analyzed by HPLC at 210nm (A) and LC-MS operating at negative mode (B). Chromatograms were obtained for three individual preparations.

A

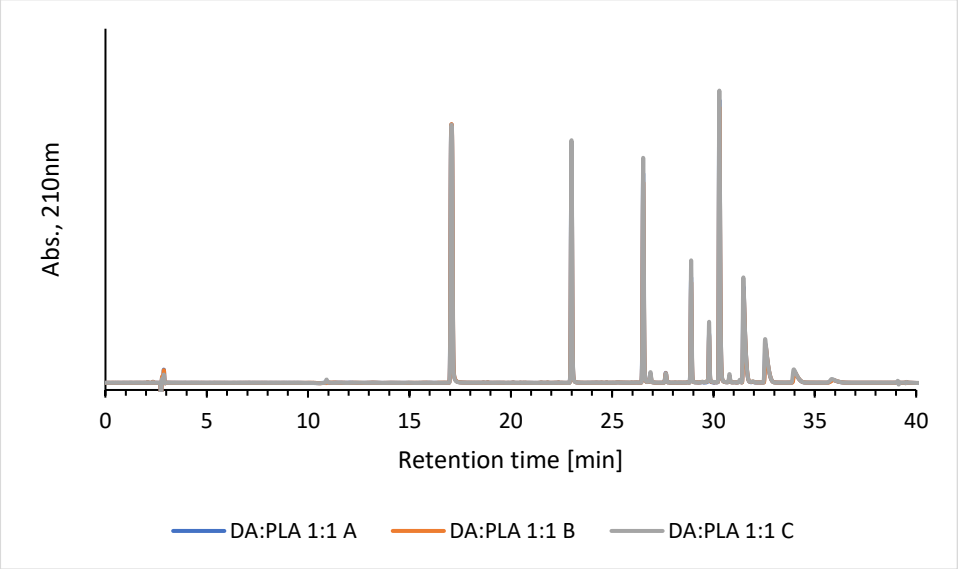

B

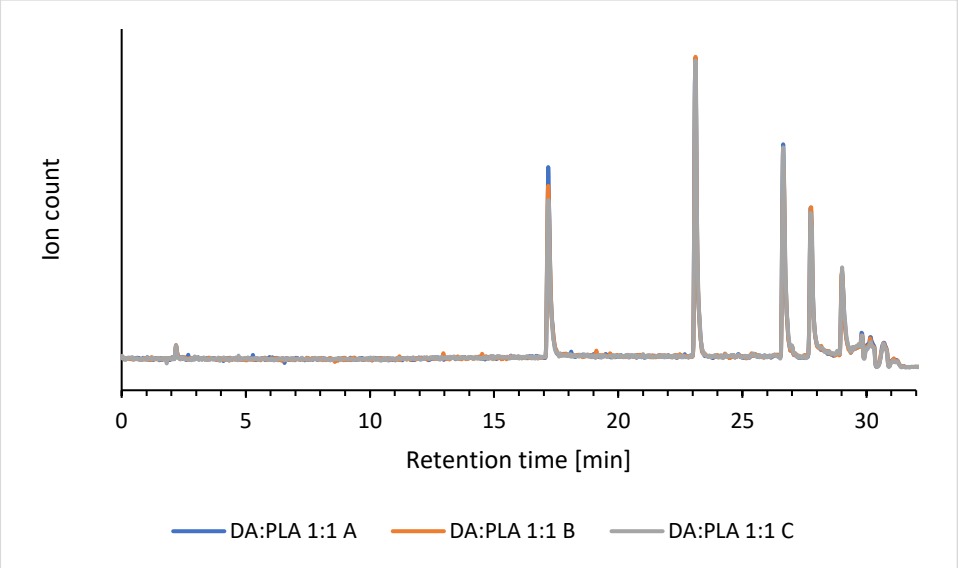

Figure S11. LC-MS analysis confirms the formation of products obtained by the reaction of DA and PLA at a 1:1 molar ratio. DA and PLA reacted under dry conditions at 85 °C for 7 days and the reaction products were analyzed by HPLC at 210nm (A) and LC-MS operating at negative mode (B). Chromatograms were obtained for three individual preparations.

A

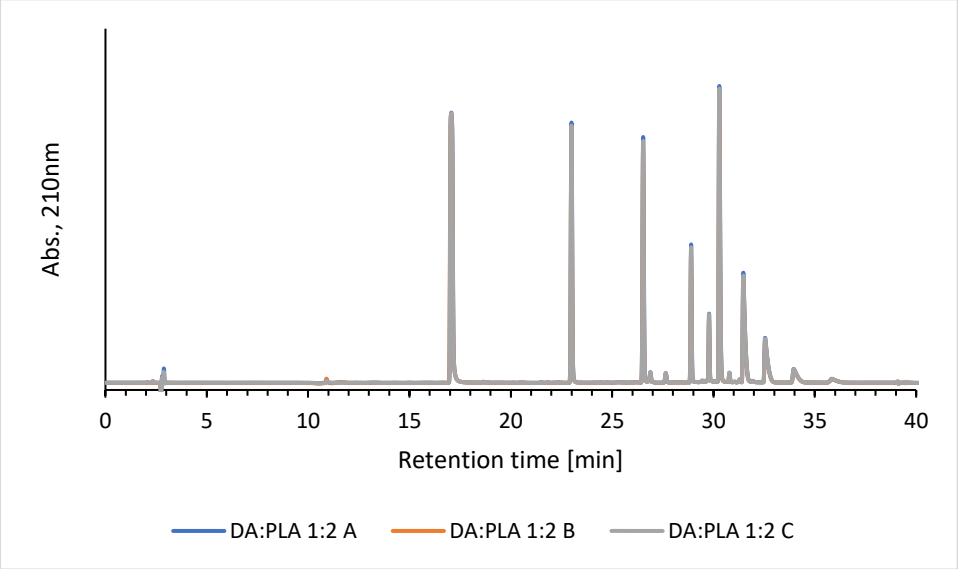

B

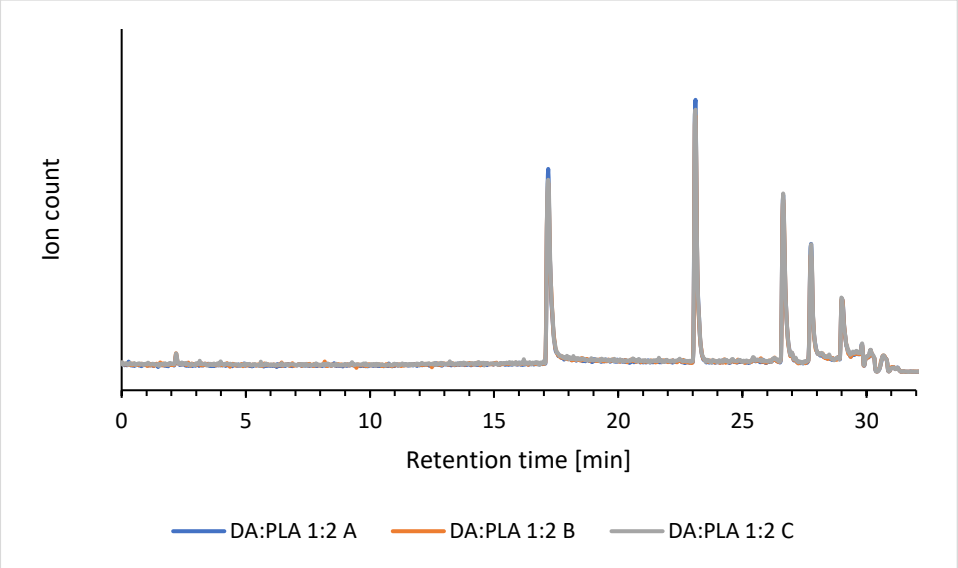

Figure S12. LC-MS analysis confirms the formation of products obtained by the reaction of DA and PLA at a 1:2 molar ratio. DA and PLA reacted under dry conditions at 85 °C for 7 days and the reaction products were analyzed by HPLC at 210nm (A) and LC-MS operating at negative mode (B). Chromatograms were obtained for three individual preparations.

A

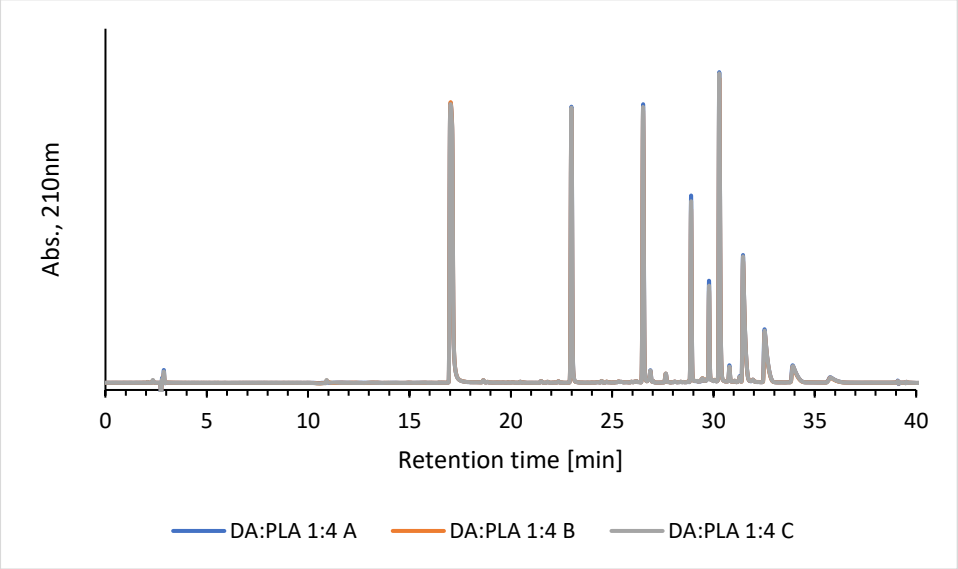

B

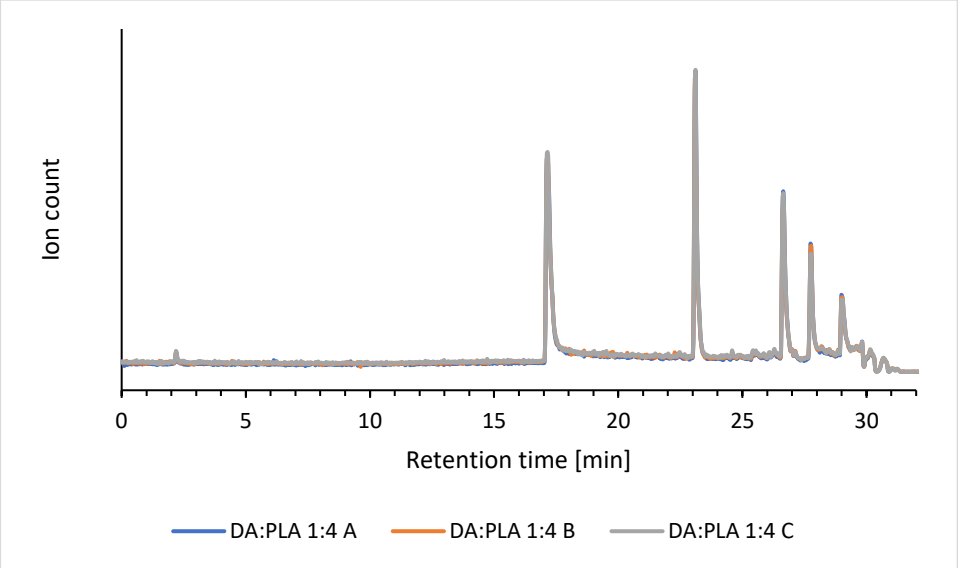

Figure S13: LC analysis confirms the formation of products obtained by the reaction of DA and PLA at a 1:4 molar ratio. DA and PLA reacted under dry conditions at 85 °C for 7 days and the reaction products were analyzed by HPLC at 210nm (A) and LC-MS operating at negative mode (B). Chromatograms were obtained for three individual preparations.

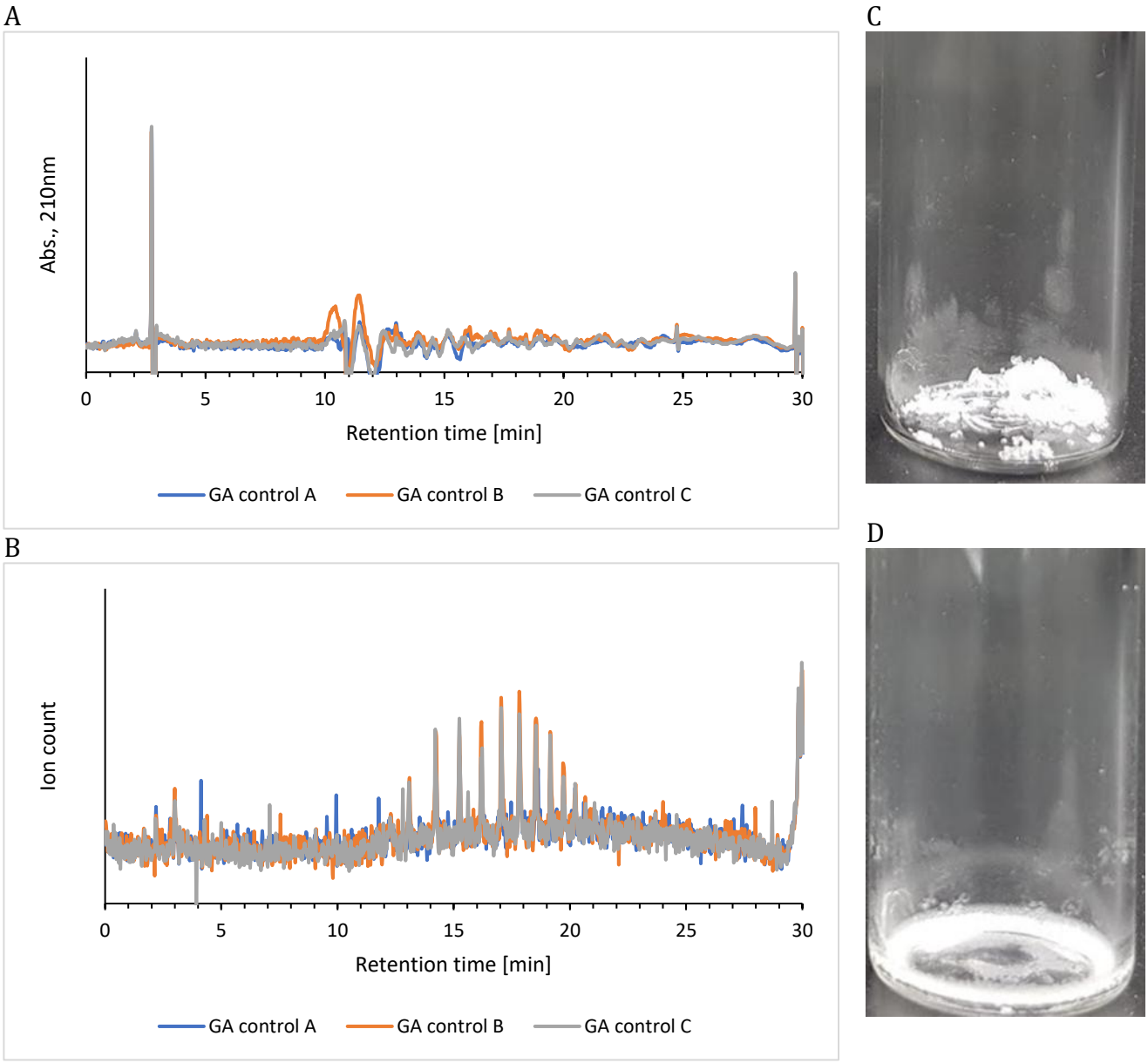

Figure S14. LC-MS analysis confirms the formation of products obtained for GA control in the absence of DA. GA (400µmol) was allowed to react under dry conditions at 85 °C for 7 days and the reaction products were analyzed by HPLC at 210nm (A) and LC-MS operating at negative mode (B). Chromatograms were obtained for three individual preparations. Images of GA sample prior to the reaction initiation (C) and after the reaction termination (D). The image of the resulting product suggests a high extent of GA oligomerization as indicated by the plastic-like appearance which was only partially soluble in the analysis diluent.

A

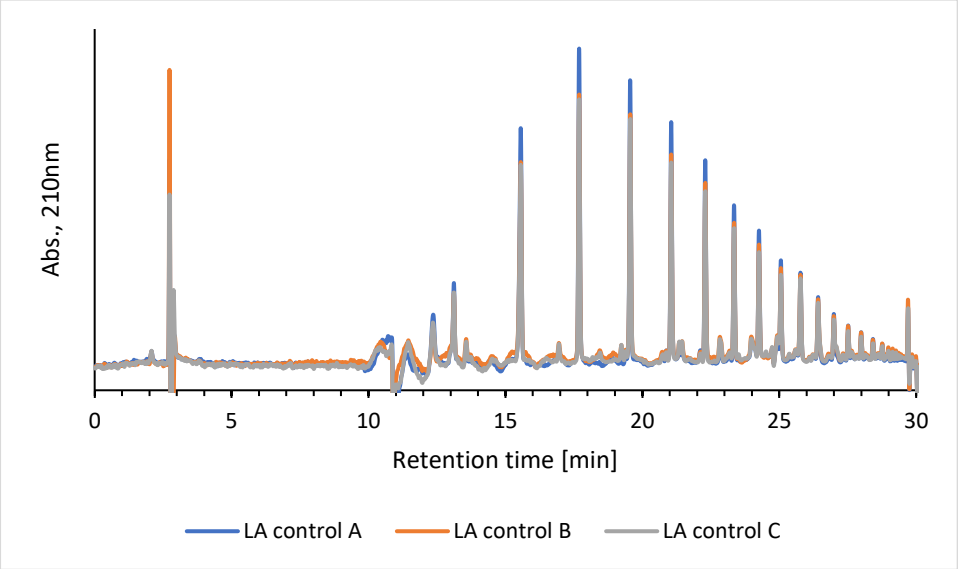

B

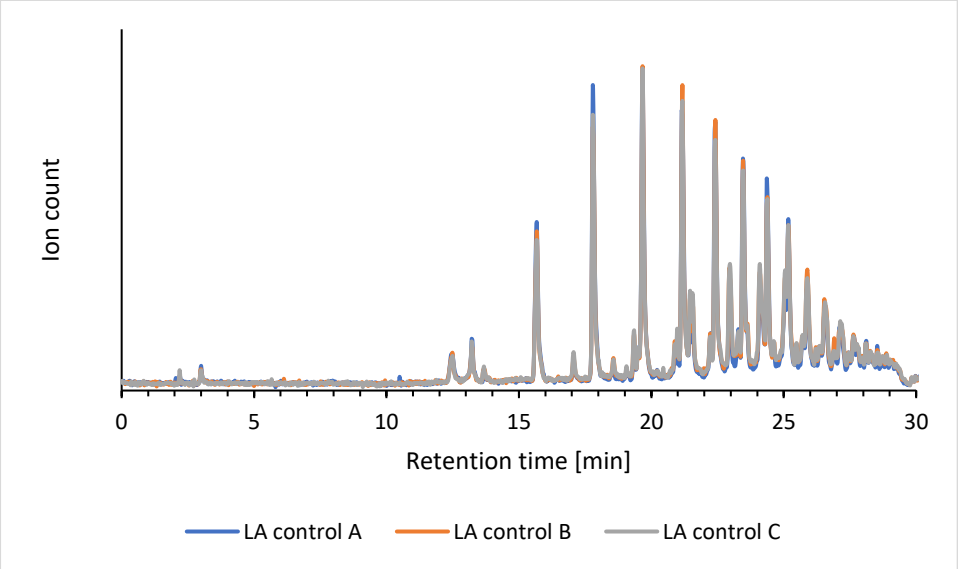

Figure S15. LC-MS analysis confirms the formation of products obtained for LA control in the absence of DA. LA (400µmol) was allowed to react under dry conditions at 85 °C for 7 days and the reaction products were analyzed by HPLC at 210nm (A) and LC-MS operating at negative mode (B). Chromatograms were obtained for three individual preparations.

A

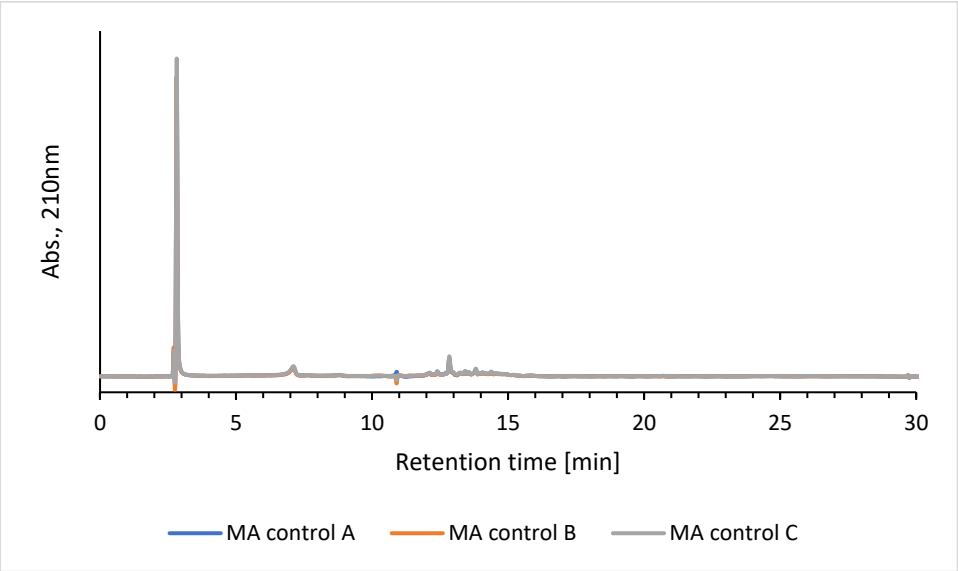

B

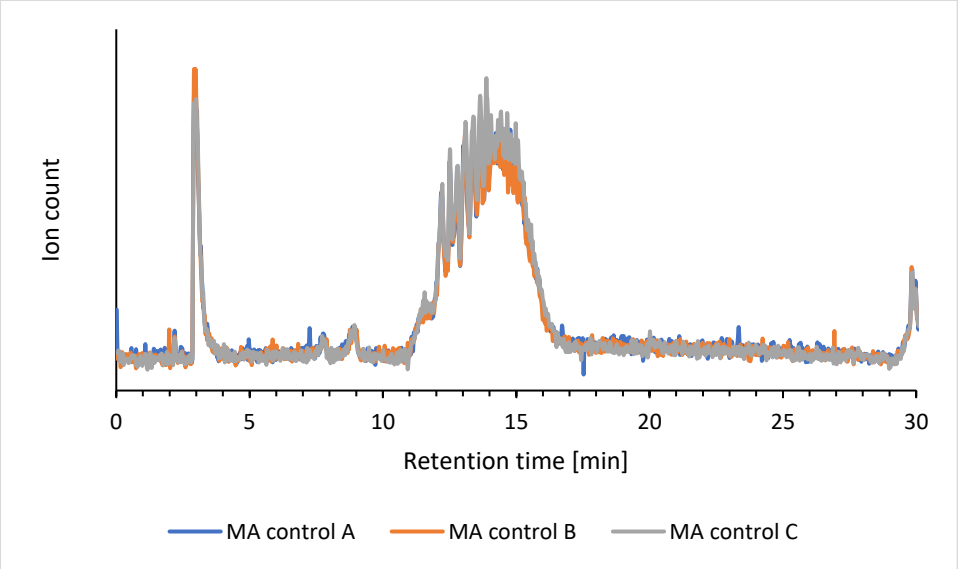

Figure S16. LC-MS analysis confirms the formation of products obtained for MA control in the absence of DA. MA (400µmol) was allowed to react under dry conditions at 85 °C for 7 days and the reaction products were analyzed by HPLC at 210nm (A) and LC-MS operating at negative mode (B). Chromatograms were obtained for three individual preparations.

A

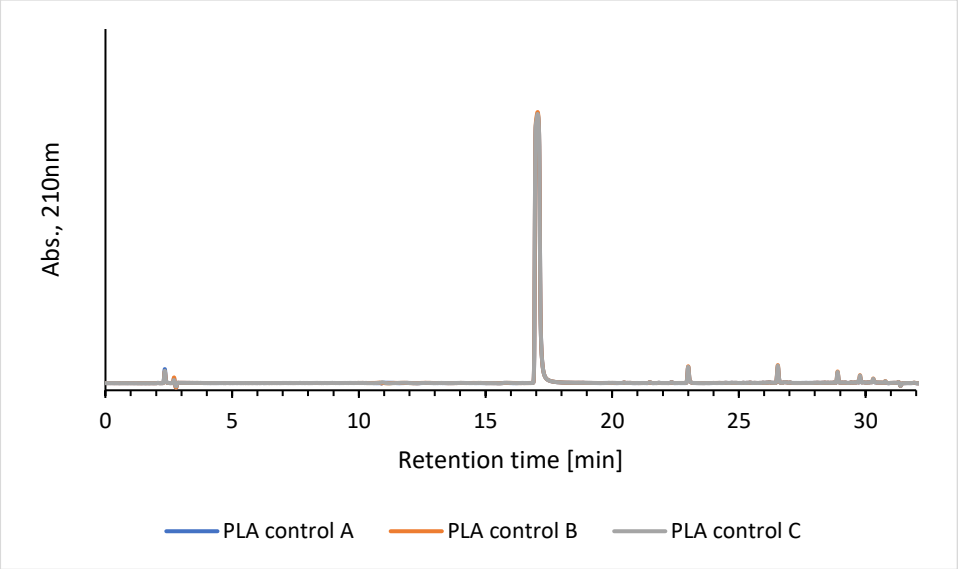

B

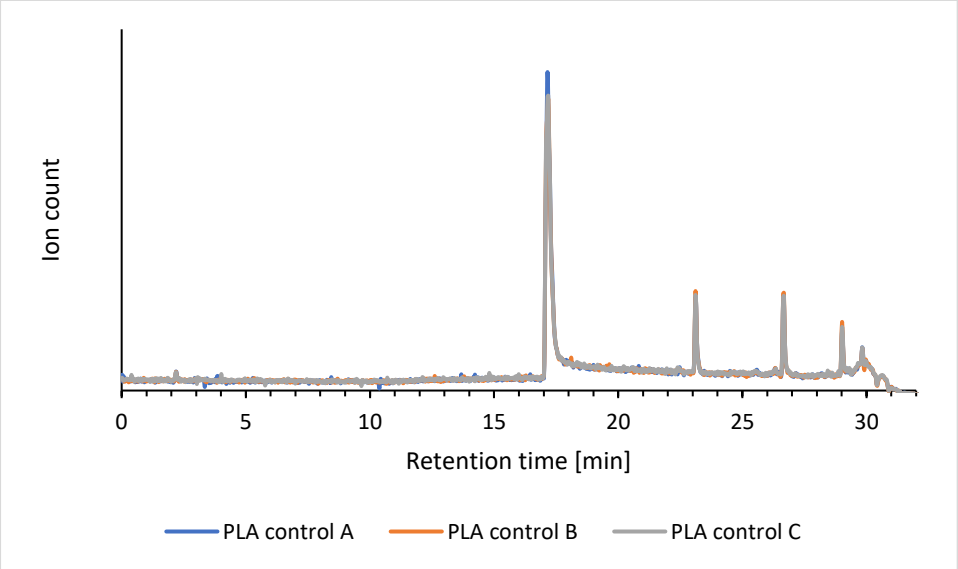

Figure S17. LC-MS analysis confirms the formation of products obtained for PLA control in the absence of DA. PLA (400µmol) was allowed to react under dry conditions at 85 °C for 7 days and the reaction products were analyzed by HPLC at 210nm (A) and LC-MS operating at negative mode (B). Chromatograms were obtained for three individual preparations.

A

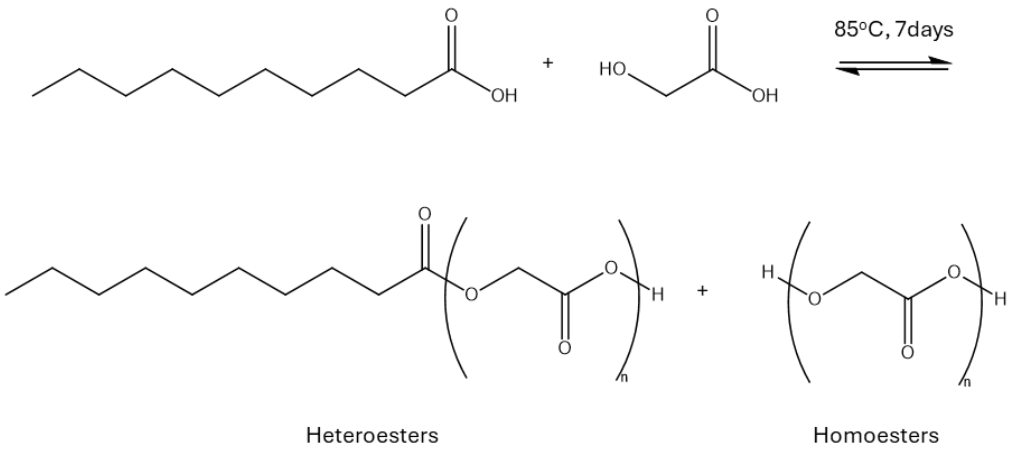

B

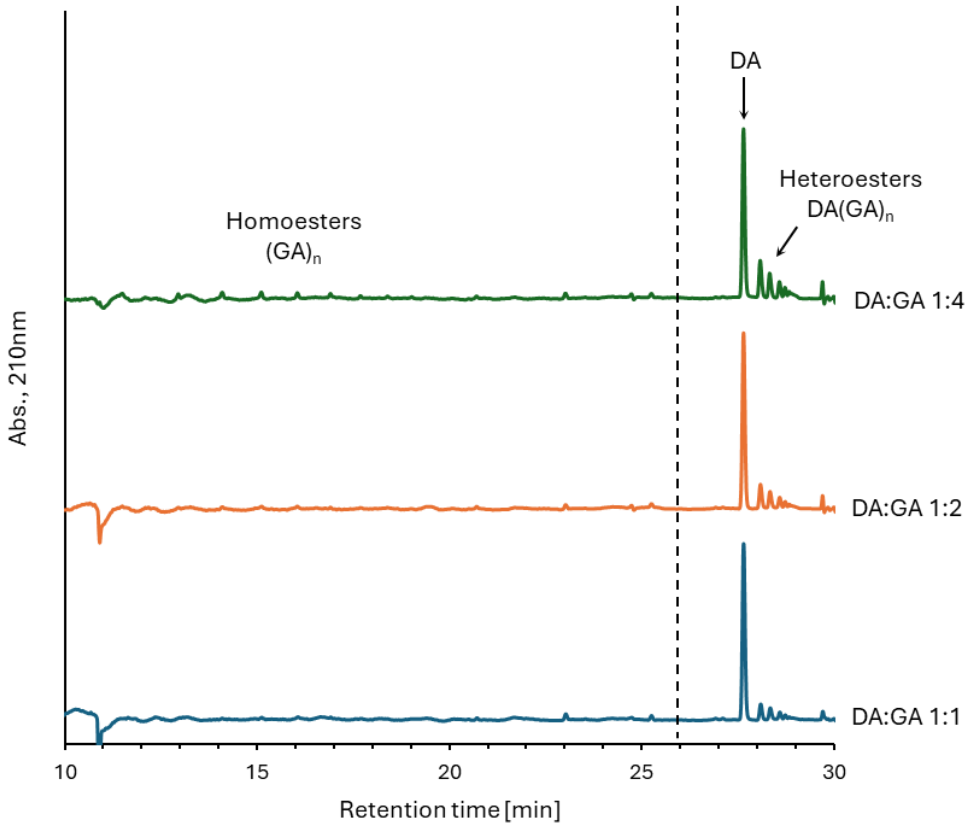

Figure S18. DA and GA react to produce two types of products: homoesters of GA and heteroesters of DA and GA. General esterification reaction that DA and GA undergo at 85 °C for 7 days. The main products obtained by the reaction are homooligomers of GA and cooligomers of single DA molecule covalently linked to GA or GA oligomers (A). HPLC chromatogram of the products obtained by the reaction of DA and GA at 1:1, 1:2, and 1:4 molar ratio (B). The products eluted at earlier retention times correspond to GA homooligomers while products of later retention times correspond to DA-GA cooligomers. A greater excess of GA results in the formation of more products at higher levels.

A

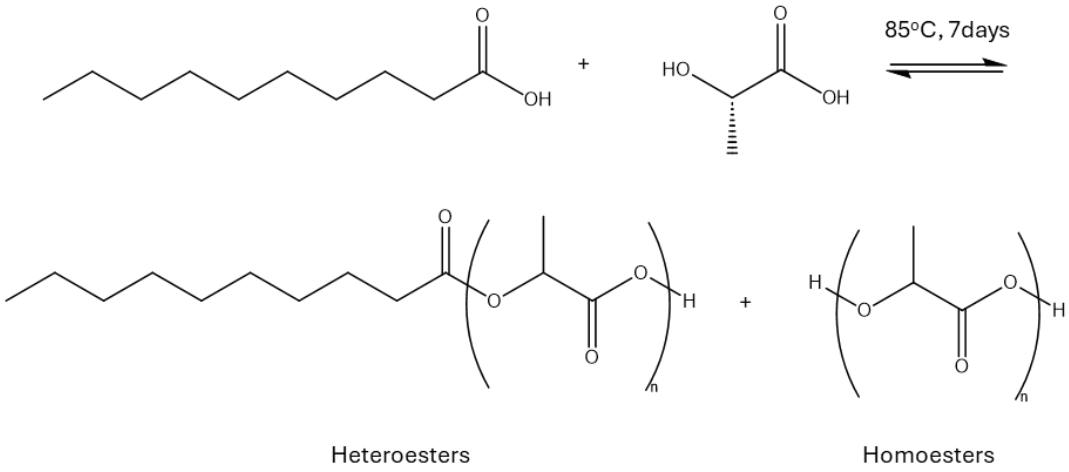

B

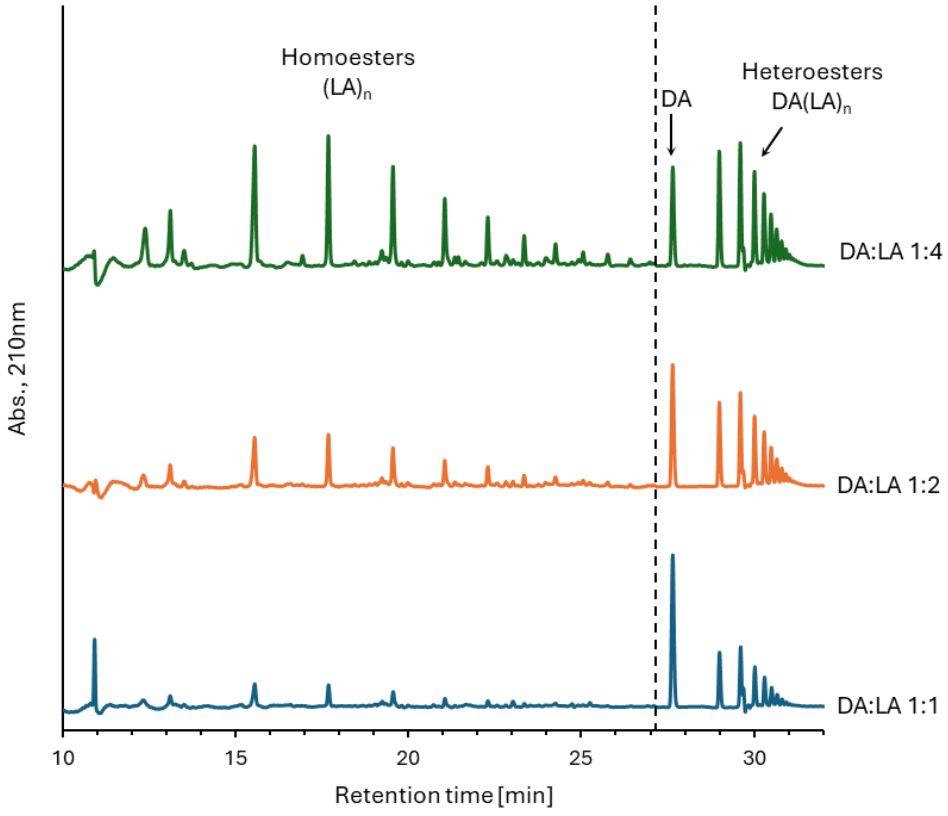

Figure S19. DA and LA react to produce two types of products: homoesters of LA and heteroesters of DA and LA. General esterification reaction that DA and LA undergo at 85 °C for 7 days. The main products obtained by the reaction are homooligomers of LA and cooligomers of single DA molecule covalently linked to LA or LA oligomers (A). HPLC chromatogram of the products obtained by the reaction of DA and LA at 1:1, 1:2, and 1:4 molar ratio (B). The products eluted at earlier retention times correspond to LA homooligomers while products of later retention times correspond to DA-LA cooligomers. A greater excess of LA results in the formation of more products at higher levels.

A

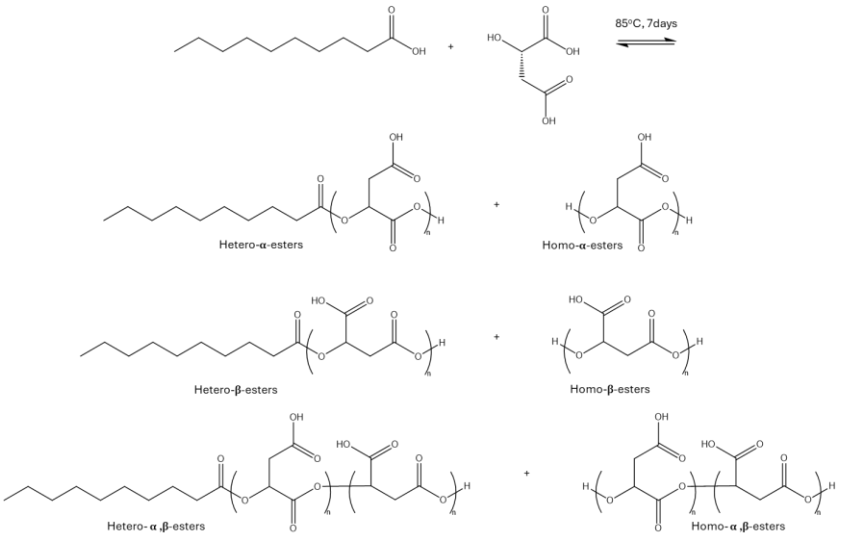

B

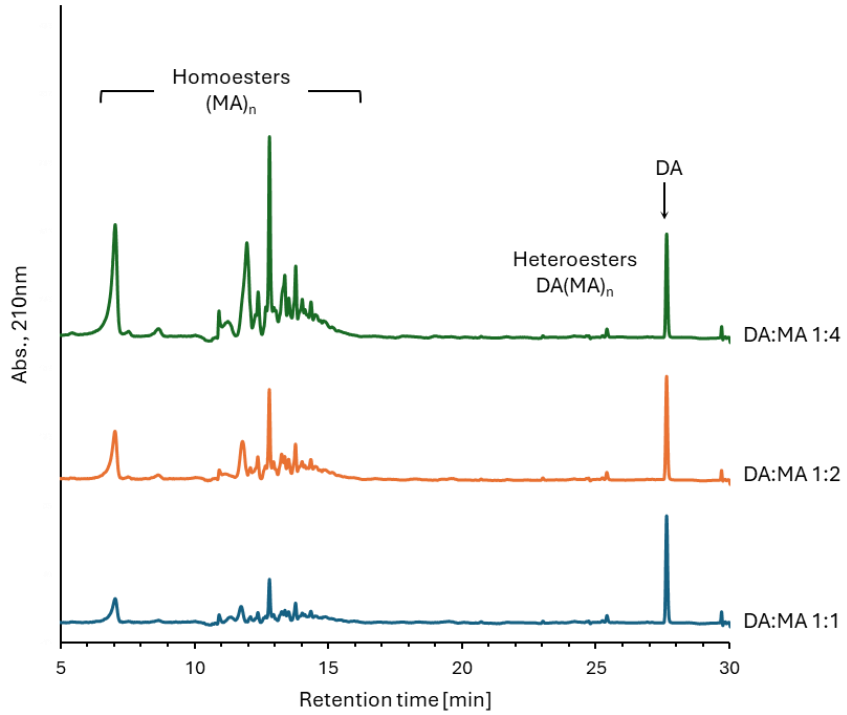

Figure S20. DA and MA react to produce two types of products: homoesters of MA and heteroesters of DA and MA. General esterification reaction that DA and LA undergo at 85 °C for 7 days. The main products obtained by the reaction are homooligomers and cooligomers of either the α-esters, β-esters, or α,β-esters. α and β esters refer to the esterification products at the α- and β- carboxylic acid of MA, respectively (A). HPLC chromatogram of the products obtained by the reaction of DA and MA at 1:1, 1:2, and 1:4 molar ratio (B). The products eluted at earlier retention times correspond to MA homooligomers. The products eluted within 20-26min correspond to DA-MA cooligomers. A greater excess of MA results in the formation of more products at higher levels.

A

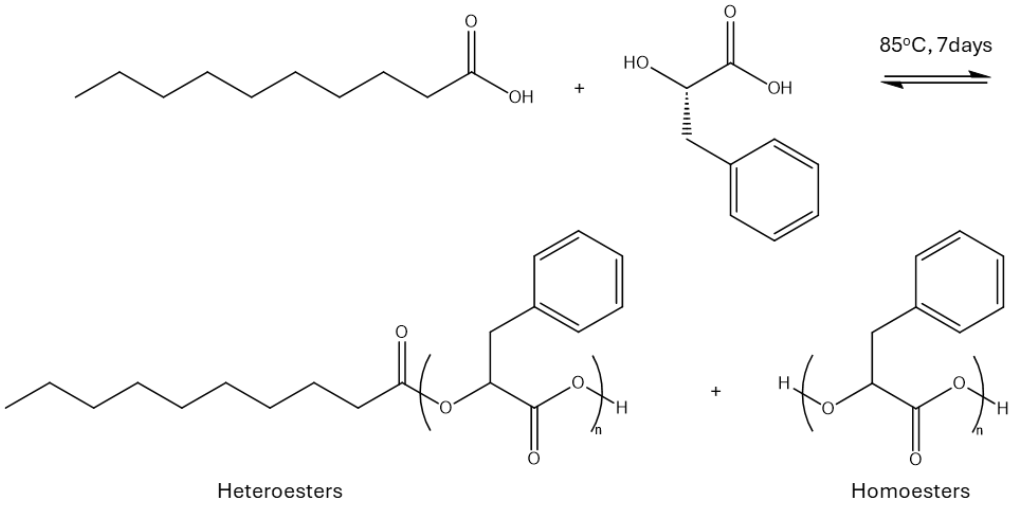

B

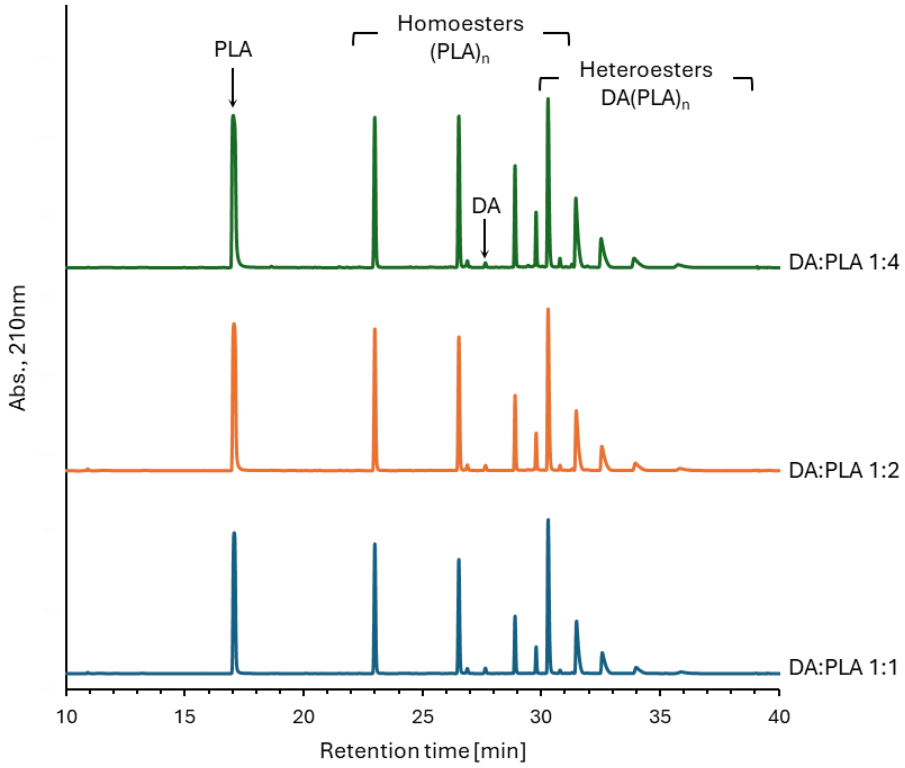

Figure S21. DA and PLA react to produce two types of products: homoesters of PLA and heteroesters of DA and PLA. General esterification reaction that DA and PLA undergo at 85 °C for 7 days. The main products obtained by the reaction are homooligomers of PLA and cooligomers of single DA molecule covalently linked to PLA or LA oligomers (A). HPLC chromatogram of the products obtained by the reaction of DA and PLA at 1:1, 1:2, and 1:4 molar ratio (B). Increasing the levels of PLA did not result in the formation of new products, but increased their concentration.

Table S1. Identification of DA-GA reaction products. The detected products based on retention time and their corresponding m/z and ionization pattern as determined by LC-MS.

Retention time (min)	Compound	M (g/mol)	Corresponding m/z (-TIC)	Ionization pattern
11.6	3GA	192.1	191.1, 383.2	$[M-H]^-$, $[2M-H]^-$
12.2	4GA	250.1	249.0, 499.3	$[M-H]^-$, $[2M-H]^-$
13.1	4GA	250.1	249.0, 499.2	$[M-H]^-$, $[2M-H]^-$
14.2	5GA	308.2	307.0, 615.3	$[M-H]^-$, $[2M-H]^-$
15.2	6GA	366.2	365.2, 731.2	$[M-H]^-$, $[2M-H]^-$
16.2	7GA	424.2	423.2, 847.4	$[M-H]^-$, $[2M-H]^-$
17.0	8GA	482.3	481.3, 963.4	$[M-H]^-$, $[2M-H]^-$
17.8	9GA	540.3	539.2, 1079.4	$[M-H]^-$, $[2M-H]^-$
18.5	10GA	598.3	597.3, 1195.5	$[M-H]^-$, $[2M-H]^-$
19.1	11GA	656.4	655.1, 1311.7	$[M-H]^-$, $[2M-H]^-$
19.7	12GA	714.4	713.3	$[M-H]^-$
28.2	1GA1DA	230.3	229.1, 459.4	$[M-H]^-$, $[2M-H]^-$
28.4	2GA1DA	288.3	287.2, 575.5	$[M-H]^-$, $[2M-H]^-$
28.7	3GA1DA	346.4	345.3, 691.5	$[M-H]^-$, $[2M-H]^-$
28.8	4GA1DA	404.4	403.3, 807.5	$[M-H]^-$, $[2M-H]^-$
28.9	5GA1DA	462.4	461.4, 923.5	$[M-H]^-$, $[2M-H]^-$
29.0	6GA1DA	520.4	519.4, 1039.6	$[M-H]^-$, $[2M-H]^-$

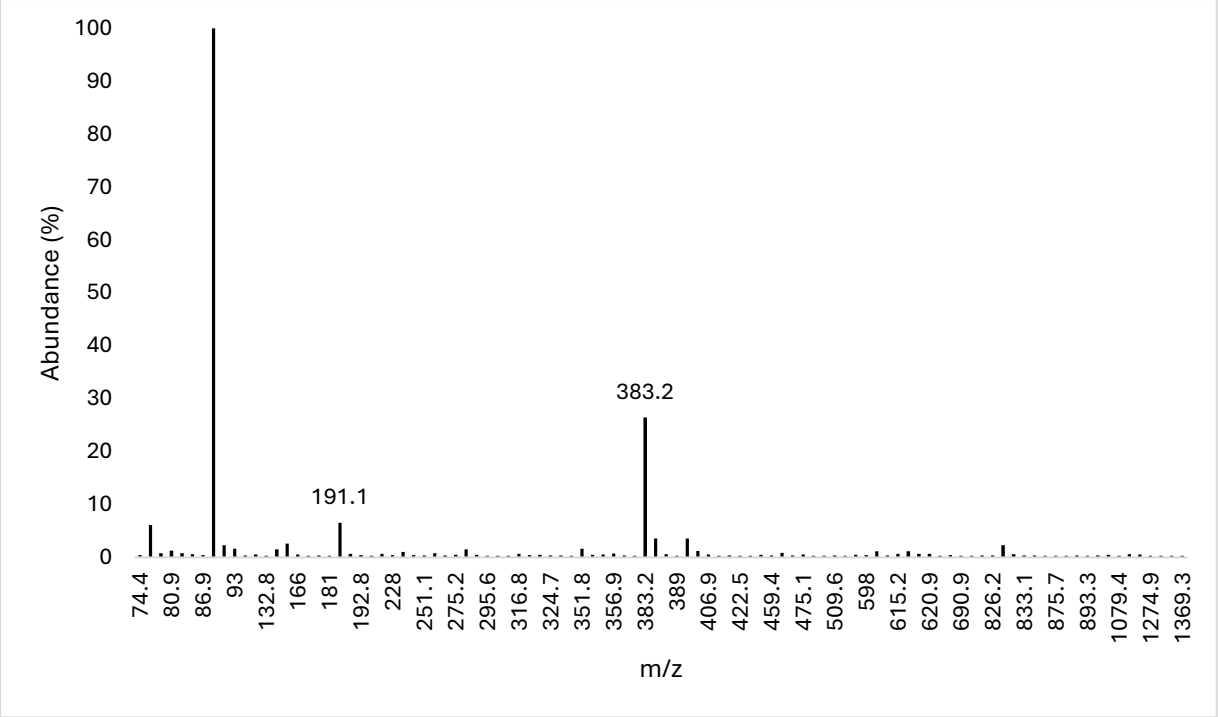

Figure S22. MS spectrum extracted from DA-GA reaction product chromatogram at retention time 11.6 min. The labeled m/z signals represent 3GA.

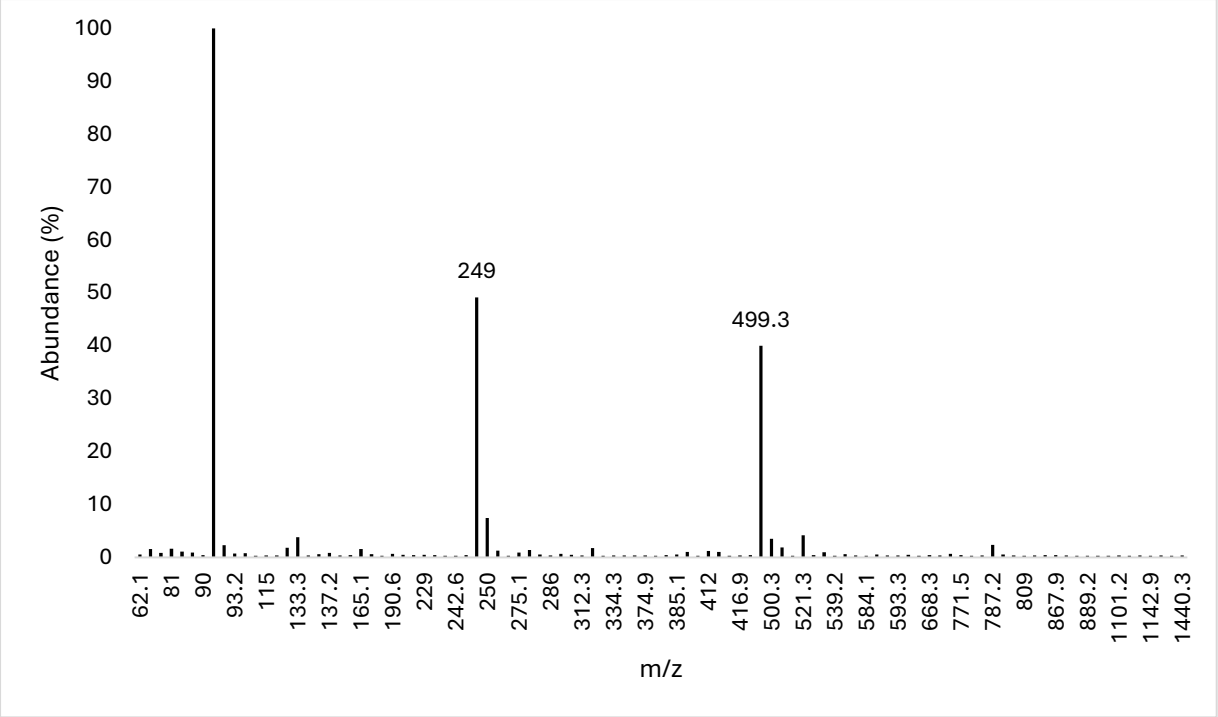

Figure S23. MS spectrum extracted from DA-GA reaction product chromatogram at retention time 12.2 min. The labeled m/z signals represent 4GA.

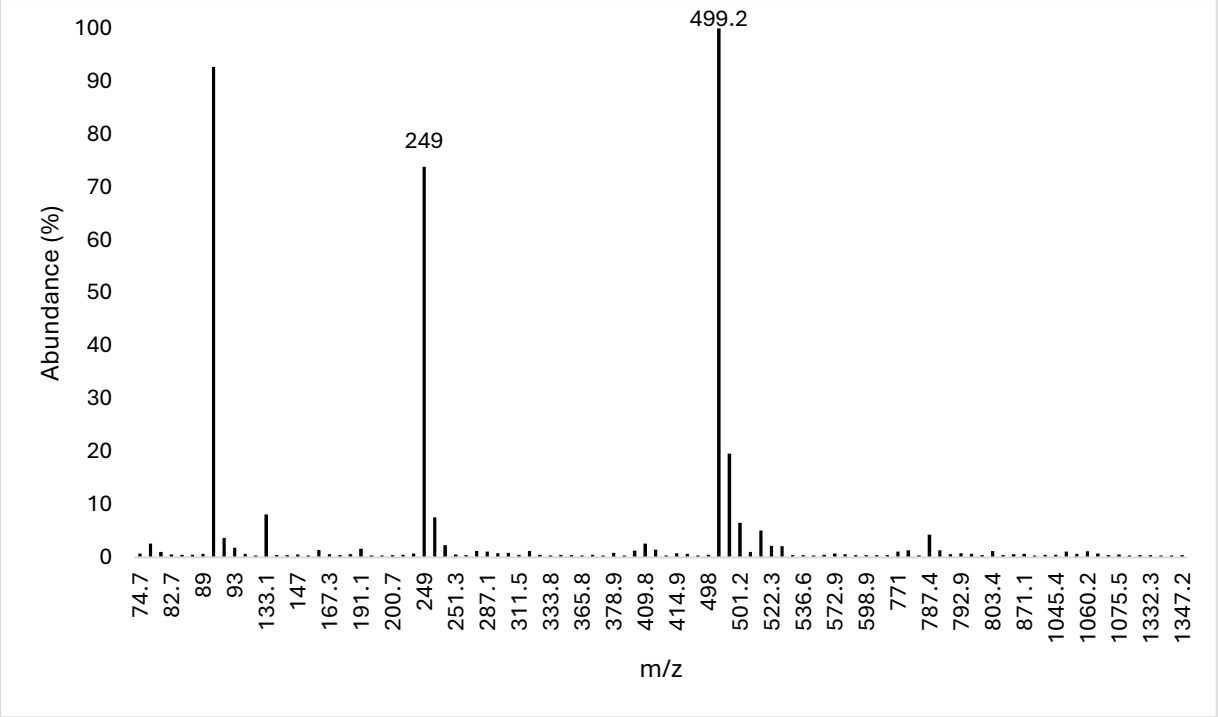

Figure S24. MS spectrum extracted from DA-GA reaction product chromatogram at retention time 13.1 min. The labeled m/z signals represent 4GA.

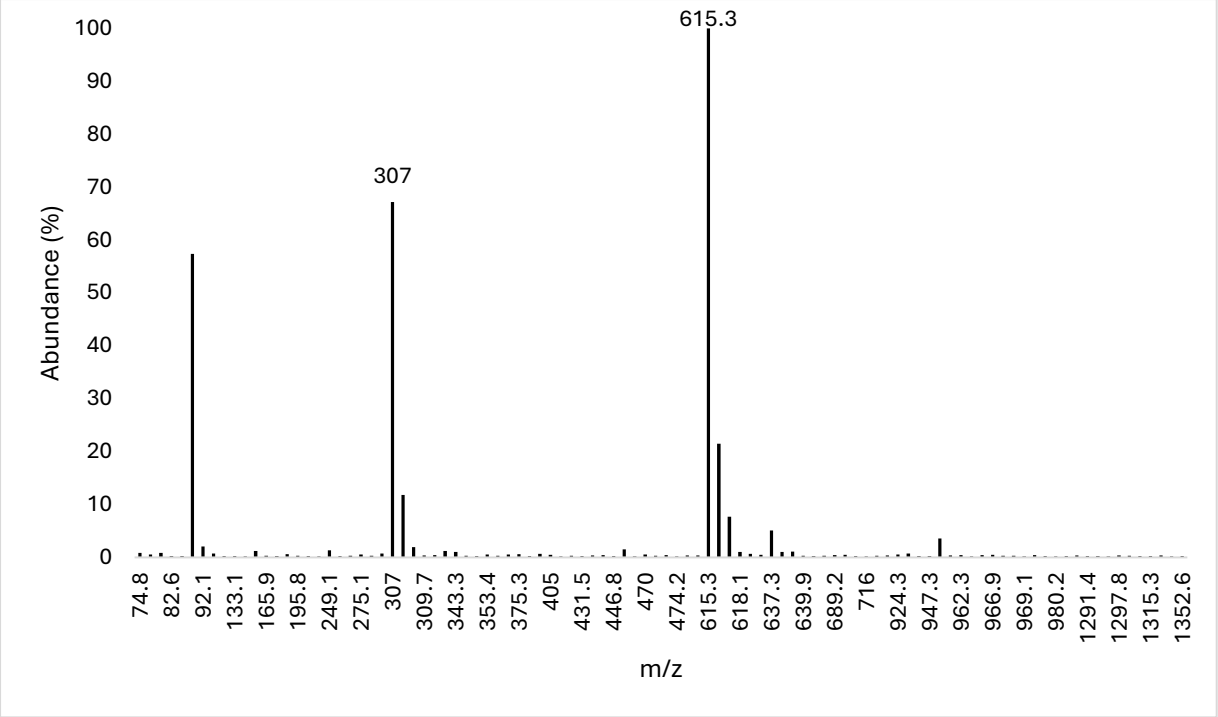

Figure S25. MS spectrum extracted from DA-GA reaction product chromatogram at retention time 14.2 min. The labeled m/z signals represent 5GA.

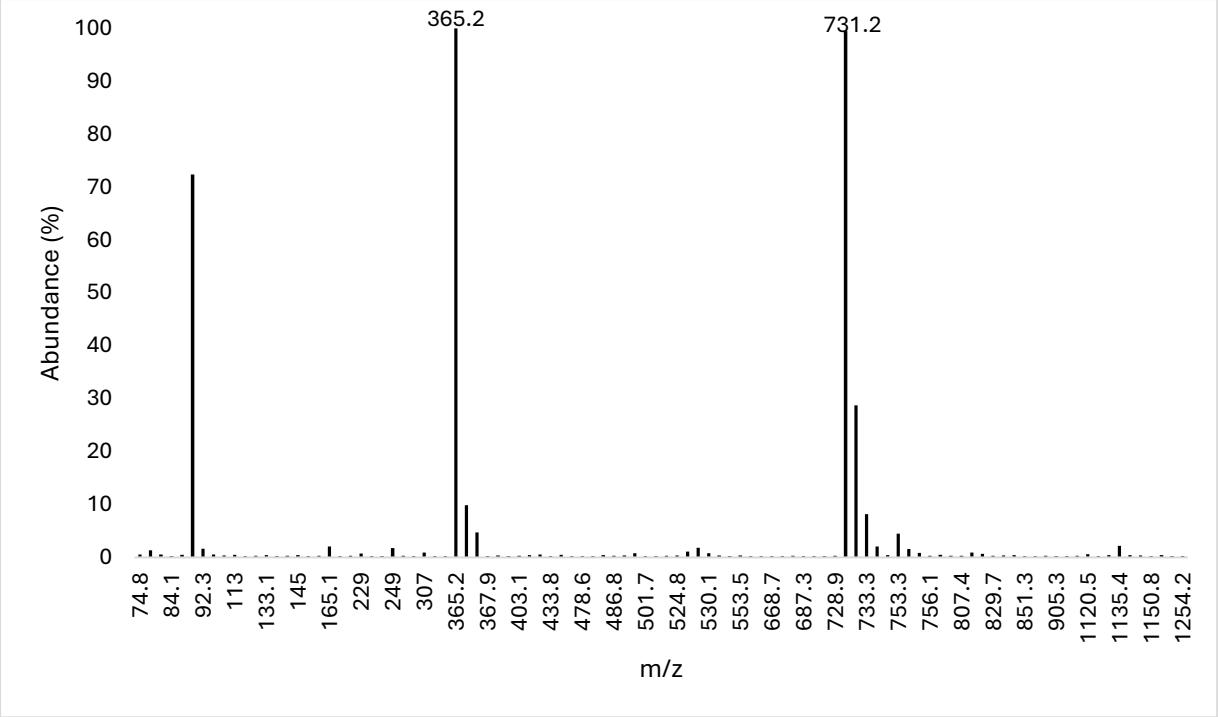

Figure S26. MS spectrum extracted from DA-GA reaction product chromatogram at retention time15.2 min. The labeled m/z signals represent 6GA.

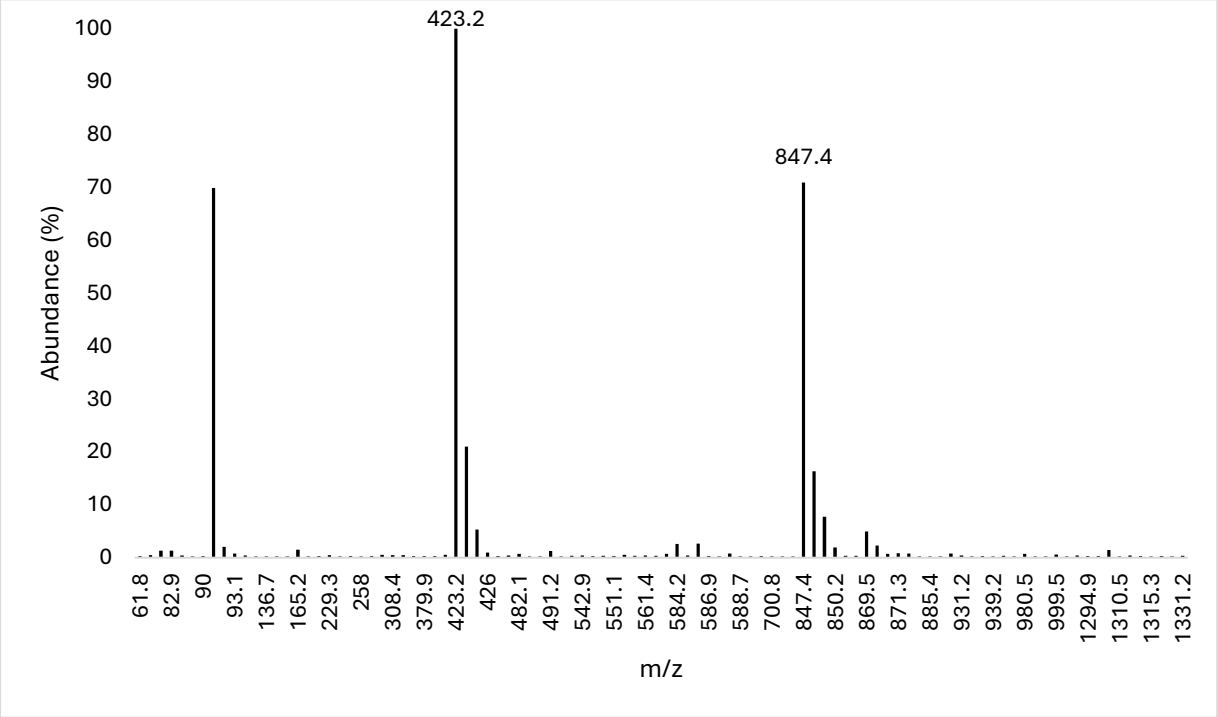

Figure S27. MS spectrum extracted from DA-GA reaction product chromatogram at retention time 16.2 min. The labeled m/z signals represent 7GA.

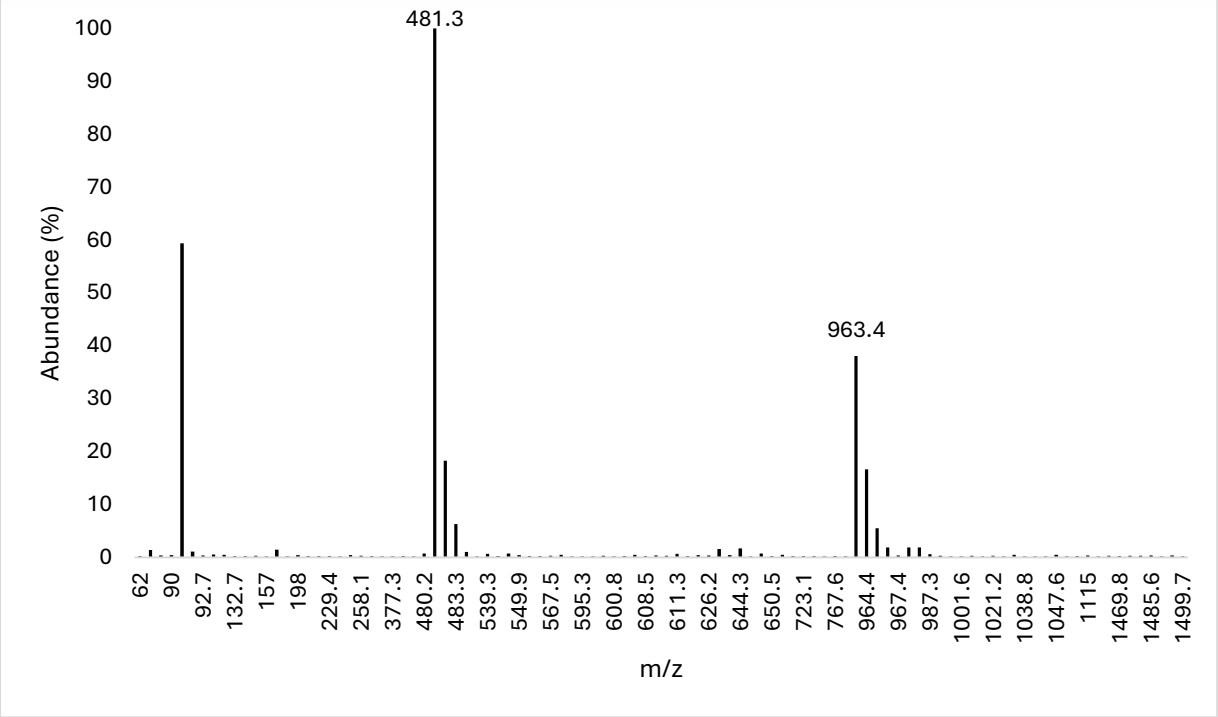

Figure S28. MS spectrum extracted from DA-GA reaction product chromatogram at retention time 17.0 min. The labeled m/z signals represent 8GA.

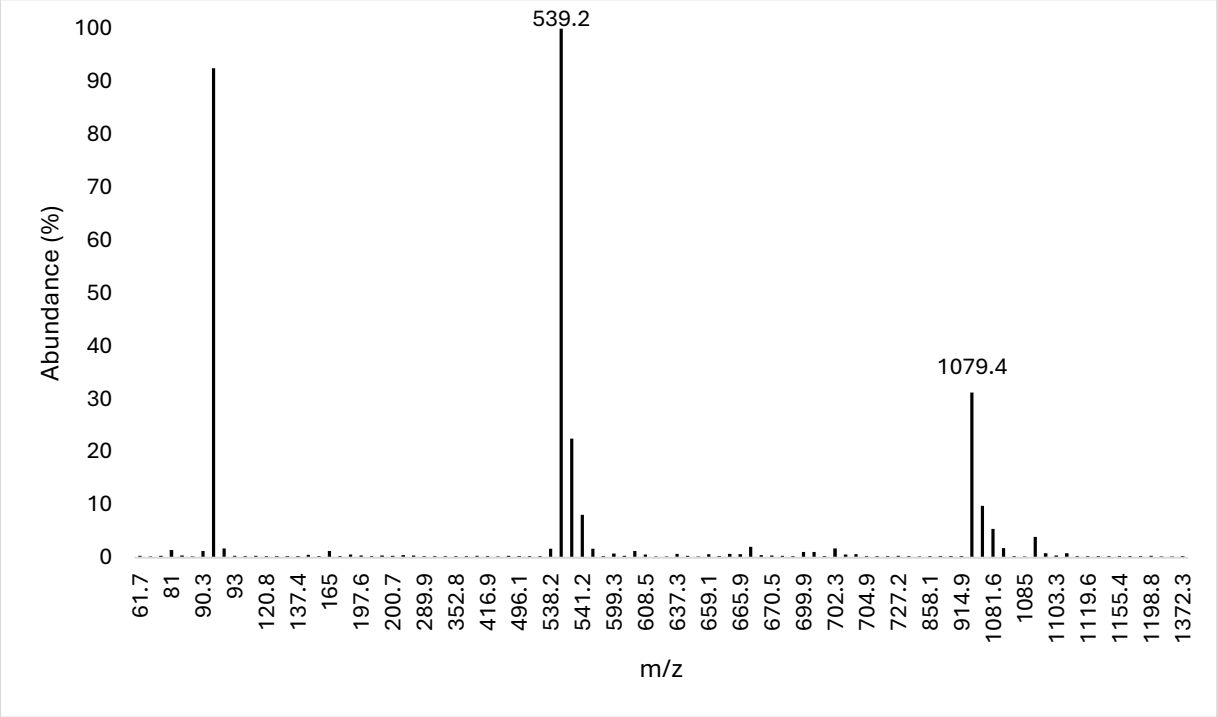

Figure S29. MS spectrum extracted from DA-GA reaction product chromatogram at retention time 17.8 min. The labeled m/z signals represent 9GA.

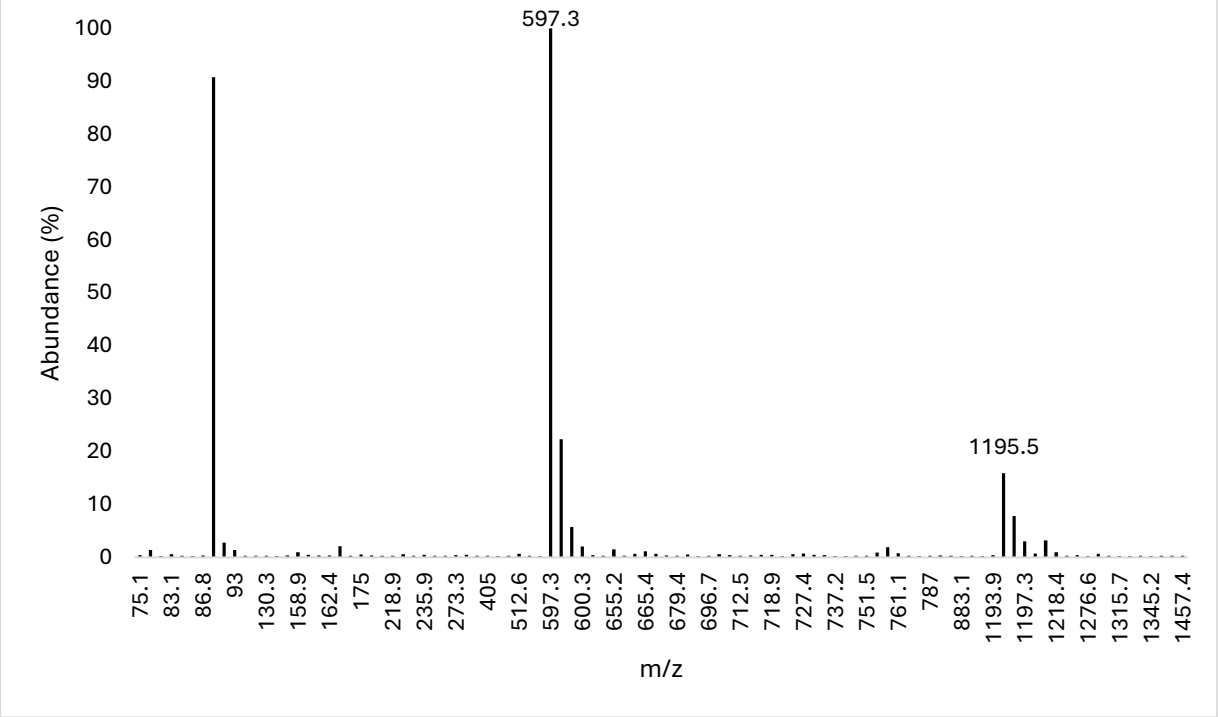

Figure S30. MS spectrum extracted from DA-GA reaction product chromatogram at retention time 18.5 min. The labeled m/z signals represent 10GA.

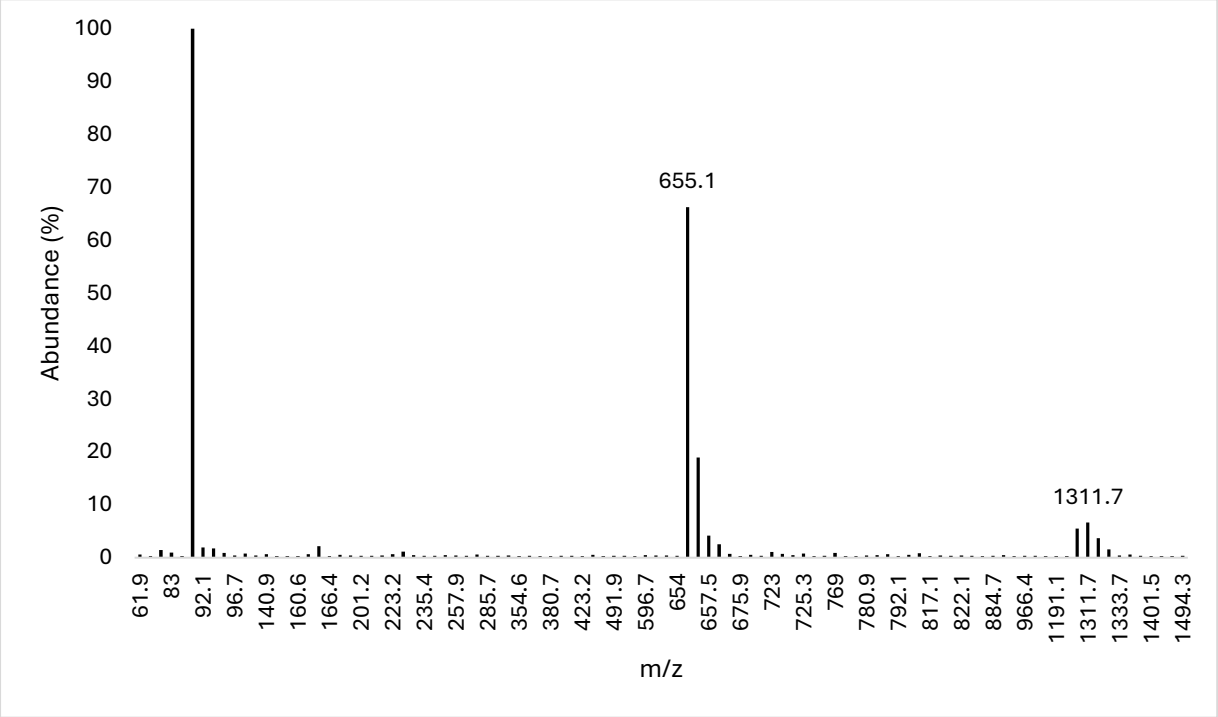

Figure S31. MS spectrum extracted from DA-GA reaction product chromatogram at retention time 19.1 min. The labeled m/z signals represent 11GA.

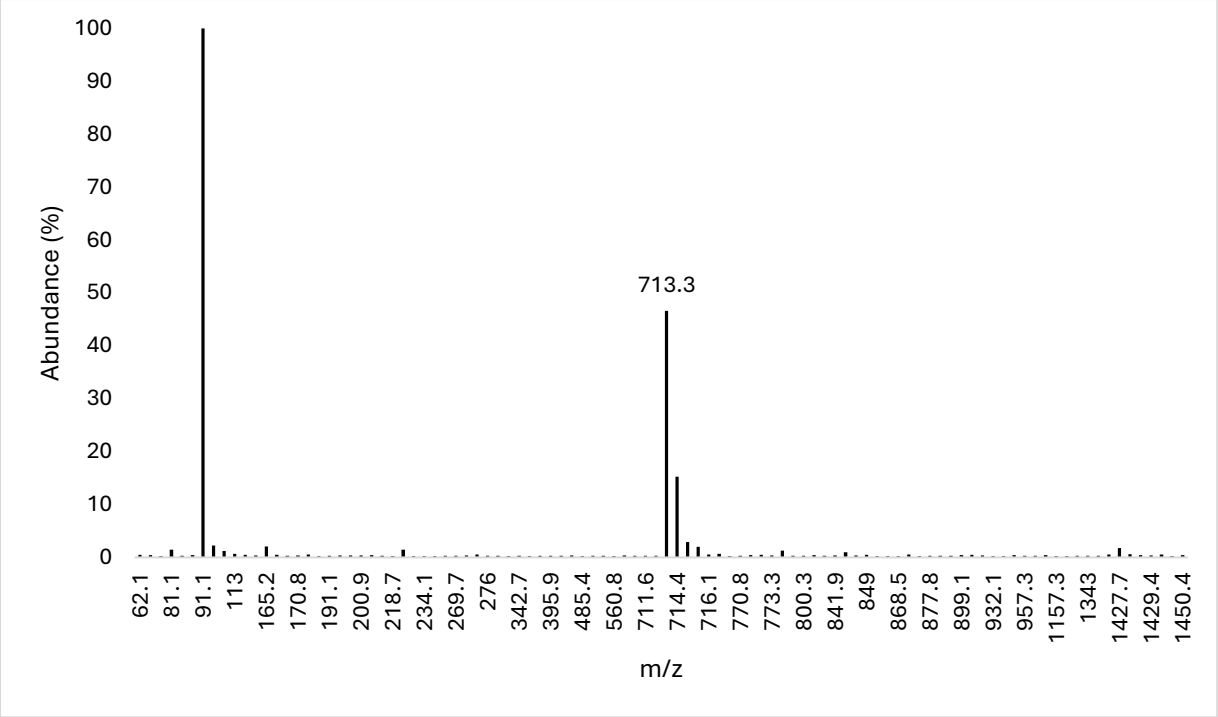

Figure S32. MS spectrum extracted from DA-GA reaction product chromatogram at retention time 19.7 min. The labeled m/z signal represents 12GA.

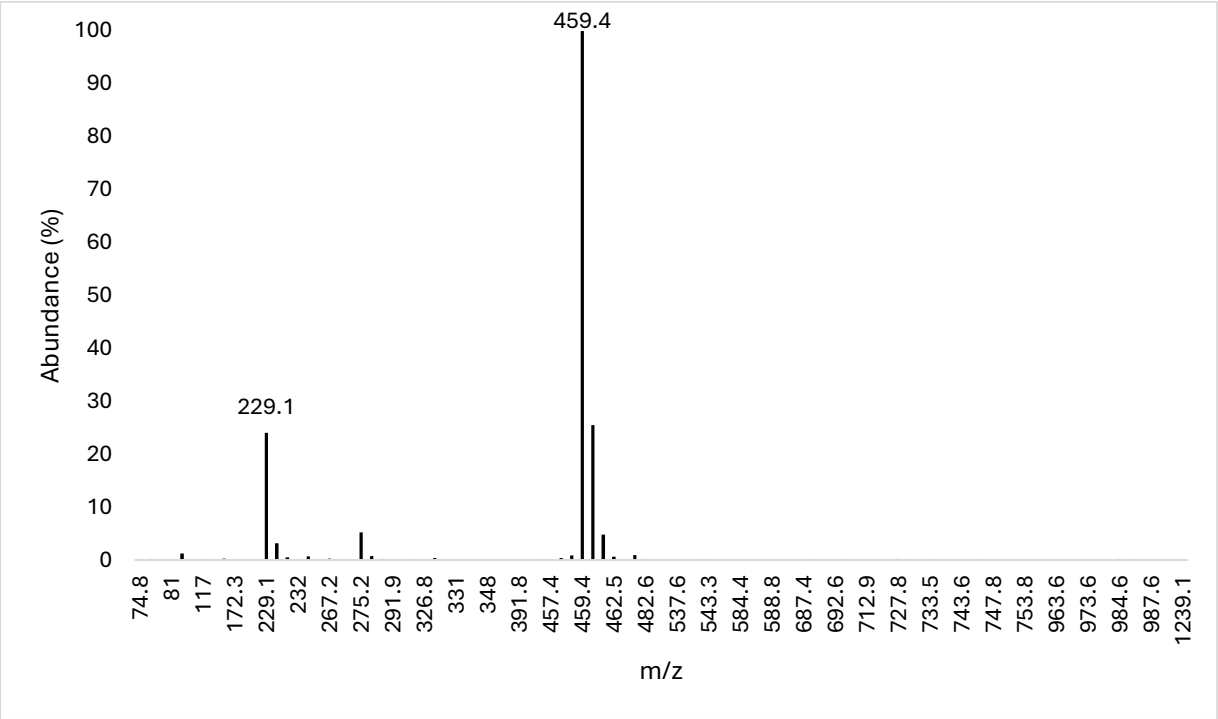

Figure S33. MS spectrum extracted from DA-GA reaction product chromatogram at retention time 28.2 min. The labeled m/z signals represent 1GA1DA.

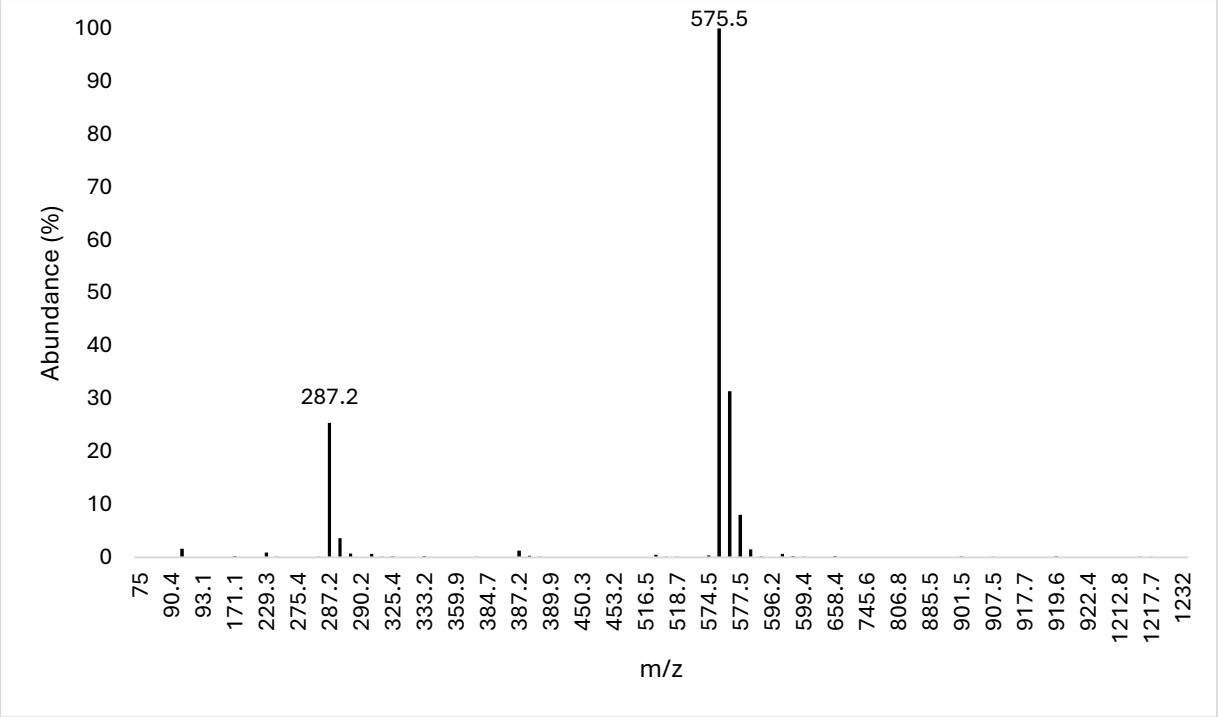

Figure S34. MS spectrum extracted from DA-GA reaction product chromatogram at retention time 28.4 min. The labeled m/z signals represent 2GA1DA.

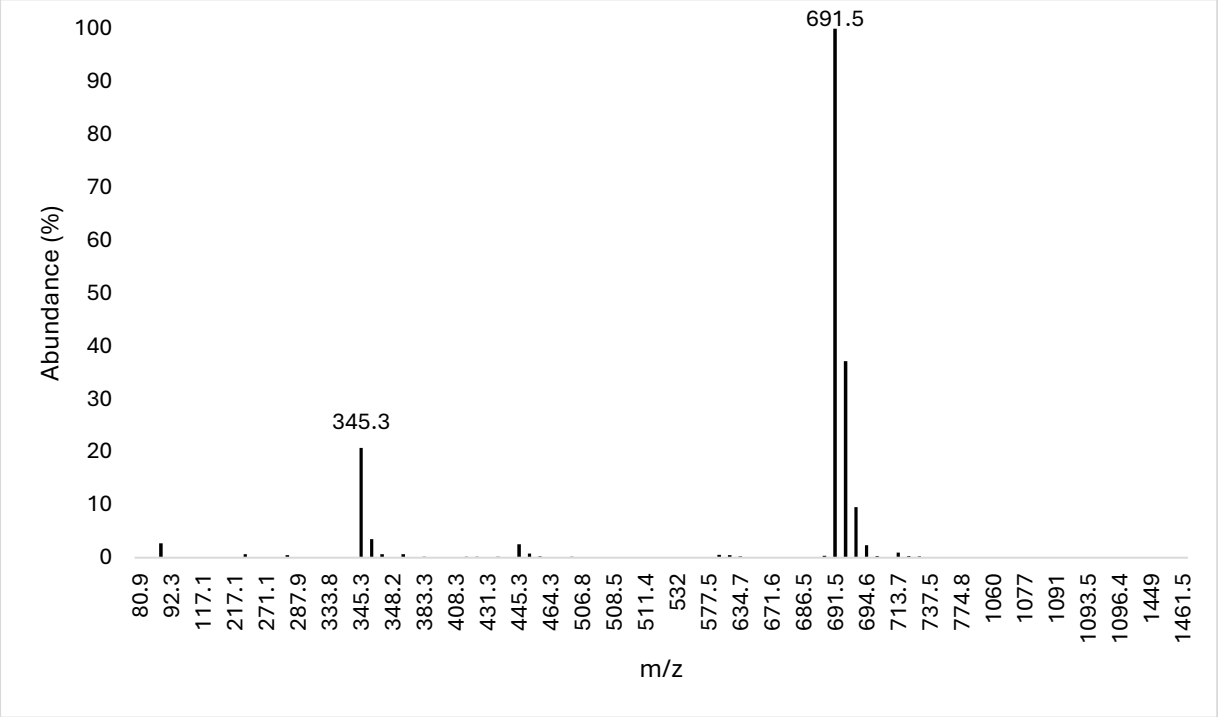

Figure S35. MS spectrum extracted from DA-GA reaction product chromatogram at retention time 28.7 min. The labeled m/z signals represent 3GA1DA.

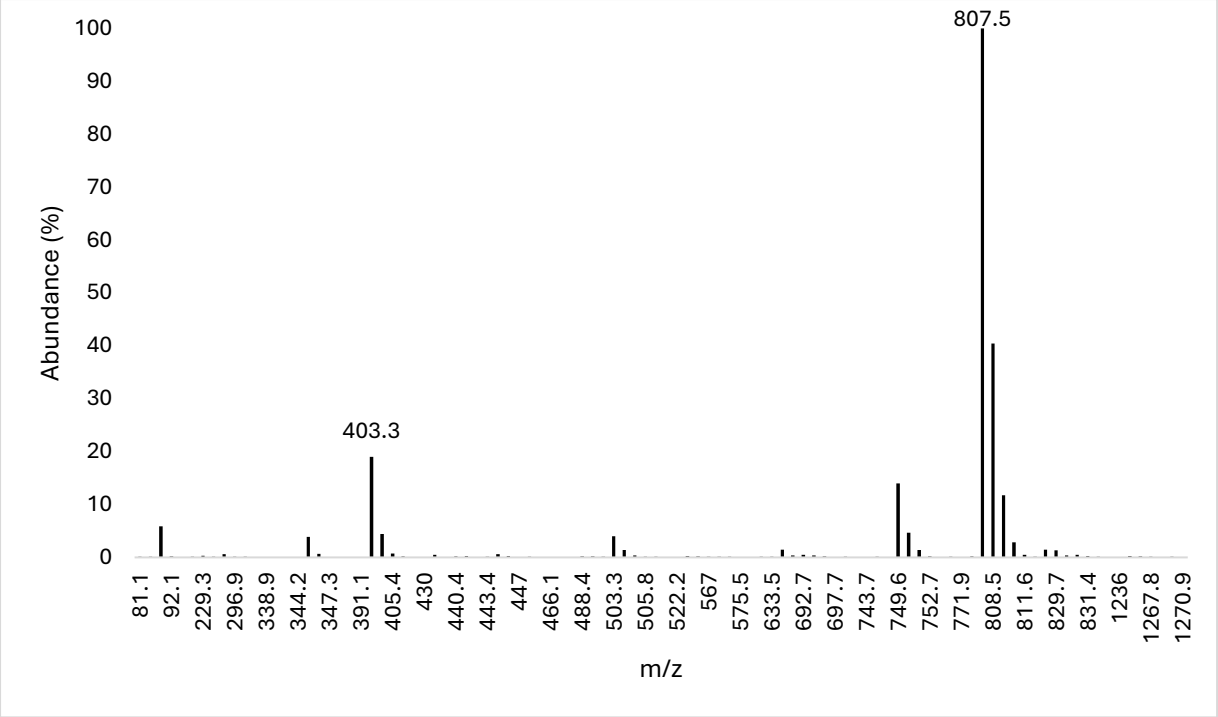

Figure S36. MS spectrum extracted from DA-GA reaction product chromatogram at retention time 28.8 min. The labeled m/z signals represent 4GA1DA.

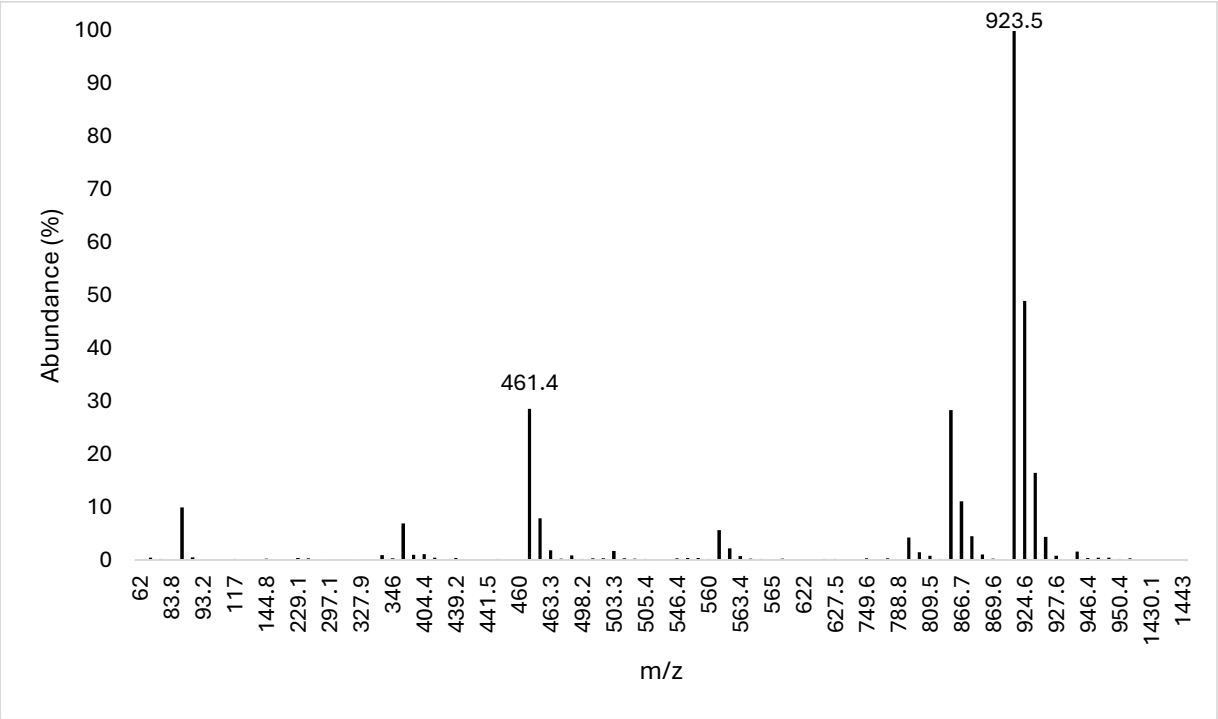

Figure S37. MS spectrum extracted from DA-GA reaction product chromatogram at retention time 28.9 min. The labeled m/z signals represent 5GA1DA.

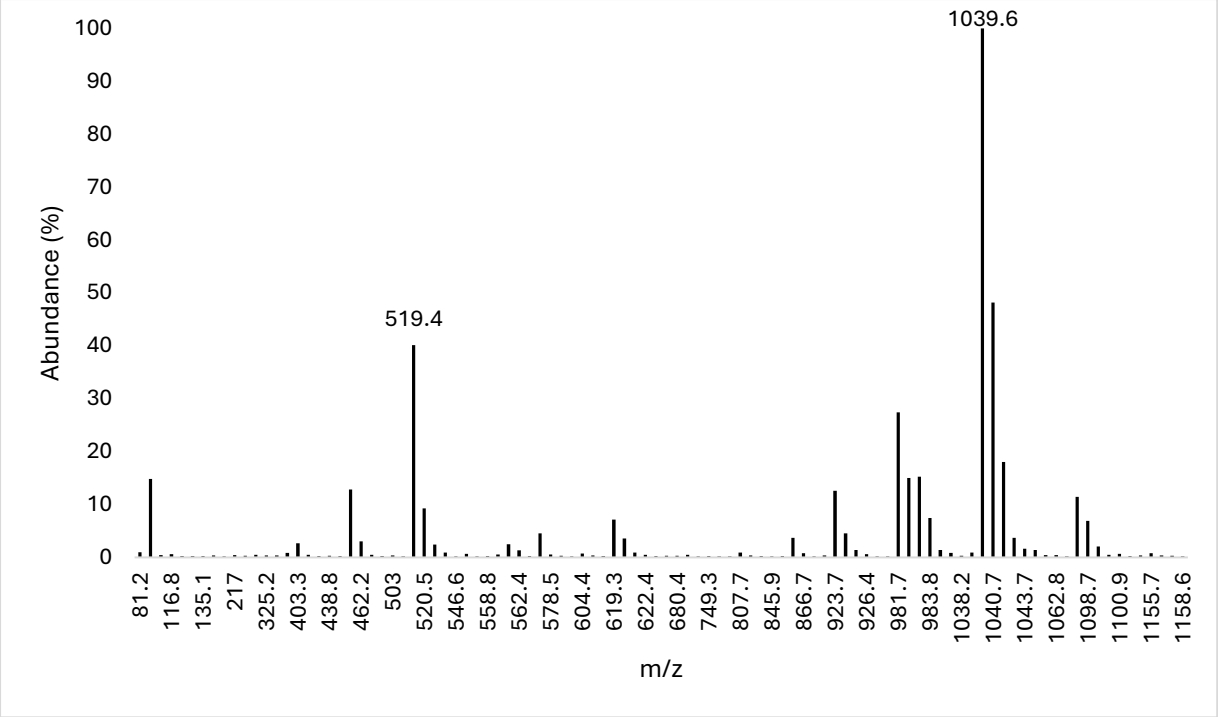

Figure S38. MS spectrum extracted from DA-GA reaction product chromatogram at retention time 29.0 min. The labeled m/z signals represent 6GA1DA.

Table S2. Identification of DA-MA reaction products. The detected products based on retention time and their corresponding m/z and ionization pattern as determined by LC-MS.

Retention time (min)	Compound	M (g/mol)	Corresponding m/z (-TIC)	Ionization pattern
7.7	2MA	250.2	249.0	$[M-H]^-$
8.7	2MA	250.2	249.1	$[M-H]^-$
11.4	3MA	366.2	365.1, 731.4	$[M-H]^-$, $[2M-H]^-$
12.1	3MA	366.2	365.2	$[M-H]^-$
	4MA	482.3	481.2	$[M-H]^-$
12.5	3MA	366.2	365.1, 731.4	$[M-H]^-$, $[2M-H]^-$
	4MA	482.3	481.2, 963.4	$[M-H]^-$, $[2M-H]^-$
12.8	4MA	482.3	481.2, 963.4	$[M-H]^-$, $[2M-H]^-$
	5MA	598.4	597.3	$[M-H]^-$
13.2	4MA	482.3	481.2	$[M-H]^-$
	5MA	598.4	597.3, 1195.6	$[M-H]^-$, $[2M-H]^-$
	6MA	714.4	713.4	$[M-H]^-$
13.4	4MA	482.3	481.2	$[M-H]^-$
	5MA	598.4	597.3, 1195.6, 298.2	$[M-H]^-$, $[2M-H]^-$, $[M-2H]^{2-}$
	6MA	714.4	713.3, 356.3	$[M-H]^-$, $[M-2H]^{2-}$
13.6	5MA	598.4	597.2, 1195.7, 297.9	$[M-H]^-$, $[2M-H]^-$, $[M-2H]^{2-}$
	6MA	714.4	713.4, 356.2	$[M-H]^-$, $[M-2H]^{2-}$
	7MA	830.5	829.5, 414.3	$[M-H]^-$, $[M-2H]^{2-}$
13.8	5MA	598.4	597.3	$[M-H]^-$
	6MA	714.4	713.3, 1427.5, 356.1	$[M-H]^-$, $[2M-H]^-$, $[M-2H]^{2-}$
	7MA	830.5	829.4, 414.2	$[M-H]^-$, $[M-2H]^{2-}$
14.0	6MA	714.4	713.4, 356.3	$[M-H]^-$, $[M-2H]^{2-}$
	7MA	830.5	829.3, 414.3	$[M-H]^-$, $[M-2H]^{2-}$
	8MA	946.6	945.3,472.3	$[M-H]^-$, $[M-2H]^{2-}$
14.4	7MA	830.5	829.3, 414.2	$[M-H]^-$, $[M-2H]^{2-}$
	8MA	946.6	945.5, 472.3	$[M-H]^-$, $[M-2H]^{2-}$
	9MA	1062.7	1061.5, 530.3	$[M-H]^-$, $[M-2H]^{2-}$
	10MA	1178.7	1177.2, 588.5	$[M-H]^-$, $[M-2H]^{2-}$
14.7	8MA	946.6	945.3, 472.4	$[M-H]^-$, $[M-2H]^{2-}$
	9MA	1062.7	1061.5, 530.3	$[M-H]^-$, $[M-2H]^{2-}$
	10MA	1178.7	1177.5, 588.4	$[M-H]^-$, $[M-2H]^{2-}$
	11MA	1294.8	1293.6, 646.4	$[M-H]^-$, $[M-2H]^{2-}$
14.9	9MA	1062.7	1061.5, 530.4	$[M-H]^-$, $[M-2H]^{2-}$
	10MA	1178.7	1177.4, 588.4	$[M-H]^-$, $[M-2H]^{2-}$
	11MA	1294.8	1293.7, 646.4	$[M-H]^-$, $[M-2H]^{2-}$
	12MA	1410.9	1409.6, 704.6	$[M-H]^-$, $[M-2H]^{2-}$
	13MA	1526.9	762.6	$[M-2H]^{2-}$
15.0	9MA	1062.7	1061.5, 530.1	$[M-H]^-$, $[M-2H]^{2-}$
	10MA	1178.7	1177.5, 588.4	$[M-H]^-$, $[M-2H]^{2-}$
	11MA	1294.8	1293.6, 646.5	$[M-H]^-$, $[M-2H]^{2-}$
	12MA	1410.9	1409.6, 704.3	$[M-H]^-$, $[M-2H]^{2-}$
	13MA	1526.9	762.8	$[M-2H]^{2-}$
15.3	10MA	1178.7	588.5	$[M-2H]^{2-}$
	11MA	1294.8	646.4	$[M-2H]^{2-}$
	12MA	1410.9	1409.7, 704.5	$[M-H]^-$, $[M-2H]^{2-}$
	13MA	1526.9	762.4	$[M-2H]^{2-}$
	14MA	1643.0	820.6	$[M-2H]^{2-}$
	15MA	1759.1	878.6	$[M-2H]^{2-}$
15.6	12MA	1410.9	704.7	$[M-2H]^{2-}$

	13MA	1526.9	762.4	$[M-2H]^{2-}$
	14MA	1643.0	820.2	$[M-2H]^{2-}$
	15MA	1759.1	878.5	$[M-2H]^{2-}$
	16MA	1875.1	936.6	$[M-2H]^{2-}$
23.6	3MA1DA	520.5	519.4	$[M-H]^-$
	4MA1DA	636.5	635.5	$[M-H]^-$
	5MA1DA	752.6	751.5	$[M-H]^-$
23.9	3MA1DA	520.5	519.4	$[M-H]^-$
	4MA1DA	636.5	635.4	$[M-H]^-$
24.3	2MA1DA	404.4	403.3, 807.8	$[M-H]^-$, $[2M-H]^-$
	3MA1DA	520.5	519.4	$[M-H]^-$
24.8	2MA1DA	404.4	403.2	$[M-H]^-$
25.5	1MA1DA	288.3	287.2, 575.5	$[M-H]^-$, $[2M-H]^-$

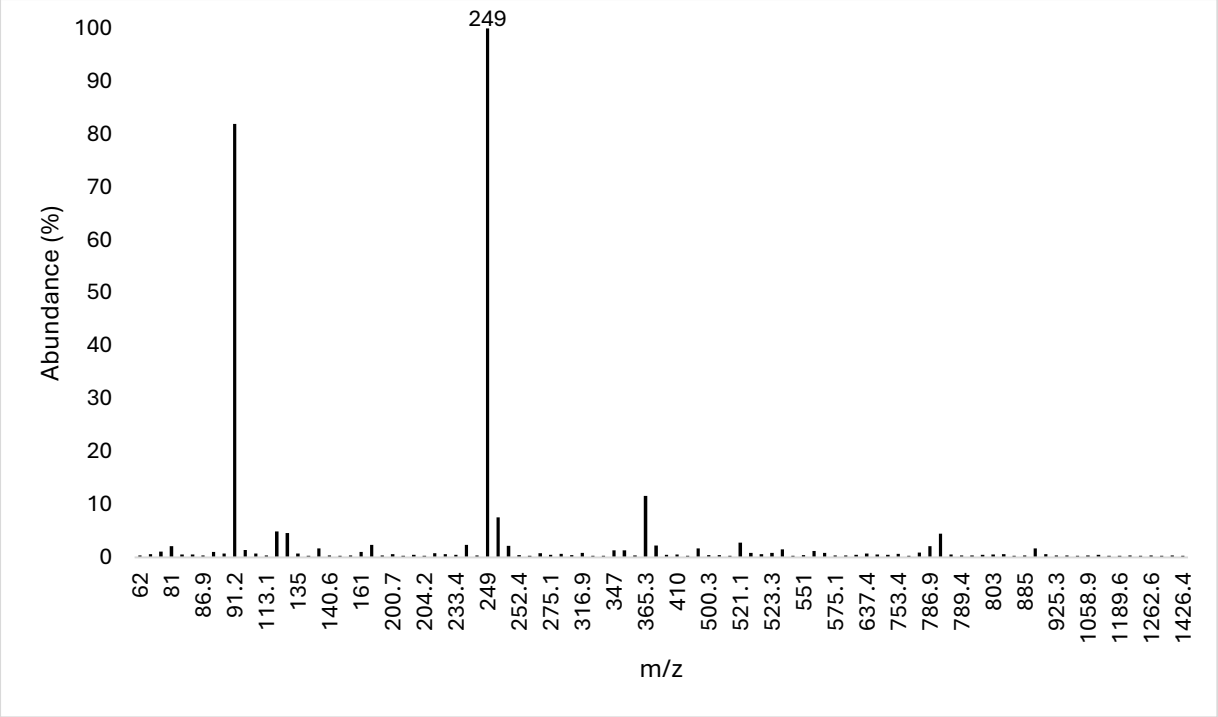

Figure S39. MS spectrum extracted from DA-MA reaction product chromatogram at retention time 7.7 min. The labeled m/z signal represents 2MA.

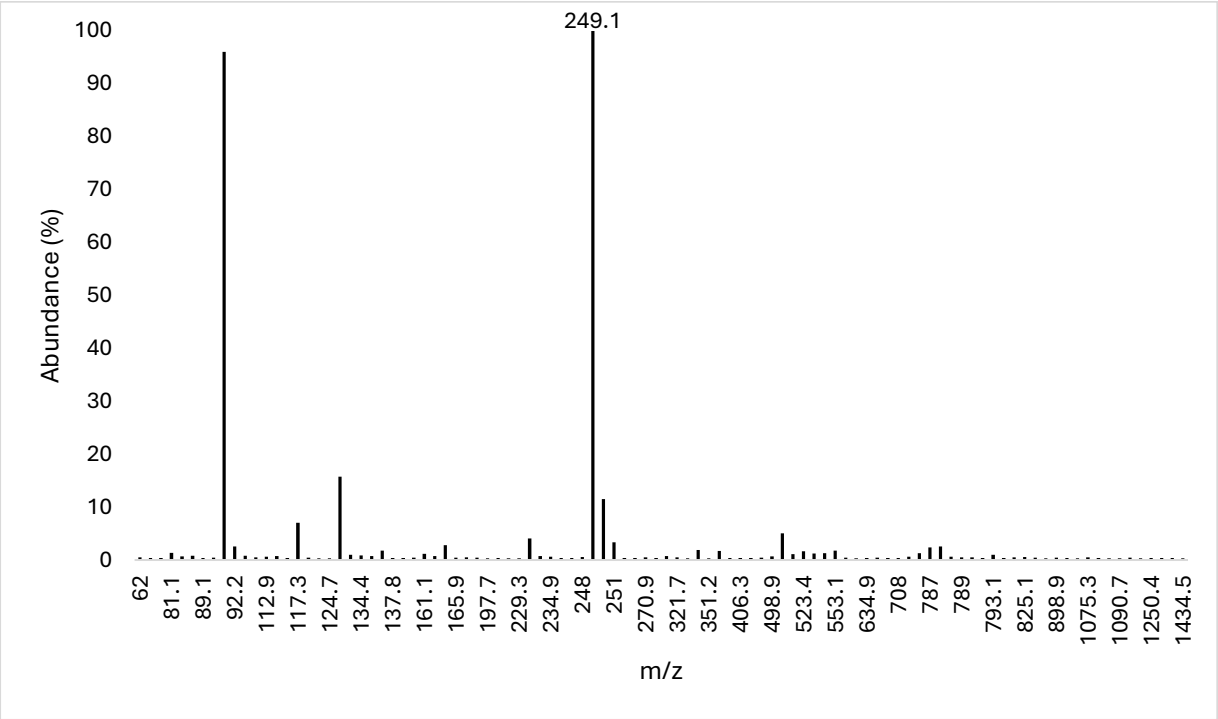

Figure S40. MS spectrum extracted from DA-MA reaction product chromatogram at retention time 8.7 min. The labeled m/z signal represents 2MA.

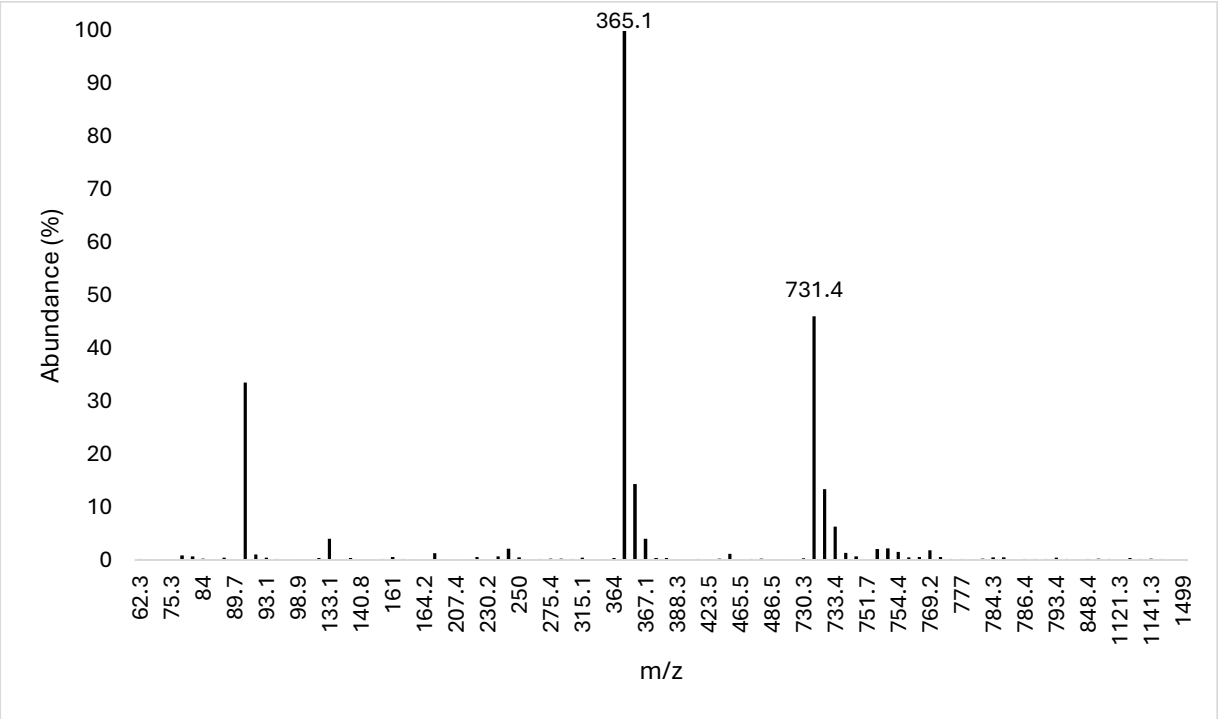

Figure S41. MS spectrum extracted from DA-MA reaction product chromatogram at retention time 11.4 min. The labeled m/z signals represent 3MA.

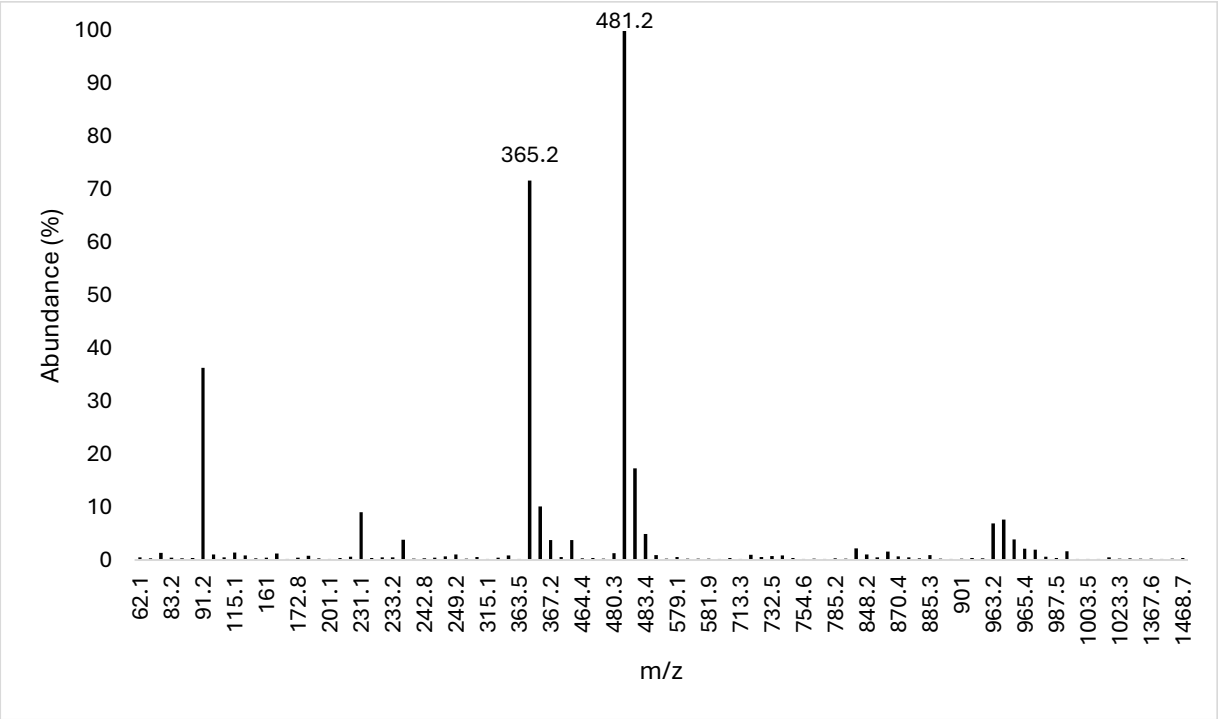

Figure S42. MS spectrum extracted from DA-MA reaction product chromatogram at retention time 12.1 min. The labeled m/z signals represent 3MA and 4MA.

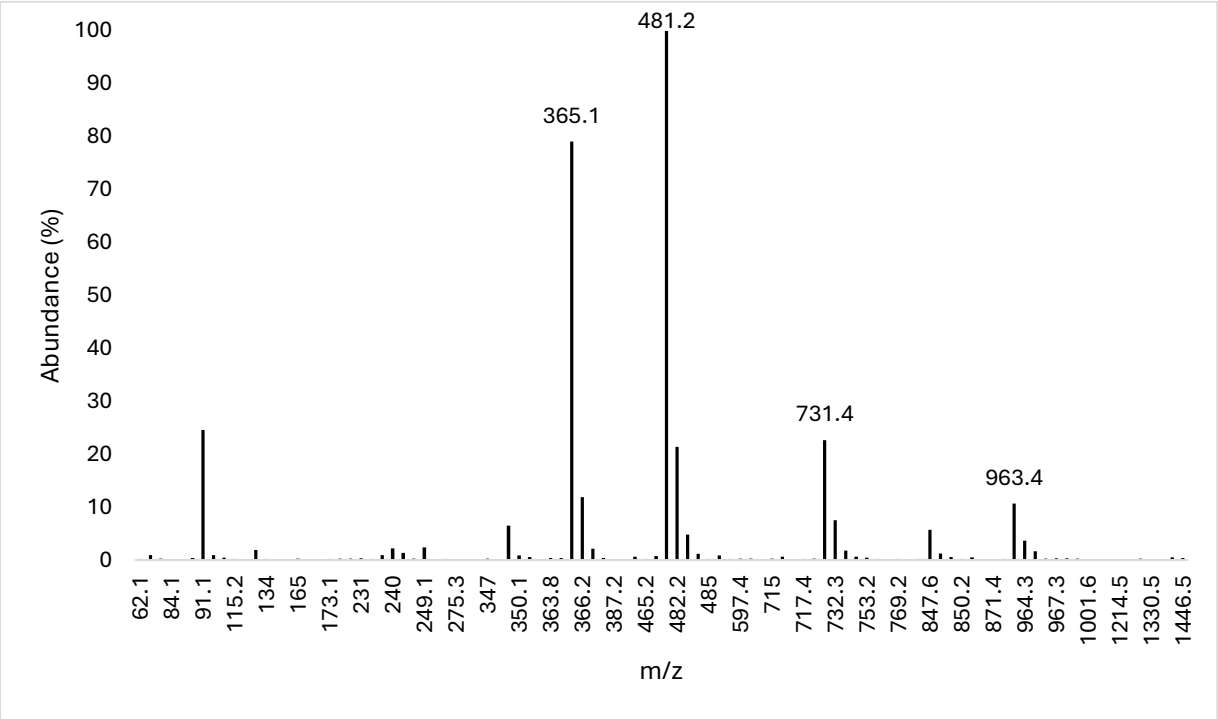

Figure S43. MS spectrum extracted from DA-MA reaction product chromatogram at retention time 12.5 min. The labeled m/z signals represent 3MA and 4MA.

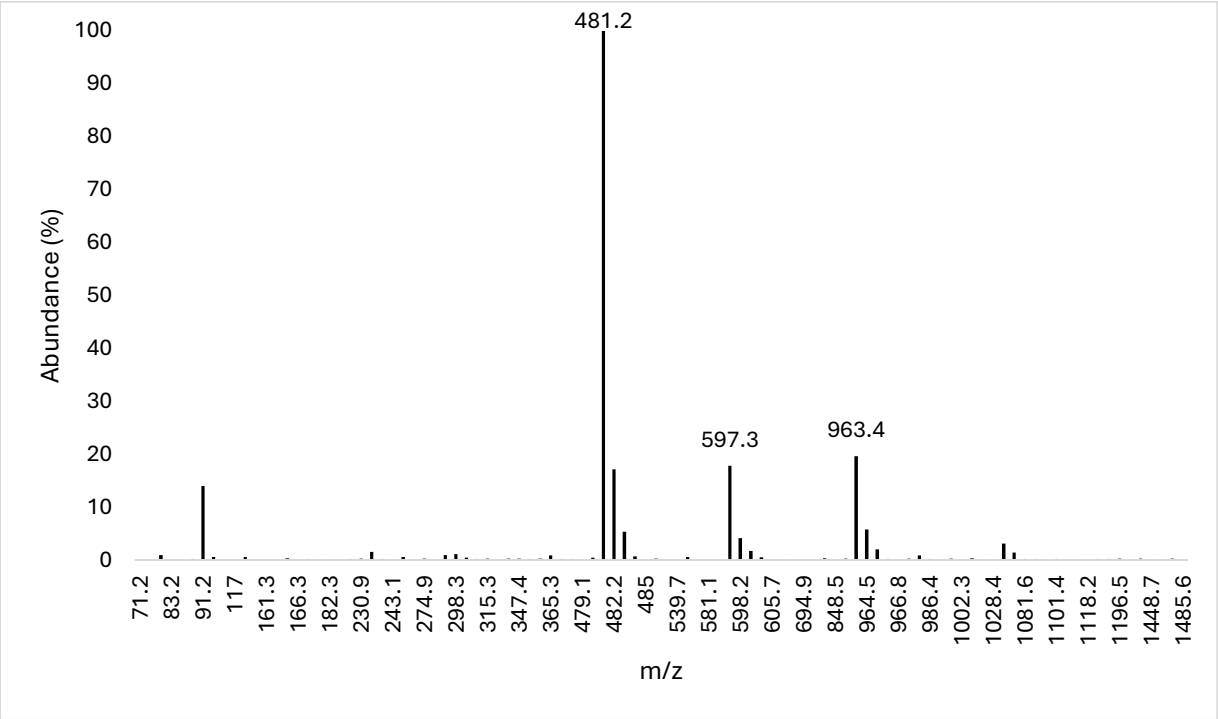

Figure S44. MS spectrum extracted from DA-MA reaction product chromatogram at retention time 12.8 min. The labeled m/z signals represent 4MA and 5MA.

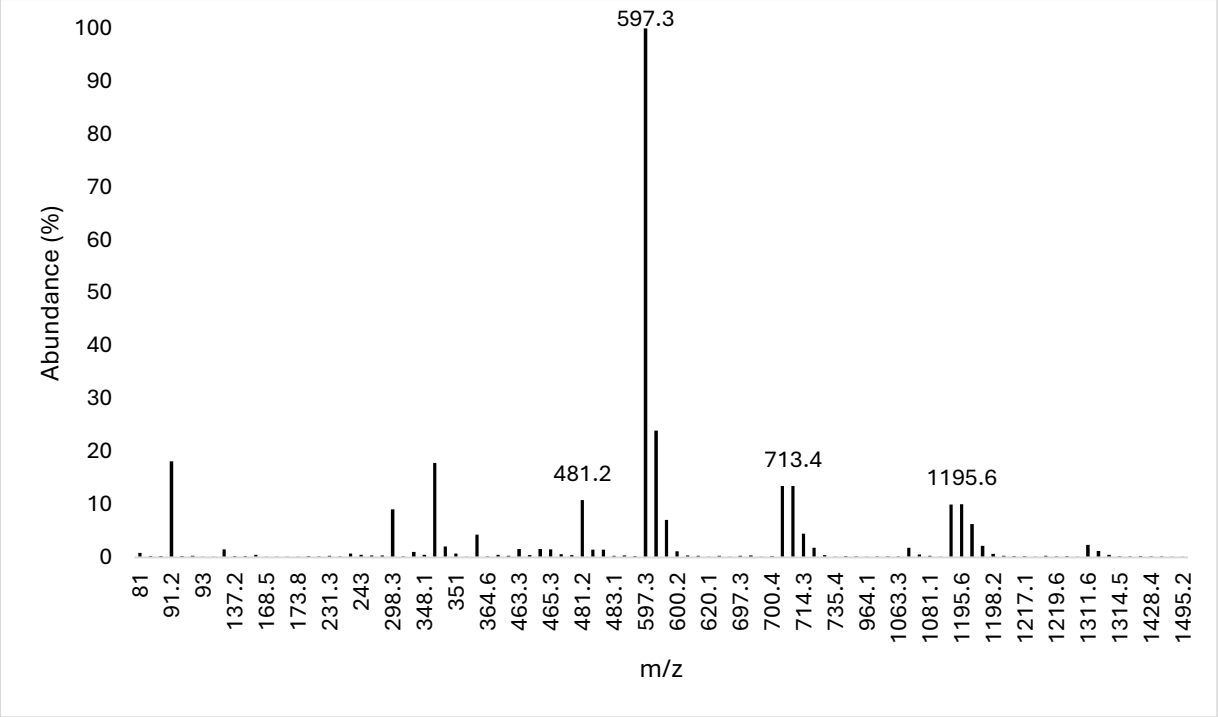

Figure S45. MS spectrum extracted from DA-MA reaction product chromatogram at retention time 13.2 min. The labeled m/z signals represent 4MA, 5MA and 6MA.

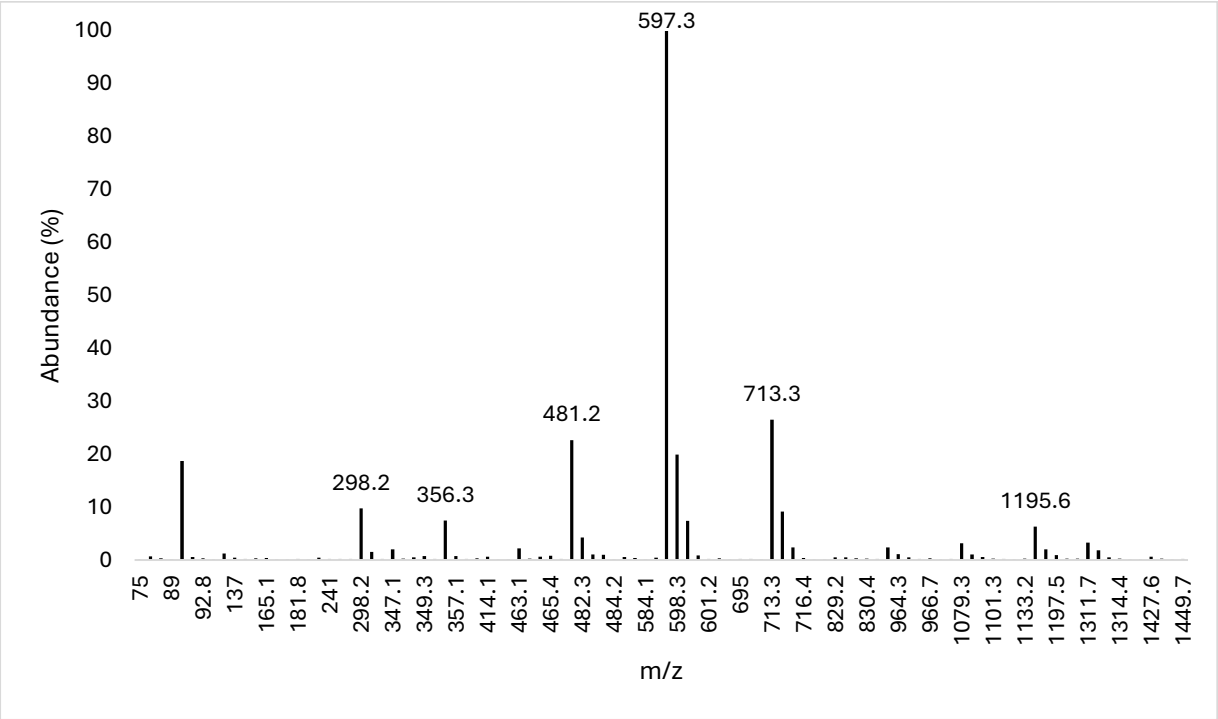

Figure S46. MS spectrum extracted from DA-MA reaction product chromatogram at retention time 13.4 min. The labeled m/z signals represent 4MA, 5MA and 6MA.

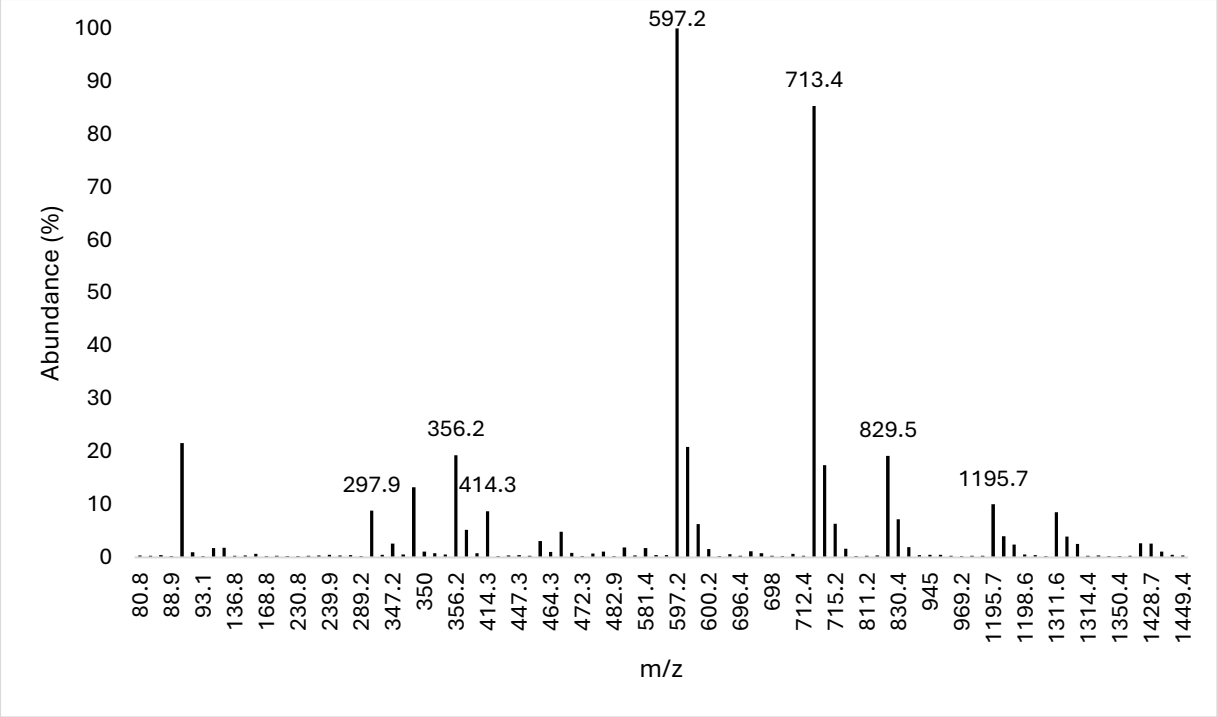

Figure S47. MS spectrum extracted from DA-MA reaction product chromatogram at retention 13.6 min. The labeled m/z signals represent 5MA, 6MA and 7MA.

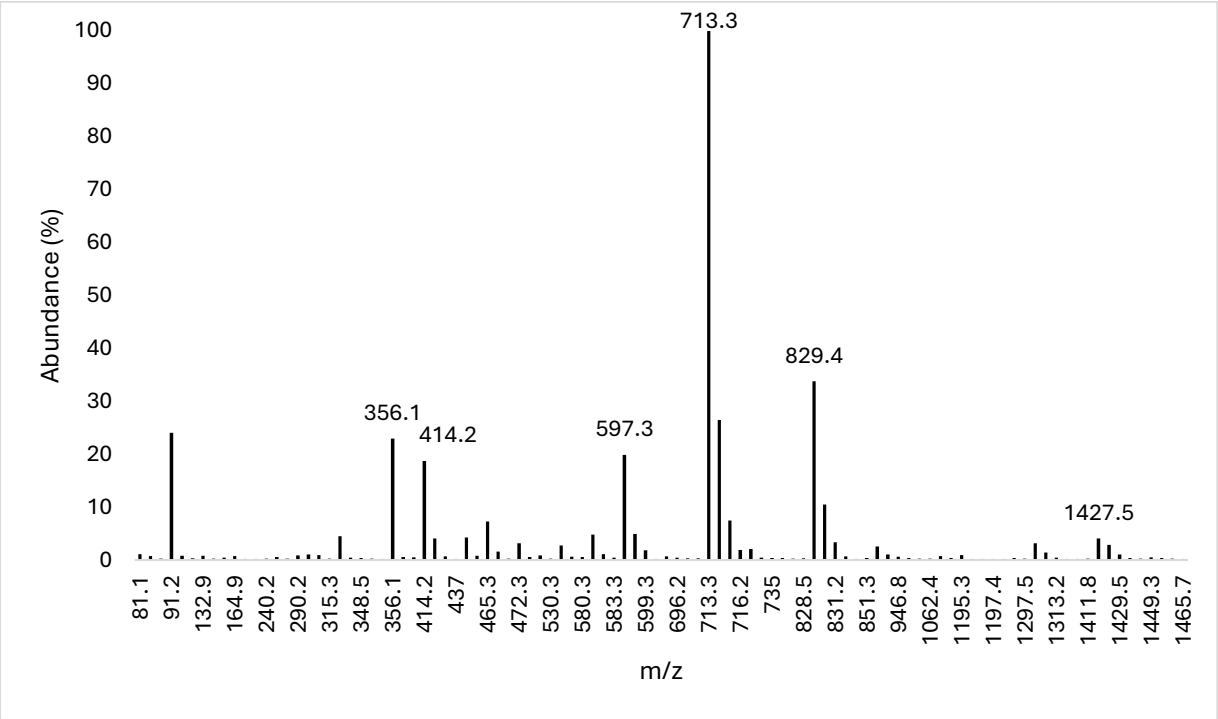

Figure S48. MS spectrum extracted from DA-MA reaction product chromatogram at retention time 13.8 min. The labeled m/z signals represent 5MA, 6MA and 7MA.

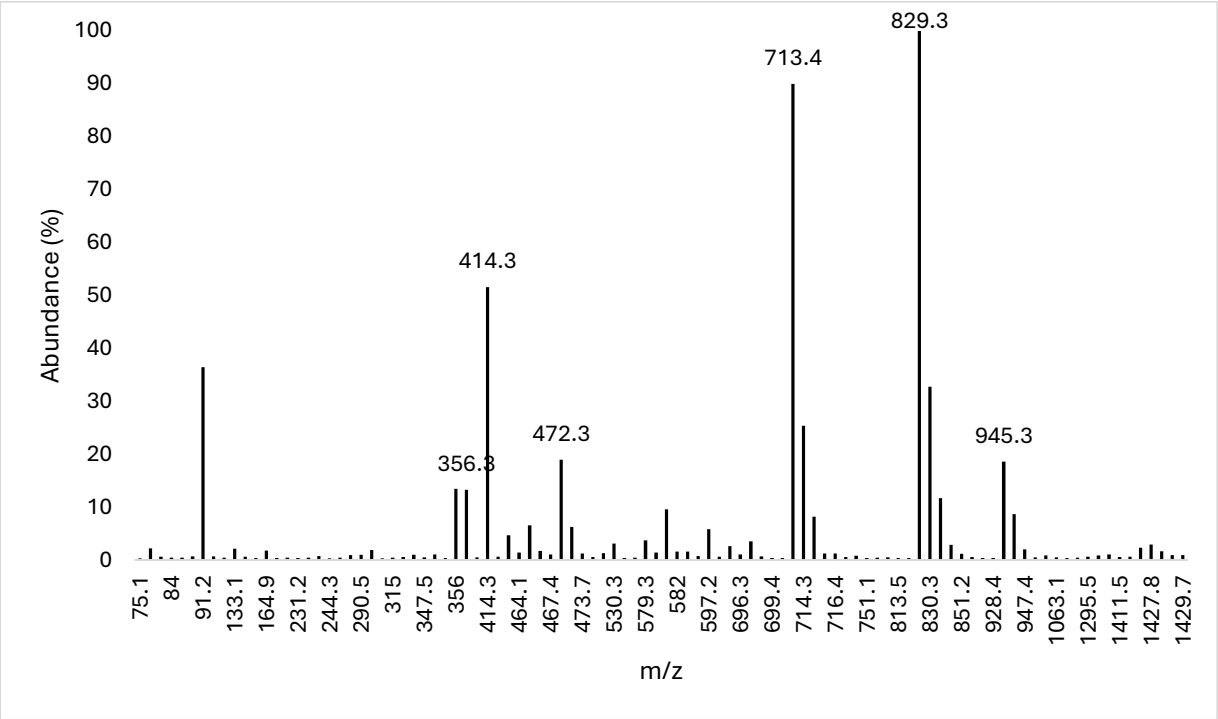

Figure S49. MS spectrum extracted from DA-MA reaction product chromatogram at retention time 14.0 min. The labeled m/z signals represent 6MA, 7MA and 8MA.

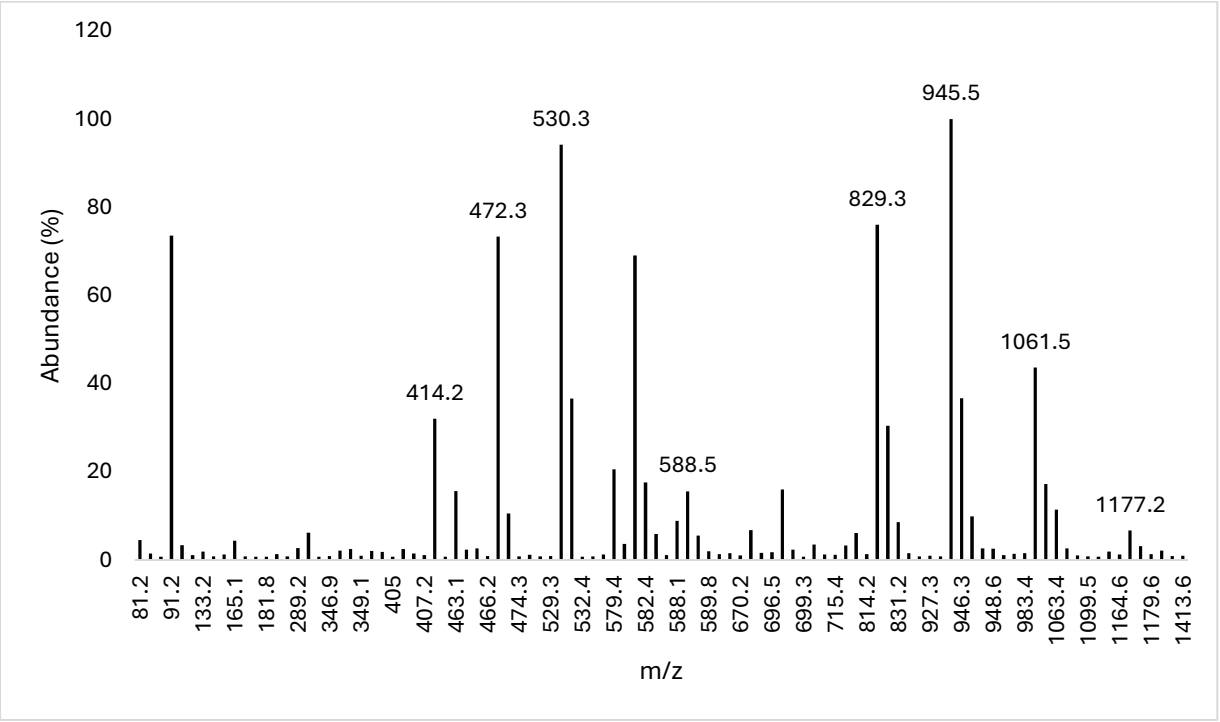

Figure S50. MS spectrum extracted from DA-MA reaction product chromatogram at retention time 14.4 min. The labeled m/z signals represent 7MA, 8MA, 9MA and 10MA.

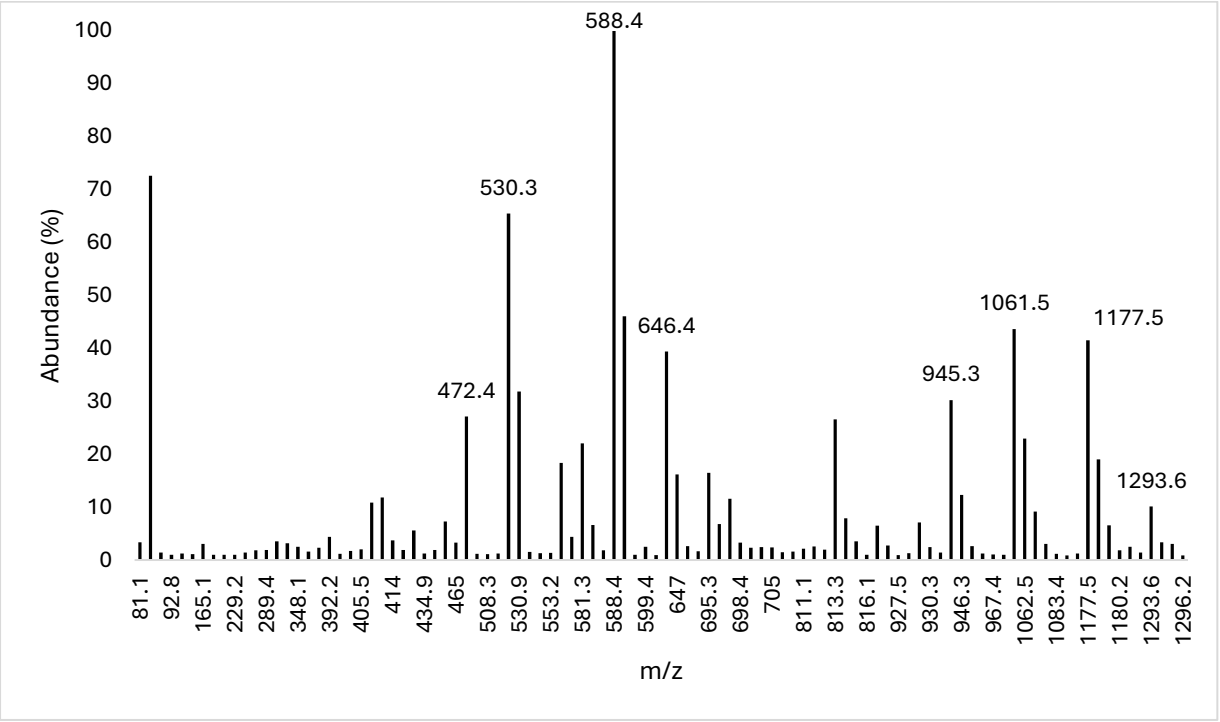

Figure S51. MS spectrum extracted from DA-MA reaction product chromatogram at retention time 14.7 min. The labeled m/z signals represent 8MA, 9MA, 10MA and 11MA.

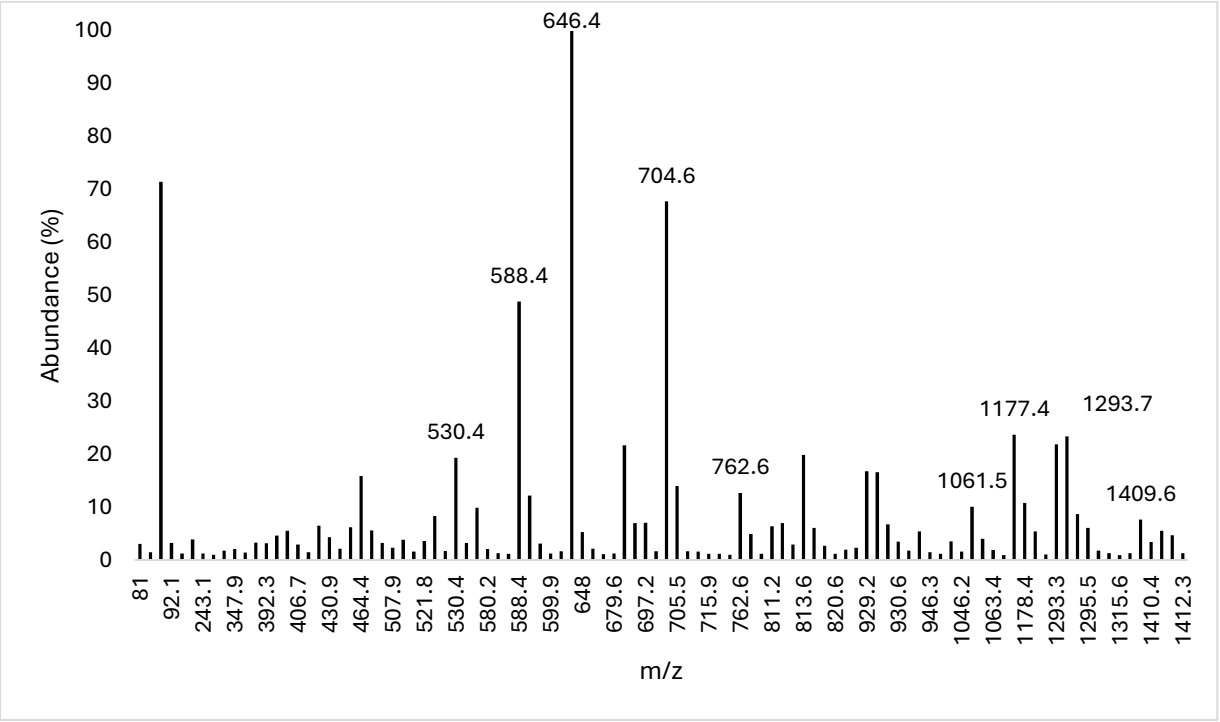

Figure S52. MS spectrum extracted from DA-MA reaction product chromatogram at retention time 14.9 min. The labeled m/z signals represent 7MA, 8MA, 9MA and 10MA.

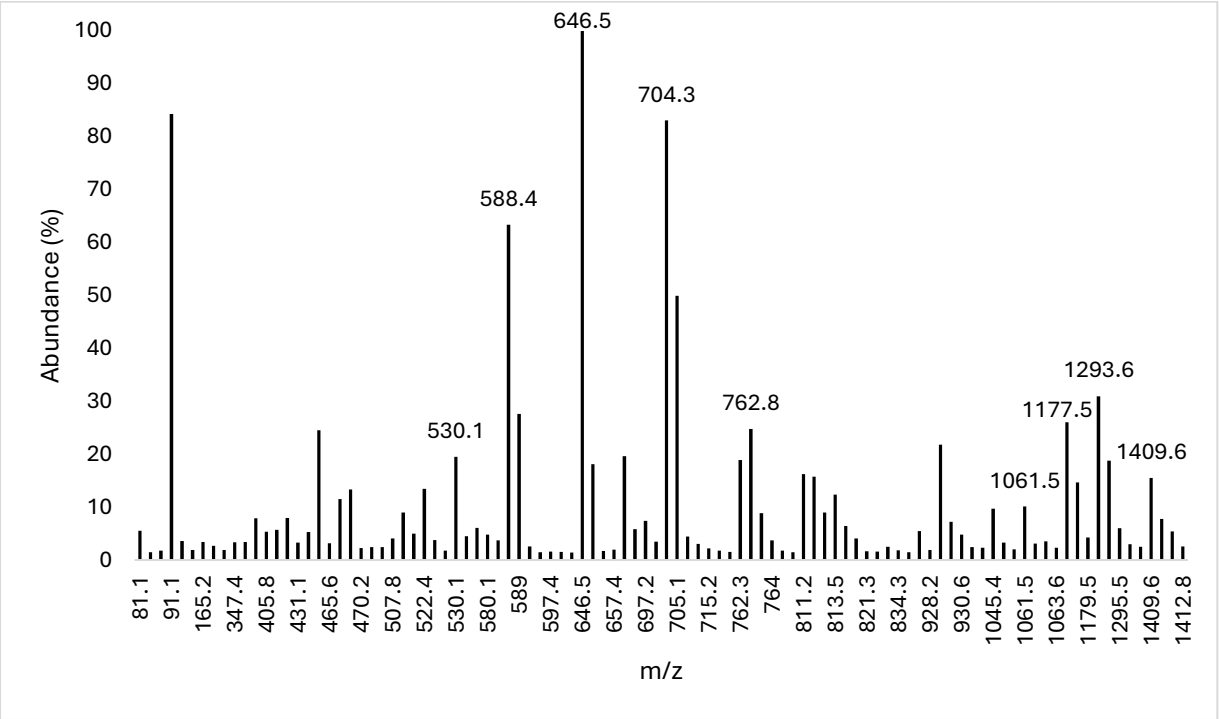

Figure S53. MS spectrum extracted from DA-MA reaction product chromatogram at retention time 15.0 min. The labeled m/z signals represent 9MA, 10MA, 11MA, 12MA and 13MA.

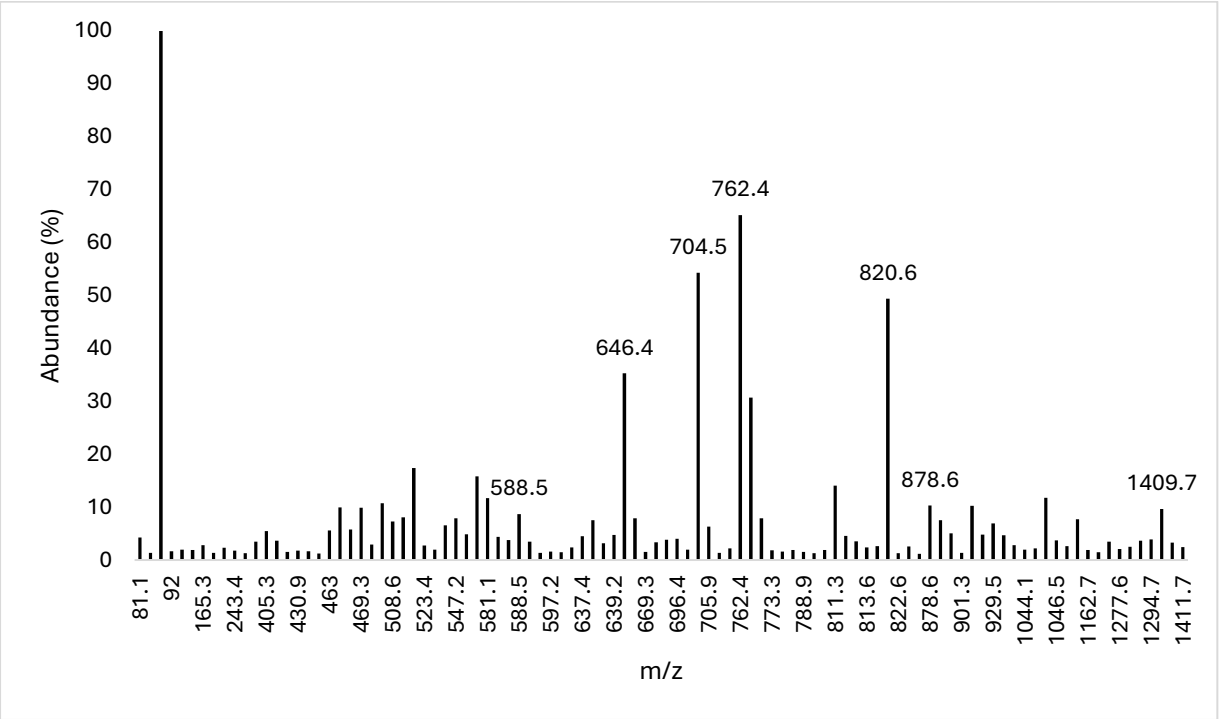

Figure S54. MS spectrum extracted from DA-MA reaction product chromatogram at retention time 15.3 min. The labeled m/z signals represent 10MA, 11MA, 12MA, 13MA, 14MA and 15MA.

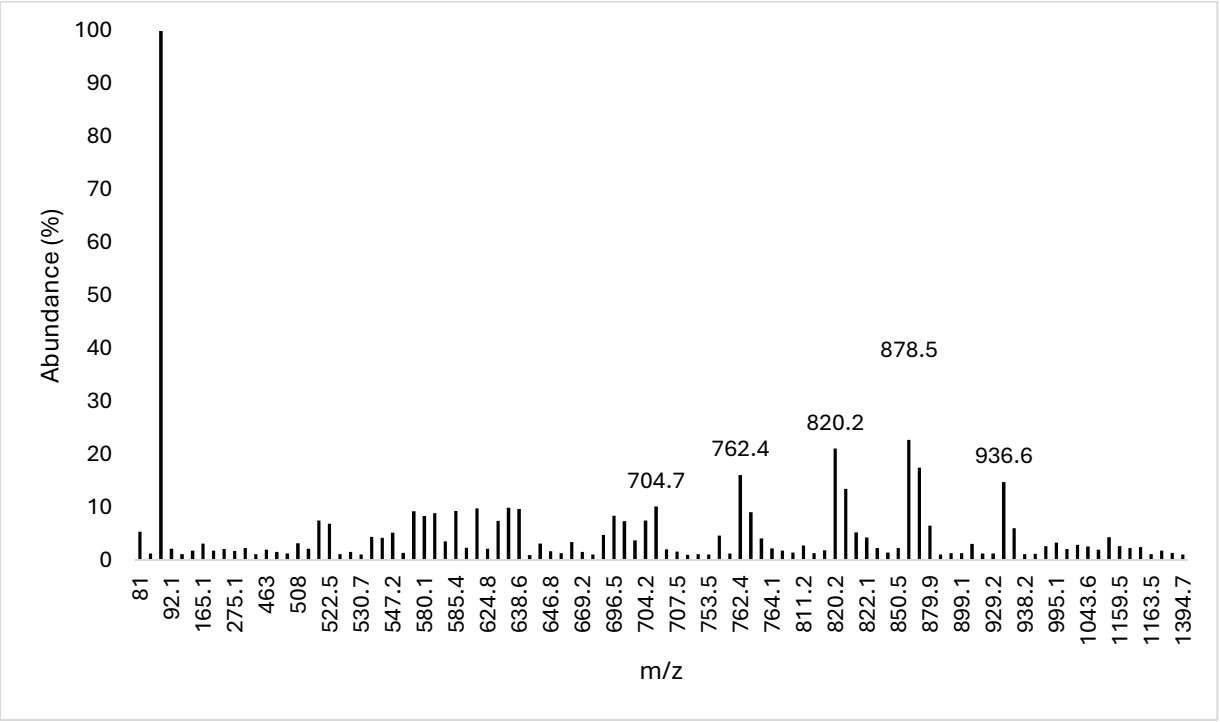

Figure S55. MS spectrum extracted from DA-MA reaction product chromatogram at retention time 15.6 min. The labeled m/z signals represent 12MA, 13MA, 14MA, 15MA and 16MA.

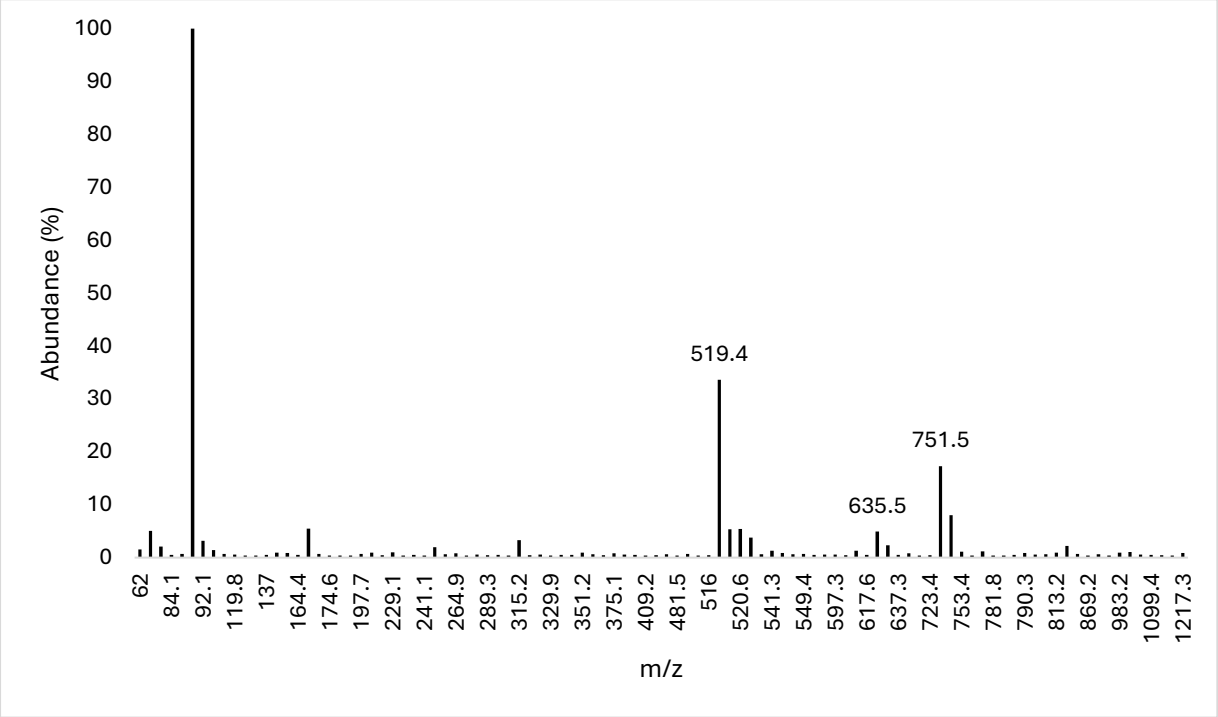

Figure S56. MS spectrum extracted from DA-MA reaction product chromatogram at retention time 23.6 min. The labeled m/z signals represent 3MA1DA, 4MA1DA and 5MA1DA.

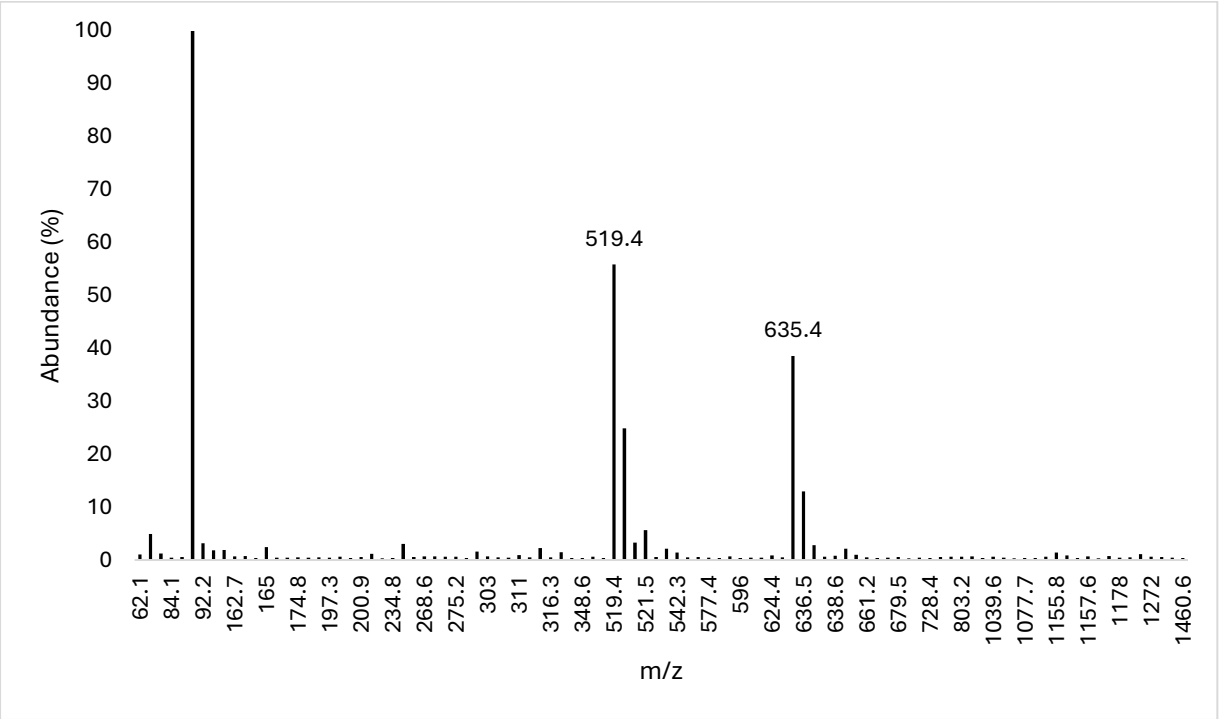

Figure S57. MS spectrum extracted from DA-MA reaction product chromatogram at retention time 23.9 min. The labeled m/z signals represent 3MA1DA, and 4MA1DA.

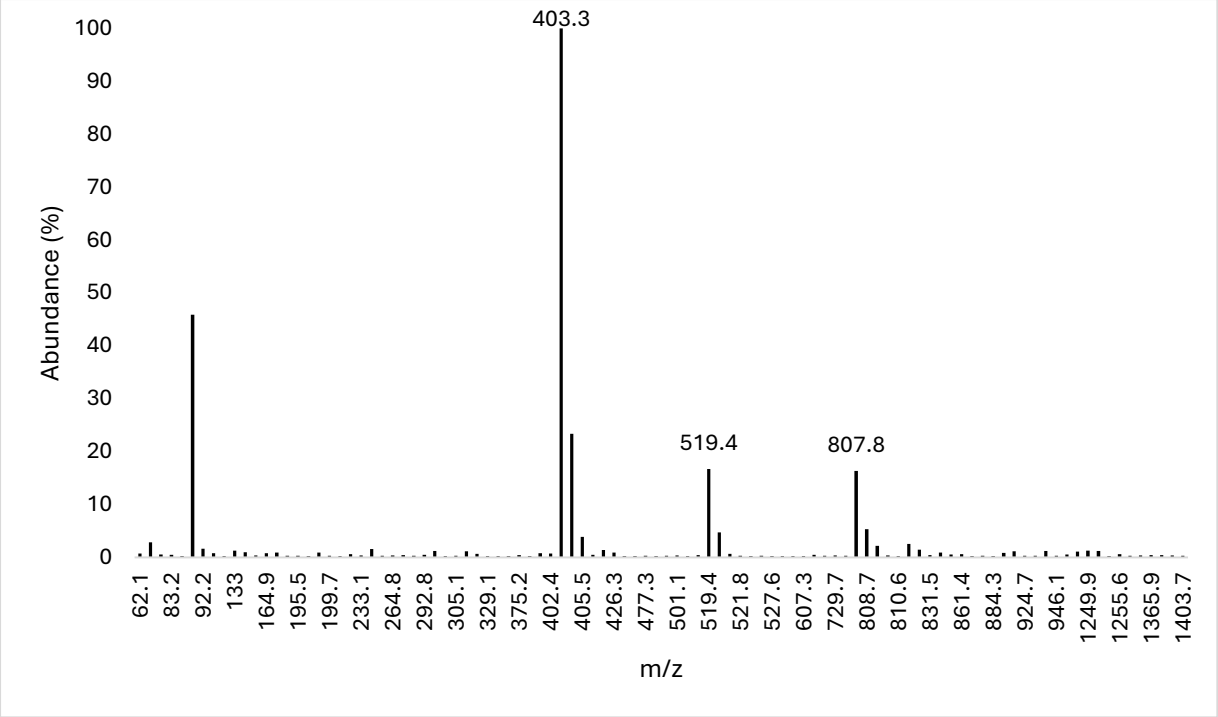

Figure S58. MS spectrum extracted from DA-MA reaction product chromatogram at retention time 24.3 min. The labeled m/z signals represent 2MA1DA, and 3MA1DA.

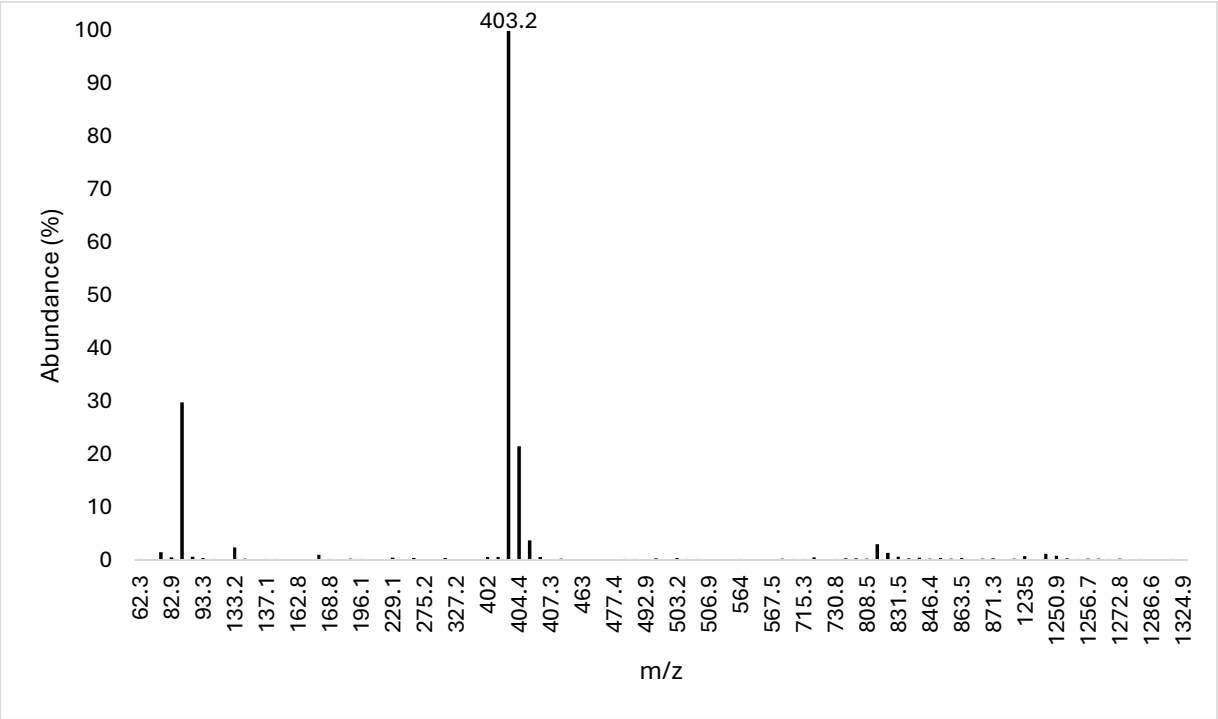

Figure S59. MS spectrum extracted from DA-MA reaction product chromatogram at retention time 24.8 min. The labeled m/z signal represents 2MA1DA.

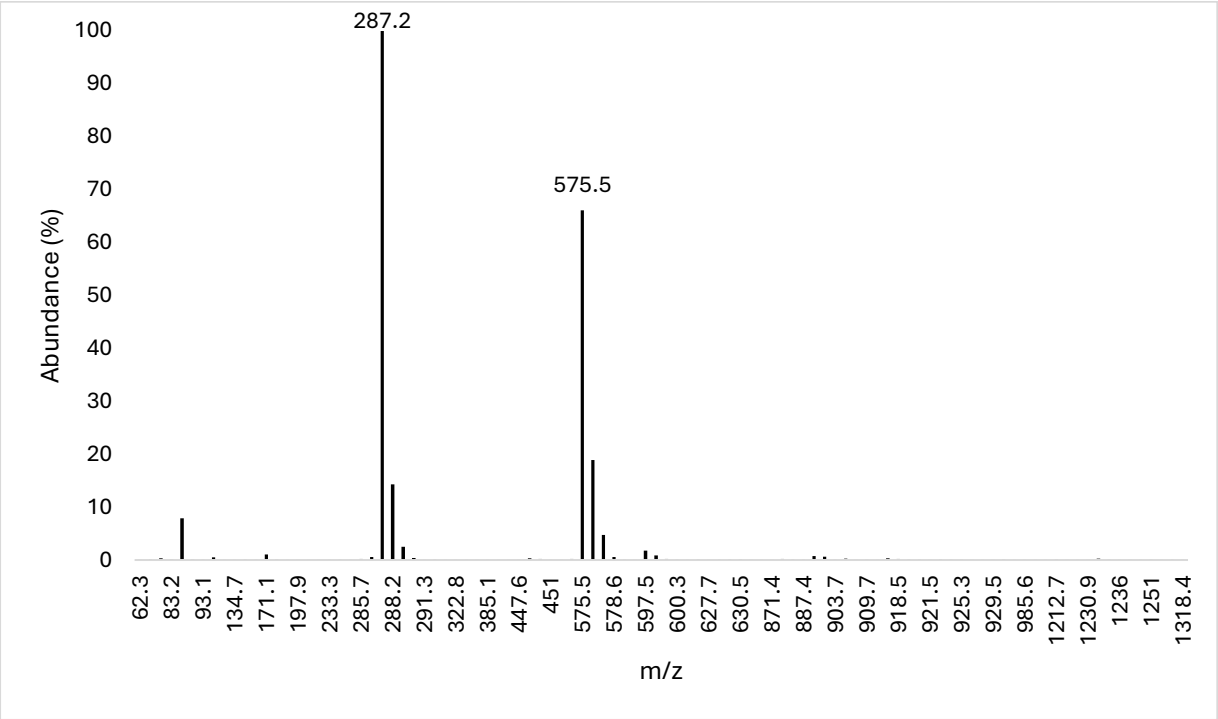

Figure S60. MS spectrum extracted from DA-MA reaction product chromatogram at retention 25.5 min. The labeled m/z signals represent 1MA1DA.

Table S3. Identification of DA-PLA reaction products. The detected products based on retention time and their corresponding m/z and ionization pattern as determined by LC-MS.

Retention time (min)	Compound	M (g/mol)	Corresponding m/z (-TIC)	Ionization pattern
23.1	2PLA	314.3	313.1, 627.5	$[M-H]^-$, $[2M-H]^-$
26.6	3PLA	462.5	461.3, 923.5	$[M-H]^-$, $[2M-H]^-$
29.0	4PLA	610.6	609.4, 1219.7	$[M-H]^-$, $[2M-H]^-$
30.0	5PLA	758.8	757.6	$[M-H]^-$
30.4	6PLA	906.9	905.5	$[M-H]^-$
	1PLA1DA	320.4	319.3, 639.7	$[M-H]^-$, $[2M-H]^-$
30.7	7PLA	1055.1	1053.7	$[M-H]^-$
	1PLA1DA	320.4	319.4, 639.7	$[M-H]^-$, $[2M-H]^-$
31.4	2PLA1DA	468.6	467.6, 936.6	$[M-H]^-$, $[2M-H]^-$
32.2	3PLA1DA	616.7	615.6, 1232.8	$[M-H]^-$, $[2M-H]^-$
33.0	4PLA1DA	764.9	763.6	$[M-H]^-$
33.8	5PLA1DA	913.0	911.7	$[M-H]^-$
34.8	6PLA1DA	1061.2	1059.6	$[M-H]^-$

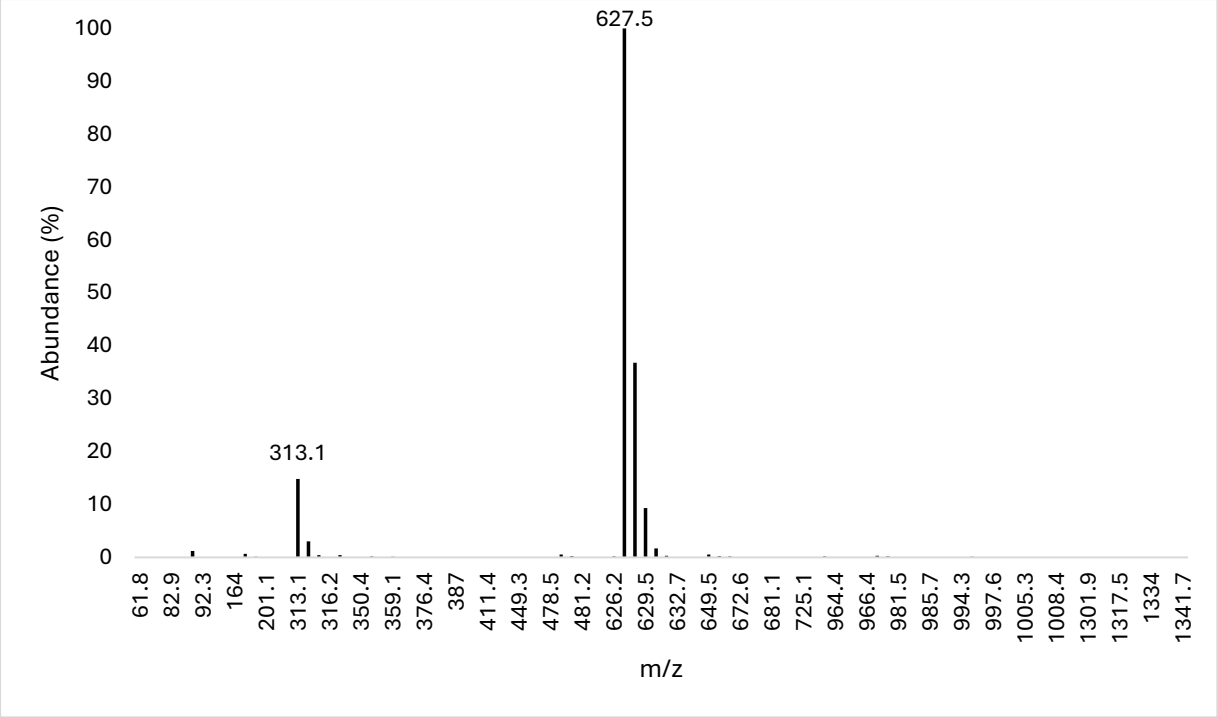

Figure S61. MS spectrum extracted from DA-PLA reaction product chromatogram at retention time 23.1 min. Labeled m/z signals represent 2PLA.

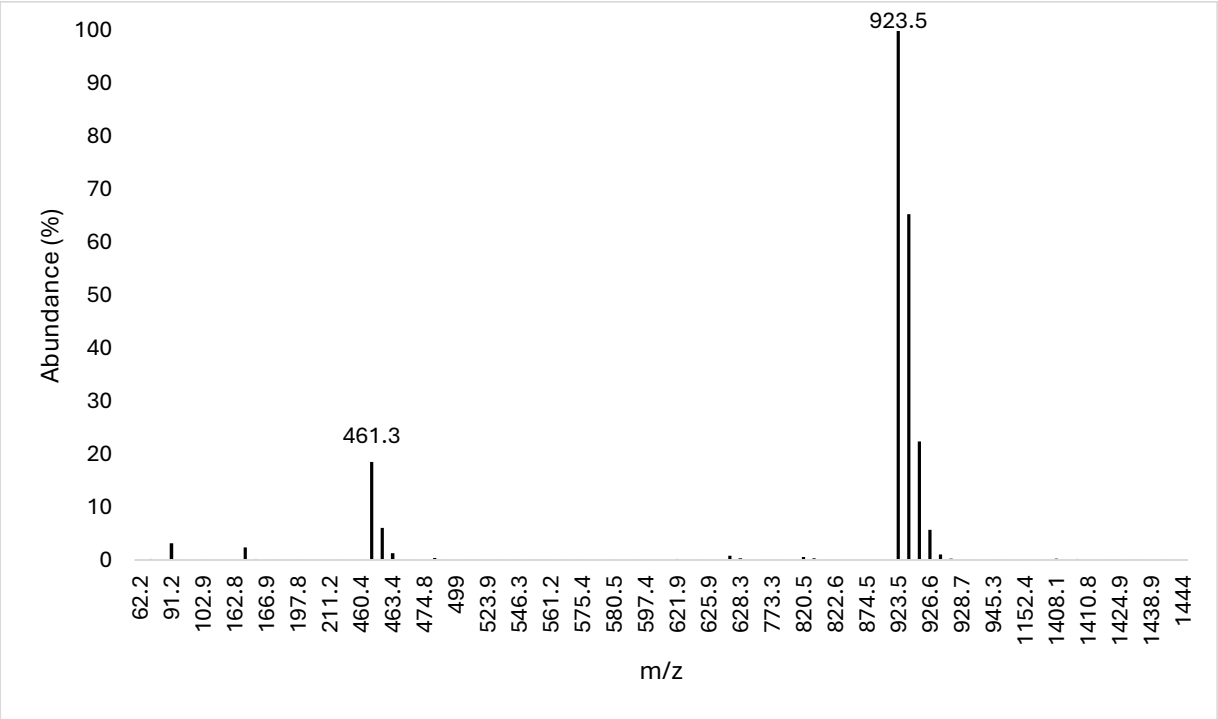

Figure S62. MS spectrum extracted from DA-PLA reaction product chromatogram at retention time 26.6 min. Labeled m/z signals represent 3PLA.

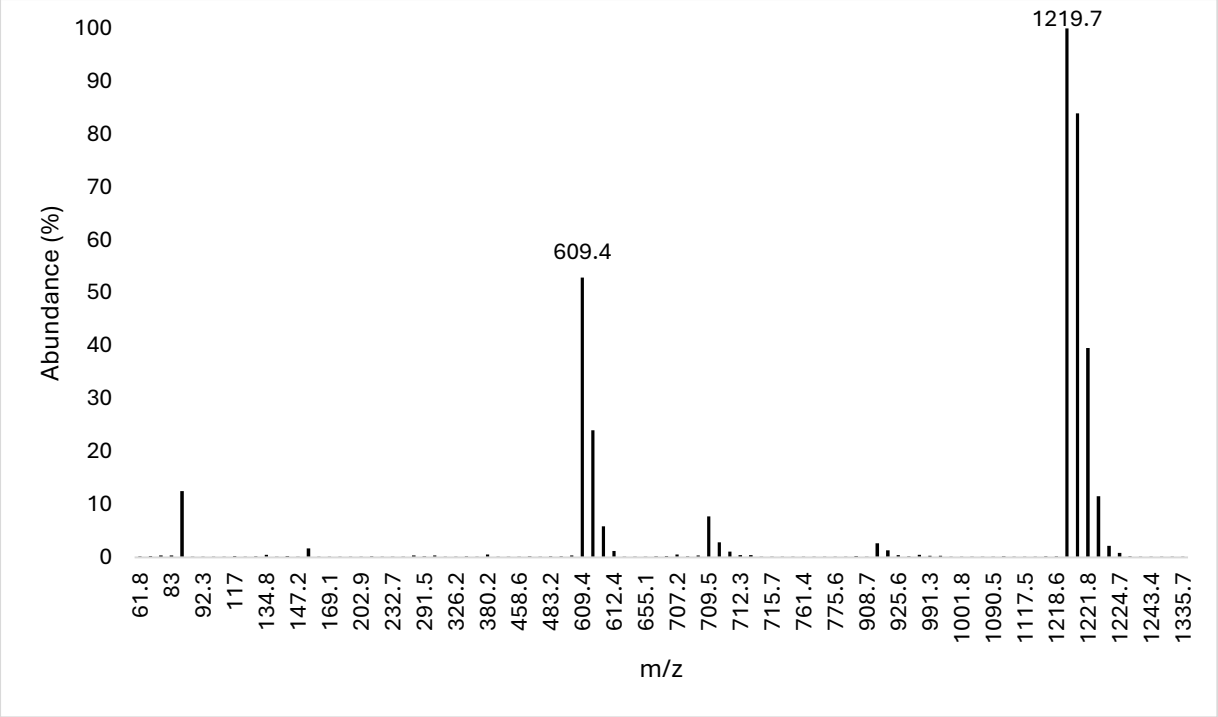

Figure S63. MS spectrum extracted from DA-PLA reaction product chromatogram at retention time 29.0 min. Labeled m/z signals represent 4PLA.

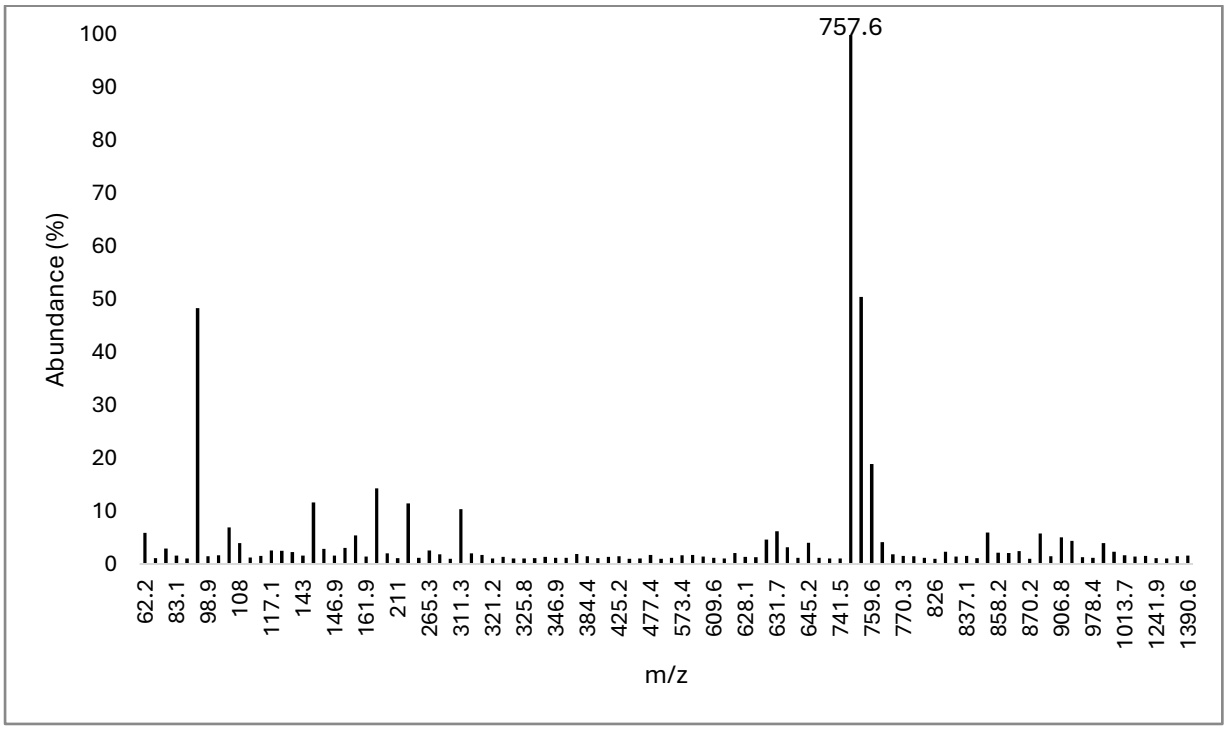

Figure S64. MS spectrum extracted from DA-PLA reaction product chromatogram at retention time 30.0 min. The labeled m/z signal represents 5PLA.

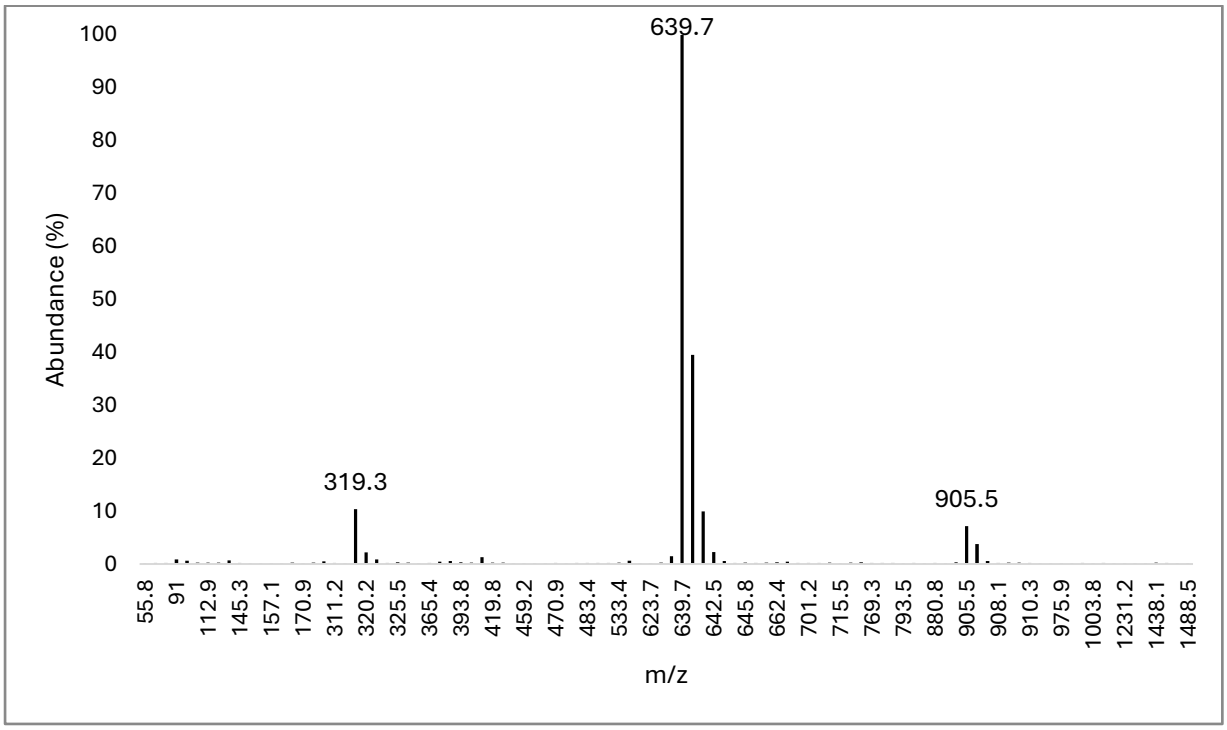

Figure S65. MS spectrum extracted from DA-PLA reaction product chromatogram at retention time 30.4 min. Labeled m/z signals represent 6PLA and 1PLA1DA.

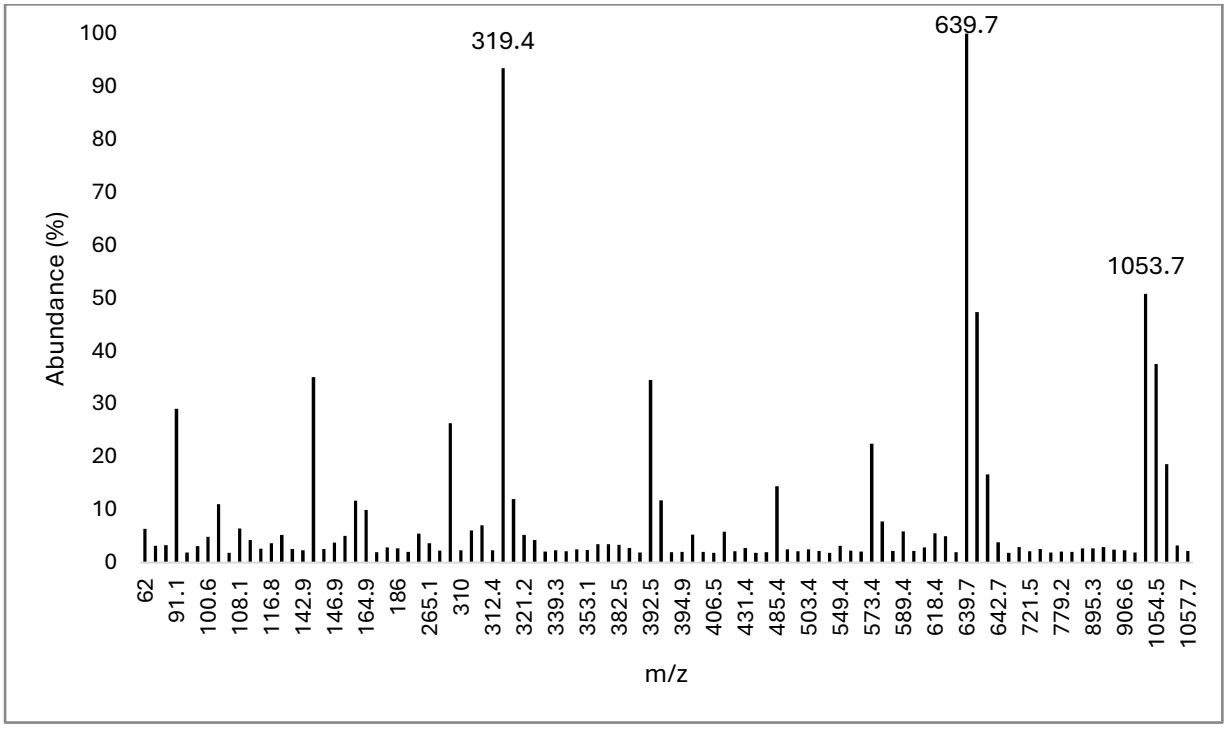

Figure S66. MS spectrum extracted from DA-PLA reaction product chromatogram at retention time 30.7 min. Labeled m/z signals represent 7PLA and 1PLA1DA.

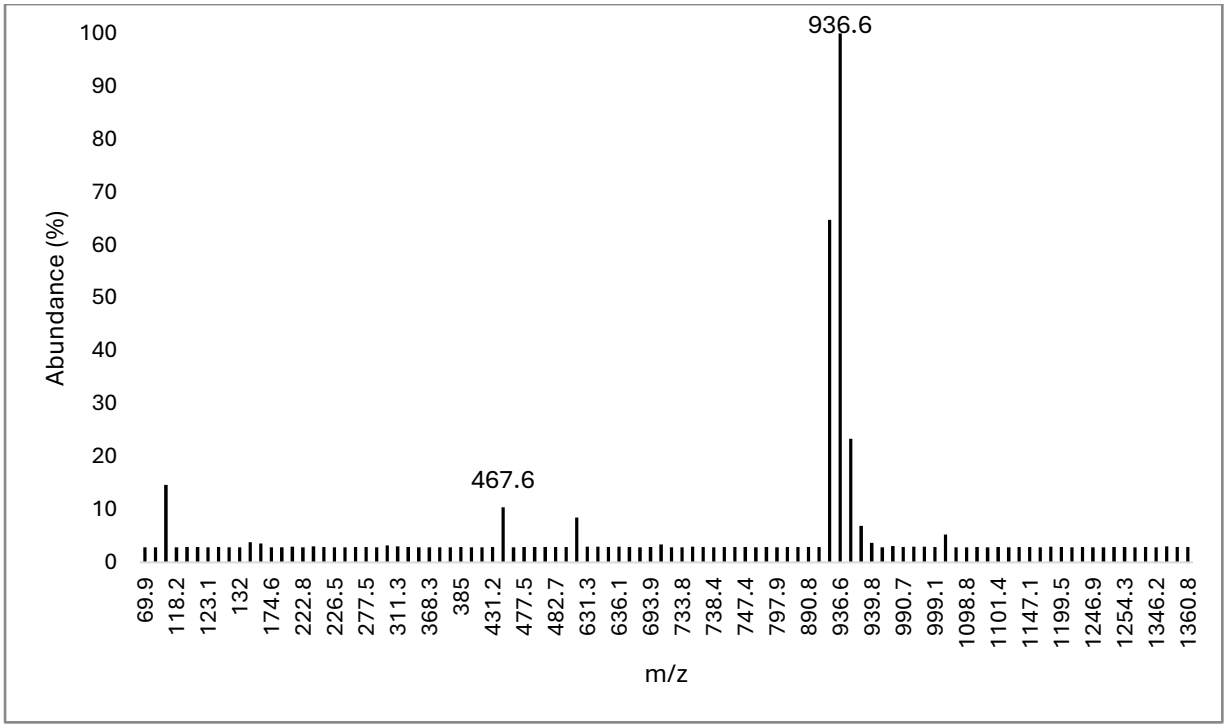

Figure S67. MS spectrum extracted from DA-PLA reaction product chromatogram at retention time 31.4 min. Labeled m/z signals represent 2PLA1DA.

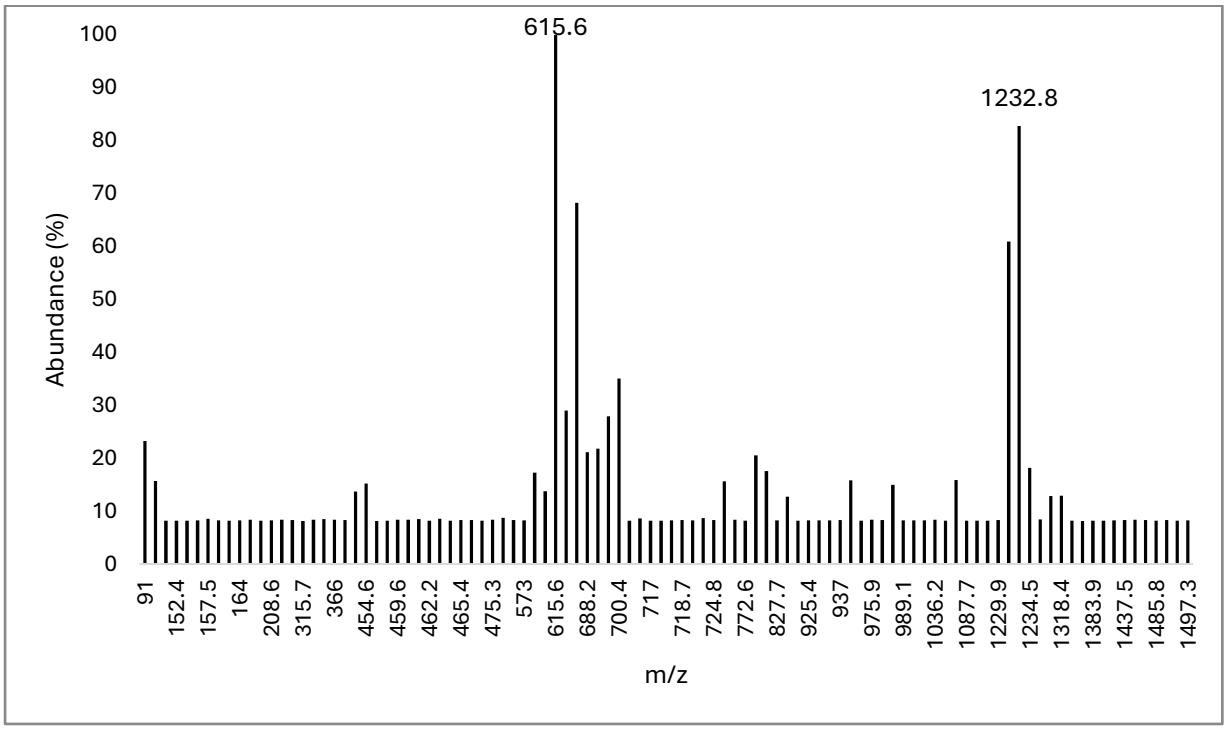

Figure S68. MS spectrum extracted from DA-PLA reaction product chromatogram at retention time 32.2 min. Labeled m/z signals represent 3PLA1DA.

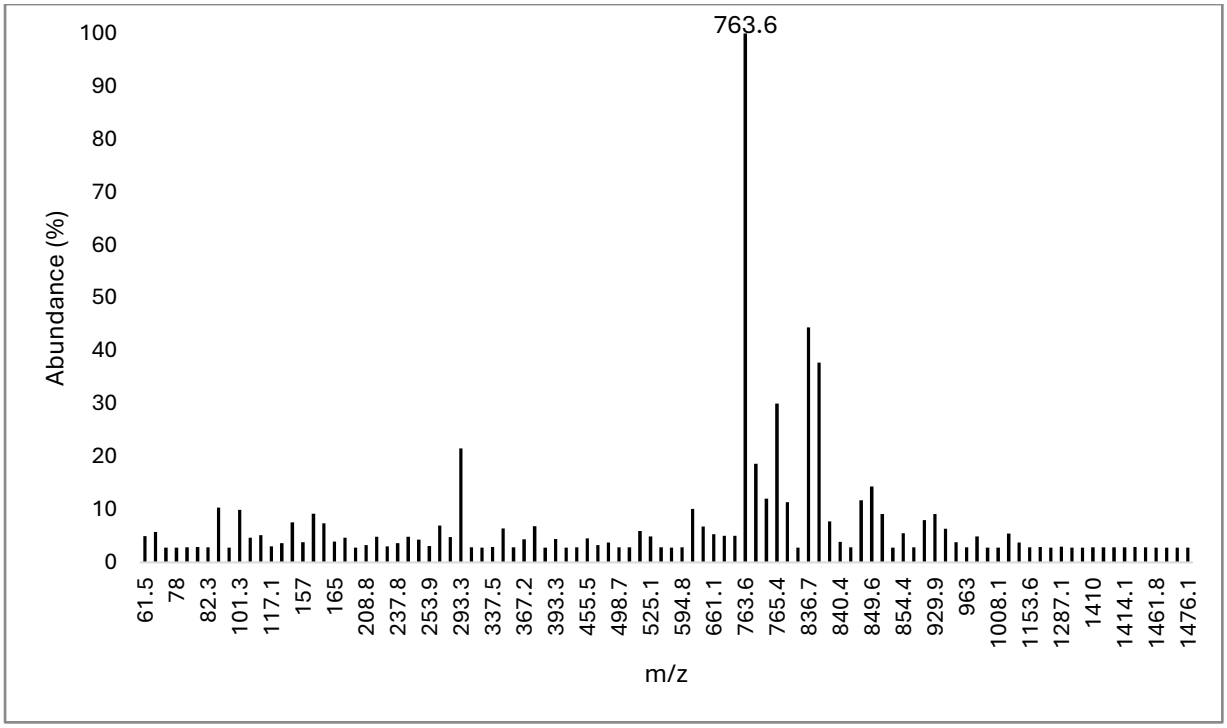

Figure S69. MS spectrum extracted from DA-PLA reaction product chromatogram at retention 33.0 min. The labeled m/z signal represents 4PLA1DA.

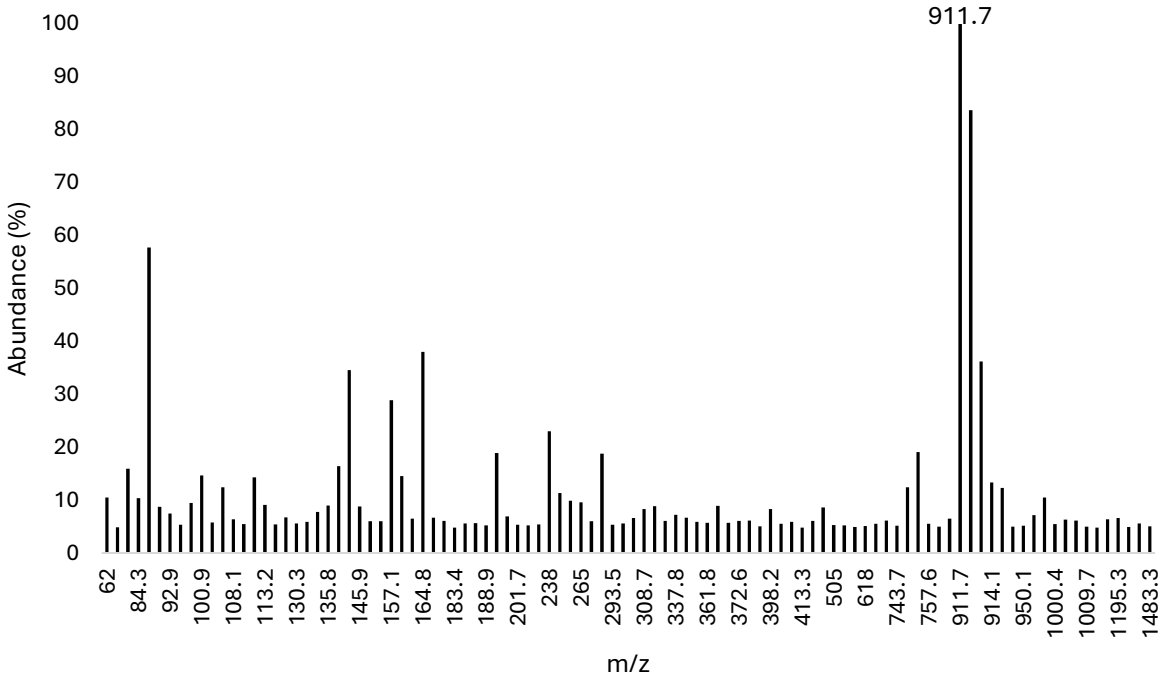

Figure S70. MS spectrum extracted from DA-PLA reaction product chromatogram at retention time 33.8 min. The labeled m/z signal represents 5PLA1DA.

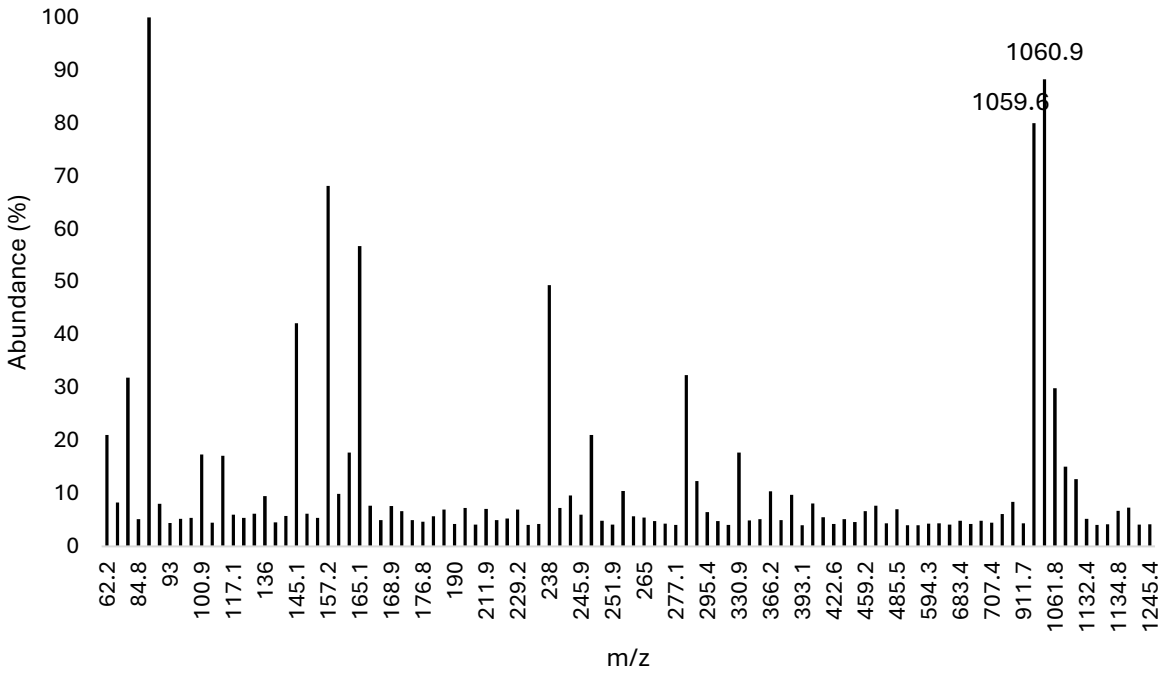

Figure S71. MS spectrum extracted from DA-PLA reaction product chromatogram at retention time 34.8 min. The labeled m/z signal represents 6PLA1DA.

Table S4. Identification of DA-LA reaction products. The detected products based on retention time and their corresponding m/z and ionization pattern as determined by LC-MS.

Retention time (min)	Compound	M (g/mol)	Corresponding m/z (-TIC)	Ionization pattern
12.5	2LA	162.1	161.1, 323.2	$[M-H]^-$, $[2M-H]^-$
13.2	2LA	162.1	161.2, 323.2	$[M-H]^-$, $[2M-H]^-$
15.7	3LA	234.2	233.1, 467.3	$[M-H]^-$, $[2M-H]^-$
17.8	4LA	306.3	305.1, 611.4	$[M-H]^-$, $[2M-H]^-$
19.5	5LA	378.3	377.2, 755.4	$[M-H]^-$, $[2M-H]^-$
19.7	5LA	378.3	377.2, 755.4	$[M-H]^-$, $[2M-H]^-$
21.0	6LA	450.4	449.3, 899.5	$[M-H]^-$, $[2M-H]^-$
21.2	6LA	450.4	449.2, 899.4	$[M-H]^-$, $[2M-H]^-$
22.2	7LA	522.4	521.3, 1043.7	$[M-H]^-$, $[2M-H]^-$
22.4	7LA	522.4	521.4, 1043.6	$[M-H]^-$, $[2M-H]^-$
23.3	8LA	594.5	593.4, 1187.8	$[M-H]^-$, $[2M-H]^-$
23.5	8LA	594.5	593.4, 1187.6	$[M-H]^-$, $[2M-H]^-$
24.4	9LA	666.6	665.5, 1331.8	$[M-H]^-$, $[2M-H]^-$
25.2	10LA	738.6	737.5, 1475.9	$[M-H]^-$, $[2M-H]^-$
25.9	11LA	810.7	809.4	$[M-H]^-$
26.6	12LA	882.7	881.6	$[M-H]^-$
27.2	13LA	954.8	953.6	$[M-H]^-$
29.1	1LA1DA	244.3	243.3, 487.5	$[M-H]^-$, $[2M-H]^-$

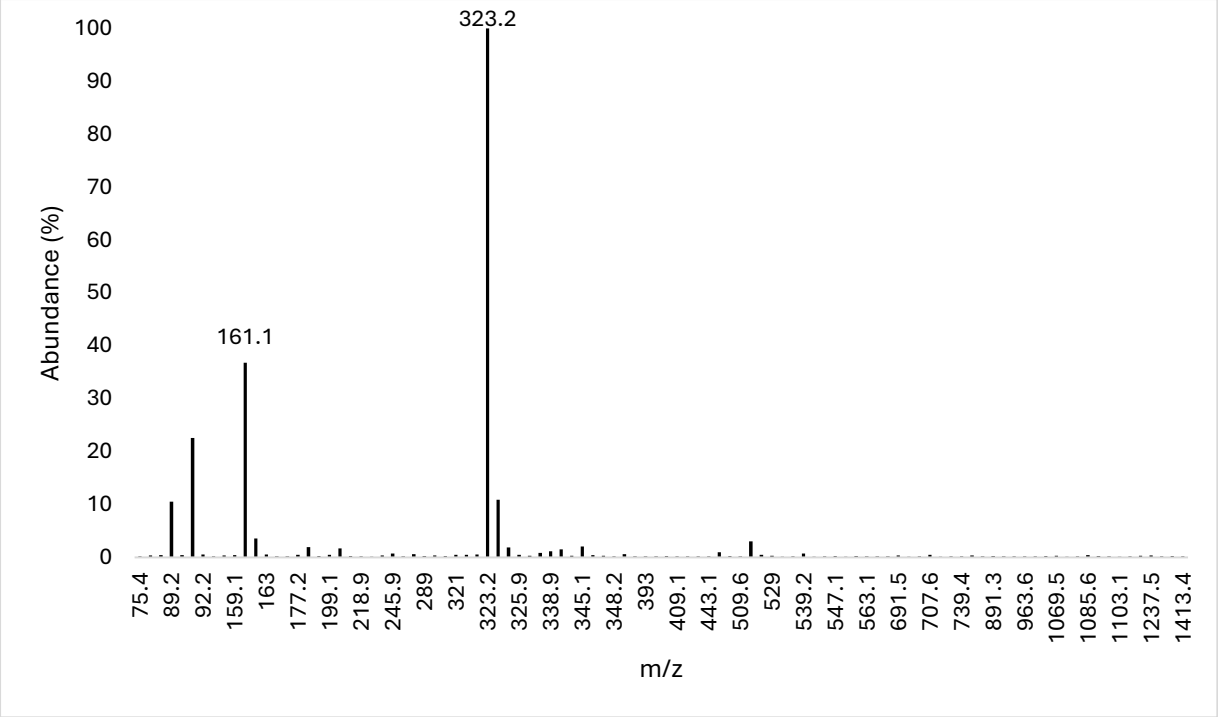

Figure S72. MS spectrum extracted from DA-LA reaction product chromatogram at retention time 12.5 min. Labeled m/z signals represent 2LA.

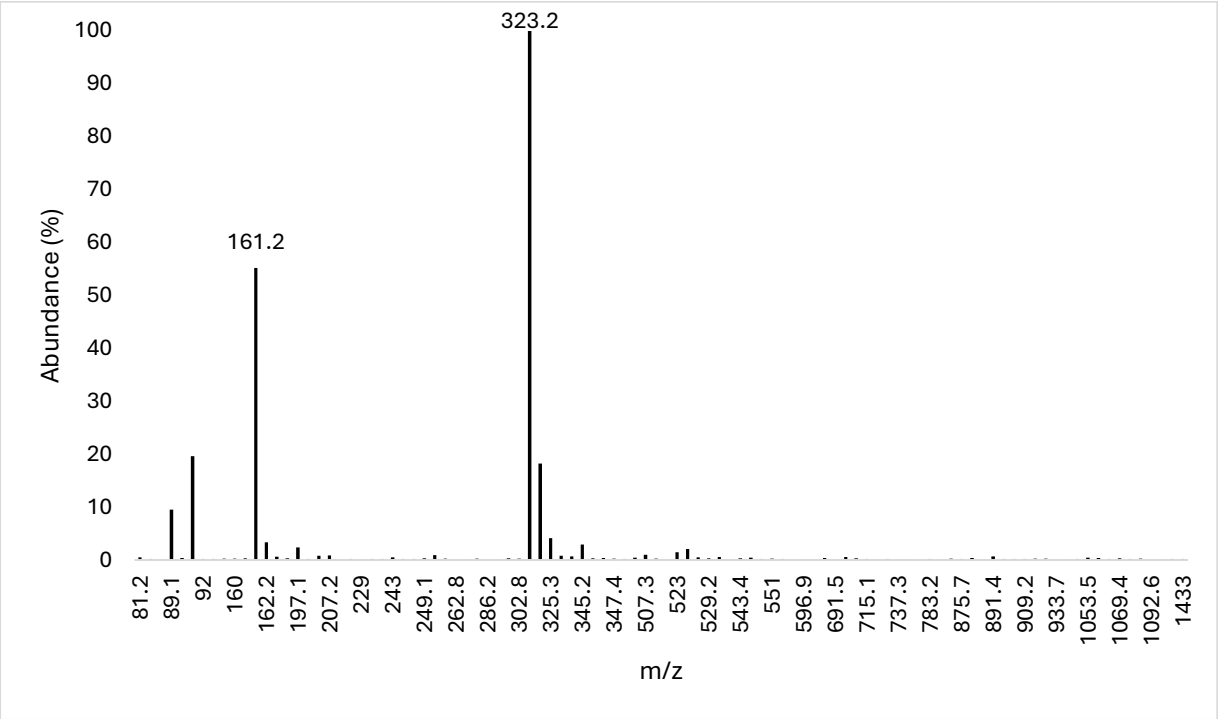

Figure S73. MS spectrum extracted from DA-LA reaction product chromatogram at retention time 13.2 min. Labeled m/z signals represent 2LA.

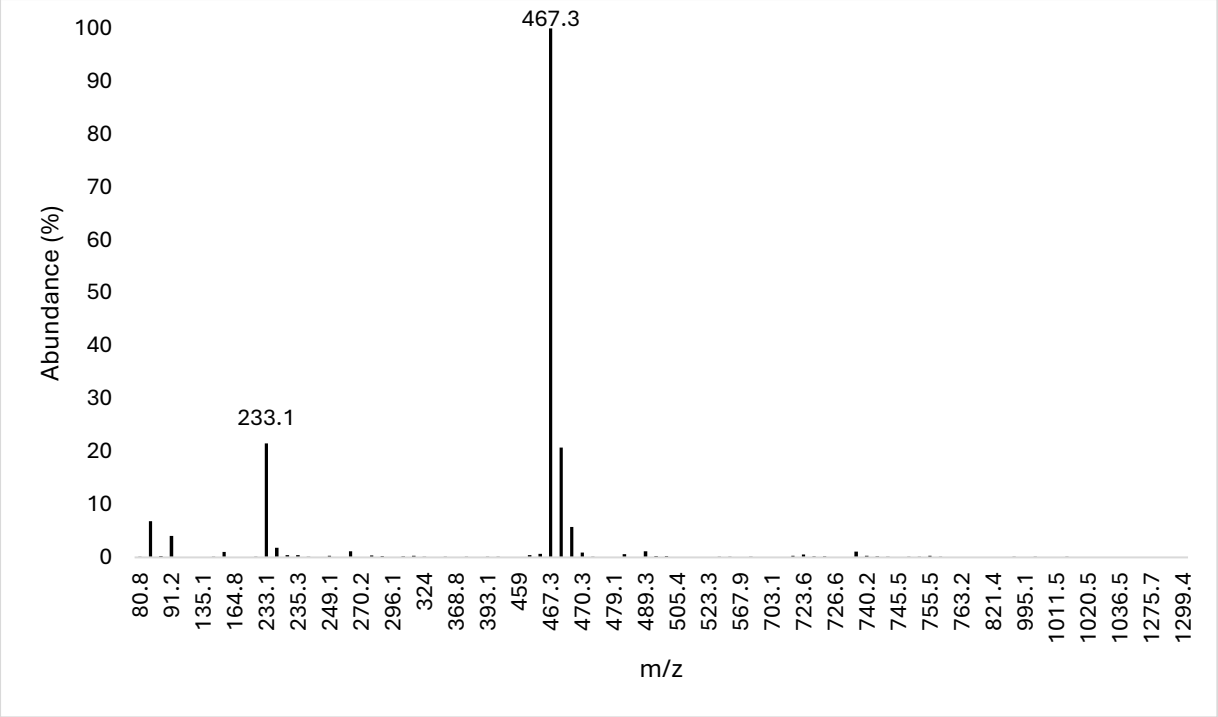

Figure S74. MS spectrum extracted from DA-LA reaction product chromatogram at retention time 15.7 min. Labeled m/z signals represent 3LA.

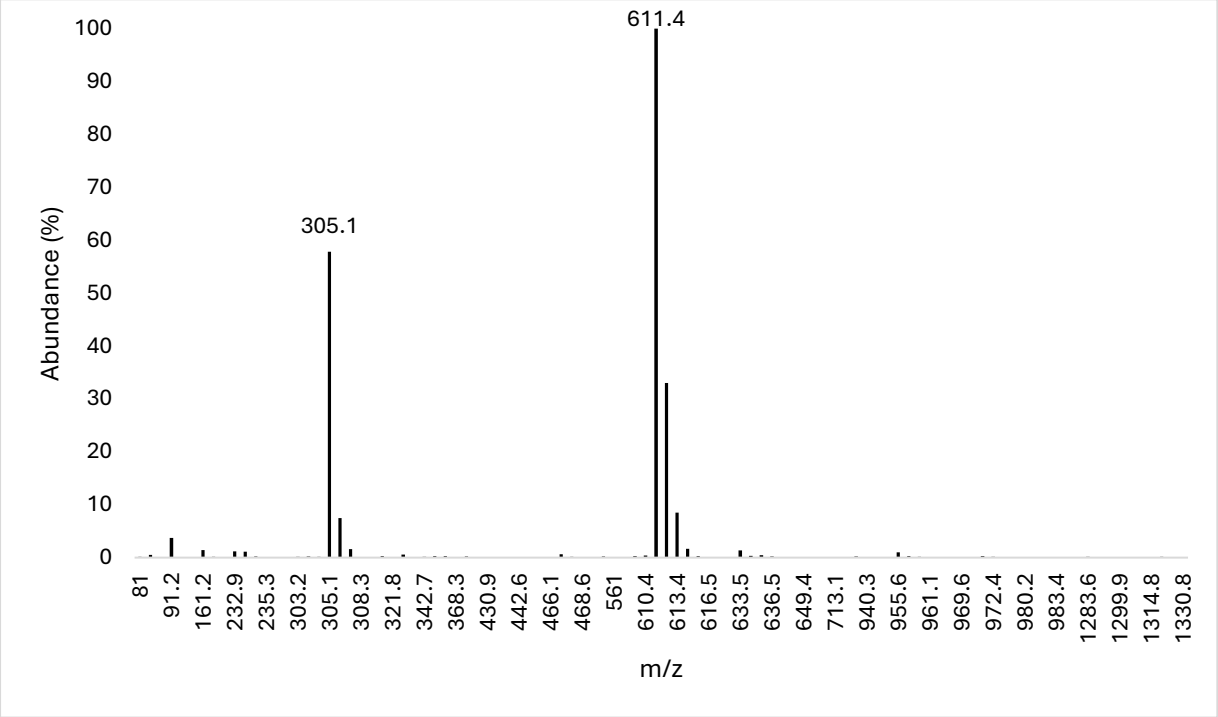

Figure S75. MS spectrum extracted from DA-LA reaction product chromatogram at retention time 17.8 min. Labeled m/z signals represent 4LA.

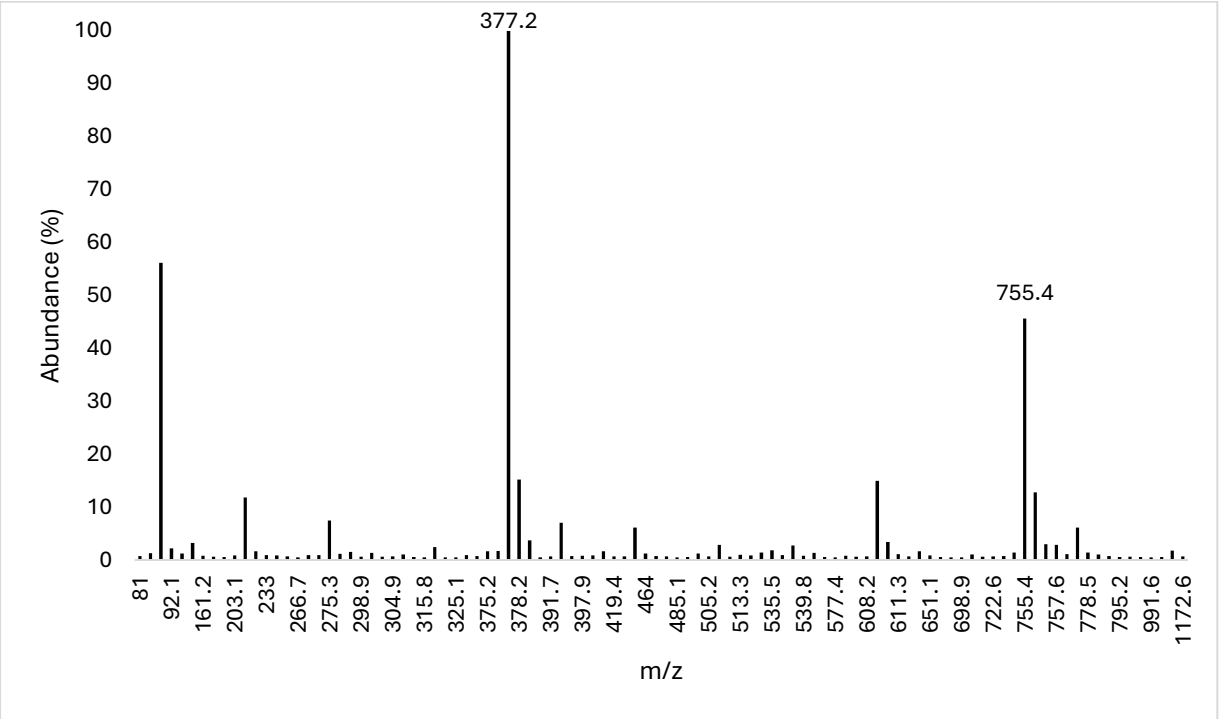

Figure S76. MS spectrum extracted from DA-LA reaction product chromatogram at retention time 19.5 min. Labeled m/z signals represent 5LA.

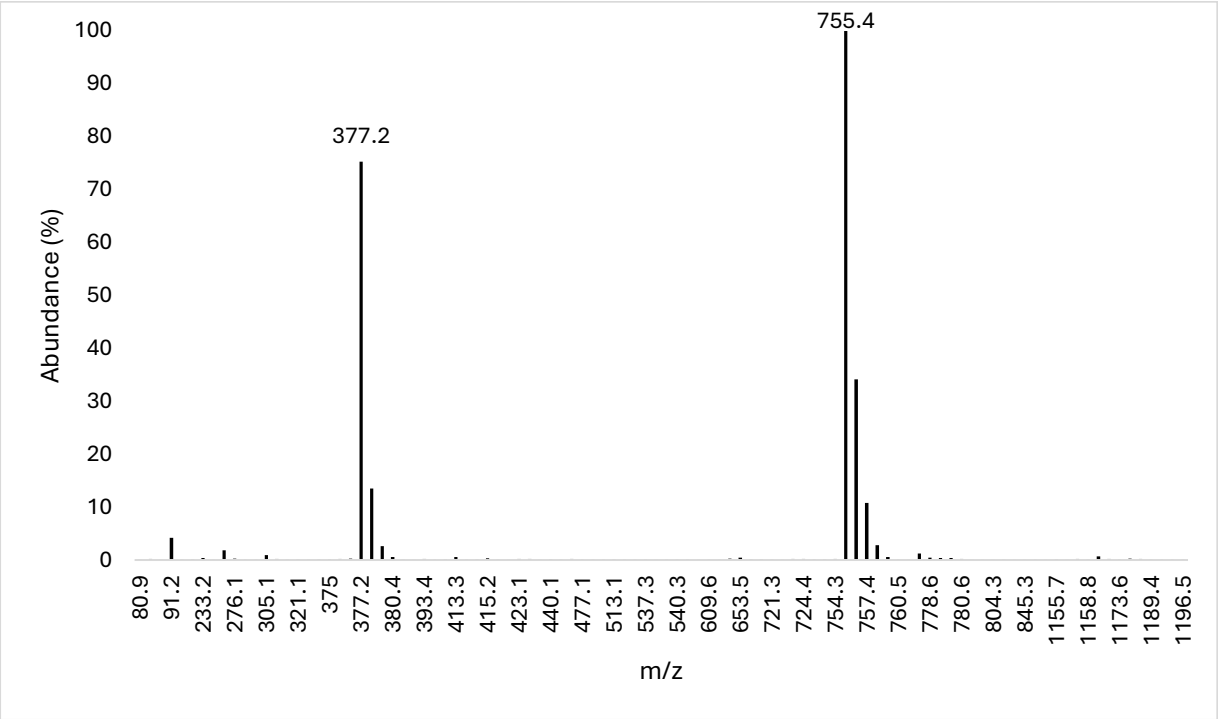

Figure S77. MS spectrum extracted from DA-LA reaction product chromatogram at retention time 19.7 min. Labeled m/z signals represent 5LA.

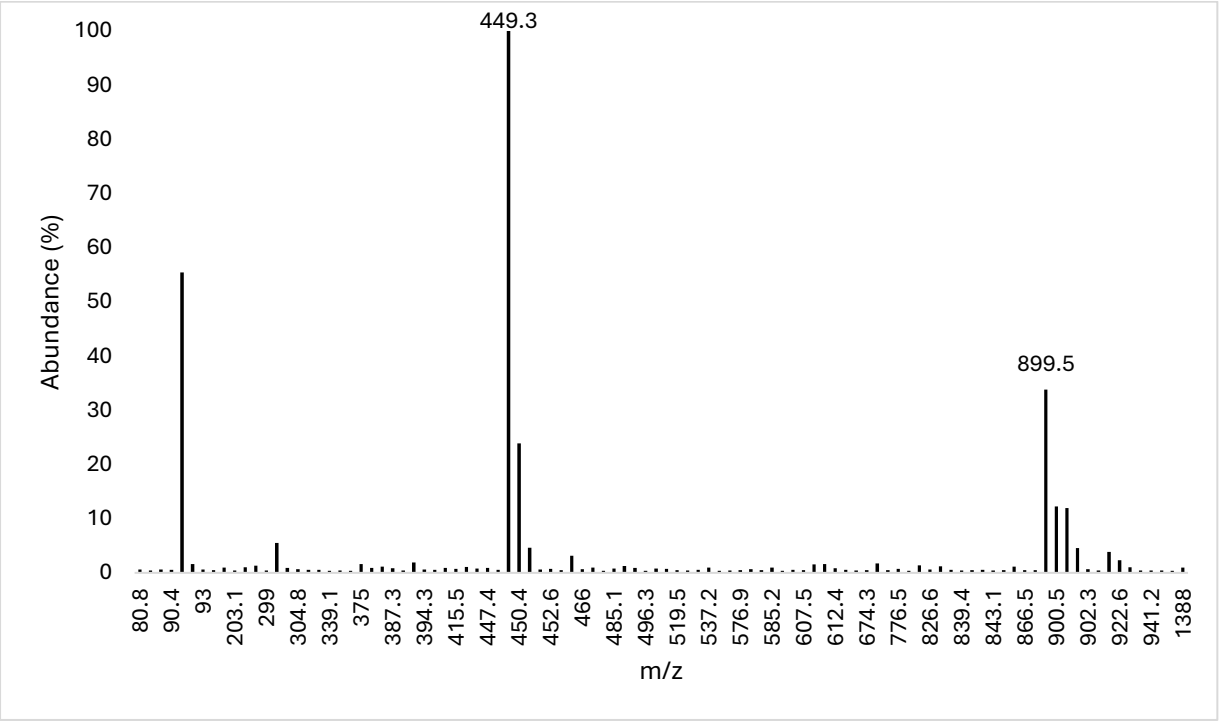

Figure S78. MS spectrum extracted from DA-LA reaction product chromatogram at retention time 21.0 min. Labeled m/z signals represent 6LA.

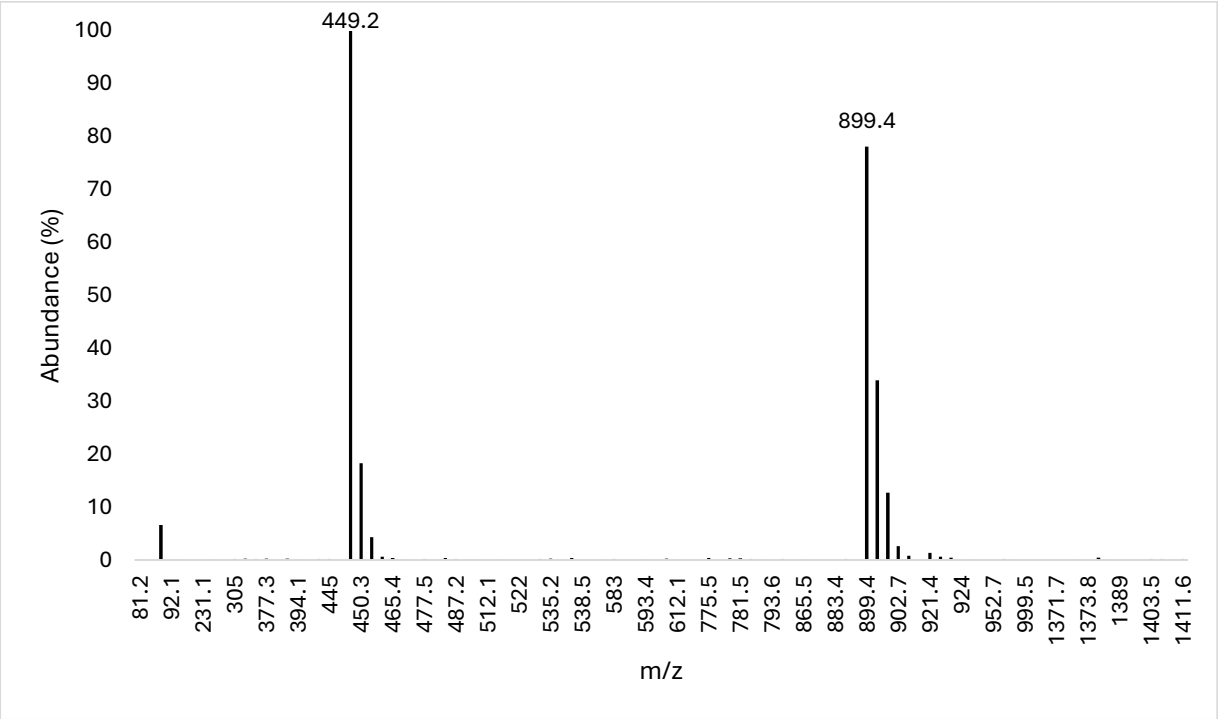

Figure S79. MS spectrum extracted from DA-LA reaction product chromatogram at retention time 21.2 min. Labeled m/z signals represent 6LA.

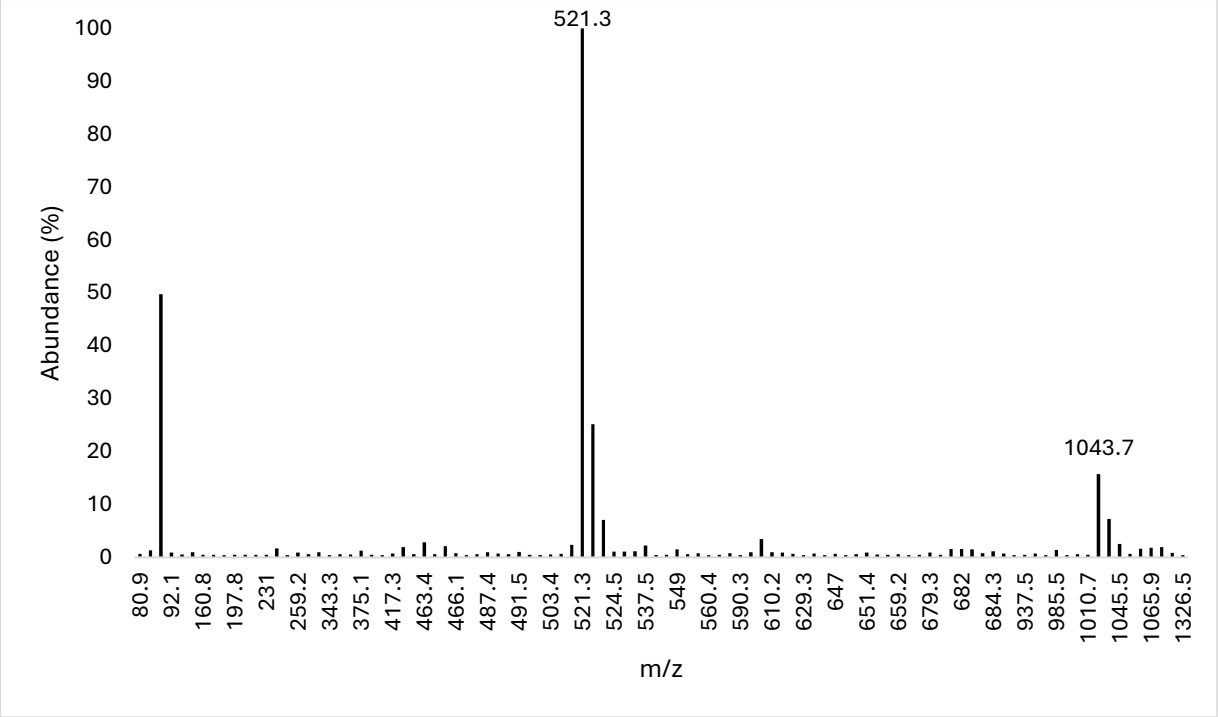

Figure S80. MS spectrum extracted from DA-LA reaction product chromatogram at retention time 22.2 min. Labeled m/z signals represent 7LA.

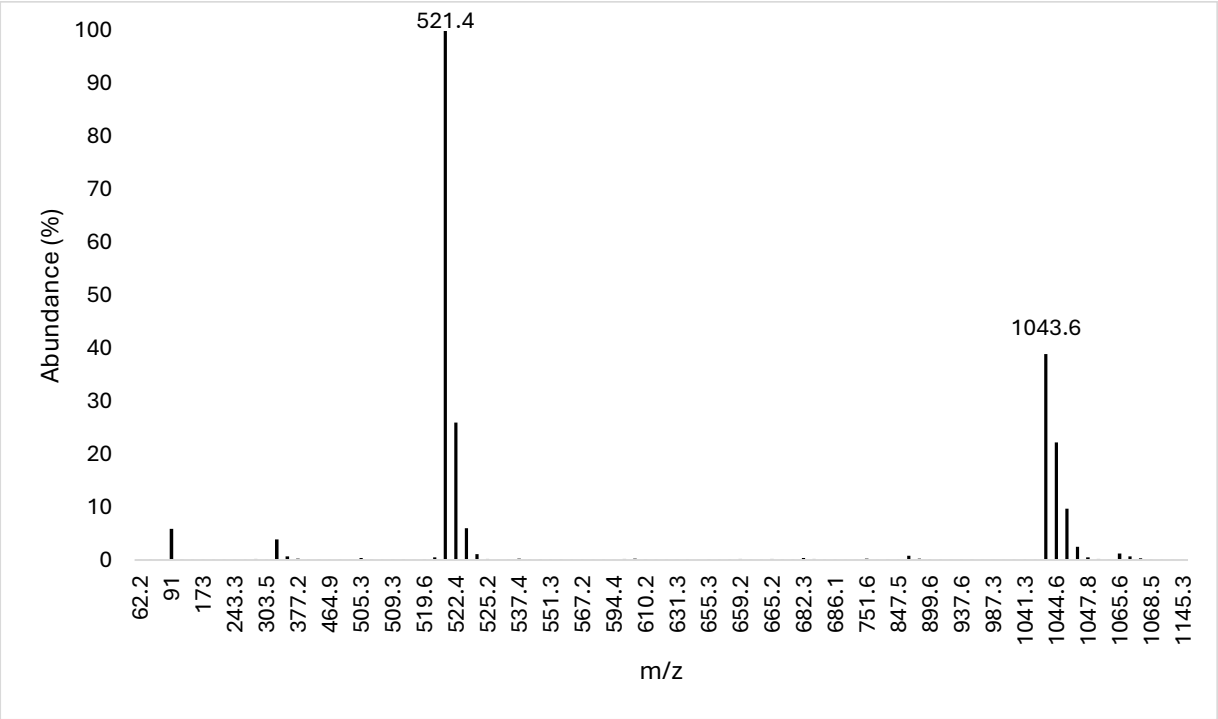

Figure S81. MS spectrum extracted from DA-LA reaction product chromatogram at retention time 22.4 min. Labeled m/z signals represent 7LA.

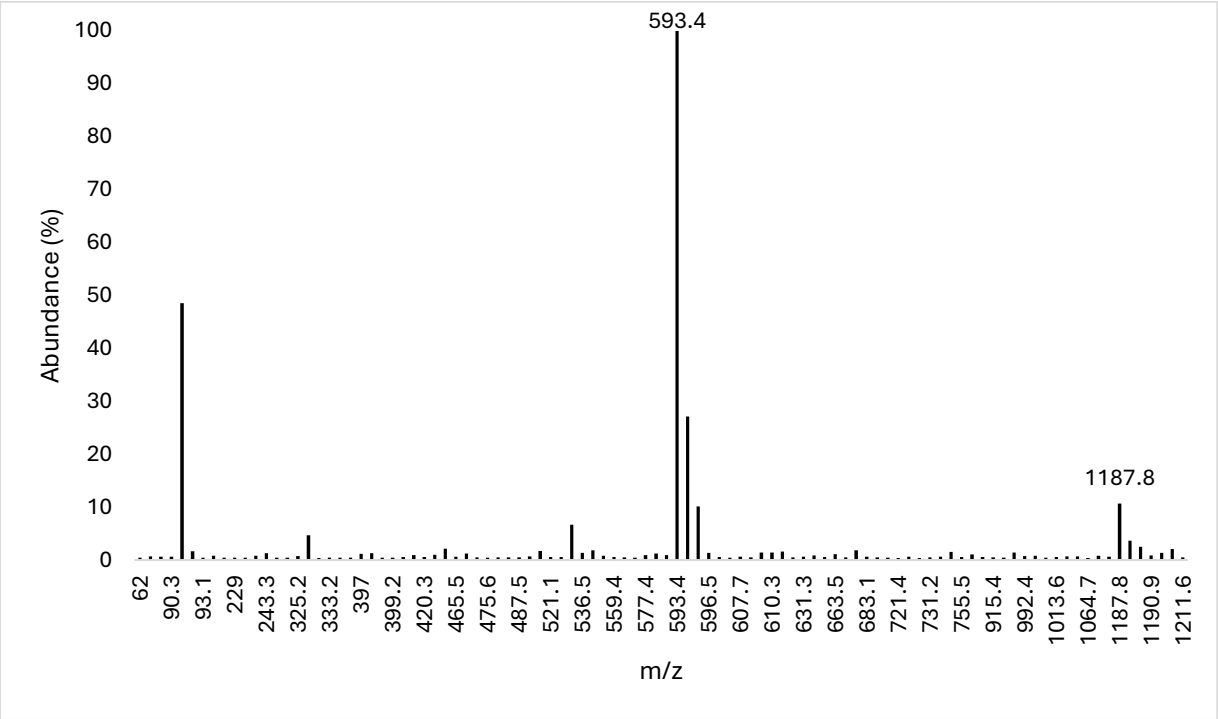

Figure S82. MS spectrum extracted from DA-LA reaction product chromatogram at retention time 23.3 min. Labeled m/z signals represent 8LA.

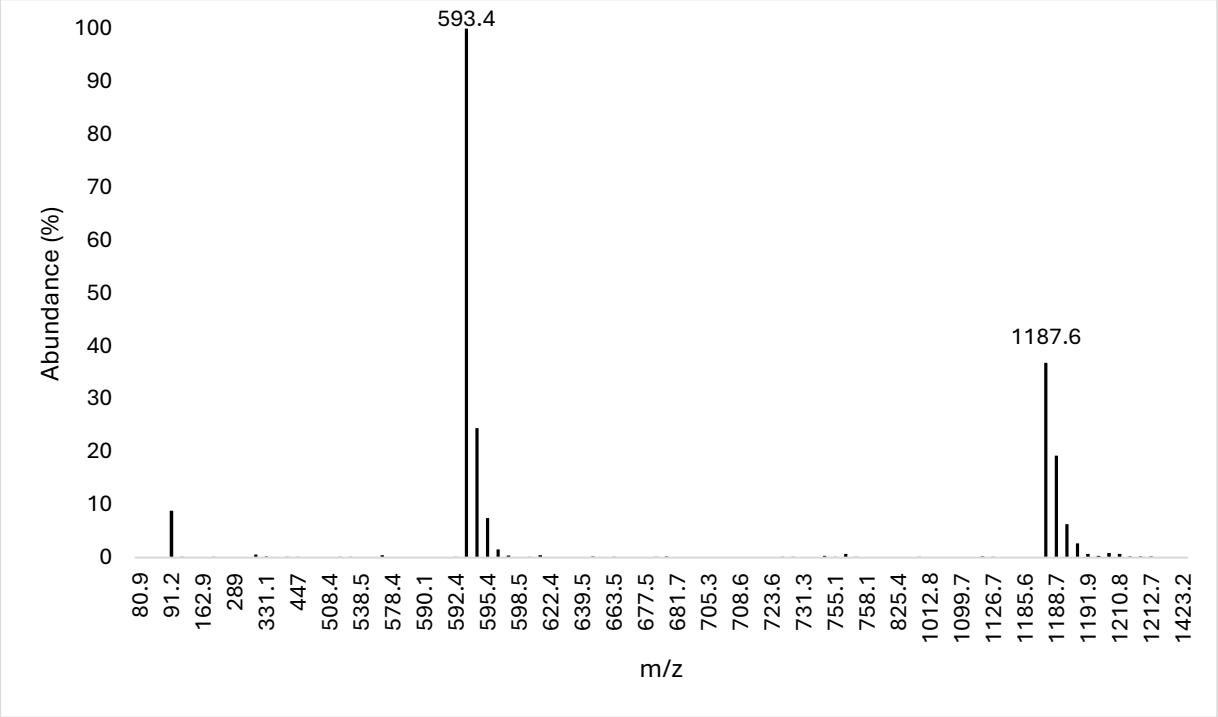

Figure S83. MS spectrum extracted from DA-LA reaction product chromatogram at retention time 23.5 min. Labeled m/z signals represent 8LA.

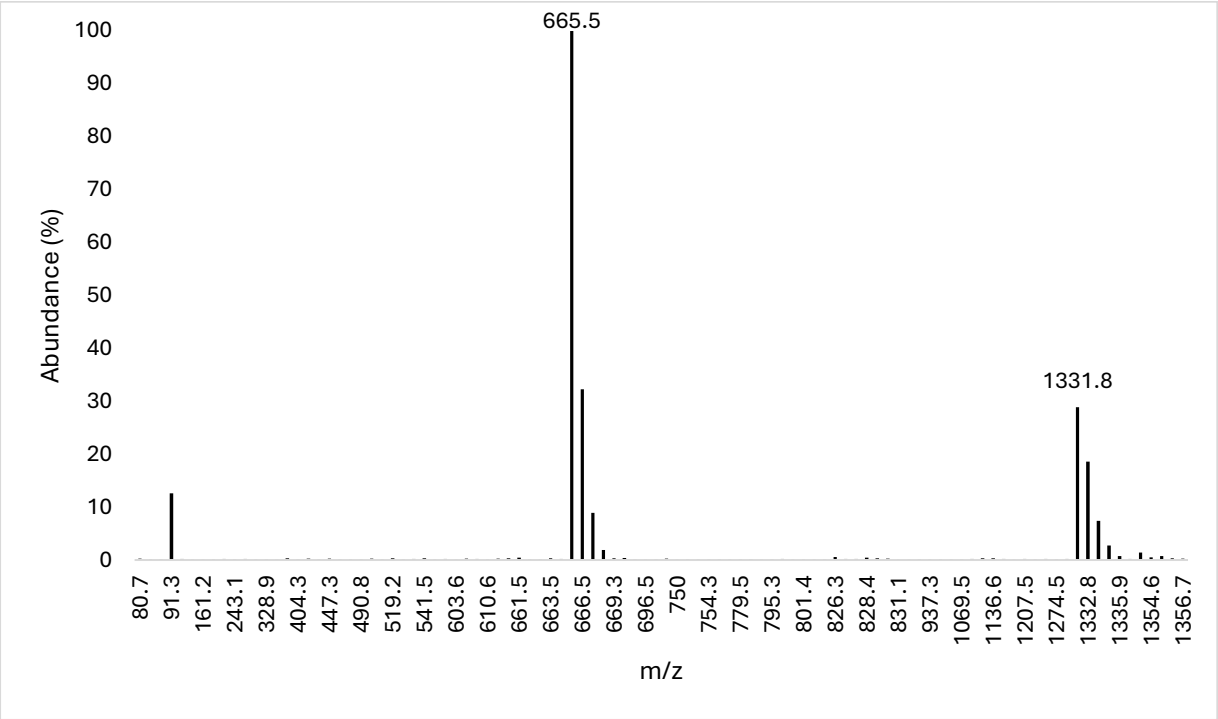

Figure S84. MS spectrum extracted from DA-LA reaction product chromatogram at retention time 24.4 min. Labeled m/z signals represent 9LA.

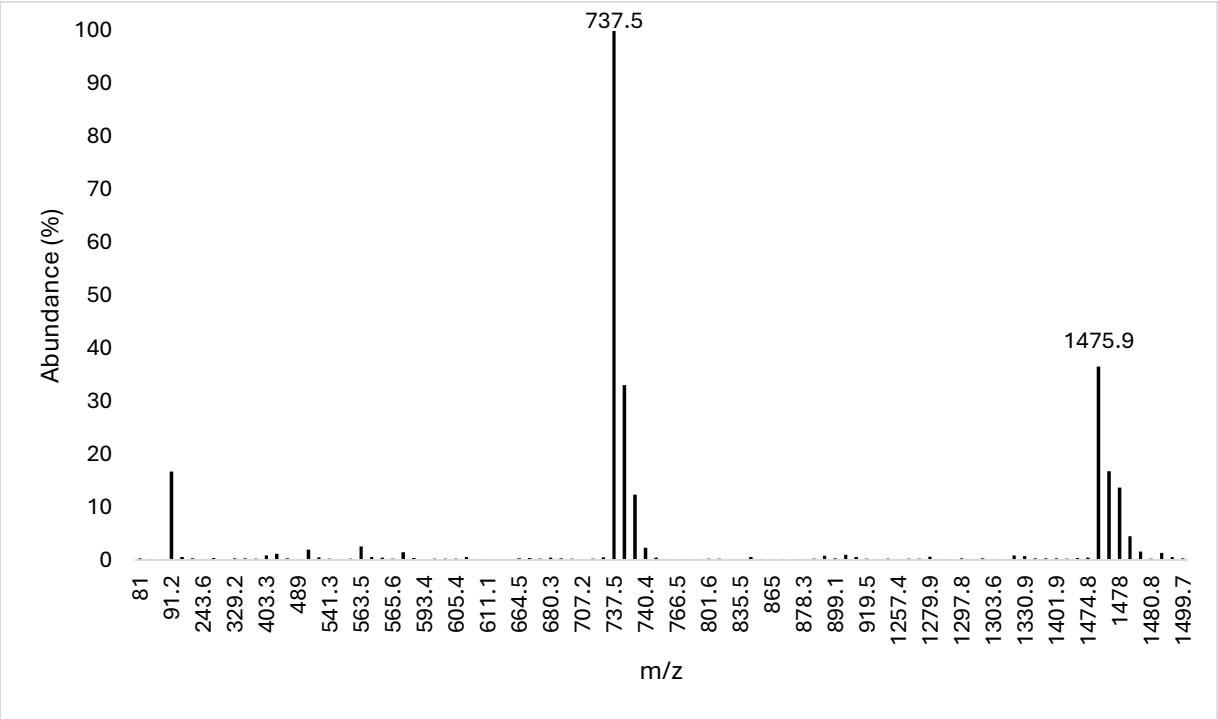

Figure S85. MS spectrum extracted from DA-LA reaction product chromatogram at retention time 25.2 min. Labeled m/z signals represent 10LA.

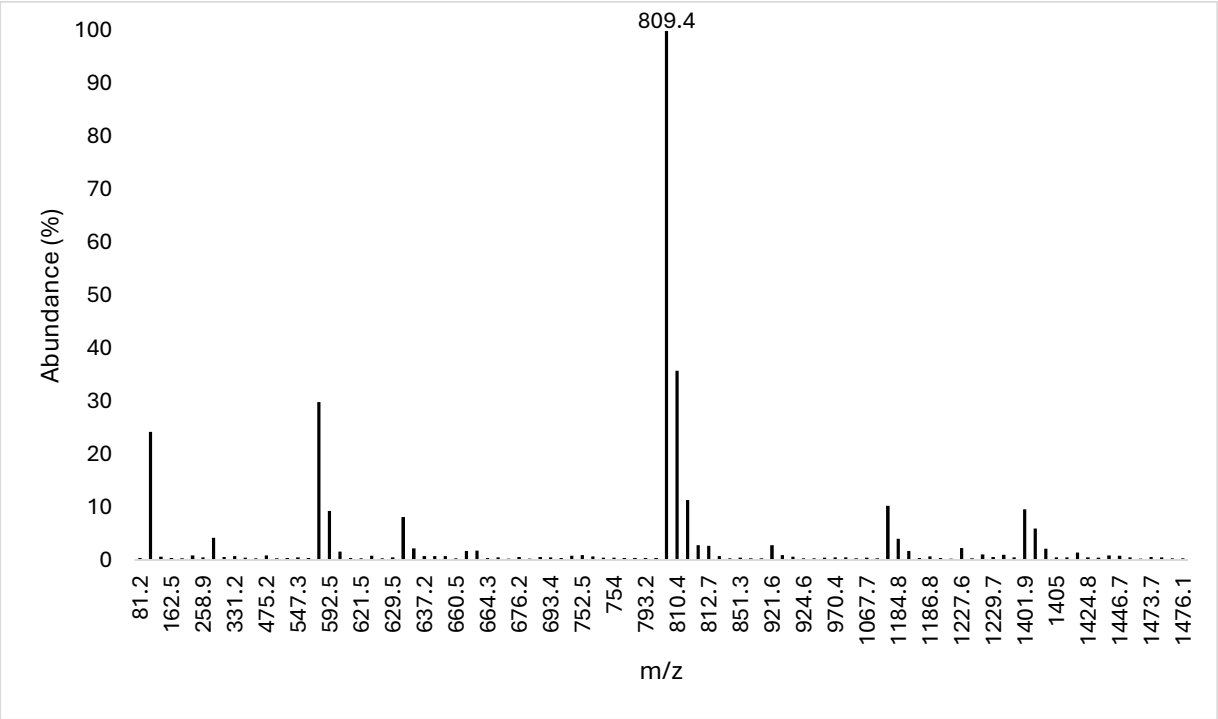

Figure S86. MS spectrum extracted from DA-LA reaction product chromatogram at retention time 25.9 min. The labeled m/z signal represents 11LA.

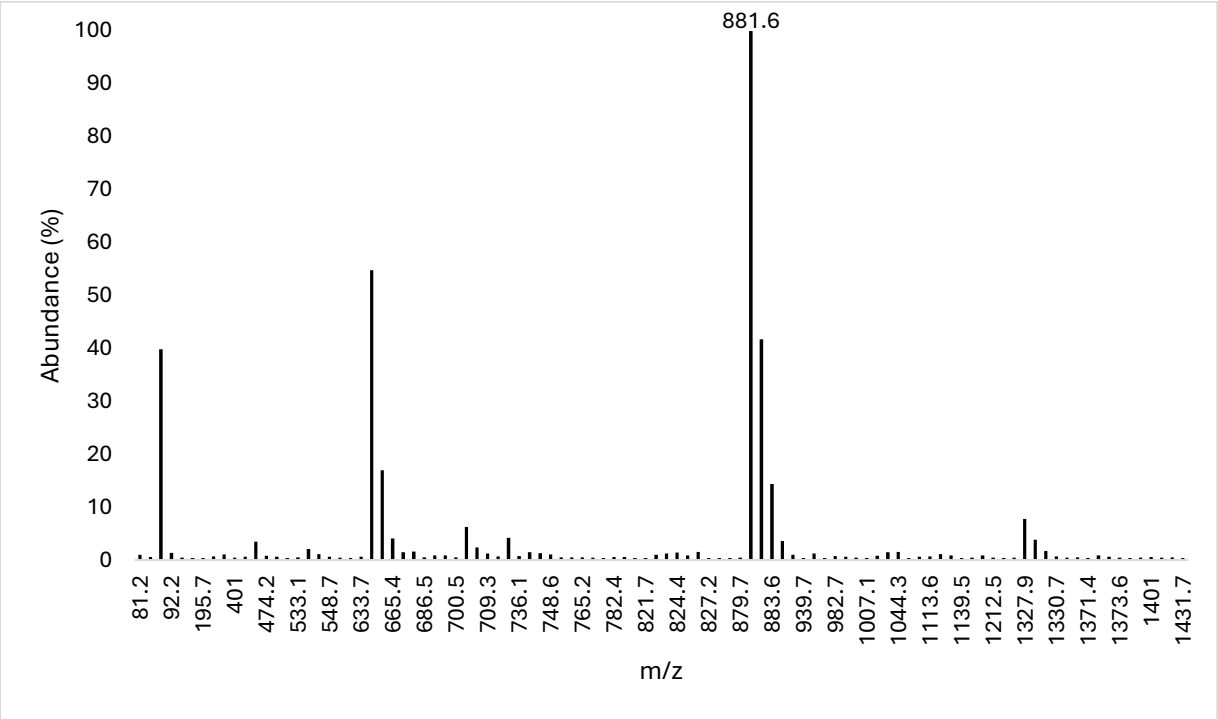

Figure S87. MS spectrum extracted from DA-LA reaction product chromatogram at retention time 26.6 min. The labeled m/z signal represents 12LA.

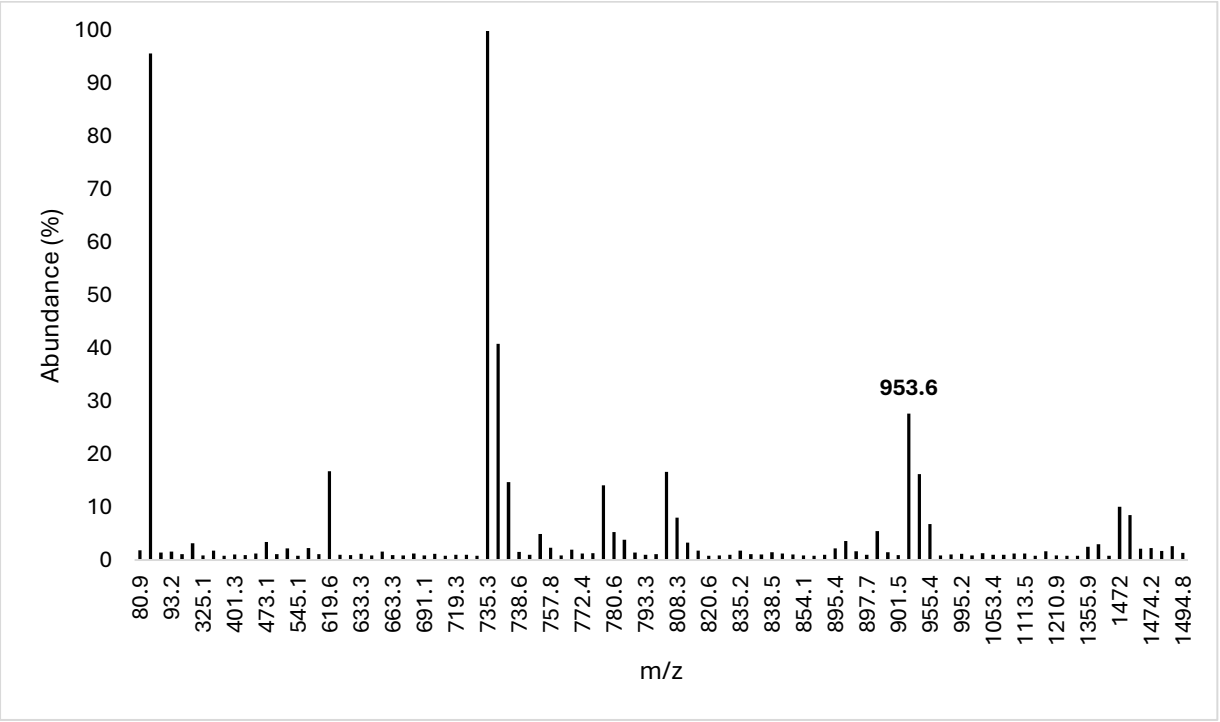

Figure S88. MS spectrum extracted from DA-LA reaction product chromatogram at retention time 27.2 min. The labeled m/z signal represents 13LA.

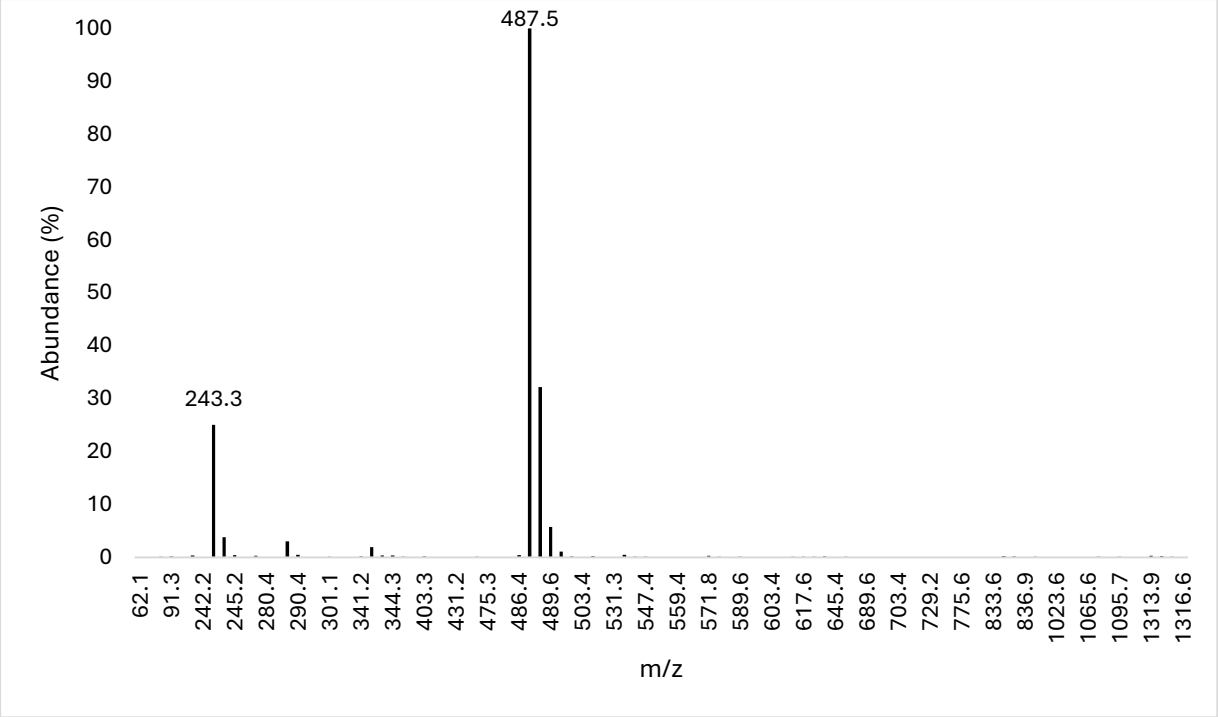

Figure S89. MS spectrum extracted from DA-LA reaction product chromatogram at retention time 29.1 min. Labeled m/z signals represent 1LA1DA.

Table S5. Identification of DA-LA reaction products. The detected products based on retention time and their corresponding m/z and ionization pattern as determined by optimized LC-MS. method

Retention time (min)	Compound	M (g/mol)	Corresponding m/z (-TIC)	Ionization pattern
10.0	1LA1DA	244.3	243.2, 487.5	$[M-H]^-$, $[2M-H]^-$
10.5	2LA1DA	316.4	315.2, 631.5	$[M-H]^-$, $[2M-H]^-$
11.0	3LA1DA	388.4	387.3, 775.6	$[M-H]^-$, $[2M-H]^-$
11.4	4LA1DA	460.5	459.4, 919.6	$[M-H]^-$, $[2M-H]^-$
11.8	5LA1DA	532.6	531.5, 1063.8	$[M-H]^-$, $[2M-H]^-$
12.2	6LA1DA	604.6	603.4, 1207.8	$[M-H]^-$, $[2M-H]^-$
12.5	7LA1DA	676.7	675.5, 1351.9	$[M-H]^-$, $[2M-H]^-$
12.8	8LA1DA	748.7	747.5, 1496.1	$[M-H]^-$, $[2M-H]^-$
13.1	9LA1DA	820.8	819.6	$[M-H]^-$
13.4	10LA1DA	892.9	891.6	$[M-H]^-$
13.7	11LA1DA	964.9	963.6	$[M-H]^-$
13.9	12LA1DA	1037.0	1035.7	$[M-H]^-$

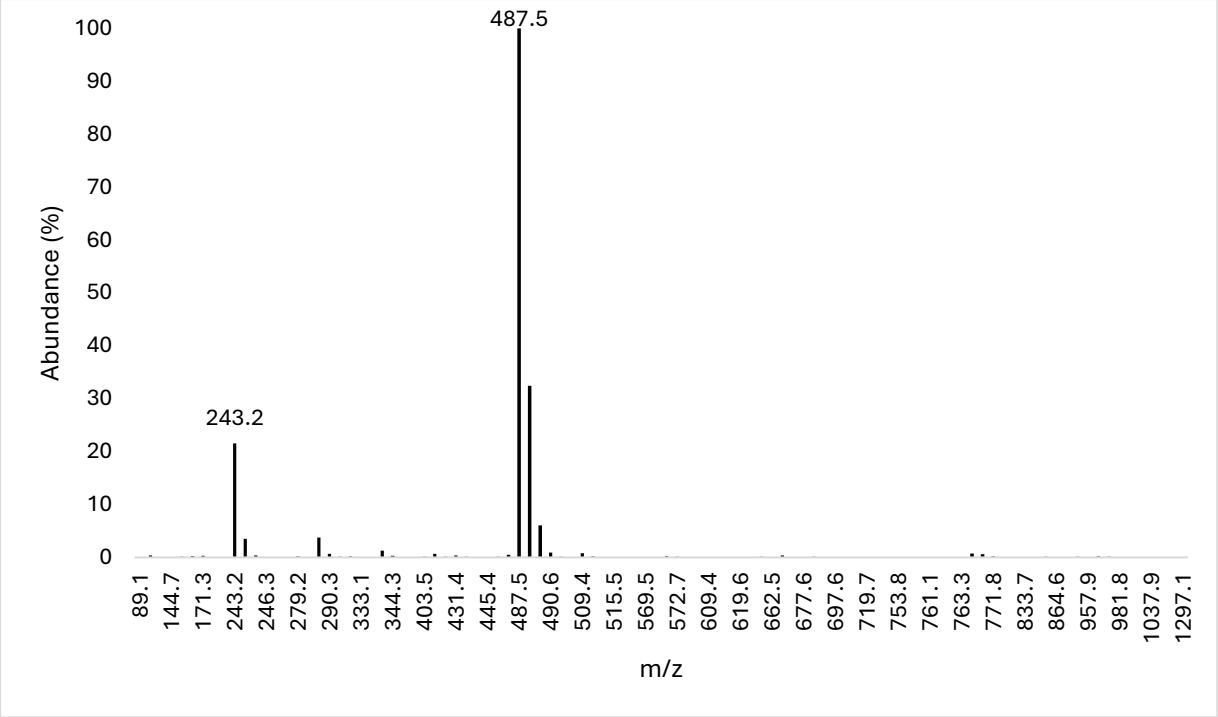

Figure S90. MS spectrum extracted from DA-LA reaction product optimized chromatogram at retention time 10.0 min. Labeled m/z signals represent 1LA1DA.

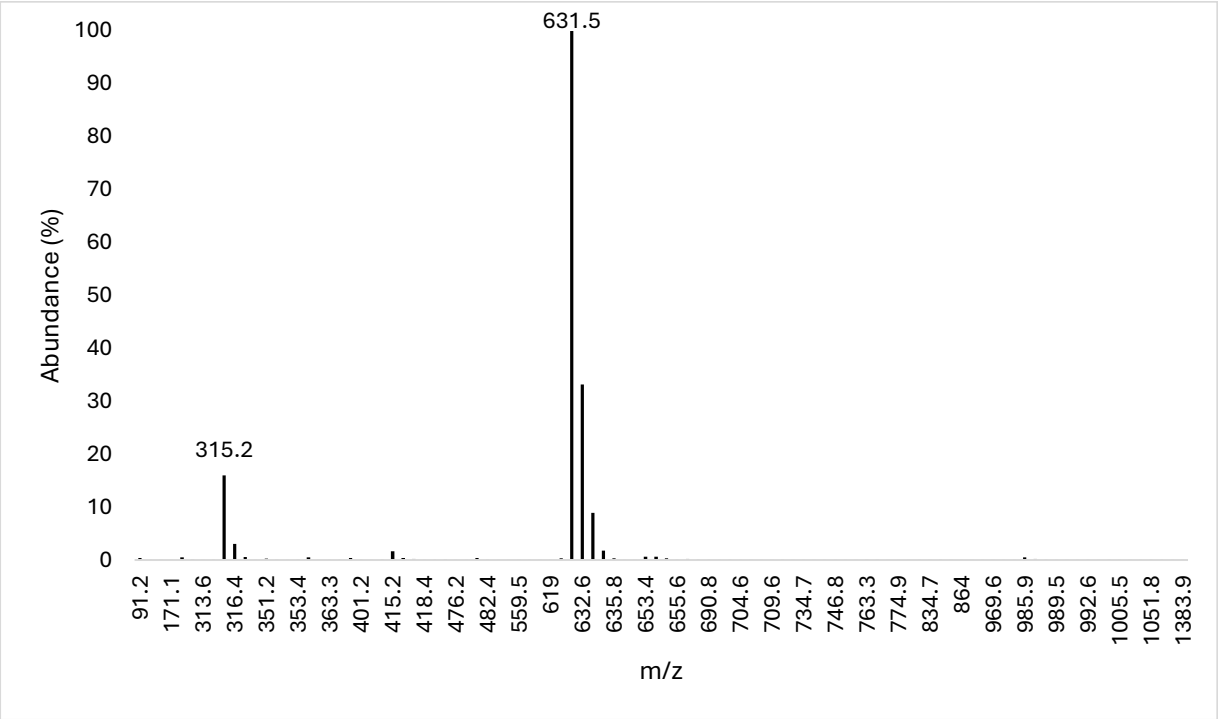

Figure S91. MS spectrum extracted from DA-LA reaction product optimized chromatogram at retention time 10.5 min. Labeled m/z signals represent 2LA1DA.

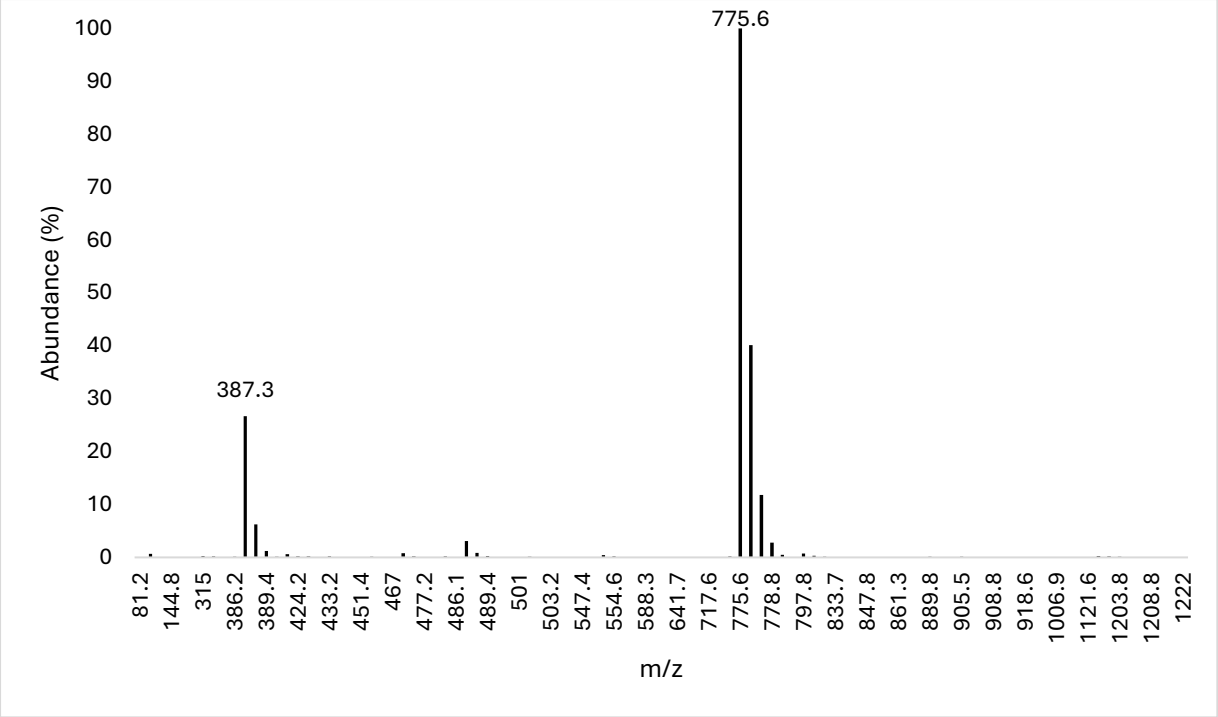

Figure S92. MS spectrum extracted from DA-LA reaction product optimized chromatogram at retention time 11.0 min. Labeled m/z signals represent 3LA1DA.

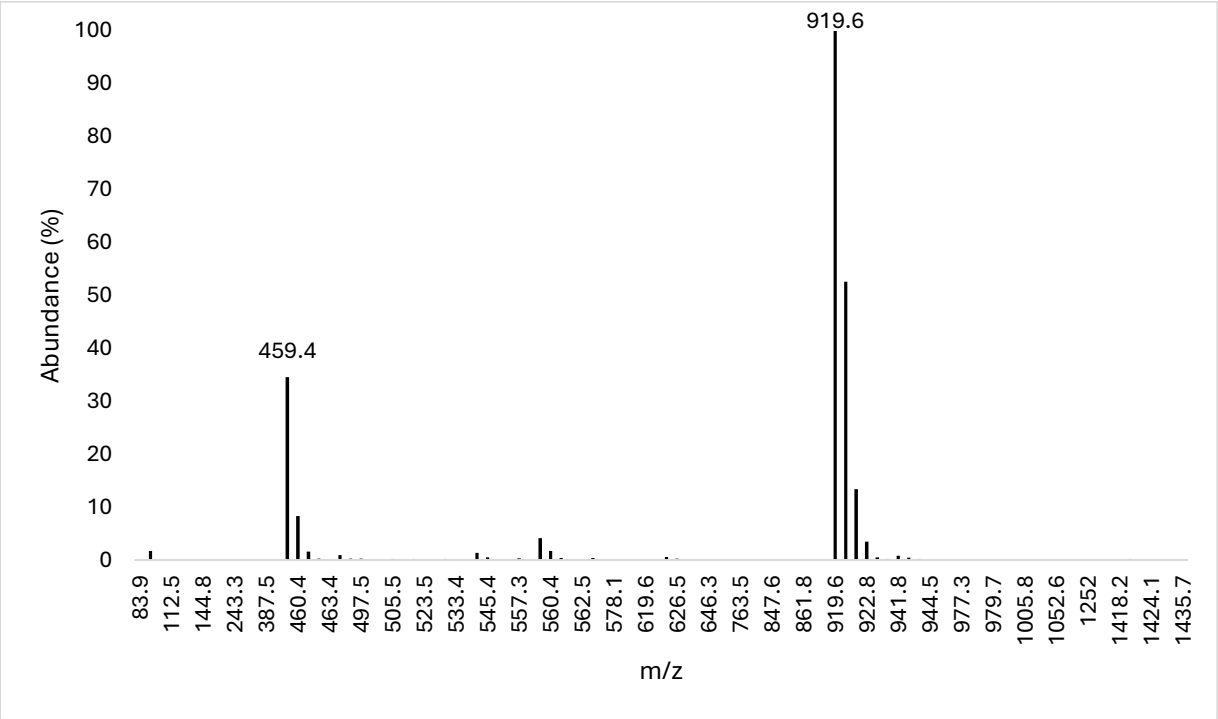

Figure S93. MS spectrum extracted from DA-LA reaction product optimized chromatogram at retention time 11.4 min. Labeled m/z signals represent 4LA1DA.

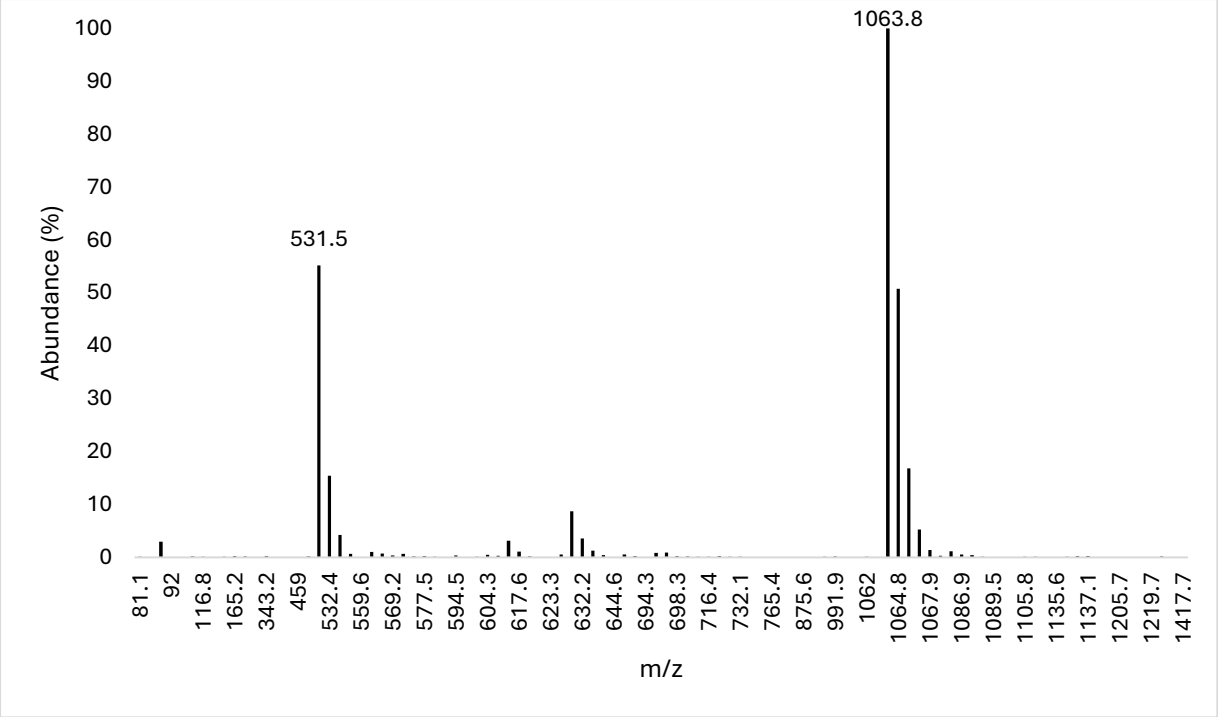

Figure S94. MS spectrum extracted from DA-LA reaction product optimized chromatogram at retention time 11.8 min. Labeled m/z signals represent 5LA1DA.

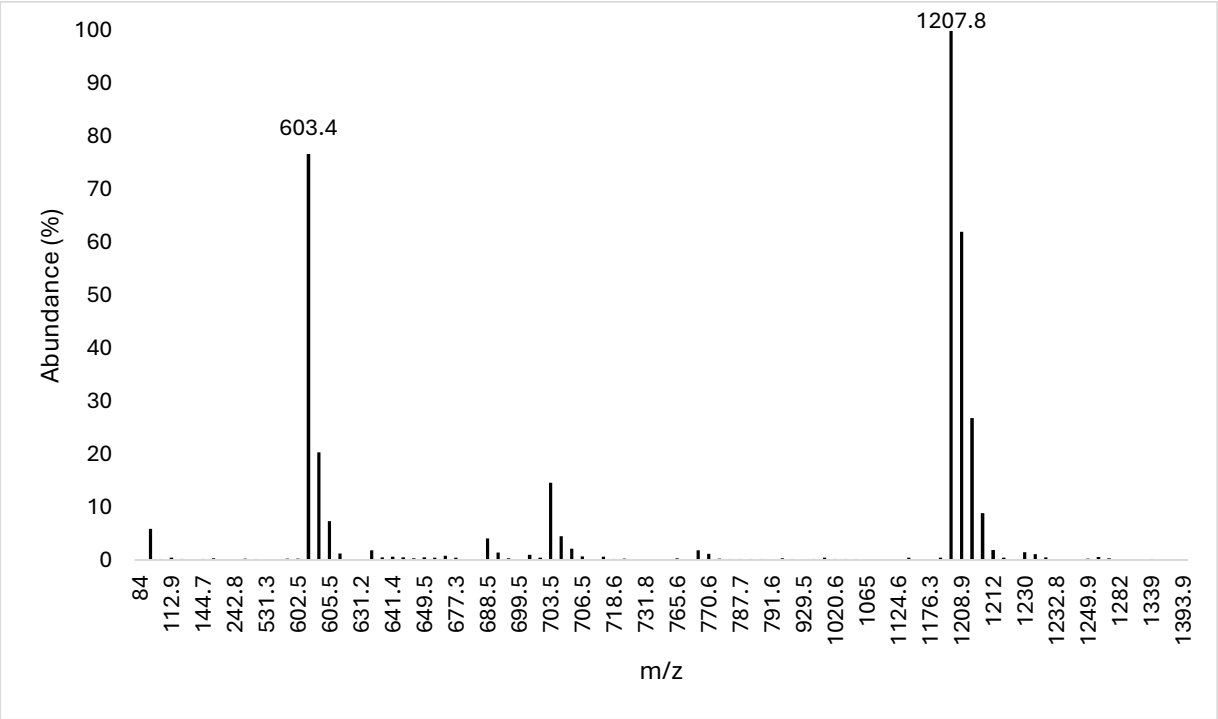

Figure S95. MS spectrum extracted from DA-LA reaction product optimized chromatogram at retention time 12.2 min. Labeled m/z signals represent 6LA1DA.

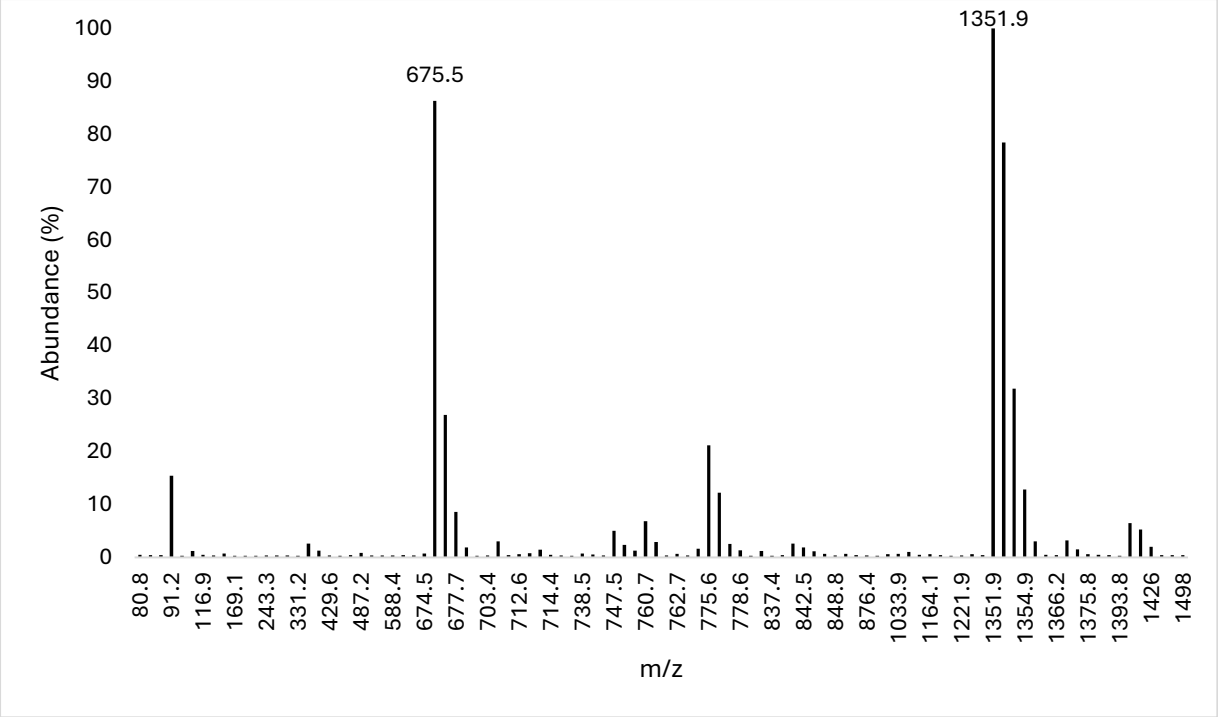

Figure S96. MS spectrum extracted from DA-LA reaction product optimized chromatogram at retention time 12.5 min. Labeled m/z signals represent 7LA1DA.

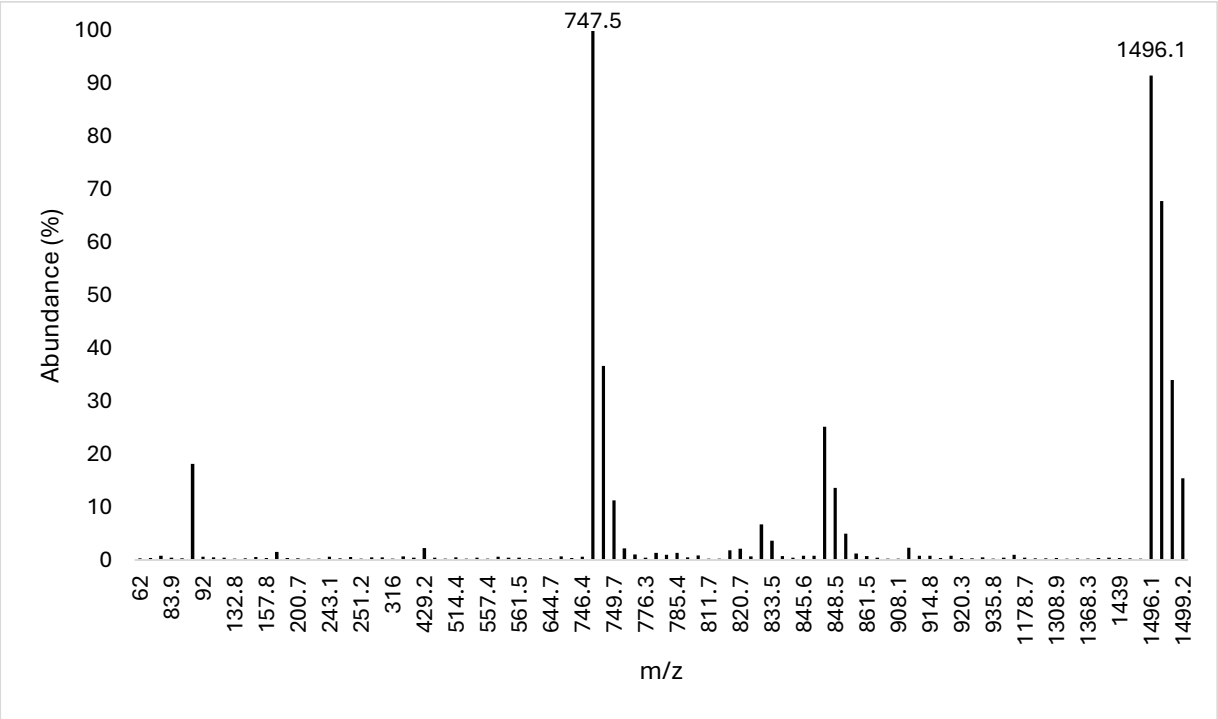

Figure S97. MS spectrum extracted from DA-LA reaction product optimized chromatogram at retention time 12.8 min. Labeled m/z signals represent 8LA1DA.

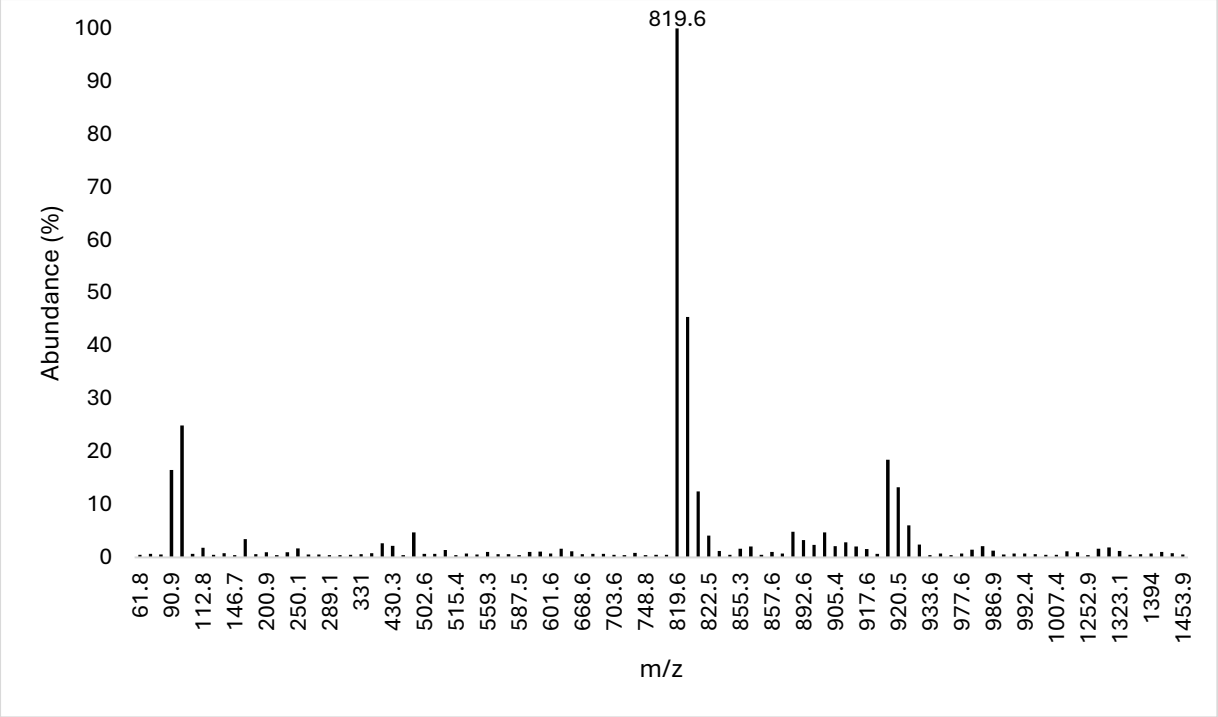

Figure S98. MS spectrum extracted from DA-LA reaction product optimized chromatogram at retention time 13.1 min. The labeled m/z signal represents 9LA1DA.

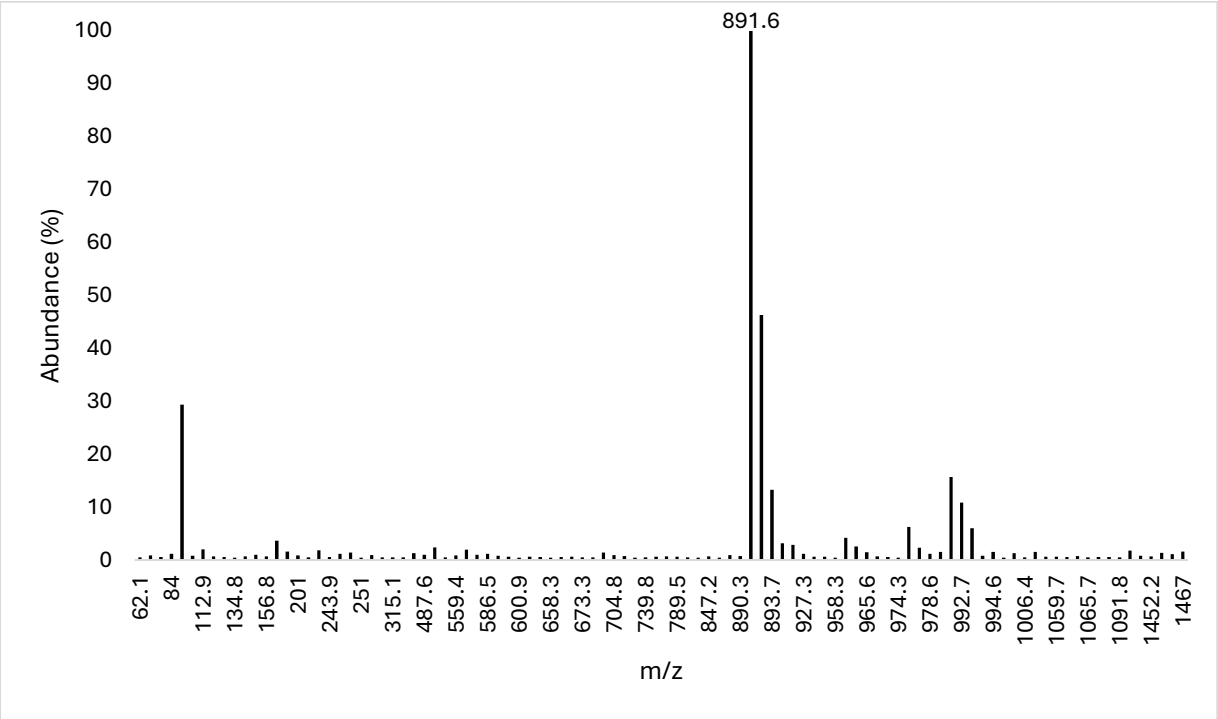

Figure S99. MS spectrum extracted from DA-LA reaction product optimized chromatogram at retention time 13.4 min. The labeled m/z signal represents 10LA1DA.

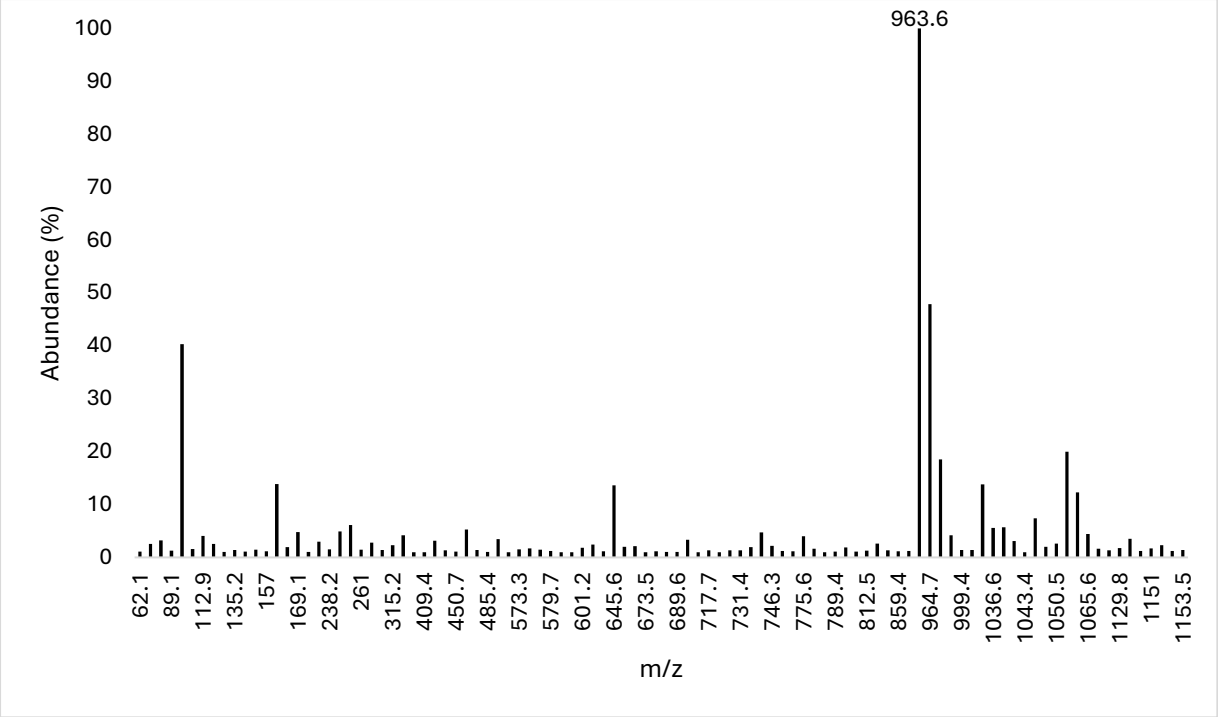

Figure S100. MS spectrum extracted from DA-LA reaction product optimized chromatogram at retention time 13.7 min. The labeled m/z signal represents 11LA1DA.

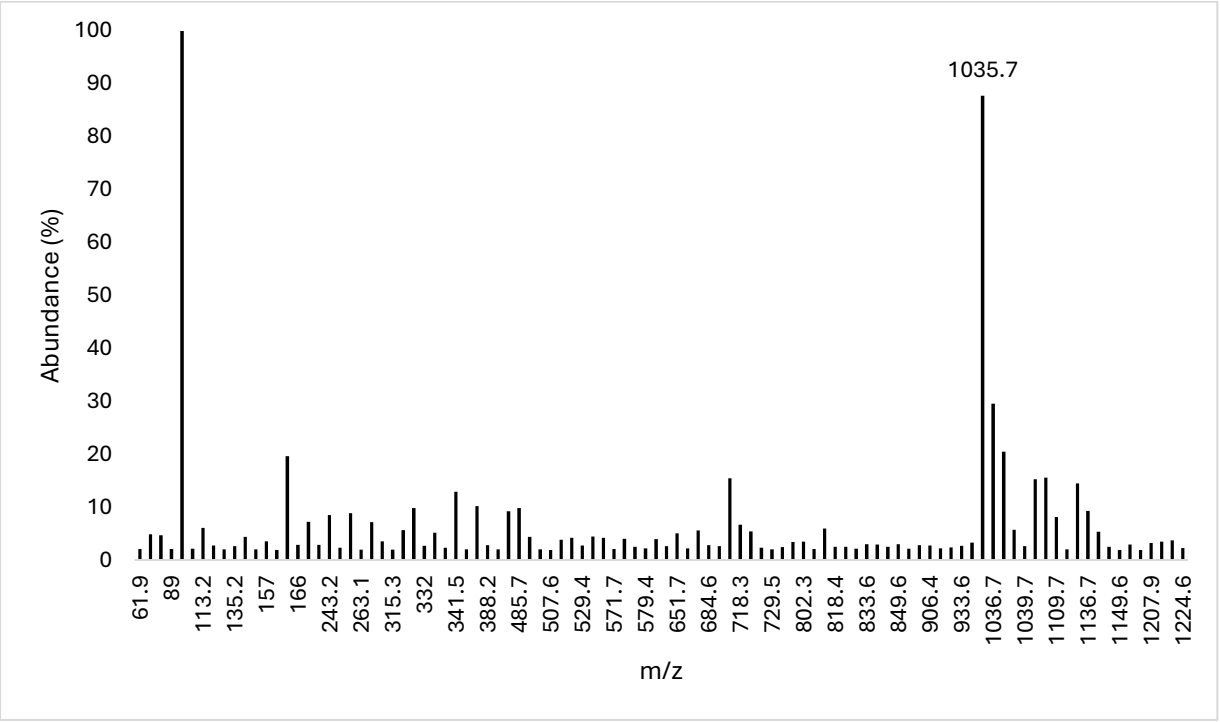

Figure S101. MS spectrum extracted from DA-LA reaction product optimized chromatogram at retention time 13.9 min. The labeled m/z signal represents 12LA1DA.

Table S6. Identification of LA reaction products (in the absence of DA). The detected products based on retention time and their corresponding m/z and ionization pattern as determined by LC-MS.

Retention time (min)	Compound	M (g/mol)	Corresponding m/z (-TIC)	Ionization pattern
12.5	2LA	162.1	161.1, 323.2	$[M-H]^-$, $[2M-H]^-$
13.2	2LA	162.1	161.3, 323.2	$[M-H]^-$, $[2M-H]^-$
15.6	3LA	234.2	233.2, 467.3	$[M-H]^-$, $[2M-H]^-$
17.8	4LA	306.3	305.2, 611.4	$[M-H]^-$, $[2M-H]^-$
19.7	5LA	378.3	377.2, 755.3	$[M-H]^-$, $[2M-H]^-$
21.0	6LA	450.4	449.2, 899.6	$[M-H]^-$, $[2M-H]^-$
21.2	6LA	450.4	449.3, 899.4	$[M-H]^-$, $[2M-H]^-$
22.2	7LA	522.4	521.3, 1043.6	$[M-H]^-$, $[2M-H]^-$
22.4	7LA	522.4	521.4, 1043.7	$[M-H]^-$, $[2M-H]^-$
23.3	8LA	594.5	593.4, 1187.7	$[M-H]^-$, $[2M-H]^-$
23.5	8LA	594.5	593.4, 1187.8	$[M-H]^-$, $[2M-H]^-$
24.4	9LA	666.6	665.4, 1331.9	$[M-H]^-$, $[2M-H]^-$
24.6	9LA	666.6	665.5	$[M-H]^-$
25.2	10LA	738.6	737.4, 1475.9	$[M-H]^-$, $[2M-H]^-$
25.7	11LA	810.7	809.4	$[M-H]^-$
25.9	11LA	810.7	809.4	$[M-H]^-$
26.6	12LA	882.7	881.6	$[M-H]^-$
27.1	13LA	954.8	953.6	$[M-H]^-$
27.6	14LA	1026.9	1025.6	$[M-H]^-$
28.1	15LA	1098.9	1097.7	$[M-H]^-$
28.5	16LA	1171.0	1169.7	$[M-H]^-$
28.9	17LA	1243.0	1241.8	$[M-H]^-$
29.1	18LA	1315.1	1313.8	$[M-H]^-$

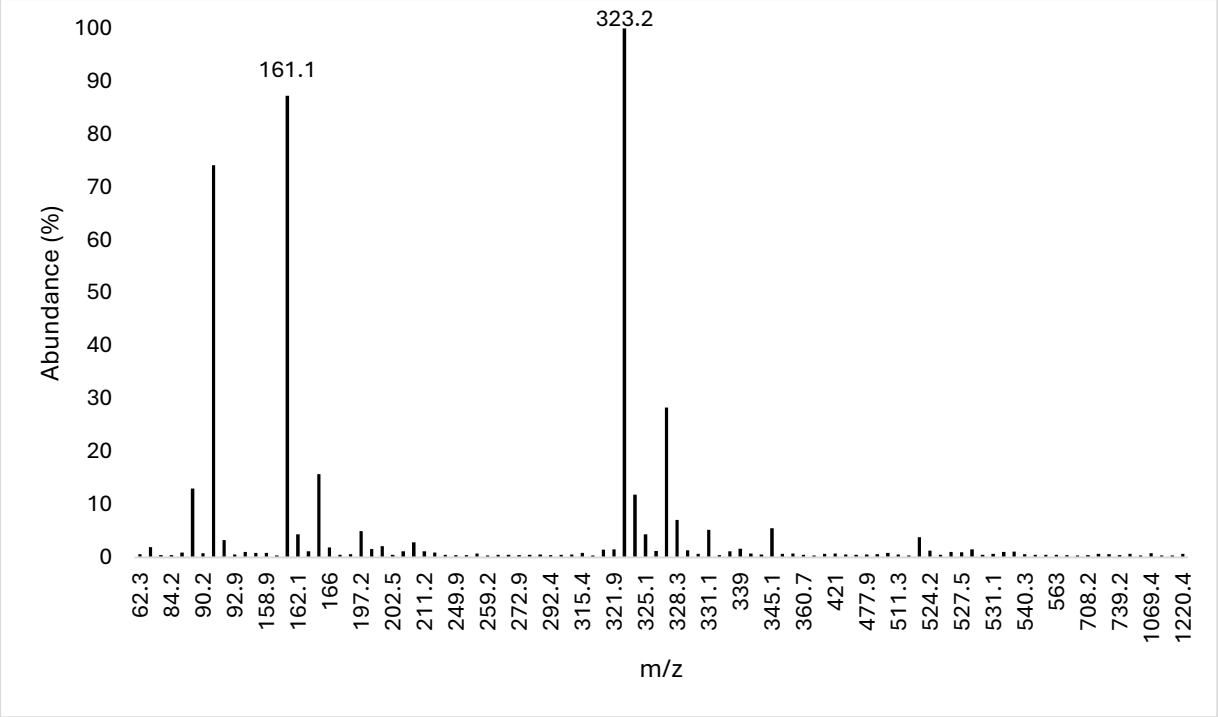

Figure S102. MS spectrum extracted from LA control chromatogram at retention time 12.5 min. Labeled m/z signals represent 2LA.

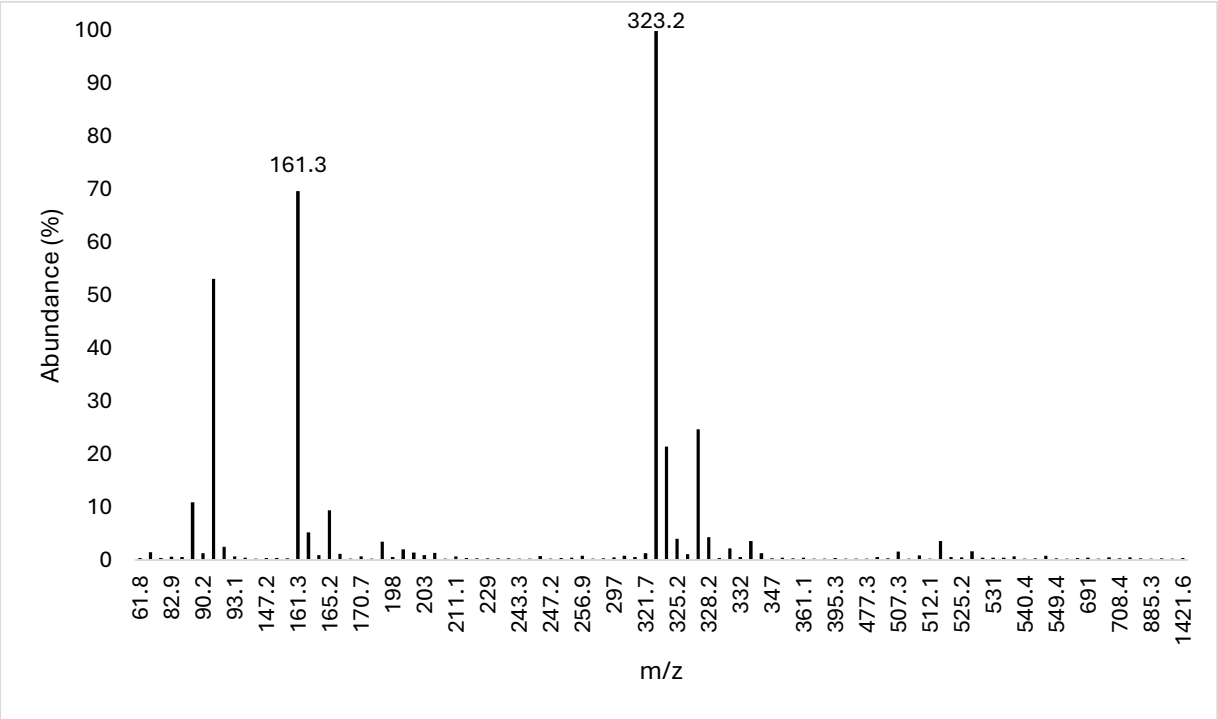

Figure S103. MS spectrum extracted from LA control chromatogram at retention time 13.2 min. Labeled m/z signals represent 2LA.

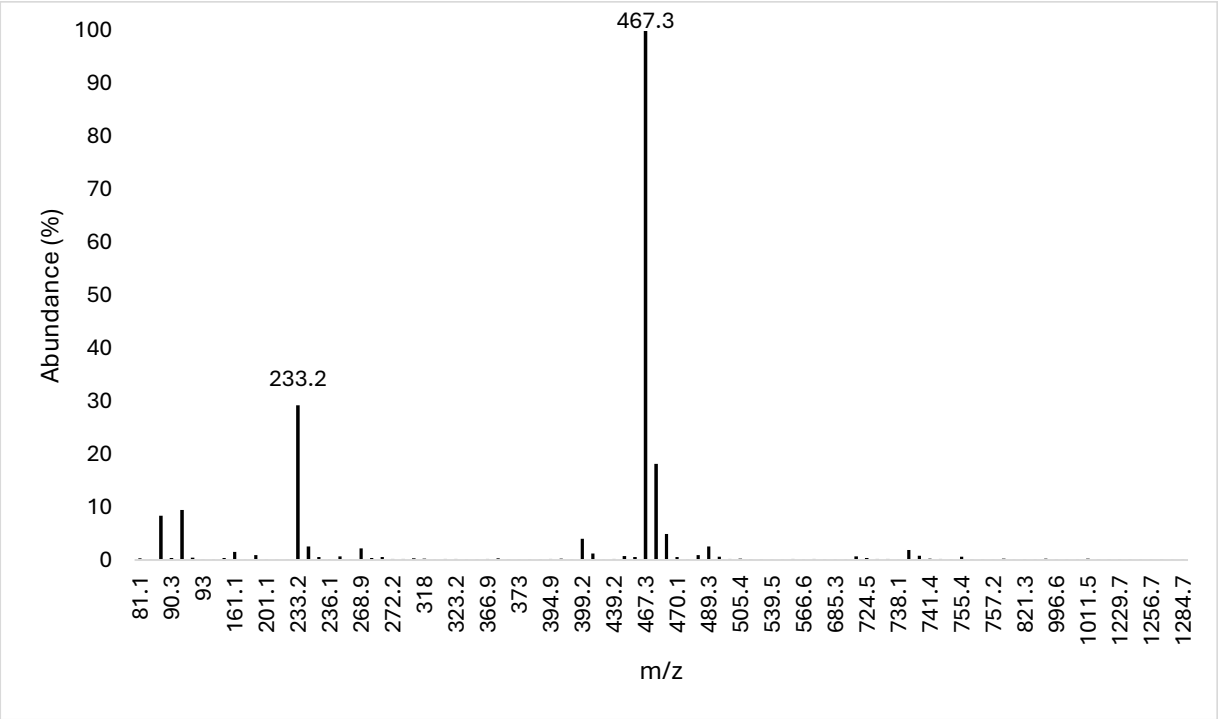

Figure S104. MS spectrum extracted from LA control chromatogram at retention time 15.6 min. Labeled m/z signals represent 3LA.

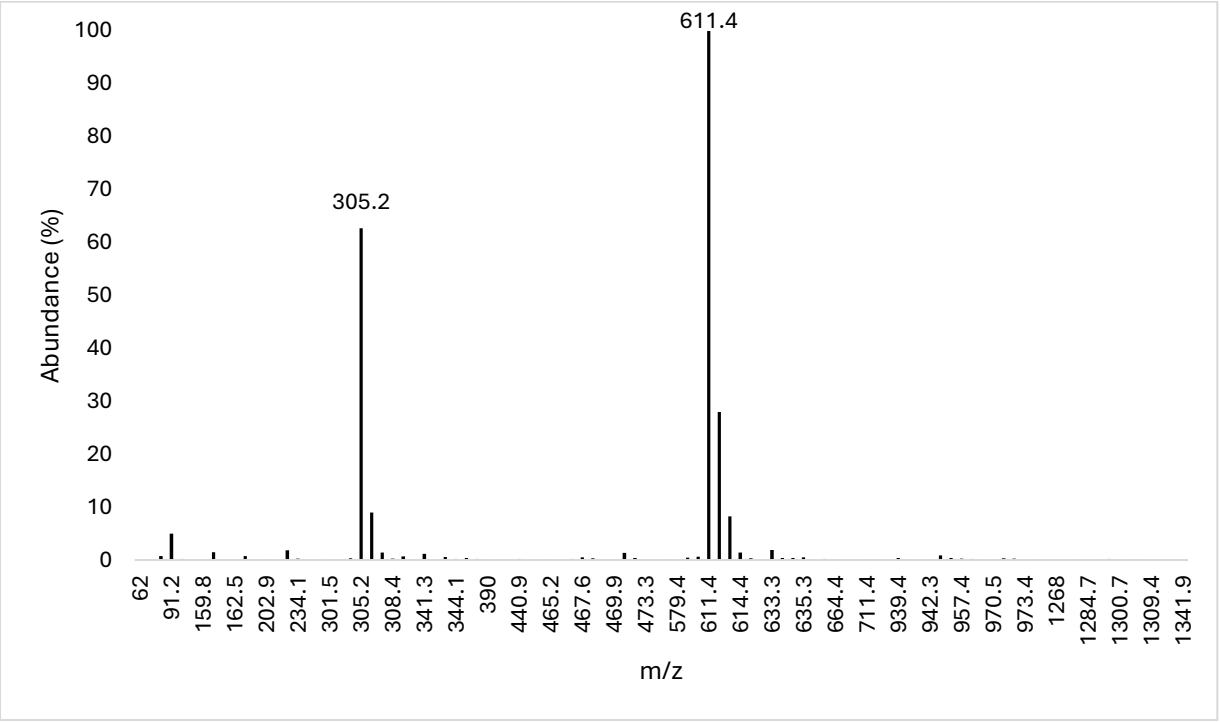

Figure S105. MS spectrum extracted from LA control chromatogram at retention time 17.8 min. Labeled m/z signals represent 4LA.

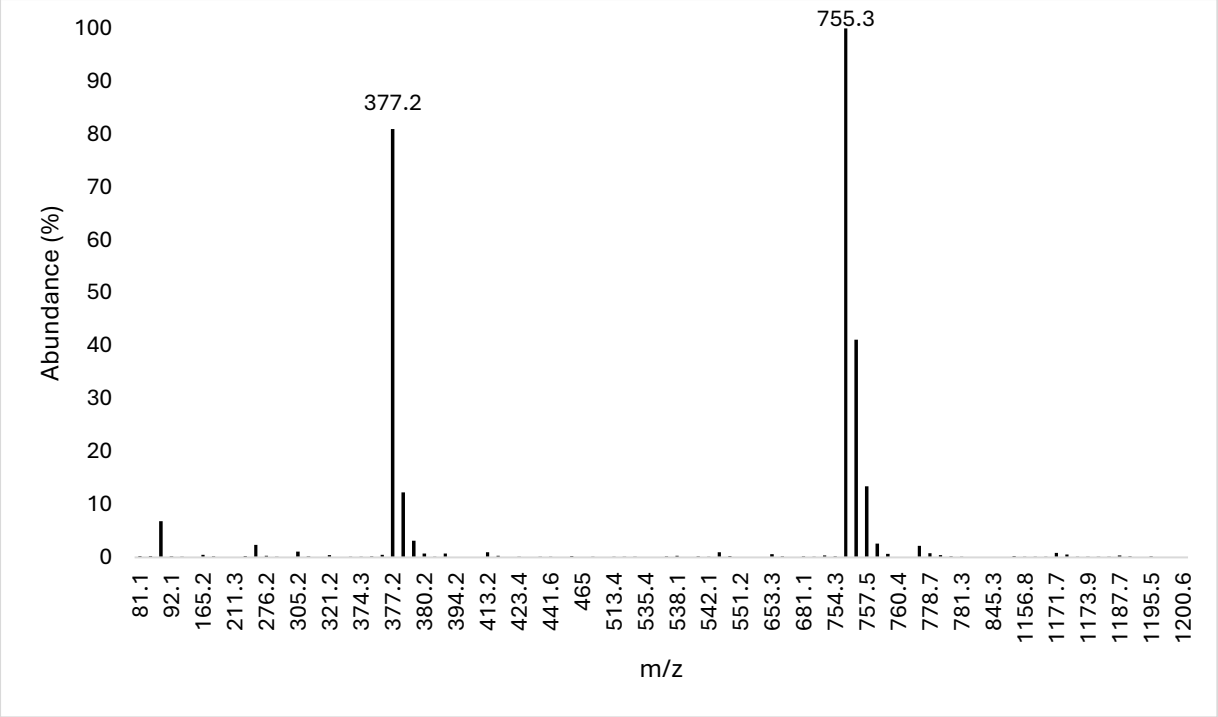

Figure S106. MS spectrum extracted from LA control chromatogram at retention time 19.7 min. Labeled m/z signals represent 5LA.

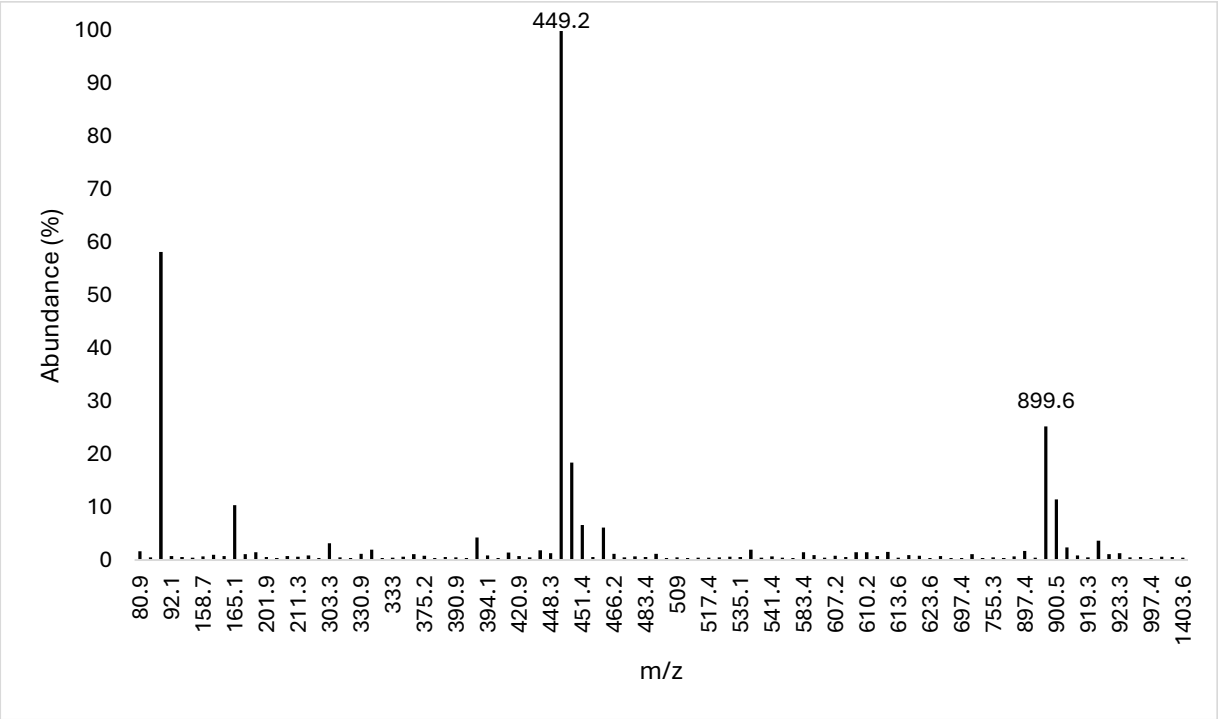

Figure S107. MS spectrum extracted from LA control chromatogram at retention time 21.0 min. Labeled m/z signals represent 6LA.

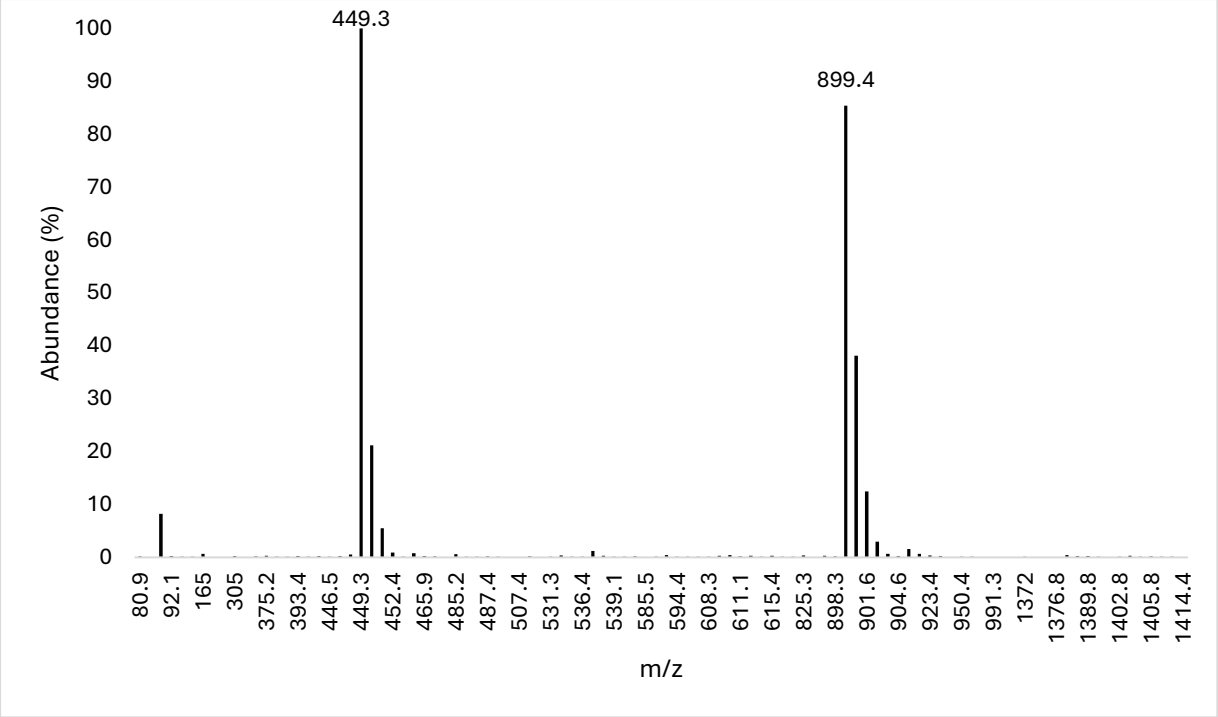

Figure S108. MS spectrum extracted from LA control chromatogram at retention time 21.2 min. Labeled m/z signals represent 6LA.

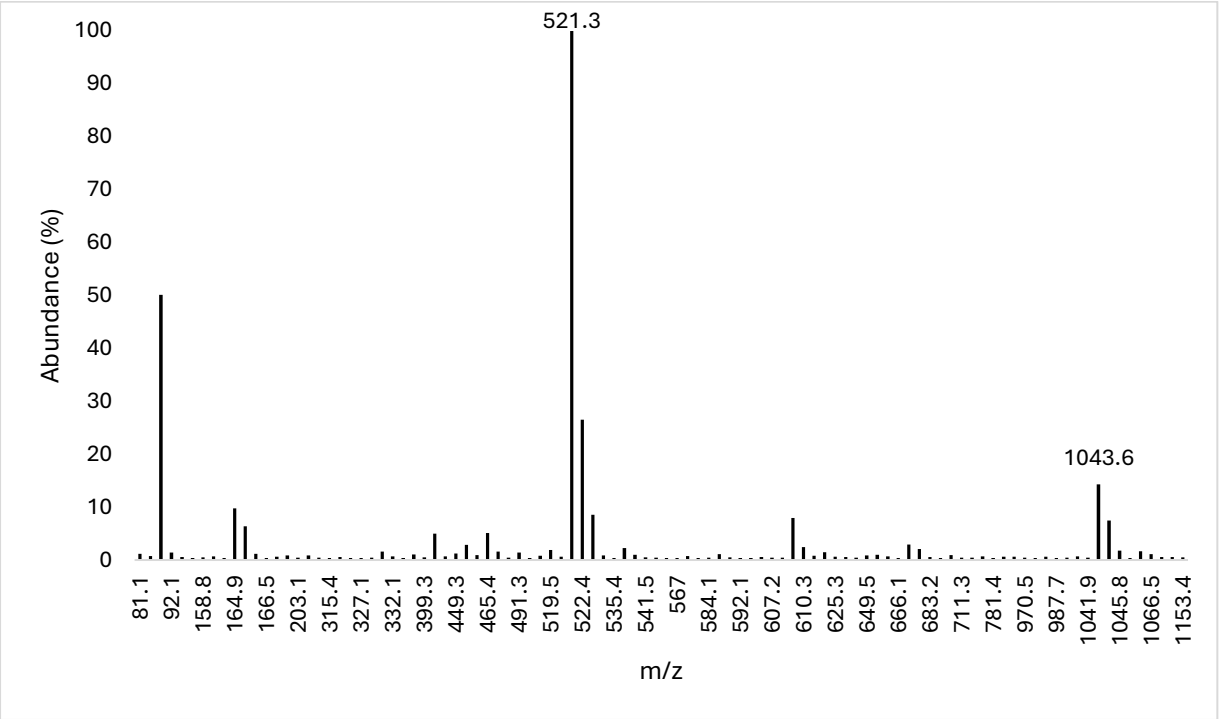

Figure S109. MS spectrum extracted from LA control chromatogram at retention time 22.2 min. Labeled m/z signals represent 7LA.

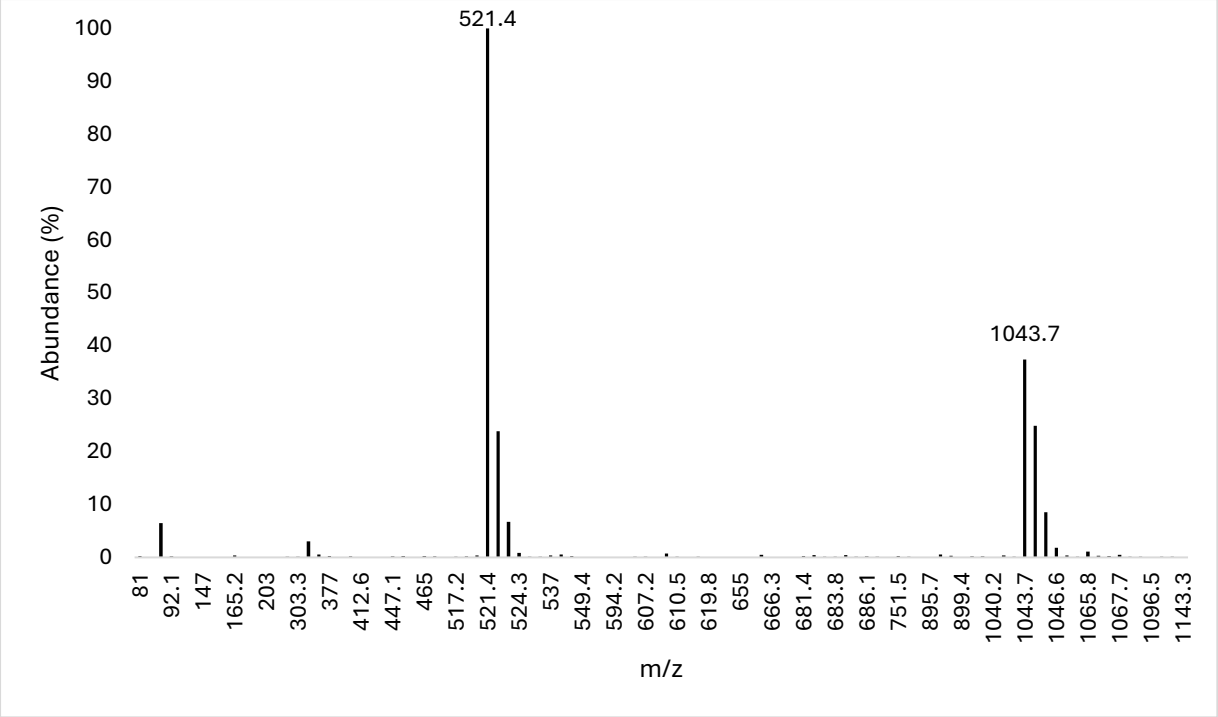

Figure S110. MS spectrum extracted from LA control chromatogram at retention time 22.4 min. Labeled m/z signals represent 7LA.

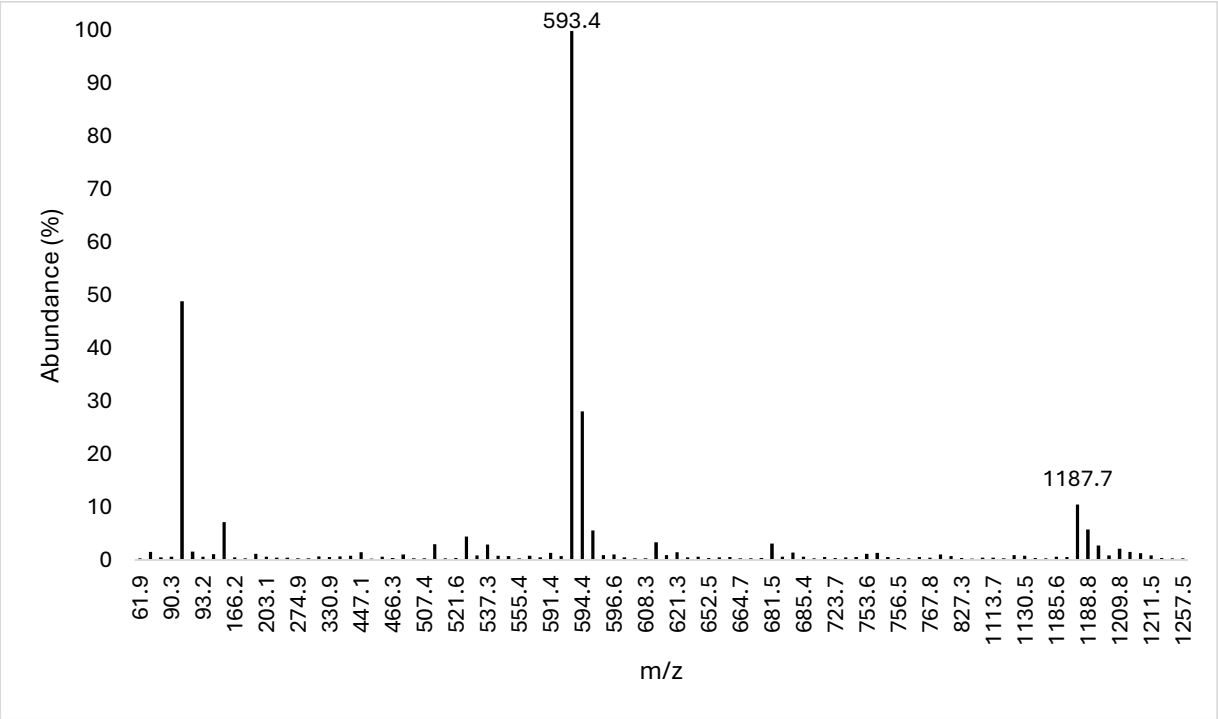

Figure S111. MS spectrum extracted from LA control chromatogram at retention time 23.3 min. Labeled m/z signals represent 8LA.

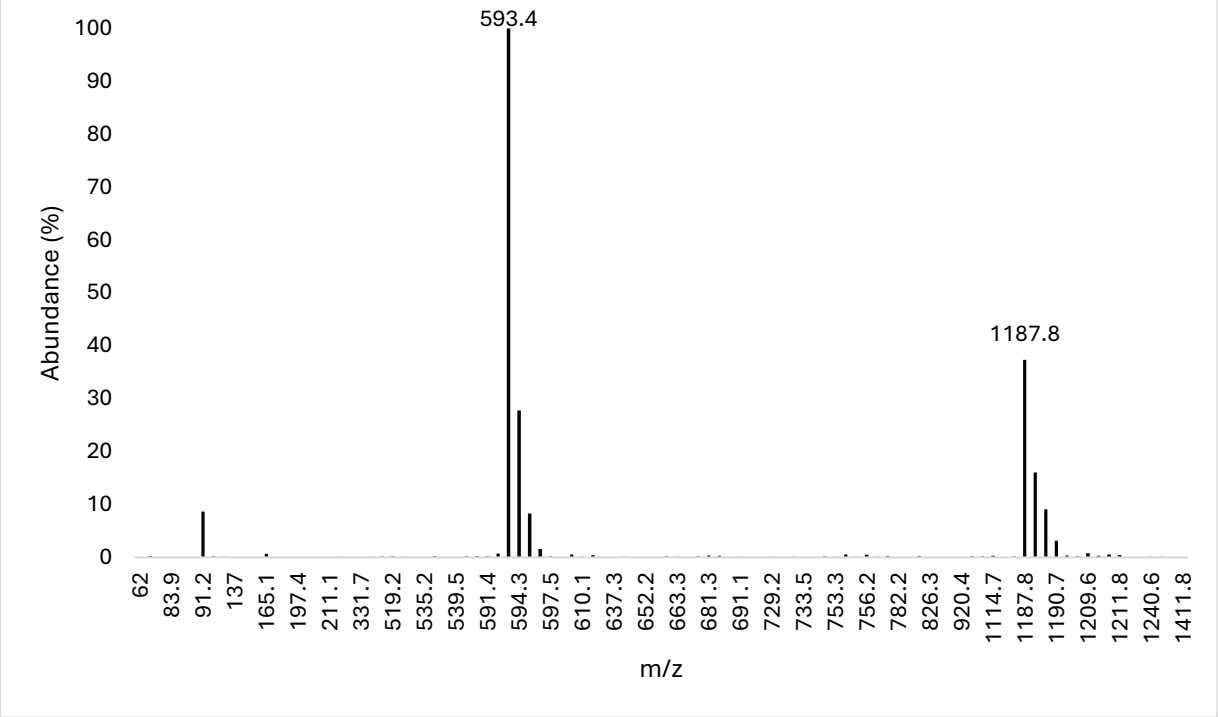

Figure S112. MS spectrum extracted from LA control chromatogram at retention time 23.5 min. Labeled m/z signals represent 8LA.

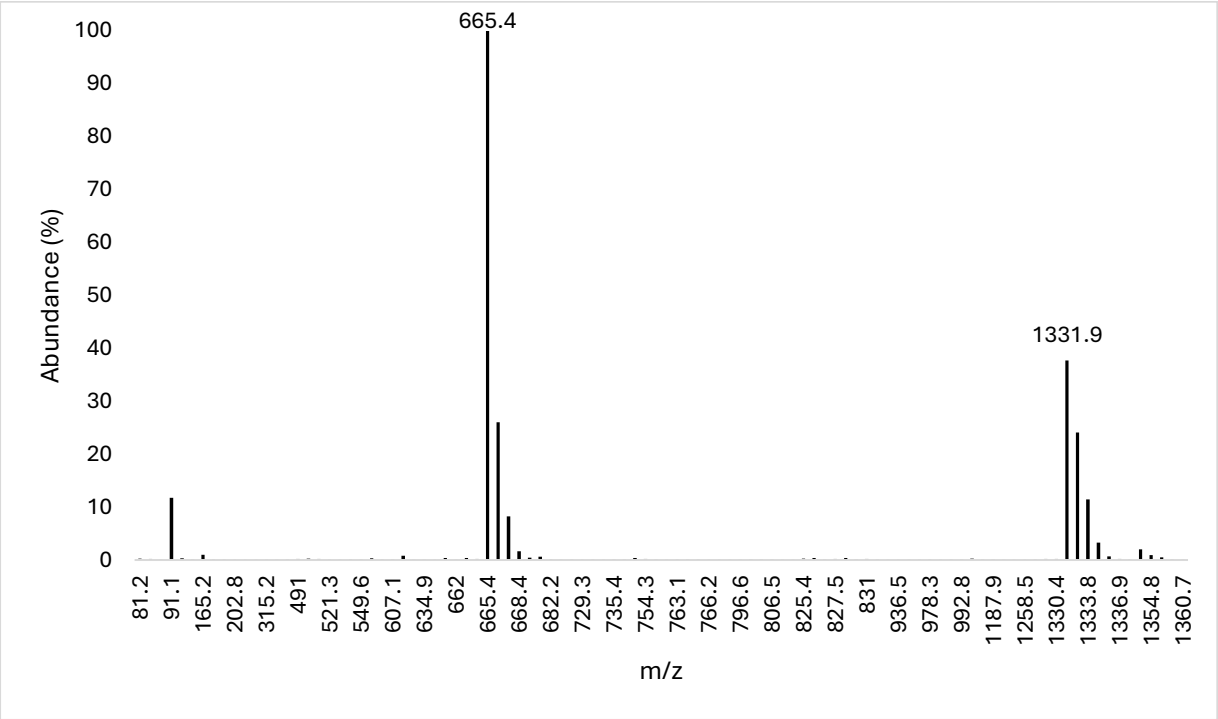

Figure S113. MS spectrum extracted from LA control chromatogram at retention time 24.4 min. Labeled m/z signals represent 9LA.

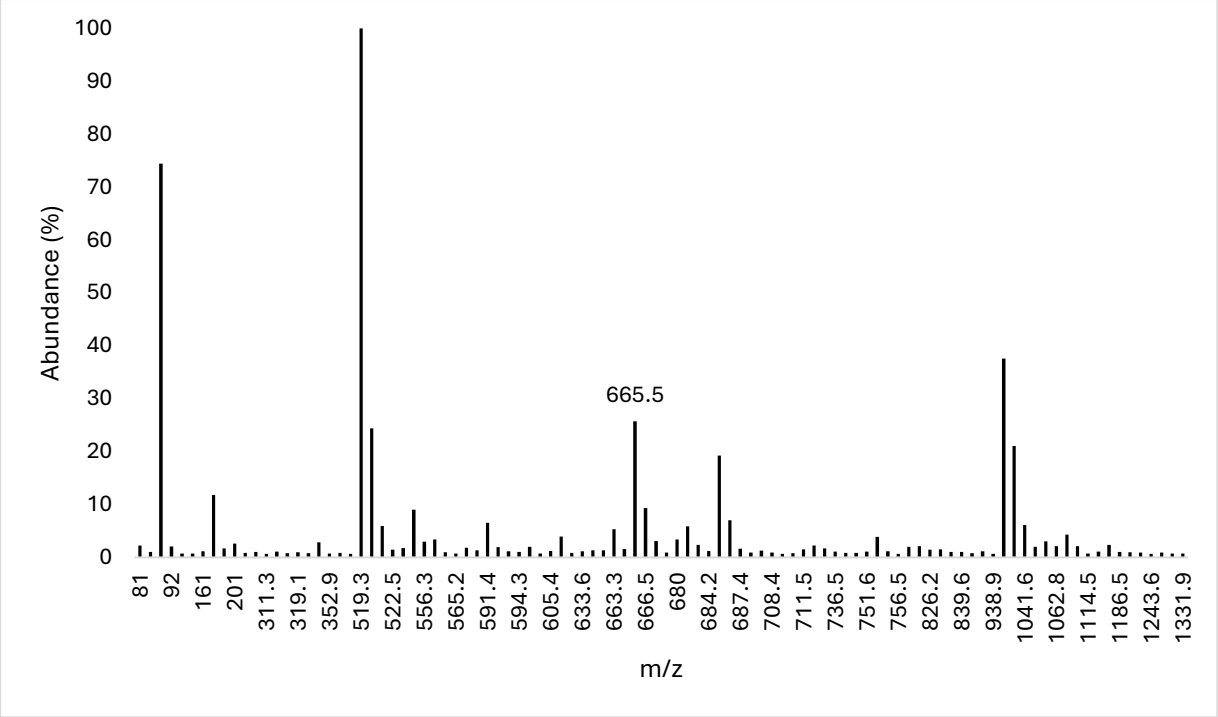

Figure S114. MS spectrum extracted from LA control chromatogram at retention time 24.6 min. Labeled m/z signals represent 9LA.

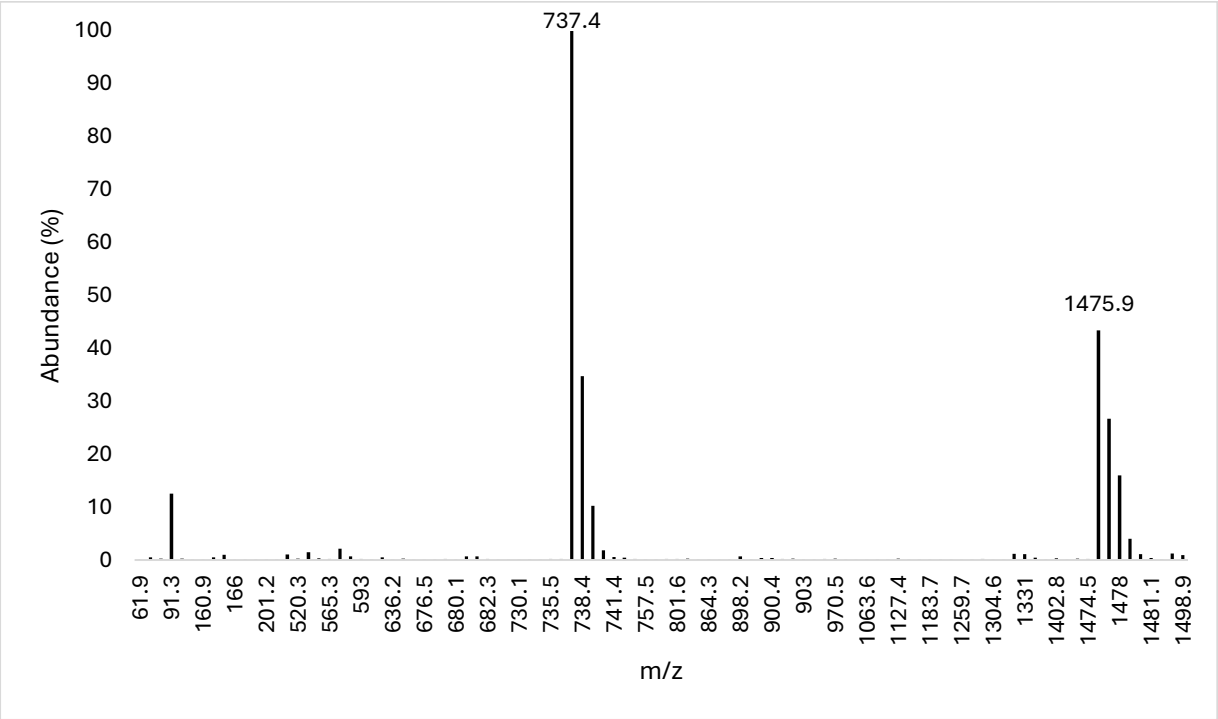

Figure S115. MS spectrum extracted from LA control chromatogram at retention time 25.2 min. Labeled m/z signals represent 10LA.

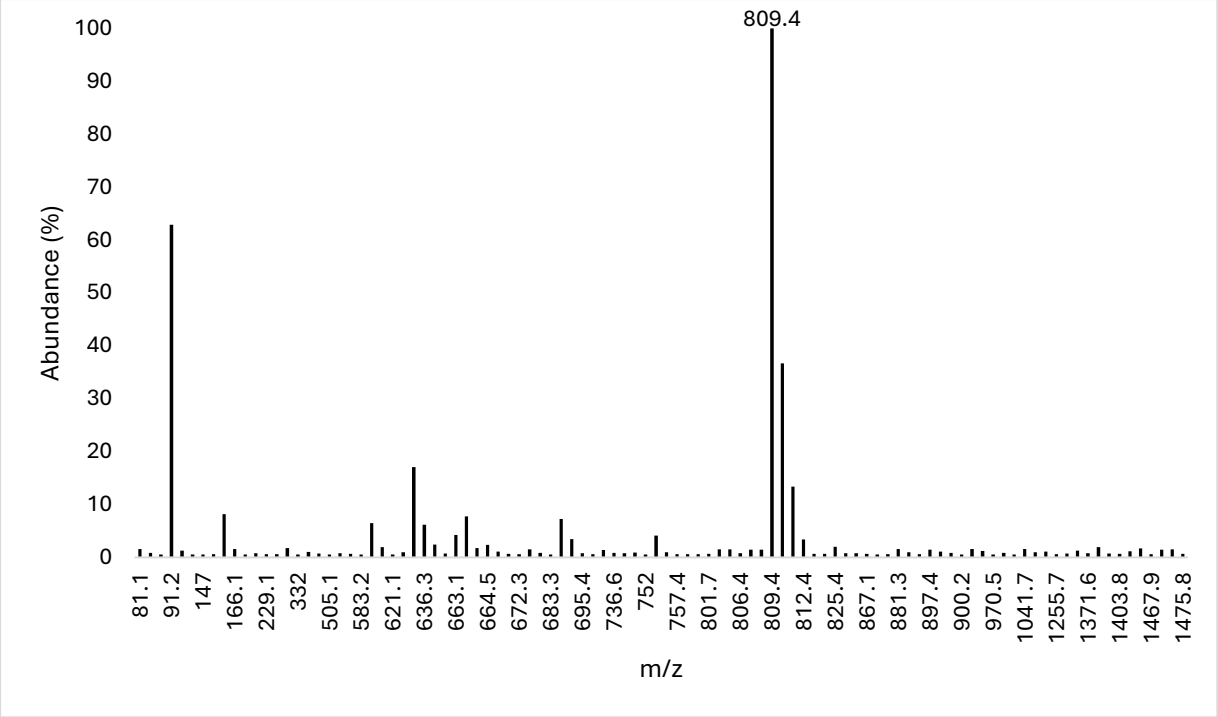

Figure S116. MS spectrum extracted from LA control chromatogram at retention time 25.7 min. Labeled m/z signal represents 11LA.

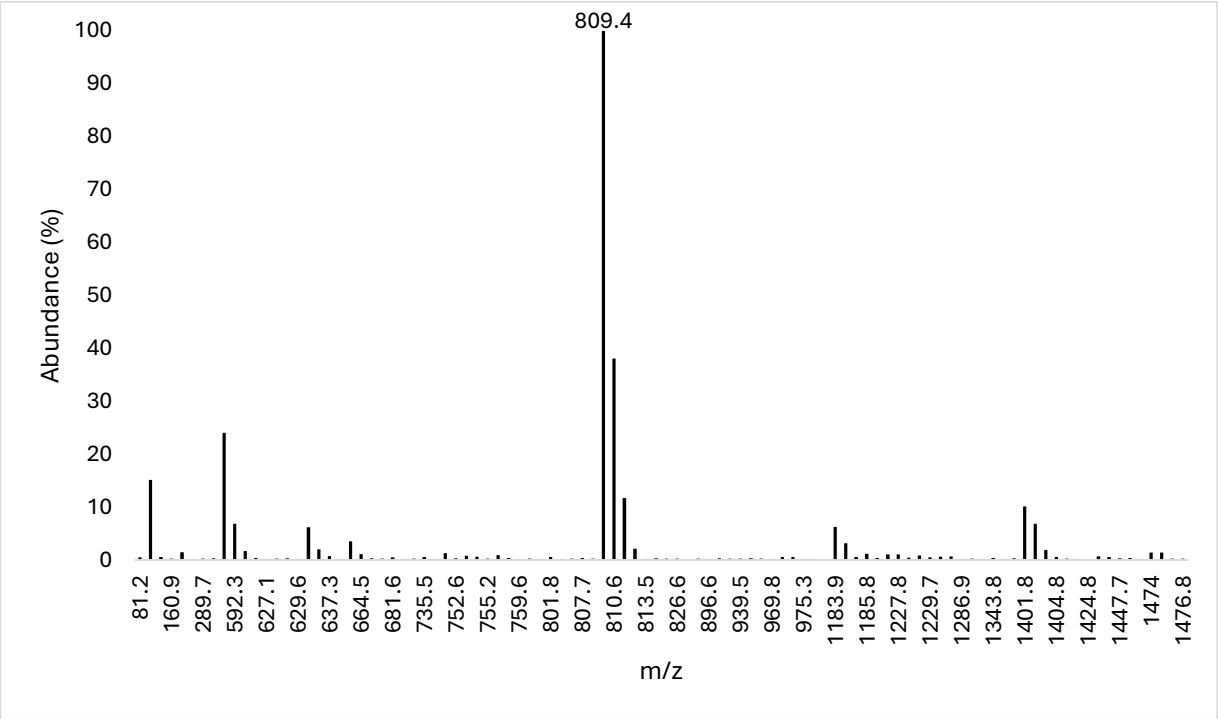

Figure S117. MS spectrum extracted from LA control chromatogram at retention time 25.9 min. Labeled m/z signal represents 11LA.

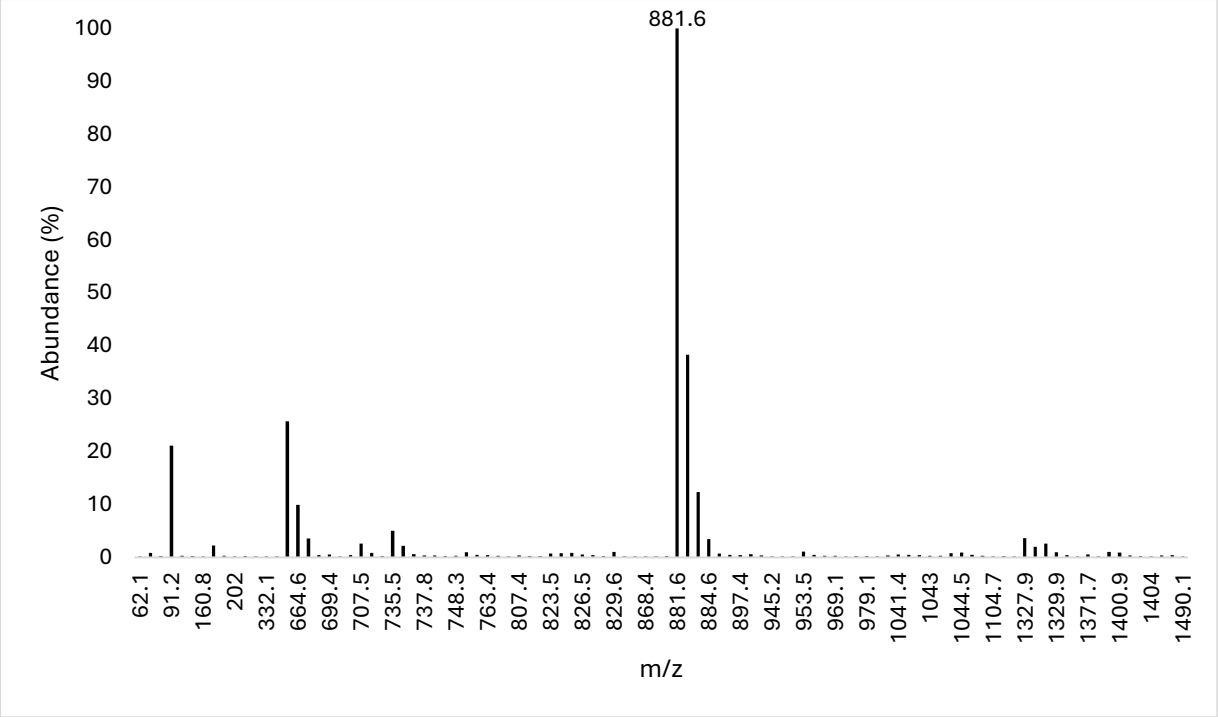

Figure S118. MS spectrum extracted from LA control chromatogram at retention time 26.6 min. Labeled m/z signal represents 12LA.

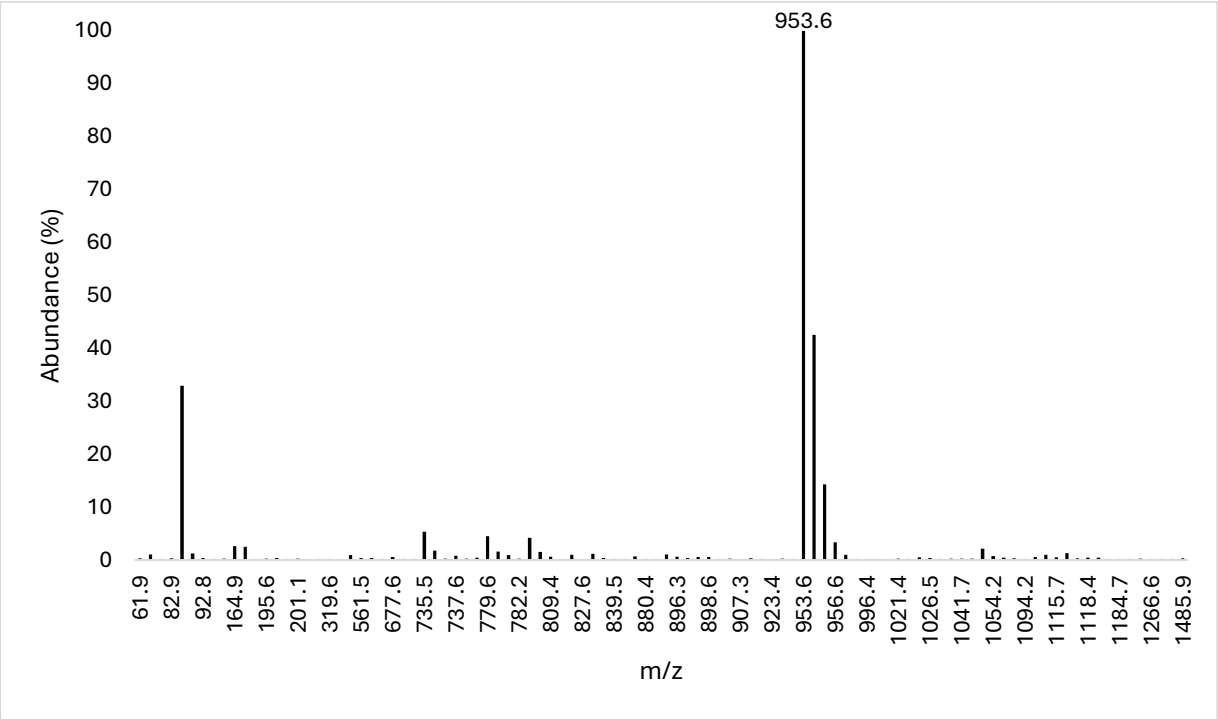

Figure S119. MS spectrum extracted from LA control chromatogram at retention time 27.1 min. Labeled m/z signal represents 13LA.

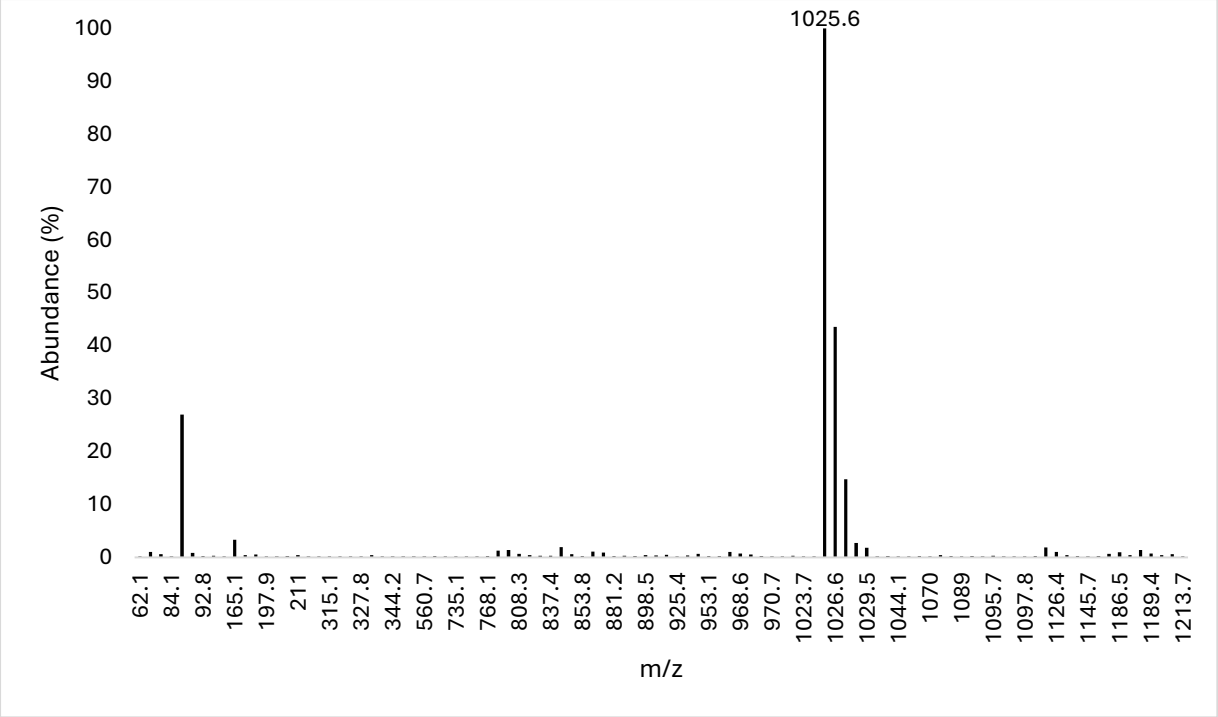

Figure S120. MS spectrum extracted from LA control chromatogram at retention time 27.6 min. Labeled m/z signal represents 14LA.

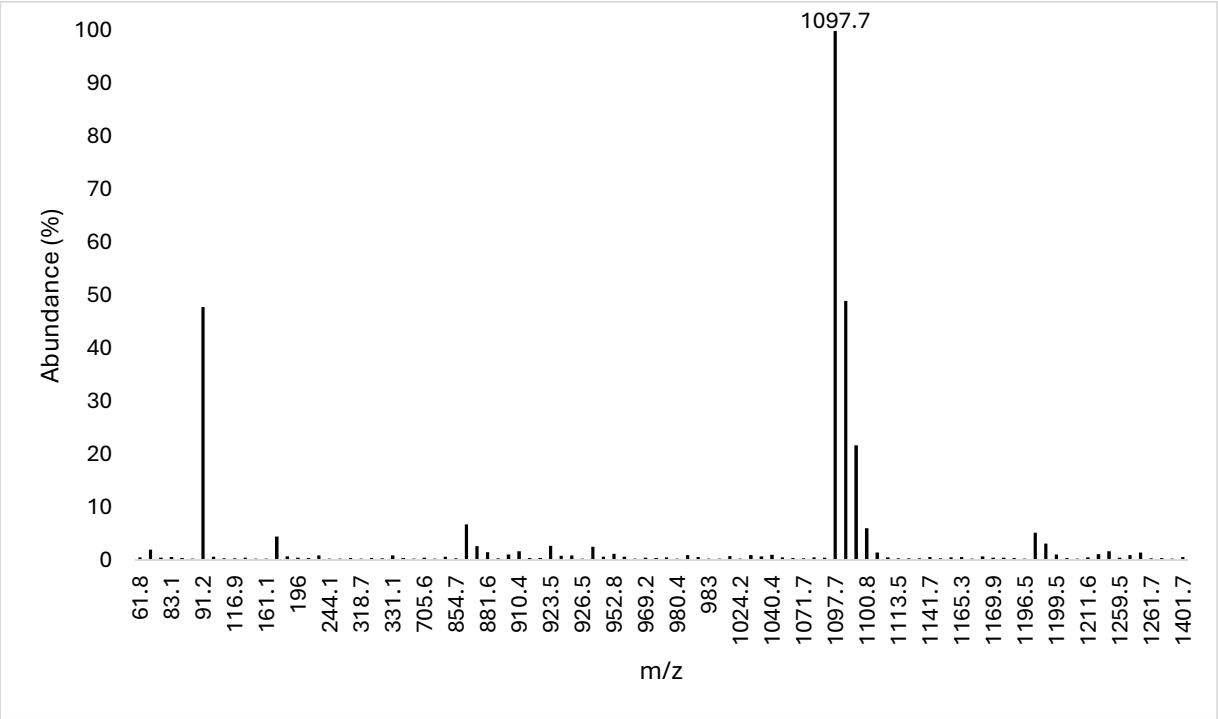

Figure S121. MS spectrum extracted from LA control chromatogram at retention time 28.1 min. Labeled m/z signal represents 15LA.

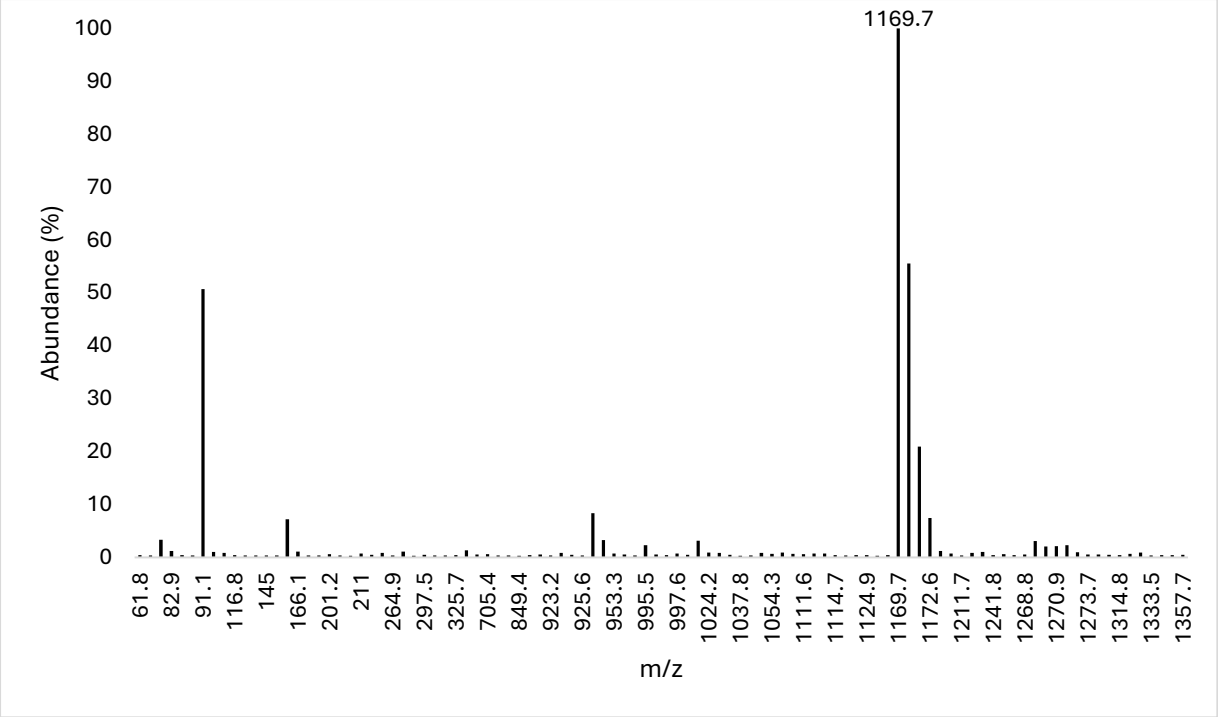

Figure S122. MS spectrum extracted from LA control chromatogram at retention time 28.5 min. Labeled m/z signal represents 16LA.

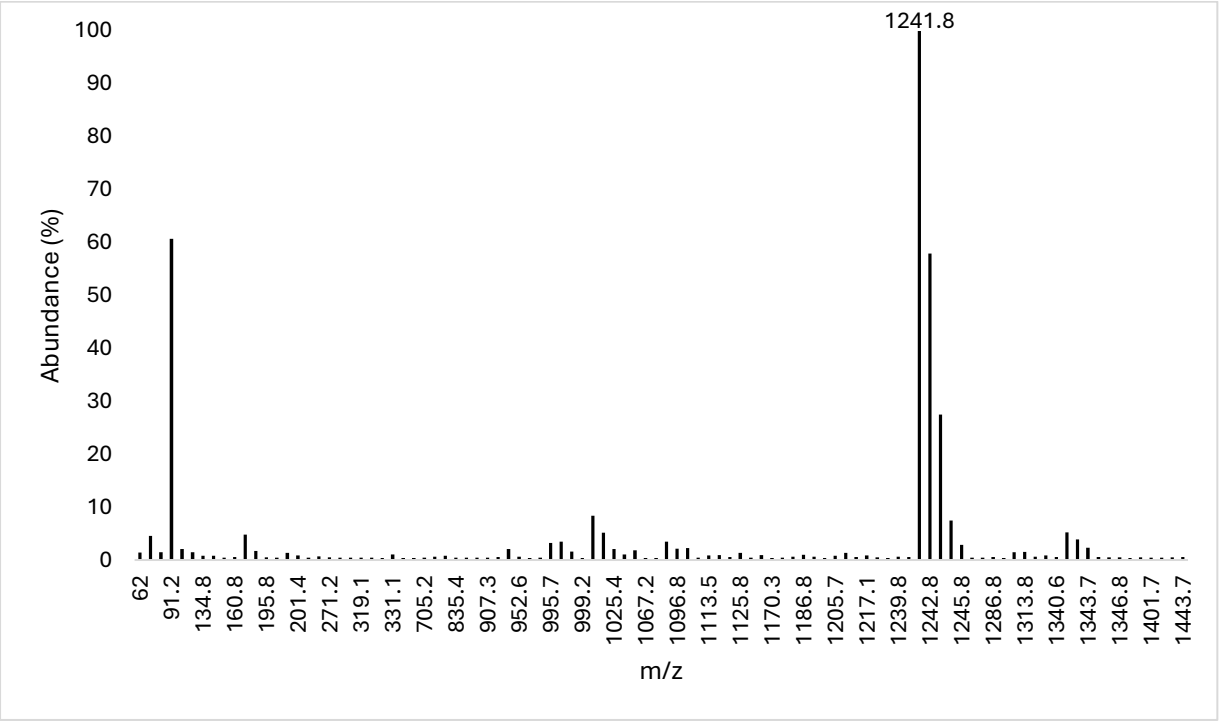

Figure S123. MS spectrum extracted from LA control chromatogram at retention time 28.9 min. Labeled m/z signal represents 17LA.

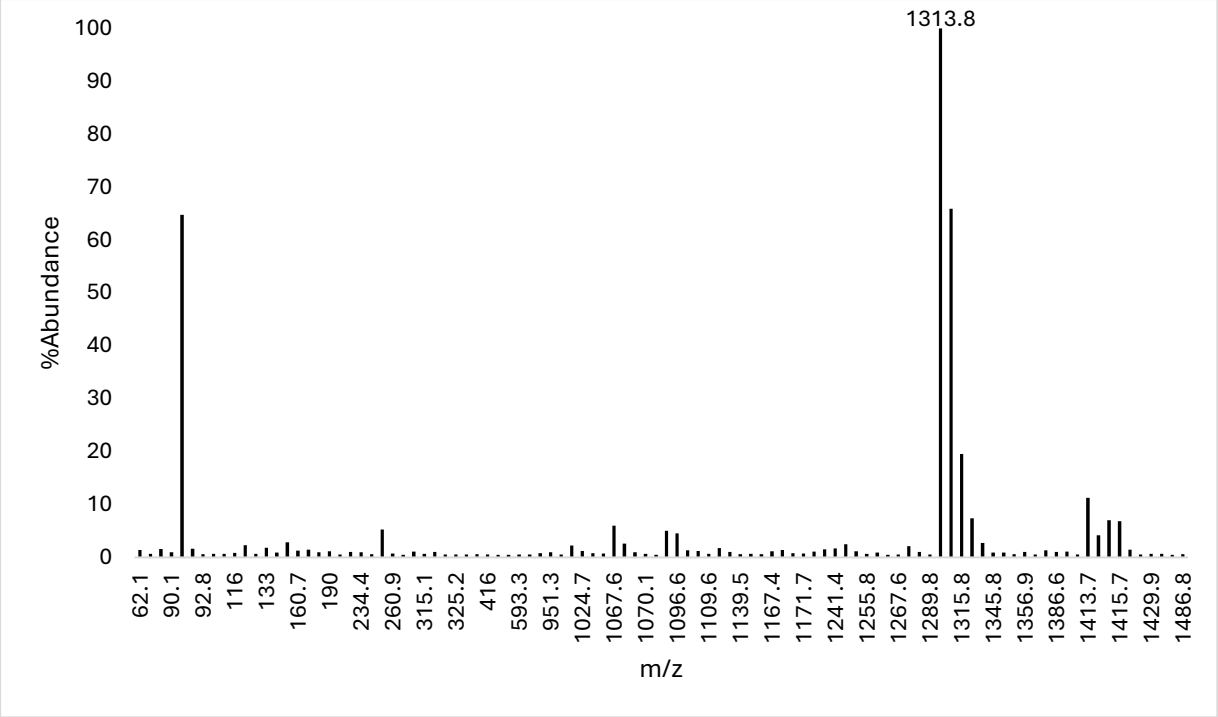

Figure S124. MS spectrum extracted from LA control chromatogram at retention time 29.1 min. Labeled m/z signal represents 18LA.

Table S7. Identification of GA reaction products (in the absence of DA). The detected products based on retention time and their corresponding m/z and ionization pattern as determined by LC-MS.

Retention time (min)	Compound	M (g/mol)	Corresponding m/z (-TIC)	Ionization pattern
13.1	4GA	250.1	249.1, 499.1	$[M-H]^-$, $[2M-H]^-$
14.2	5GA	308.2	307.1, 615.3	$[M-H]^-$, $[2M-H]^-$
15.2	6GA	366.2	365.1, 731.4	$[M-H]^-$, $[2M-H]^-$
16.2	7GA	424.2	423.2, 847.3	$[M-H]^-$, $[2M-H]^-$
17.0	8GA	482.3	481.2, 963.5	$[M-H]^-$, $[2M-H]^-$
17.8	9GA	540.3	539.2, 1079.5	$[M-H]^-$, $[2M-H]^-$
18.5	10GA	598.3	597.2, 1195.6	$[M-H]^-$, $[2M-H]^-$
19.2	11GA	656.4	655.3, 1311.7	$[M-H]^-$, $[2M-H]^-$
19.7	12GA	714.4	713.1, 1427.5	$[M-H]^-$, $[2M-H]^-$
20.2	13GA	772.4	771.1	$[M-H]^-$
20.7	14GA	830.4	829.3	$[M-H]^-$

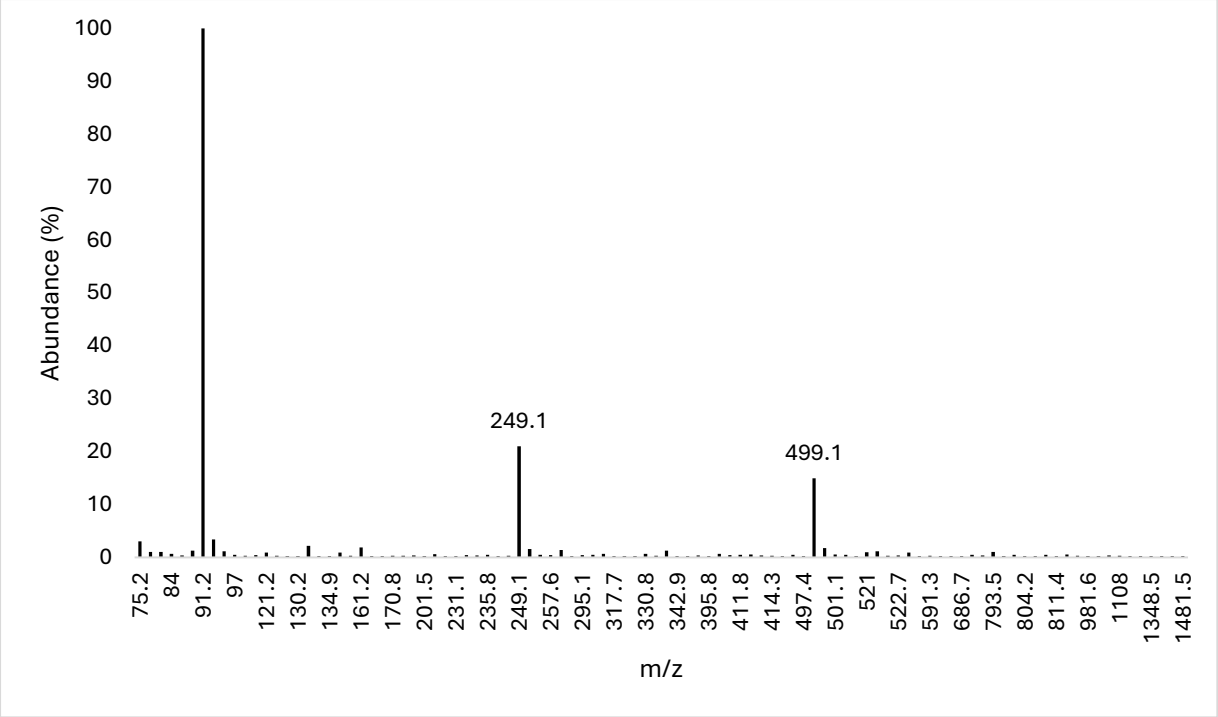

Figure S125. MS spectrum extracted from GA control chromatogram at retention time 13.1 min. Labeled m/z signals represent 4GA.

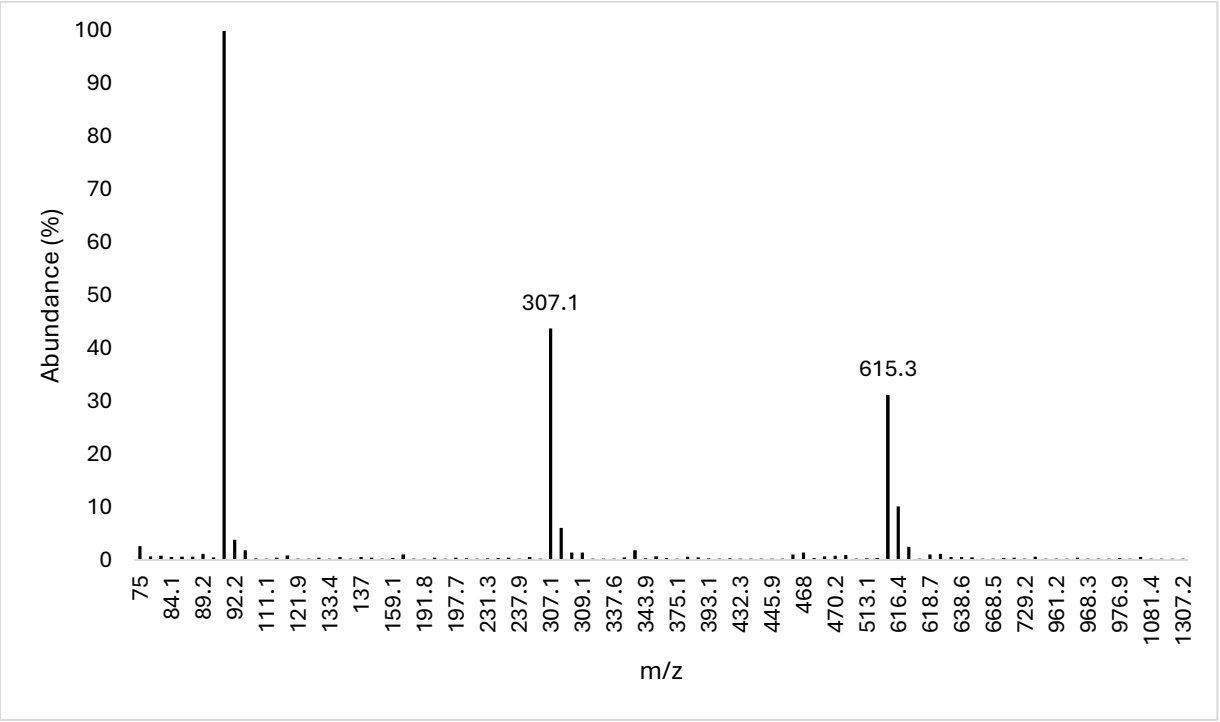

Figure S126. MS spectrum extracted from GA control chromatogram at retention time 14.2 min. Labeled m/z signals represent 5GA.

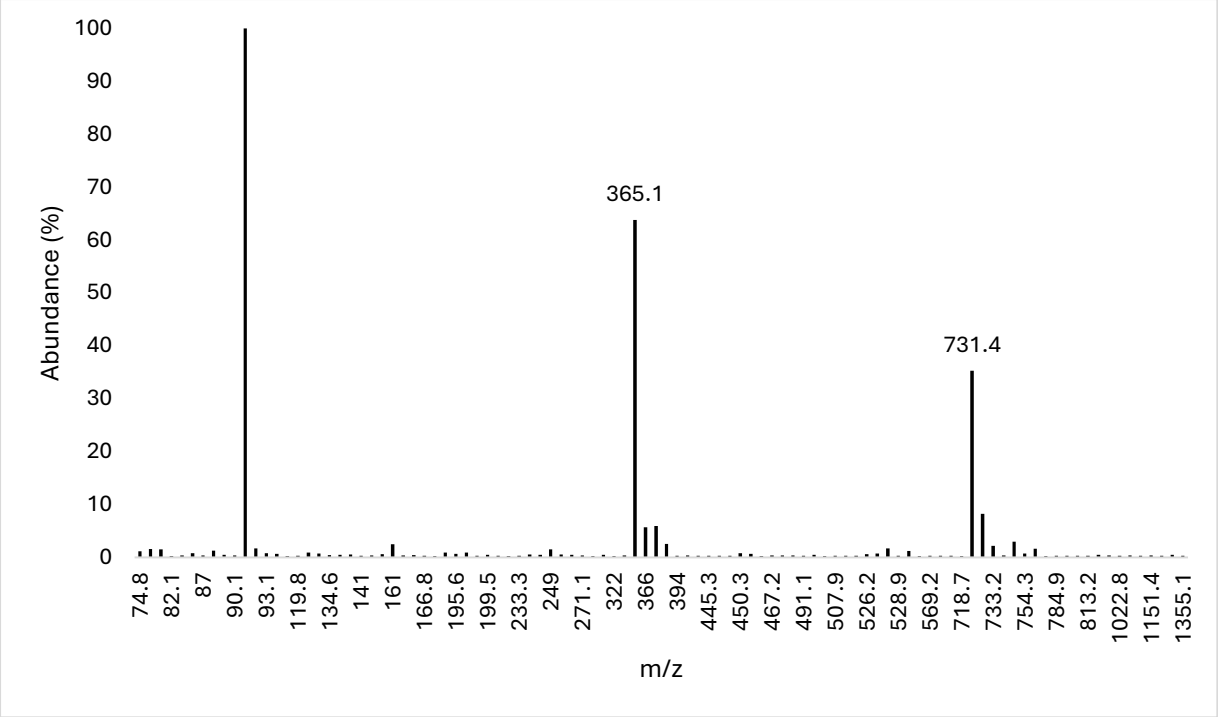

Figure S127. MS spectrum extracted from GA control chromatogram at retention time 15.2 min. Labeled m/z signals represent 6GA.

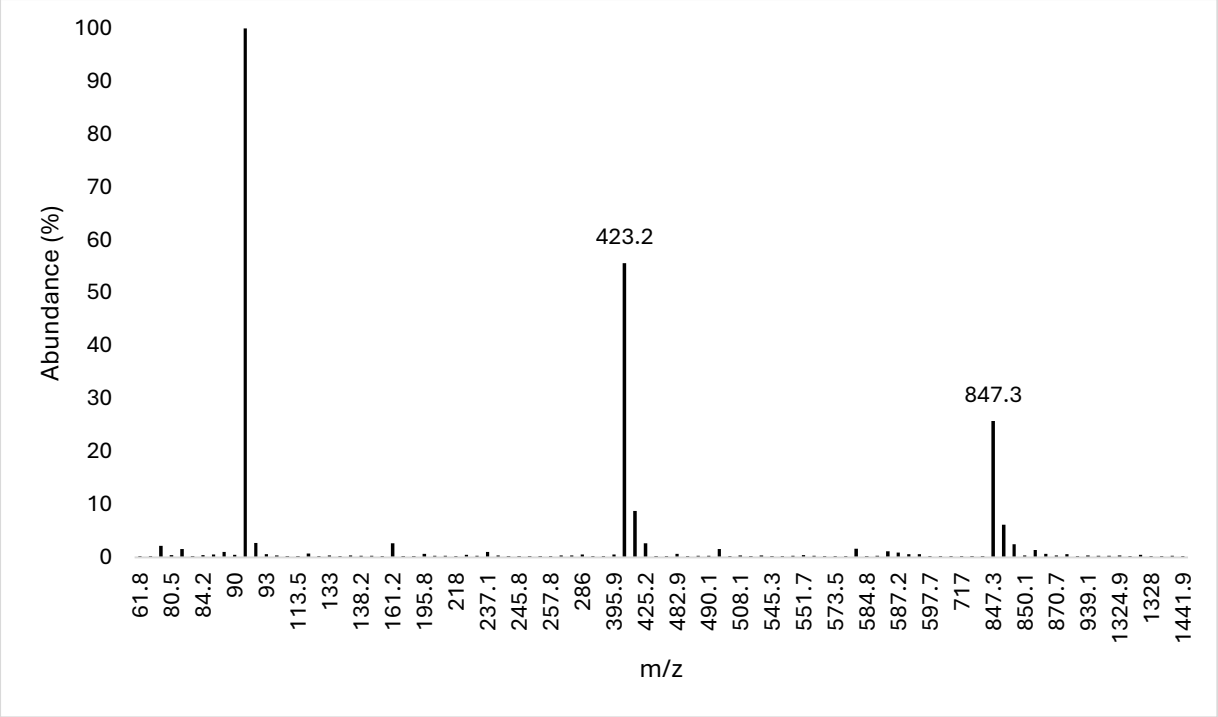

Figure S128. MS spectrum extracted from GA control chromatogram at retention time 16.2 min. Labeled m/z signals represent 7GA.

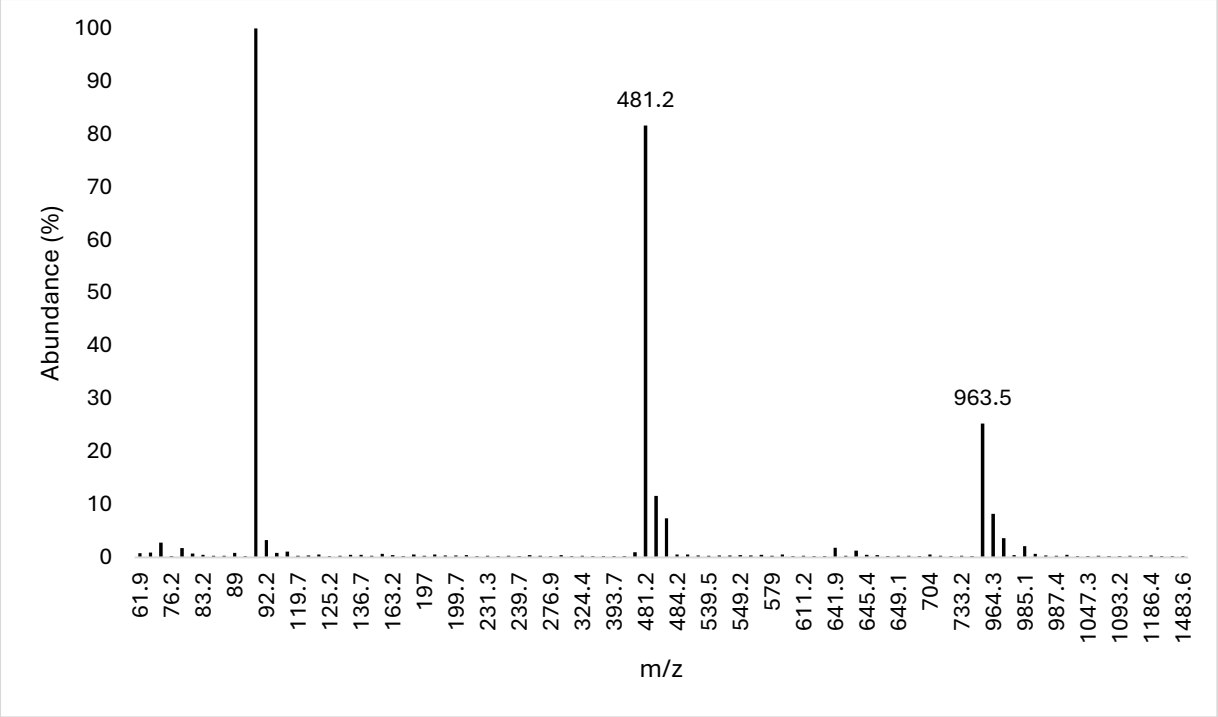

Figure S129. MS spectrum extracted from GA control chromatogram at retention time 17.0 min. Labeled m/z signals represent 8GA.

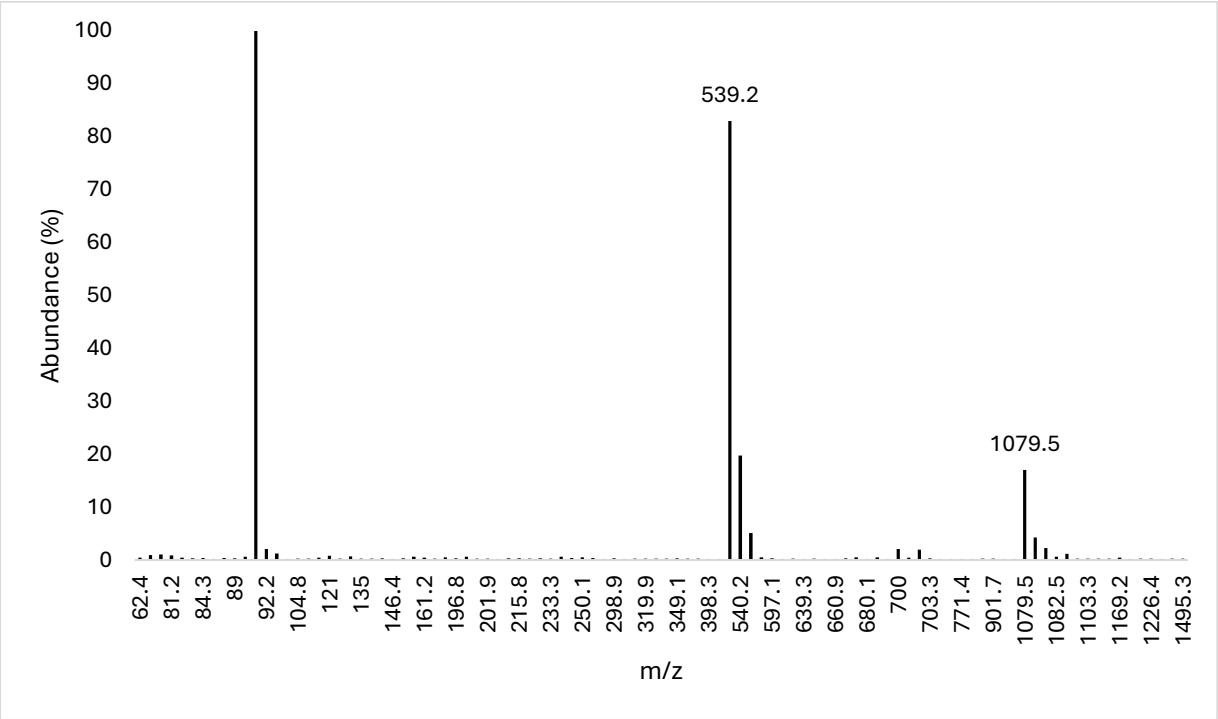

Figure S130. MS spectrum extracted from GA control chromatogram at retention time 17.8 min. Labeled m/z signals represent 9GA.

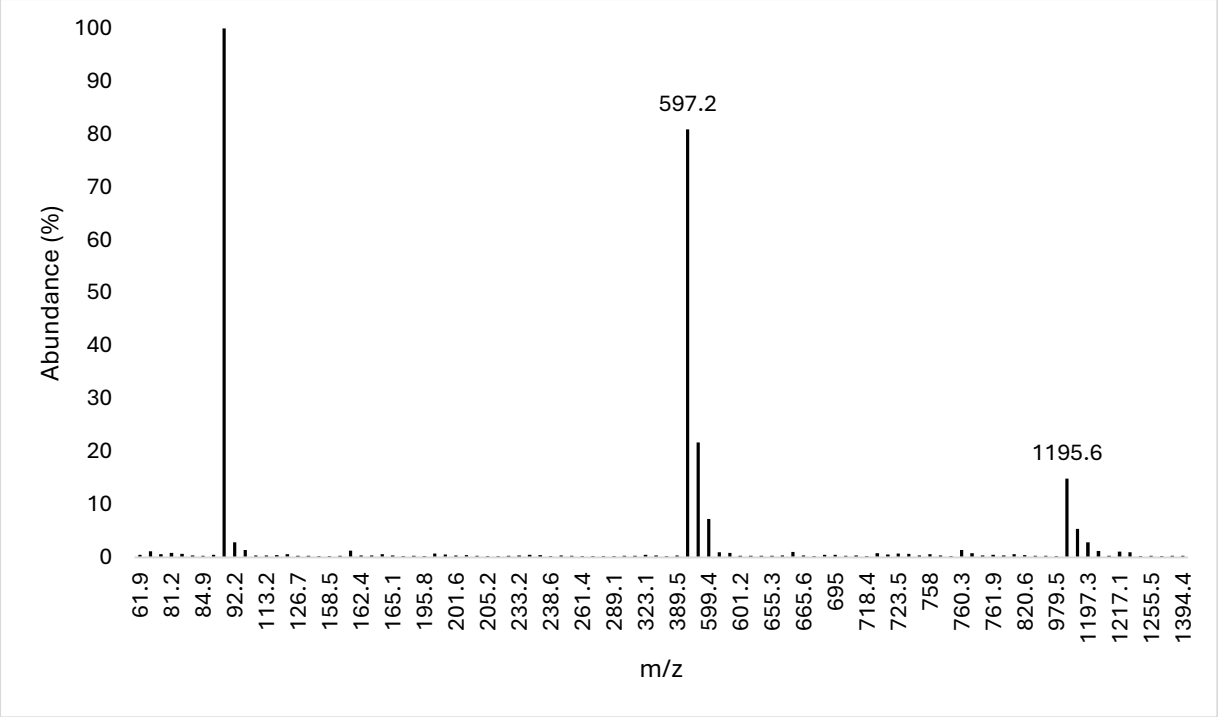

Figure S131. MS spectrum extracted from GA control chromatogram at retention time 18.5 min. Labeled m/z signals represent 10GA.

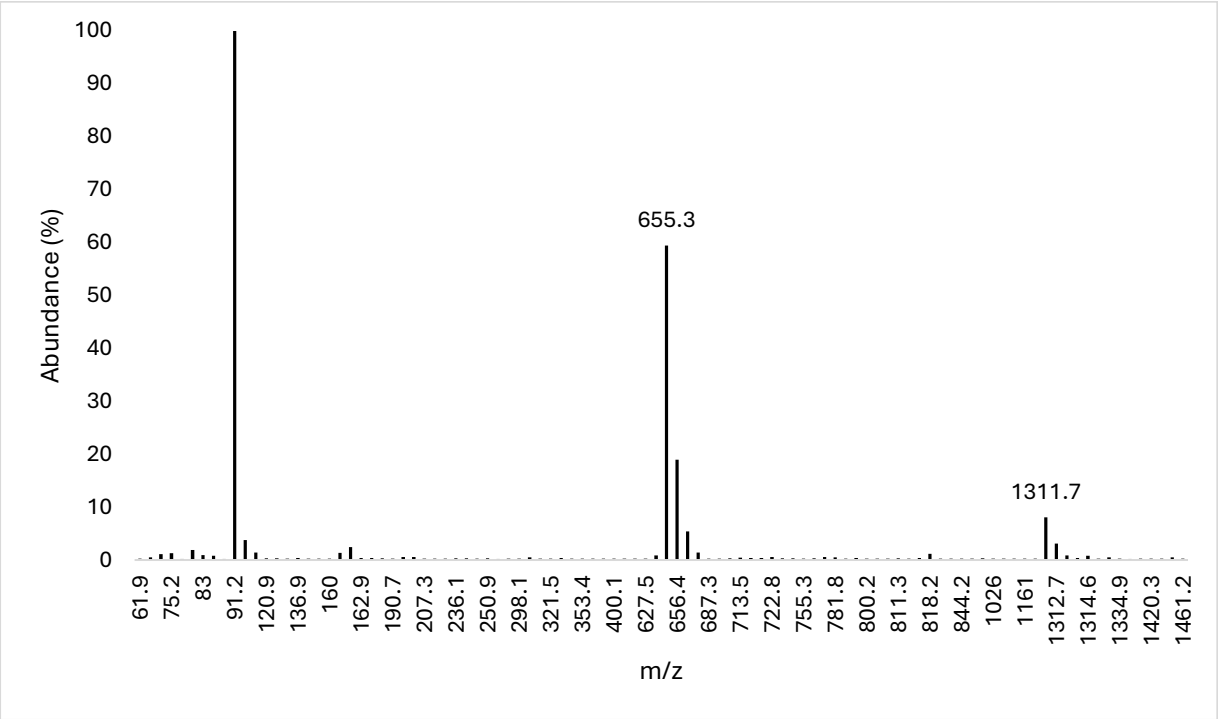

Figure S132. MS spectrum extracted from GA control chromatogram at retention time 19.2 min. Labeled m/z signals represent 11GA.

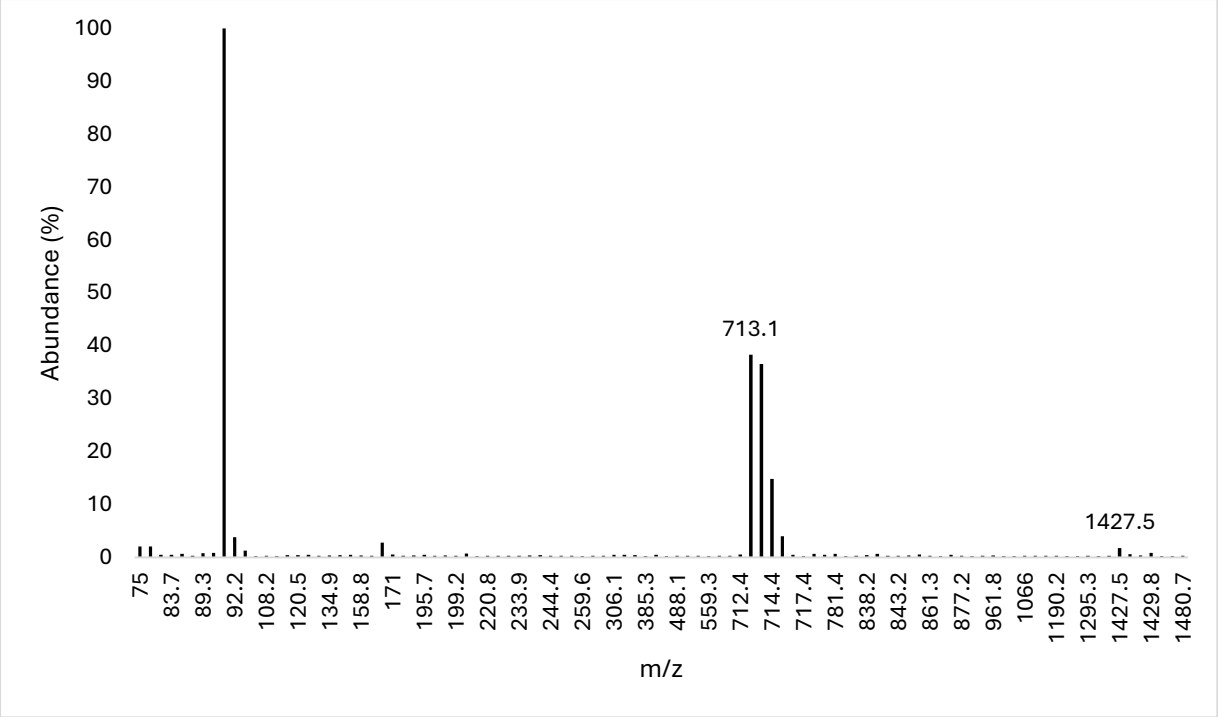

Figure S133. MS spectrum extracted from GA control chromatogram at retention time 19.7 min. Labeled m/z signals represent 12GA.

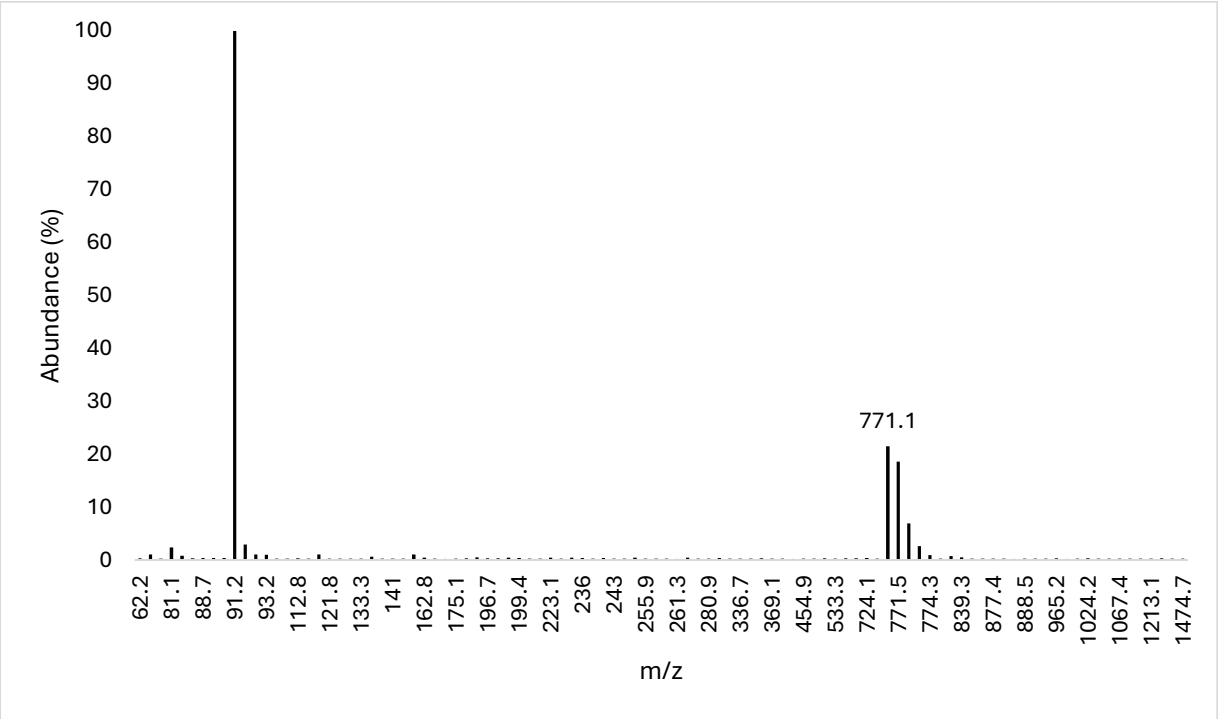

Figure S134. MS spectrum extracted from GA control chromatogram at retention time 20.2 min. Labeled m/z signal represents 13GA.

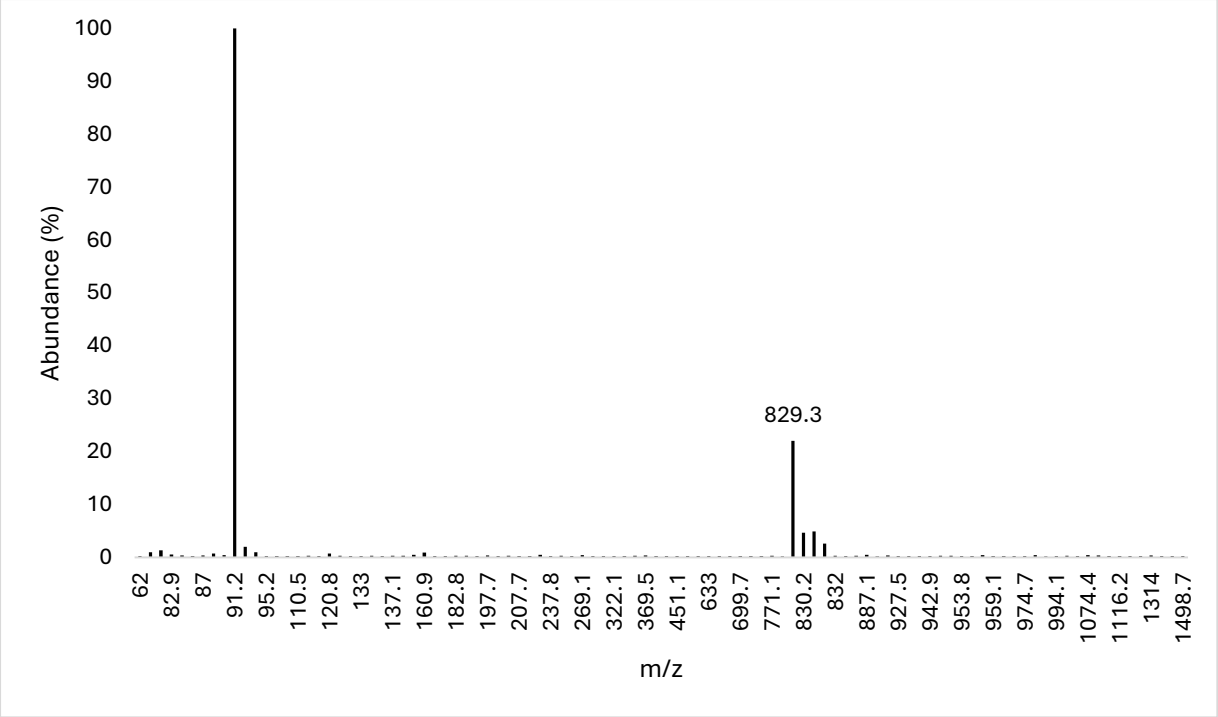

Figure S135. MS spectrum extracted from GA control chromatogram at retention time 20.7 min. Labeled m/z signal represents 14GA.

Table S8. Identification of MA reaction products (in the absence of DA). The detected products based on retention time and their corresponding m/z and ionization pattern as determined by LC-MS.

Retention time (min)	Compound	M (g/mol)	Corresponding m/z (-TIC)	Ionization pattern
7.7	2MA	250.2	249.0	$[M-H]^-$
8.7	2MA	250.2	249.1	$[M-H]^-$
11.3	3MA	366.2	365.2, 731.1	$[M-H]^-$, $[2M-H]^-$
12.5	3MA	366.2	365.2, 731.3	$[M-H]^-$, $[2M-H]^-$
	4MA	482.3	481.3, 963.4	$[M-H]^-$, $[2M-H]^-$
12.8	4MA	482.3	481.2, 963.4	$[M-H]^-$, $[2M-H]^-$
	5MA	598.4	597.4	$[M-H]^-$
13.1	4MA	482.3	481.3, 963.3	$[M-H]^-$, $[2M-H]^-$
	5MA	598.4	597.2	$[M-H]^-$
13.4	4MA	482.3	481.3	$[M-H]^-$
	5MA	598.4	597.2, 1195.4	$[M-H]^-$, $[2M-H]^-$
	6MA	714.4	713.2	$[M-H]^-$
13.6	5MA	598.4	597.3, 1195.5	$[M-H]^-$, $[2M-H]^-$
	6MA	714.4	713.4, 356.2	$[M-H]^-$, $[M-2H]^{2-}$
13.9	5MA	598.4	597.3	$[M-H]^-$
	6MA	714.4	713.3, 356.2	$[M-H]^-$, $[M-2H]^{2-}$
	7MA	830.5	829.3	$[M-H]^-$
14.1	6MA	714.4	713.3, 356.2	$[M-H]^-$, $[M-2H]^{2-}$
	7MA	830.5	829.3, 414.2	$[M-H]^-$, $[M-2H]^{2-}$
	8MA	946.6	945.5, 472.2	$[M-H]^-$, $[M-2H]^{2-}$
14.5	7MA	830.5	829.3, 414.0	$[M-H]^-$, $[M-2H]^{2-}$
	8MA	946.6	945.4, 472.2	$[M-H]^-$, $[M-2H]^{2-}$
	9MA	1062.7	1061.5, 530.3	$[M-H]^-$, $[M-2H]^{2-}$
	10MA	1178.7	1177.5, 588.5	$[M-H]^-$, $[M-2H]^{2-}$
14.9	8MA	946.6	945.5, 472.2	$[M-H]^-$, $[M-2H]^{2-}$
	9MA	1062.7	1061.4, 530.3	$[M-H]^-$, $[M-2H]^{2-}$
	10MA	1178.7	1177.5, 588.1	$[M-H]^-$, $[M-2H]^{2-}$
	11MA	1294.8	1293.5, 646.2	$[M-H]^-$, $[M-2H]^{2-}$
	12MA	1410.9	704.4	$[M-2H]^{2-}$
15.0	9MA	1062.7	530.2	$[M-2H]^{2-}$
	10MA	1178.7	1177.5, 588.3	$[M-H]^-$, $[M-2H]^{2-}$
	11MA	1294.8	1293.4, 646.3	$[M-H]^-$, $[M-2H]^{2-}$
	12MA	1410.9	704.4	$[M-2H]^{2-}$
	13MA	1526.9	762.4	$[M-2H]^{2-}$
15.6	12MA	1410.9	704.8	$[M-2H]^{2-}$
	13MA	1526.9	762.6	$[M-2H]^{2-}$
	14MA	1643	820.2	$[M-2H]^{2-}$
	15MA	1759.1	878.6	$[M-2H]^{2-}$
	16MA	1875.1	936.5	$[M-2H]^{2-}$
16.0	16MA	1875.1	963.5	$[M-2H]^{2-}$
	17MA	1991.2	994.1	$[M-2H]^{2-}$

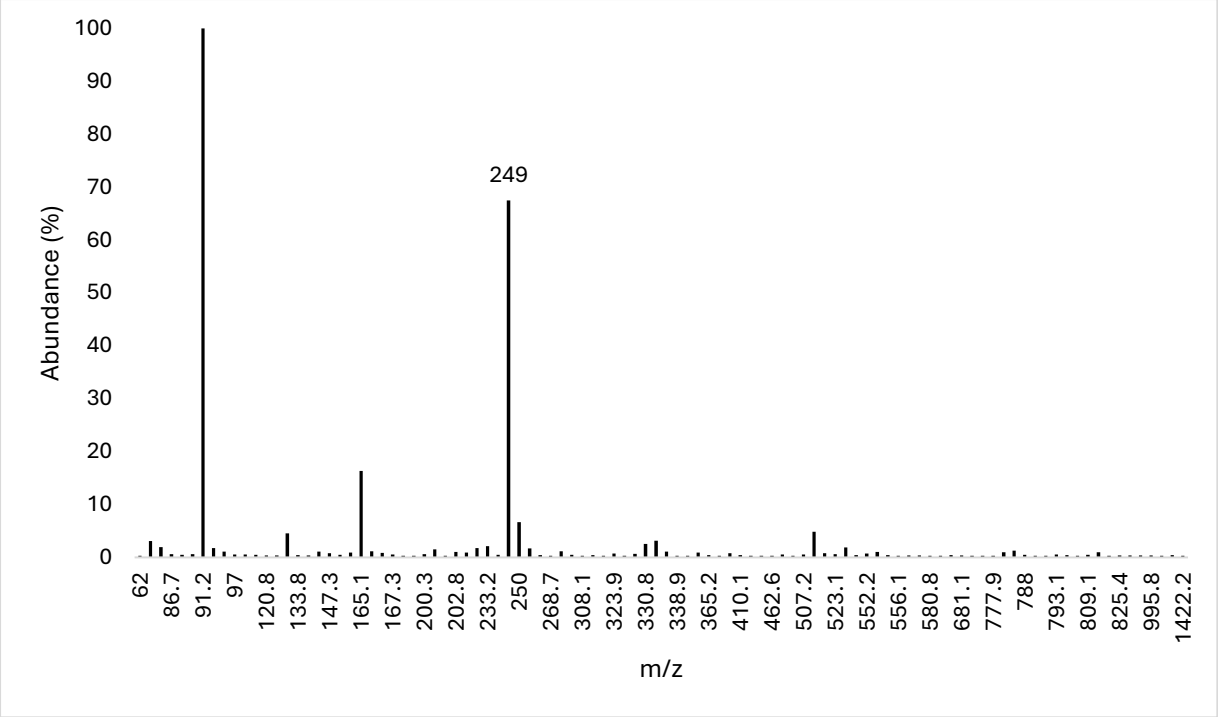

Figure S136. MS spectrum extracted from MA control chromatogram at retention time 7.7 min. Labeled m/z signal represents 2MA.

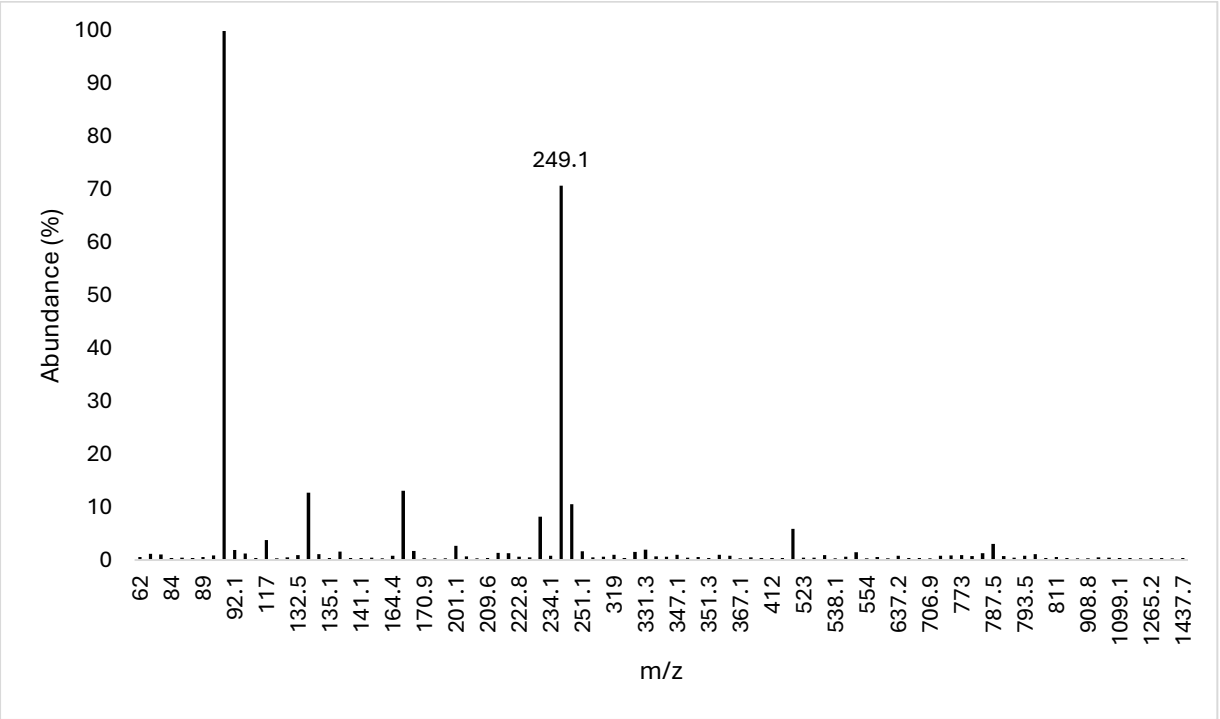

Figure S137. MS spectrum extracted from MA control chromatogram at retention time 8.7 min. Labeled m/z signal represents 2MA.

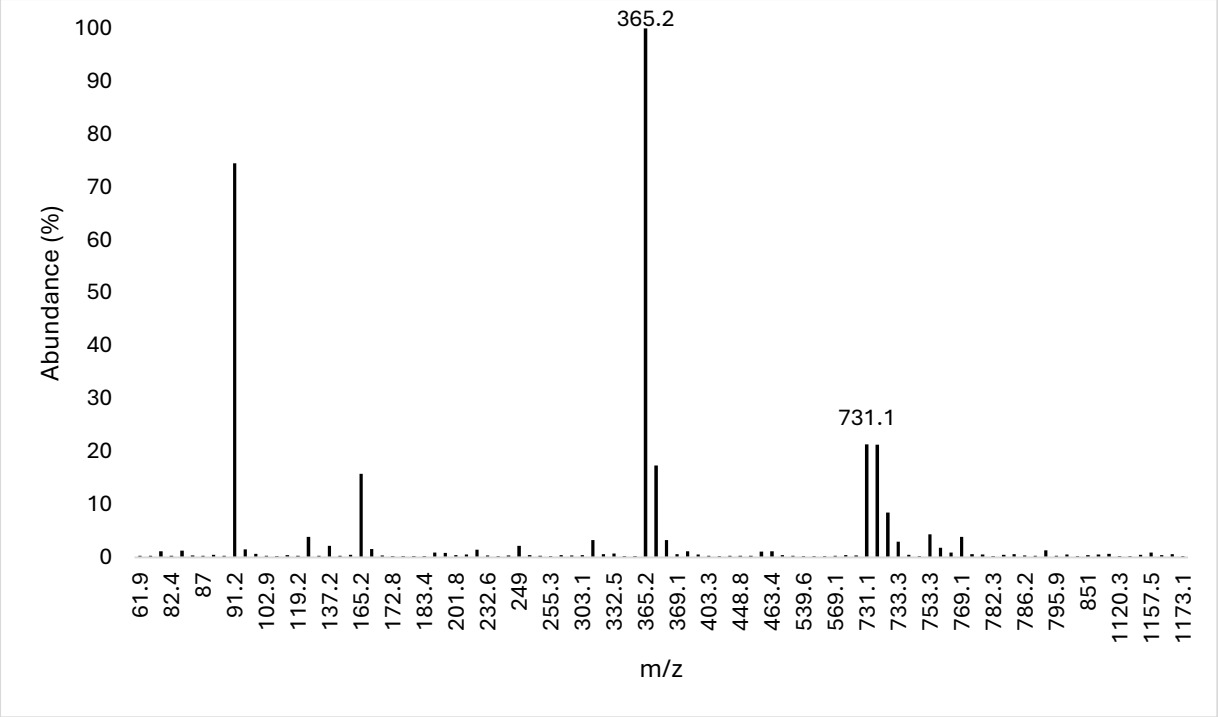

Figure S138. MS spectrum extracted from MA control chromatogram at retention time 11.3 min. Labeled m/z signals represent 3MA.

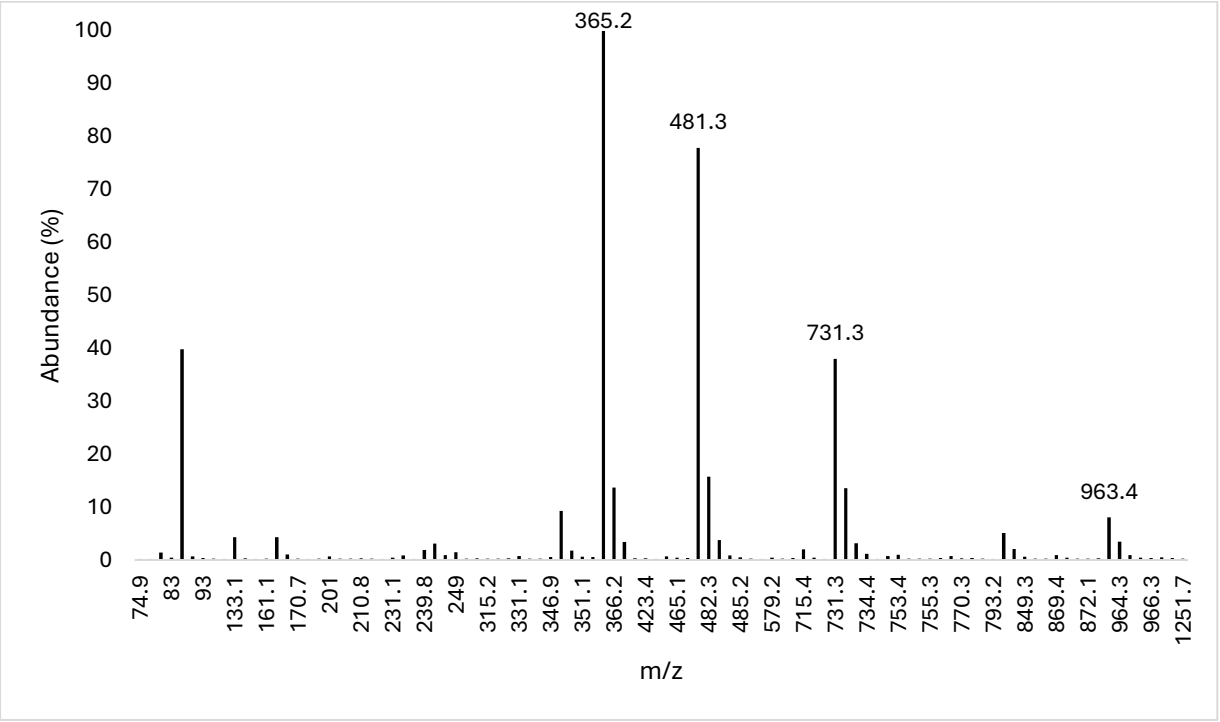

Figure S139. MS spectrum extracted from MA control chromatogram at retention time 12.5 min. Labeled m/z signals represent 3MA and 4MA.

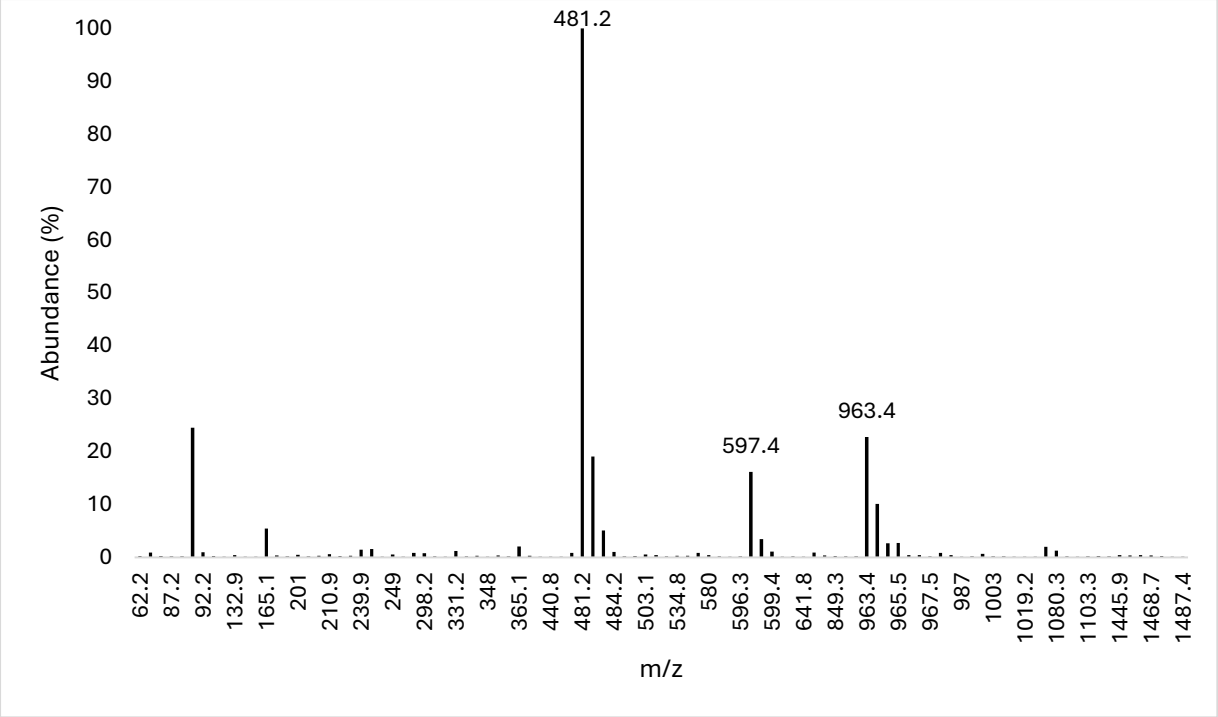

Figure S140. MS spectrum extracted from MA control chromatogram at retention time 12.8 min. Labeled m/z signals represent 4MA and 5MA.

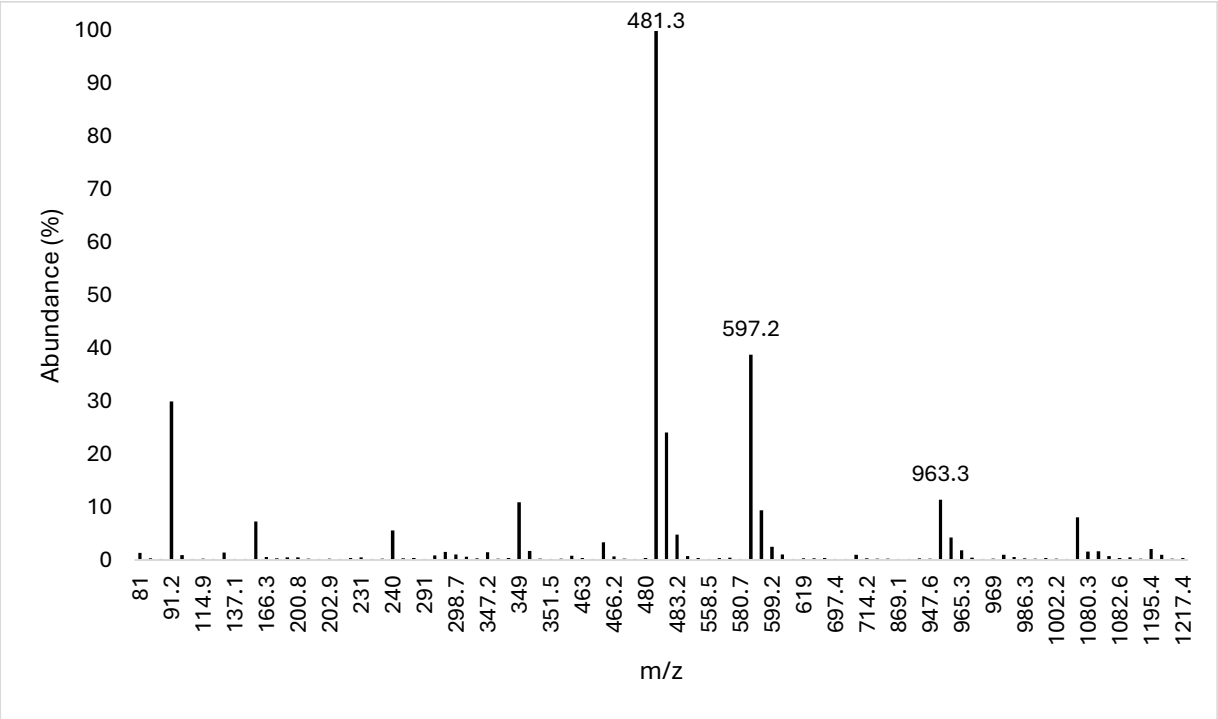

Figure S141. MS spectrum extracted from MA control chromatogram at retention time 13.1 min. Labeled m/z signals represent 4MA and 5MA.

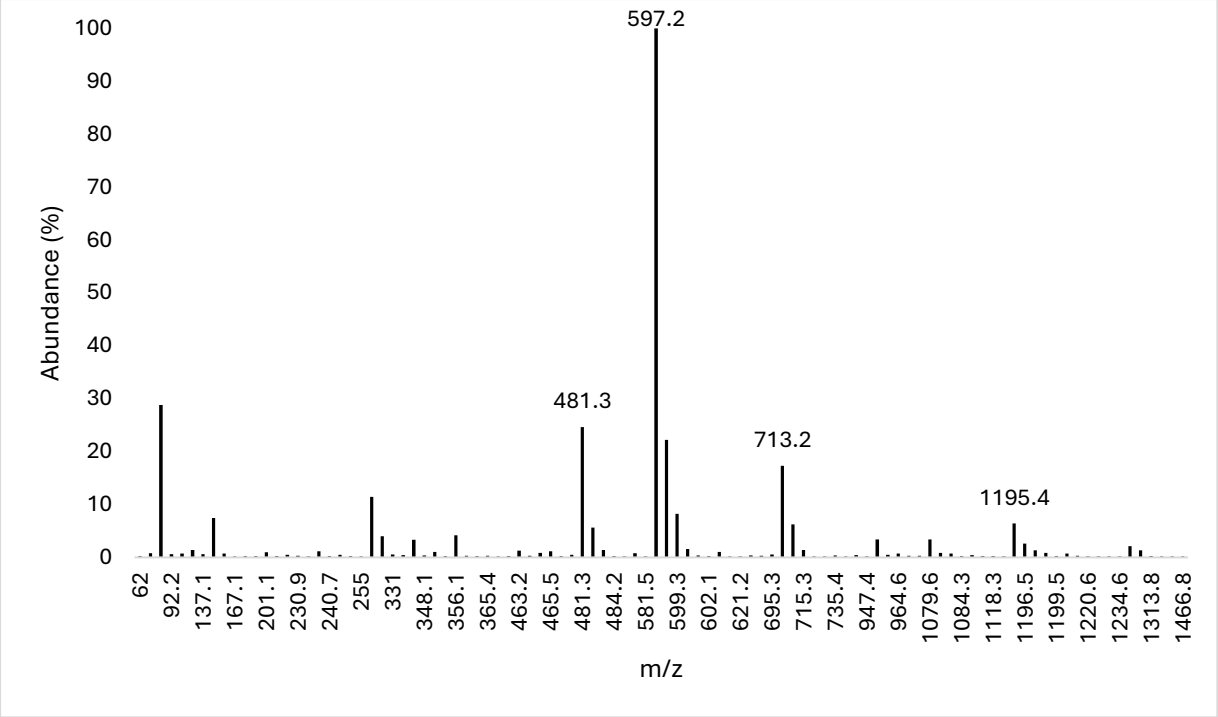

Figure S142. MS spectrum extracted from MA control chromatogram at retention time 13.4 min. Labeled m/z signals represent 4MA, 5MA and 6MA.

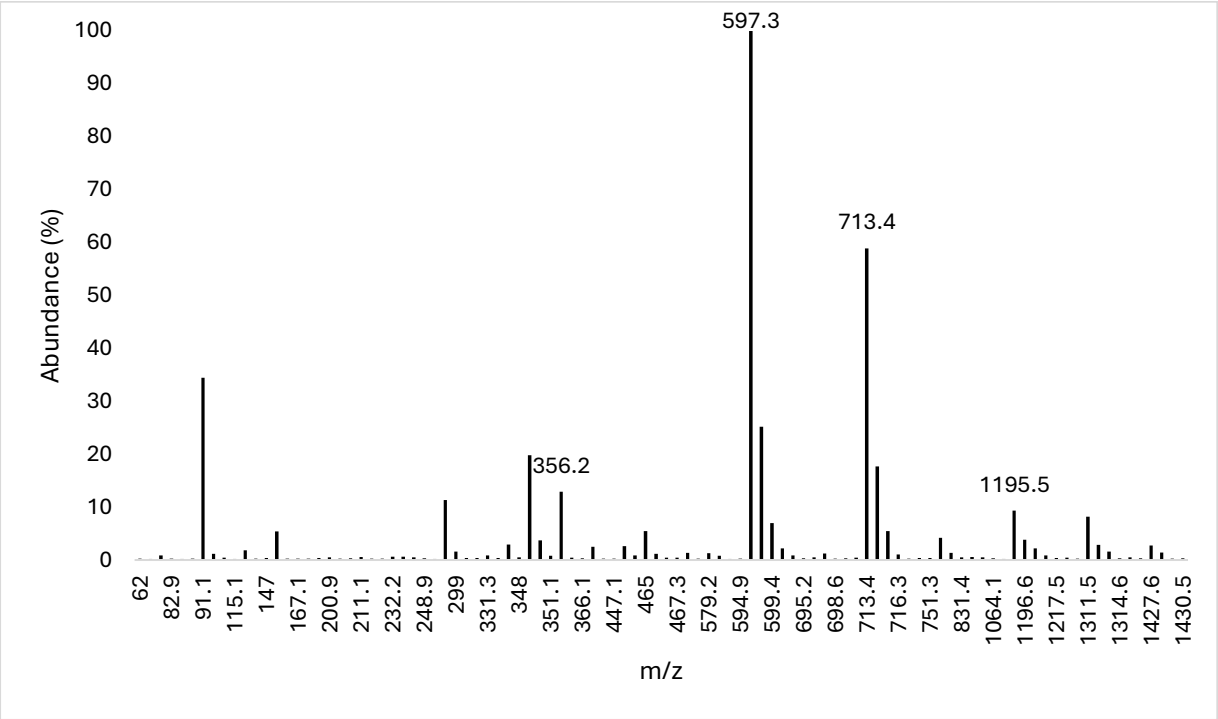

Figure S143. MS spectrum extracted from MA control chromatogram at retention time 13.6 min. Labeled m/z signals represent 5MA and 6MA.

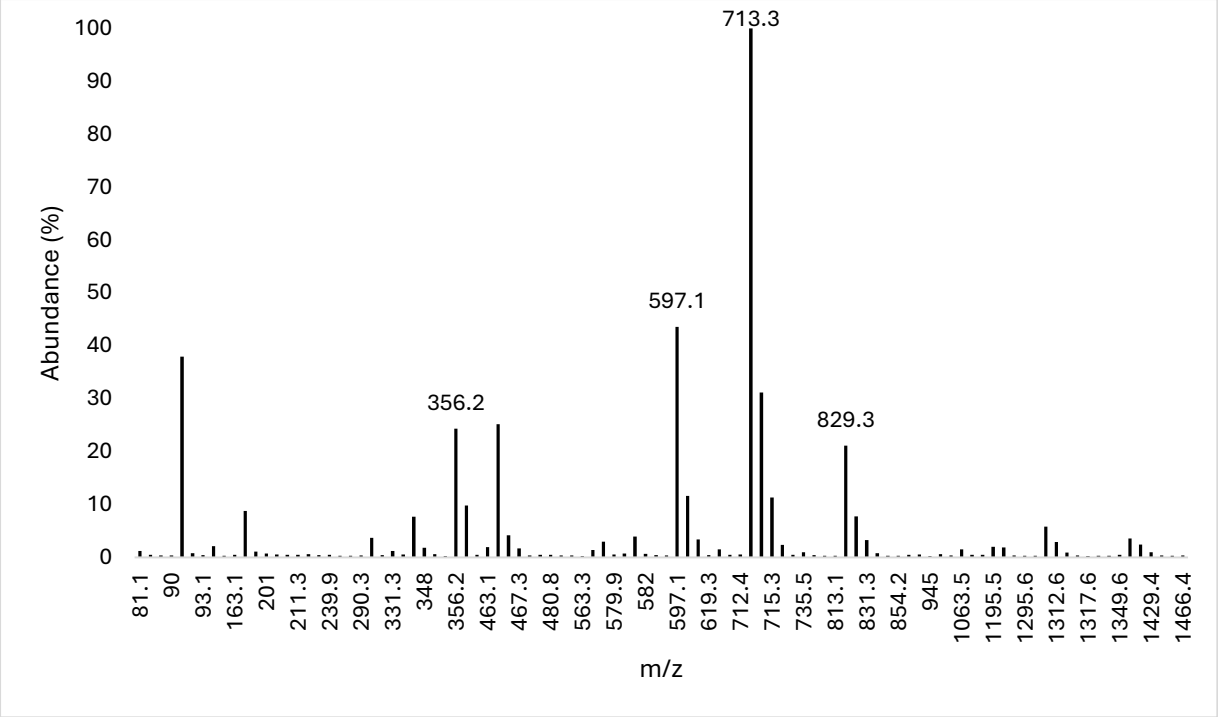

Figure S144. MS spectrum extracted from MA control chromatogram at retention time 13.9 min. Labeled m/z signals represent 5MA, 6MA and 7MA.

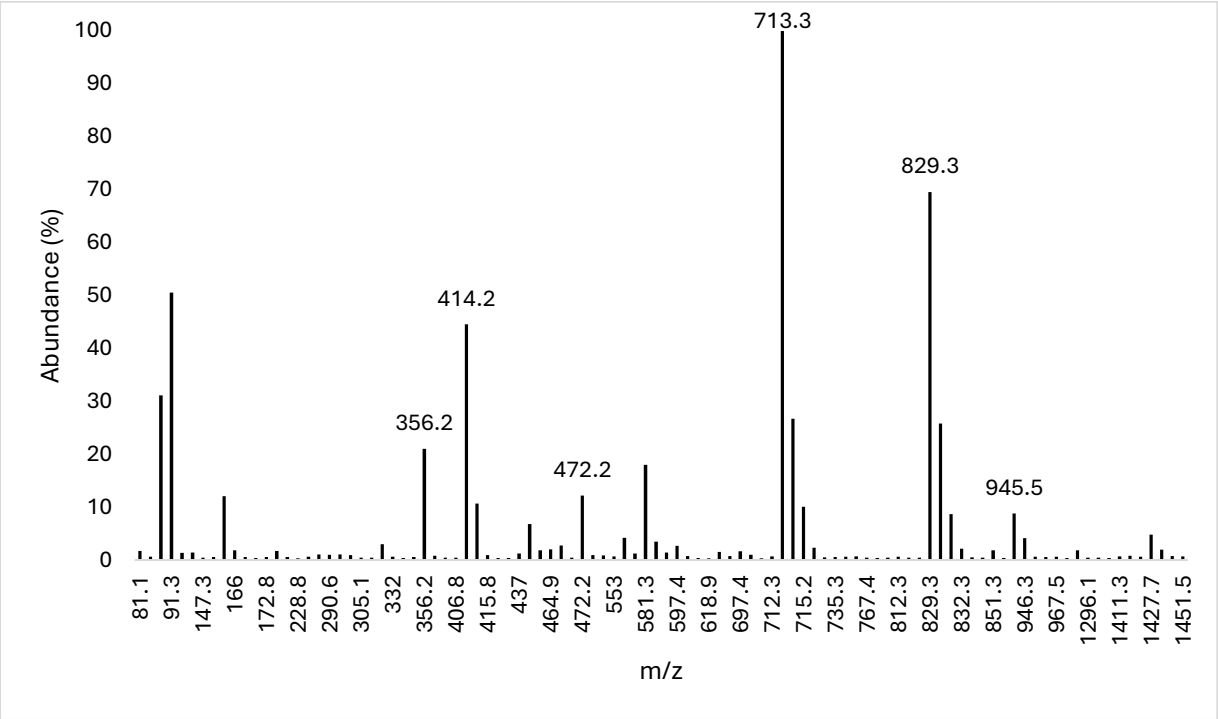

Figure S145. MS spectrum extracted from MA control chromatogram at retention time 14.1 min. Labeled m/z signals represent 6MA, 7MA and 8MA.

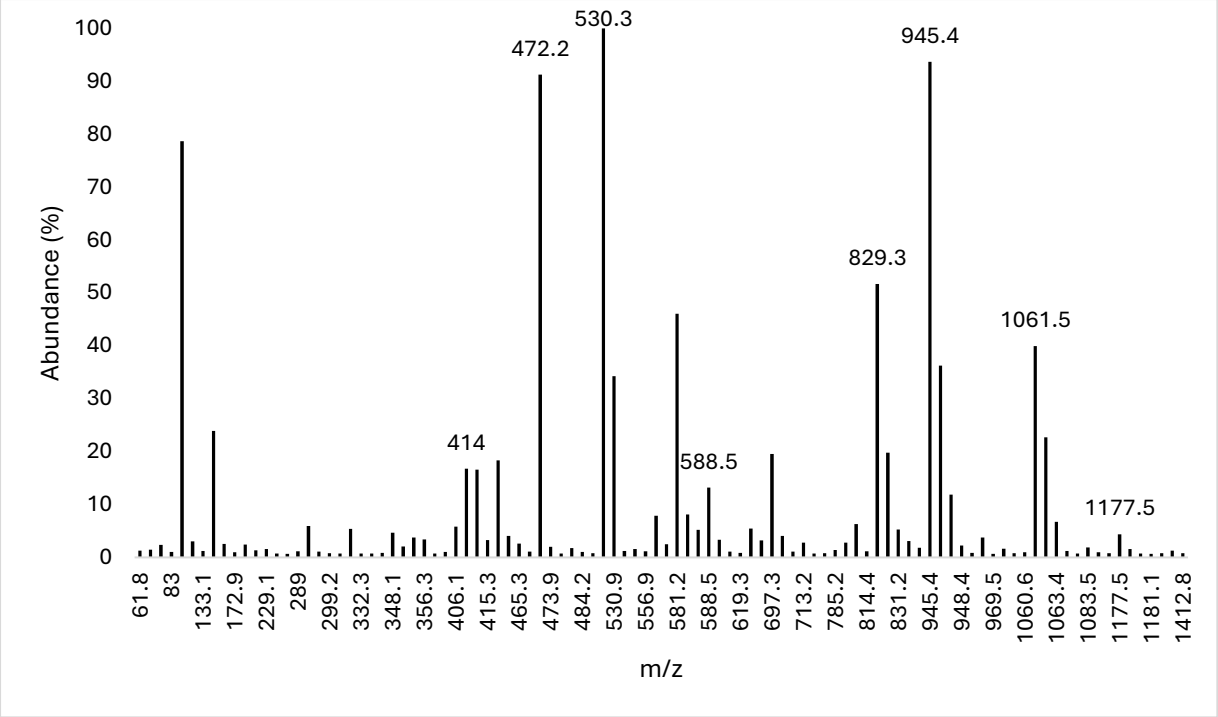

Figure S146. MS spectrum extracted from MA control chromatogram at retention time 14.5 min. Labeled m/z signals represent 7MA, 8MA, 9MA and 10MA.

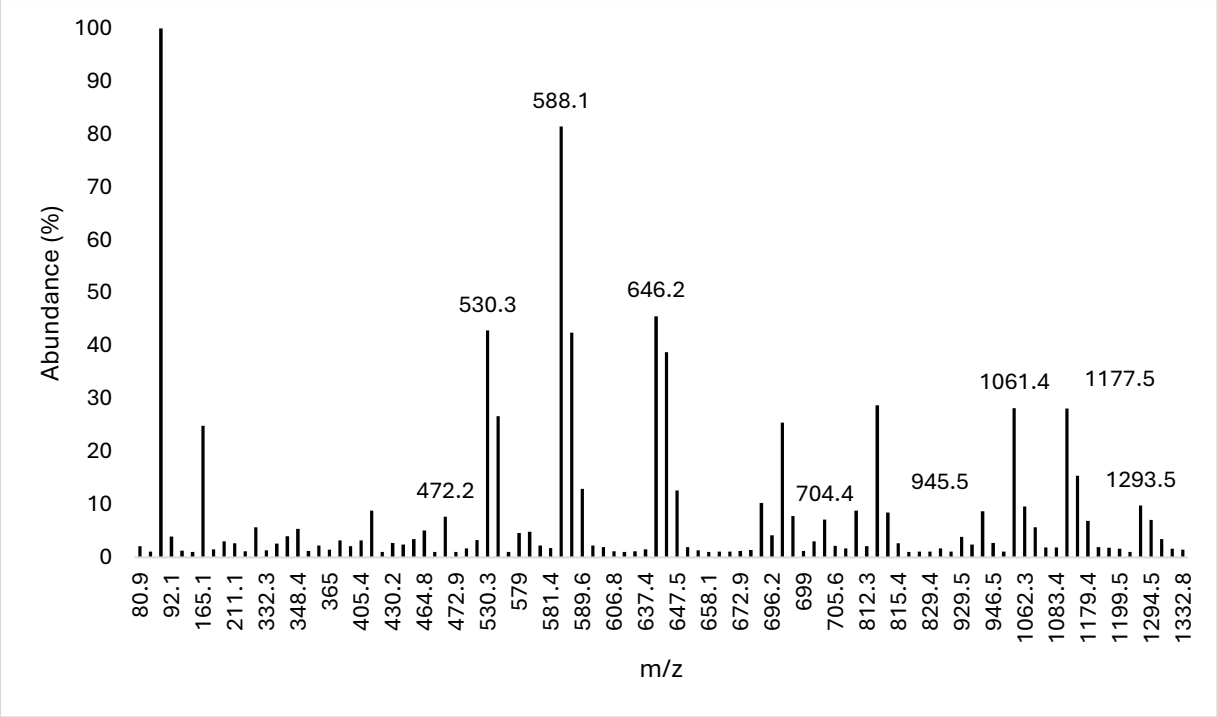

Figure S147. MS spectrum extracted from MA control chromatogram at retention time 14.9 min. Labeled m/z signals represent 8MA, 9MA, 10MA, 11MA and 12MA**.**

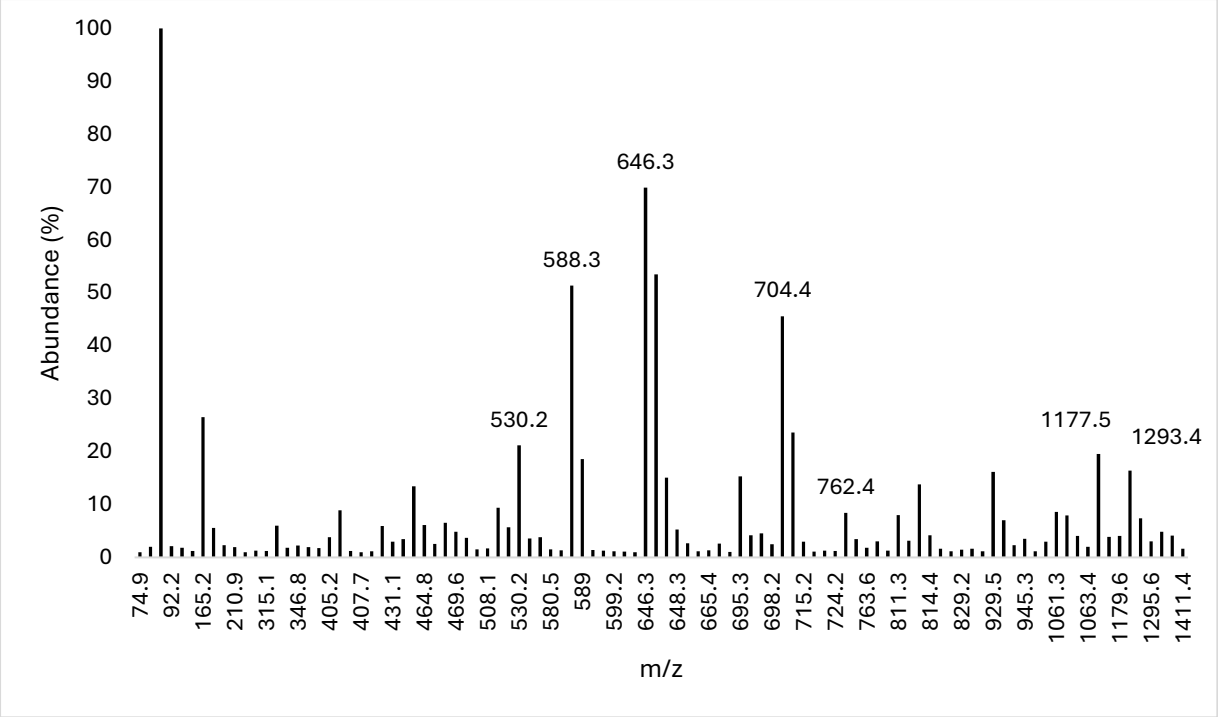

Figure S148. MS spectrum extracted from MA control chromatogram at retention time 15.0 min. Labeled m/z signals represent 9MA, 10MA, 11MA, 12MA and 13MA.

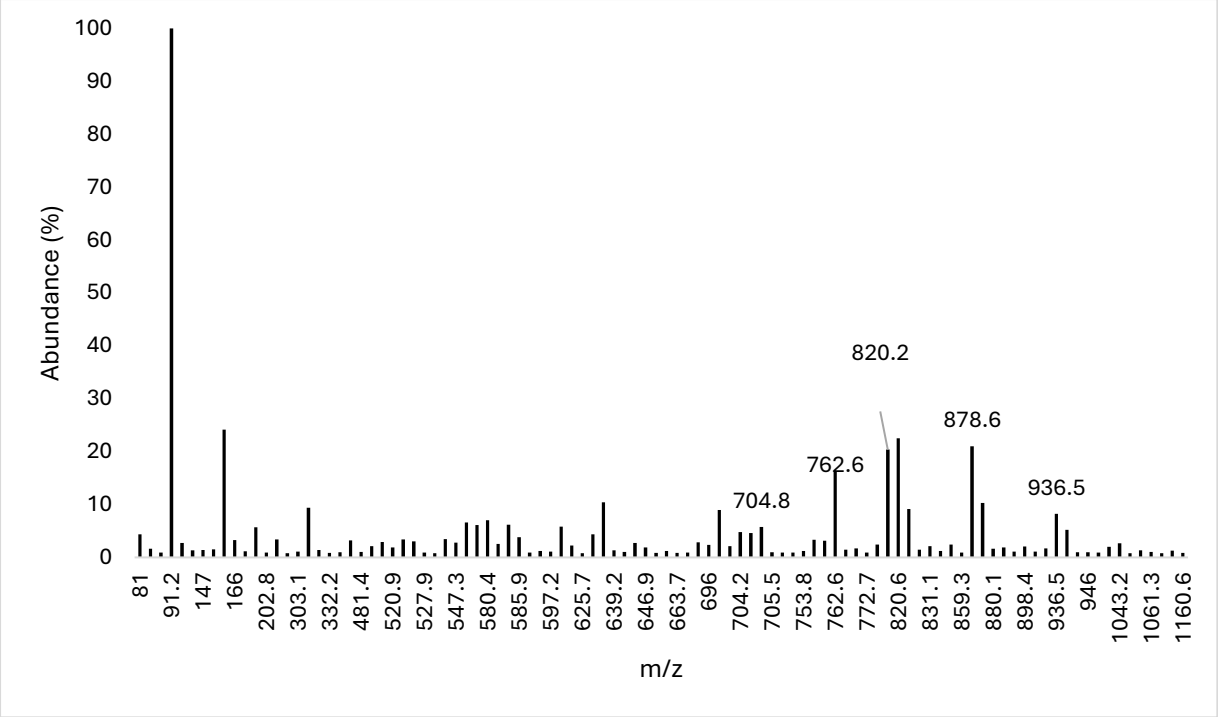

Figure S149. MS spectrum extracted from MA control chromatogram at retention time 15.6 min. Labeled m/z signals represent 12MA, 13MA, 14MA, 15MA and 16MA.

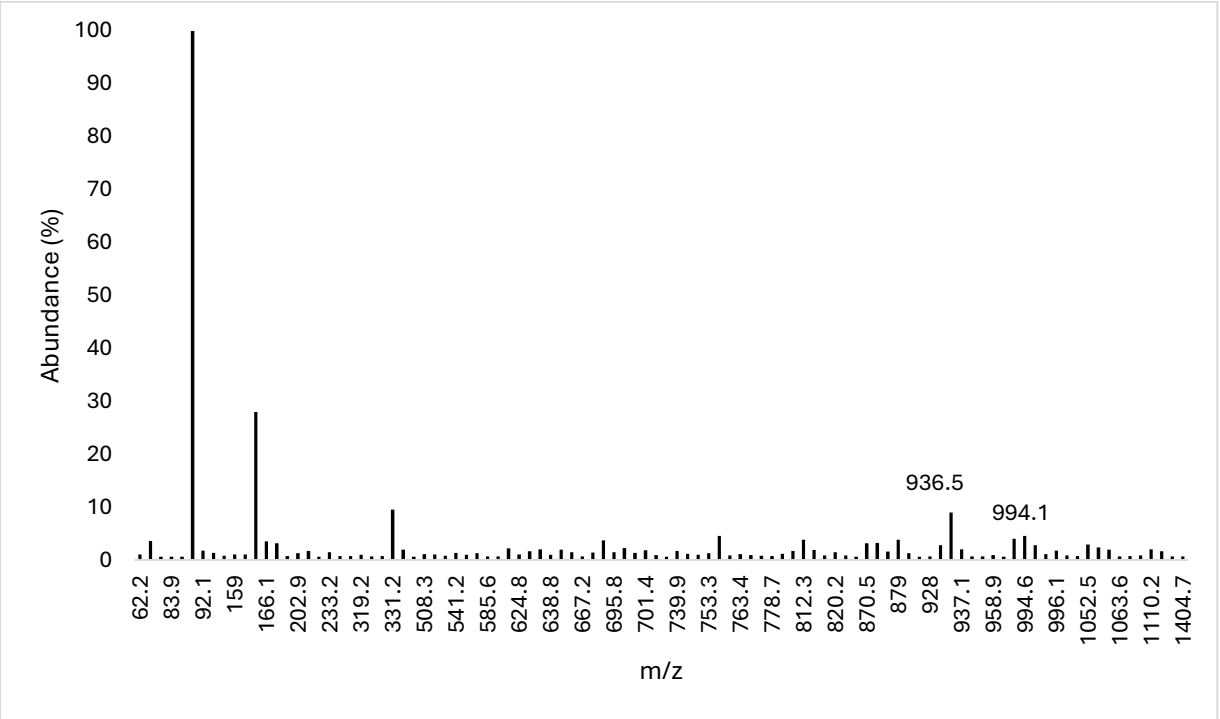

Figure S150. MS spectrum extracted from MA control chromatogram at retention time 16.0 min. Labeled m/z signals represent 16MA and 17MA.

Table S9. Identification of PLA reaction products (in the absence of DA). The detected products based on retention time and their corresponding m/z and ionization pattern as determined by LC-MS.

Retention time (min)	Compound	M (g/mol)	Corresponding m/z (-TIC)	Ionization pattern
23.1	2PLA	314.3	313.2, 627.4	$[M-H]^-$, $[2M-H]^-$
26.7	3PLA	462.5	461.3, 923.5	$[M-H]^-$, $[2M-H]^-$
29.0	4PLA	610.6	609.5, 1219.8	$[M-H]^-$, $[2M-H]^-$
29.8	5PLA	758.8	757.4	$[M-H]^-$
30.6	6PLA	906.9	905.7	$[M-H]^-$
	7PLA	1055.1	1053.9	$[M-H]^-$

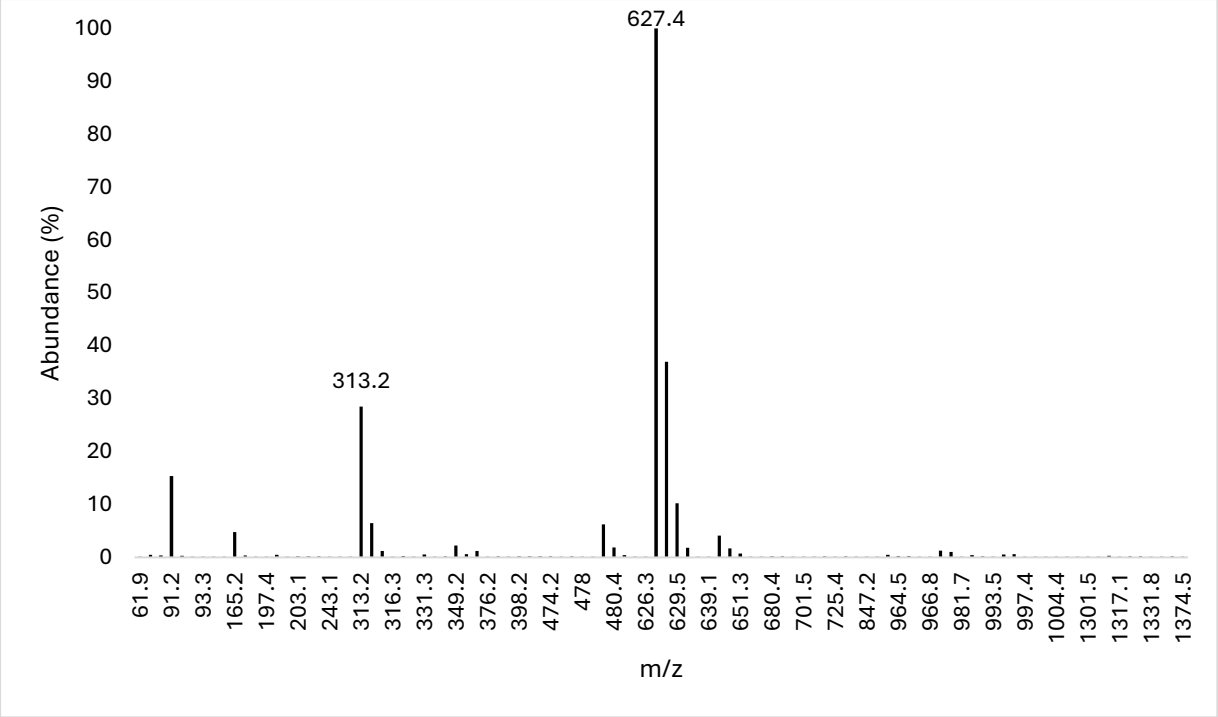

Figure S151. MS spectrum extracted from PLA control chromatogram at retention time 23.1 min. Labeled m/z signals represent 2PLA.

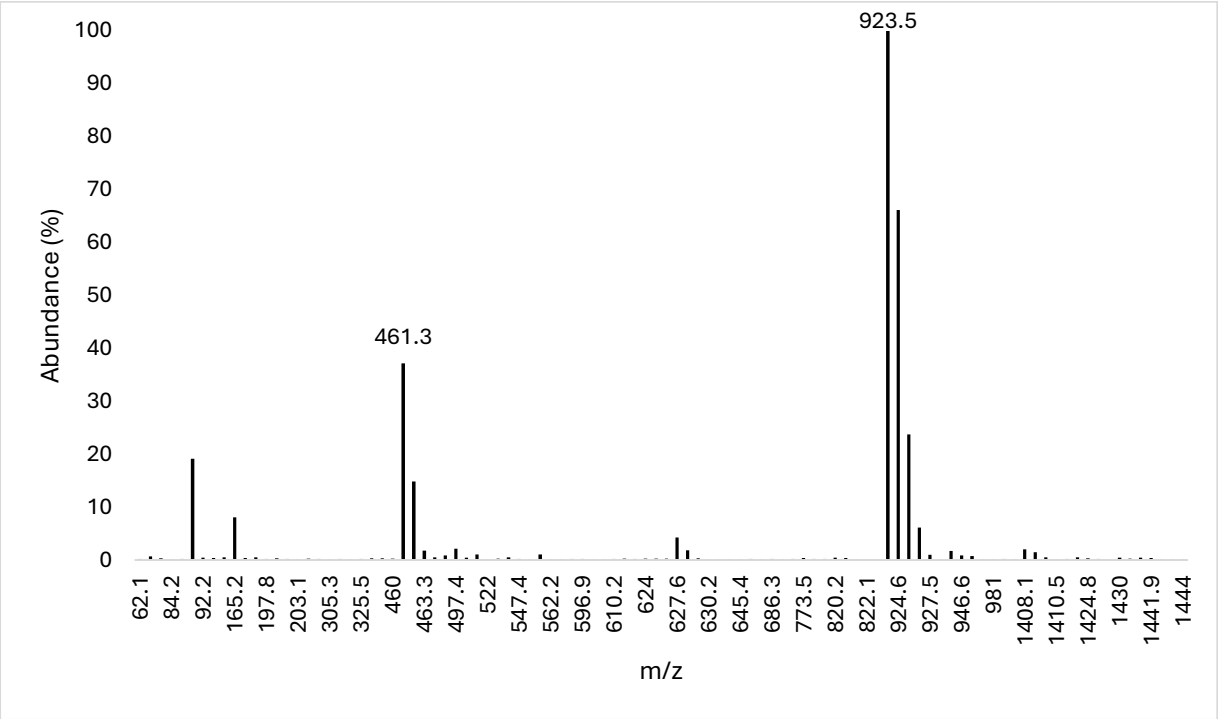

Figure S152. MS spectrum extracted from PLA control chromatogram at retention time 26.7 min. Labeled m/z signals represent 3PLA.

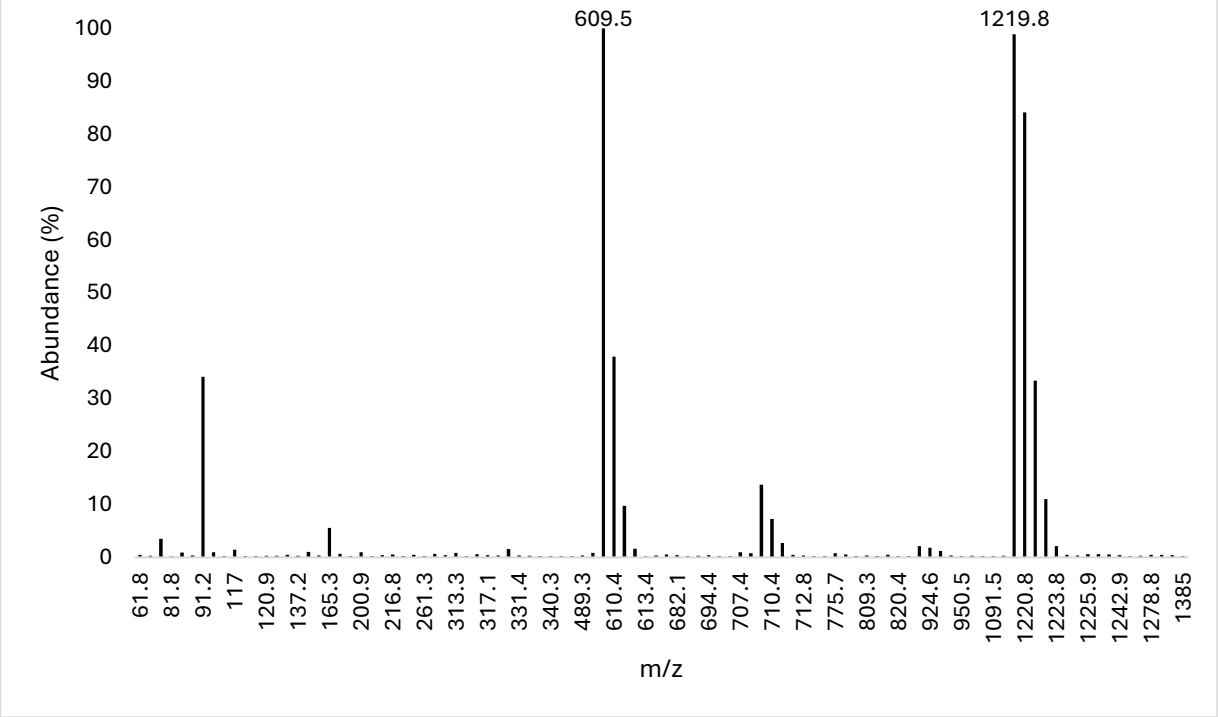

Figure S153. MS spectrum extracted from PLA control chromatogram at retention time 29.0 min. Labeled m/z signals represent 4PLA.

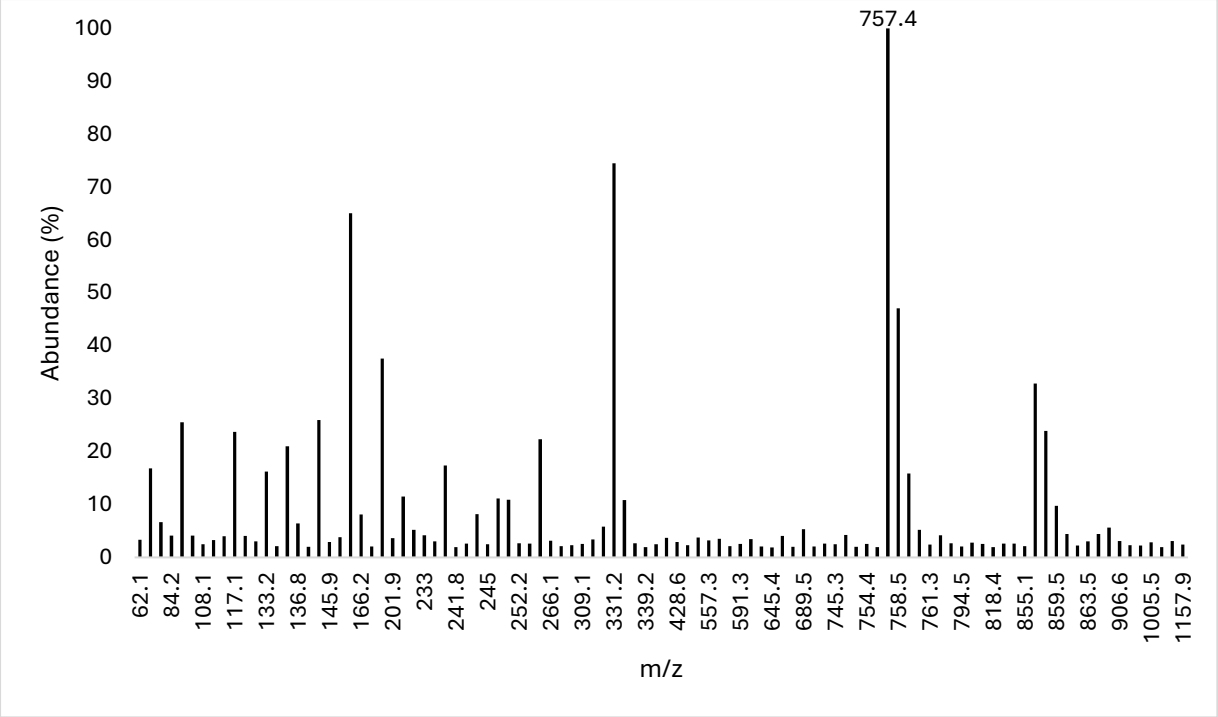

Figure S154. MS spectrum extracted from PLA control chromatogram at retention time 29.8 min. Labeled m/z signal represents 5PLA.

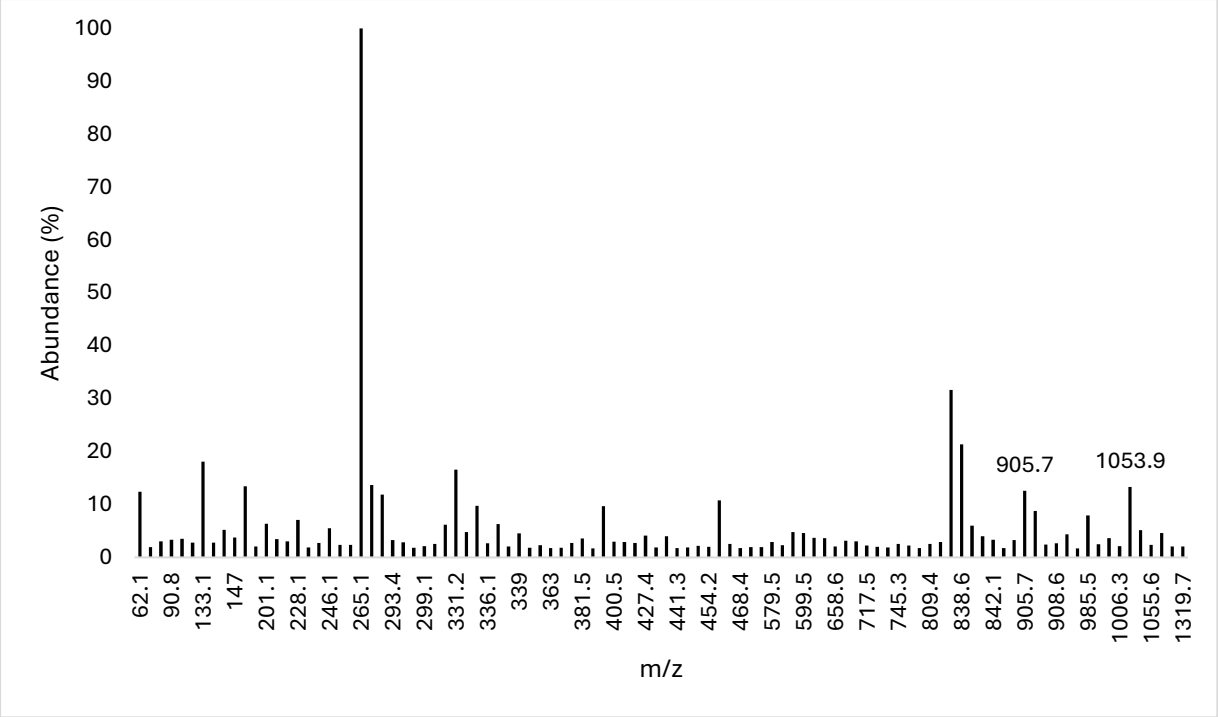

Figure S155. MS spectrum extracted from PLA control chromatogram at retention time 30.6 min. Labeled m/z signals represent 6PLA and 7PLA.

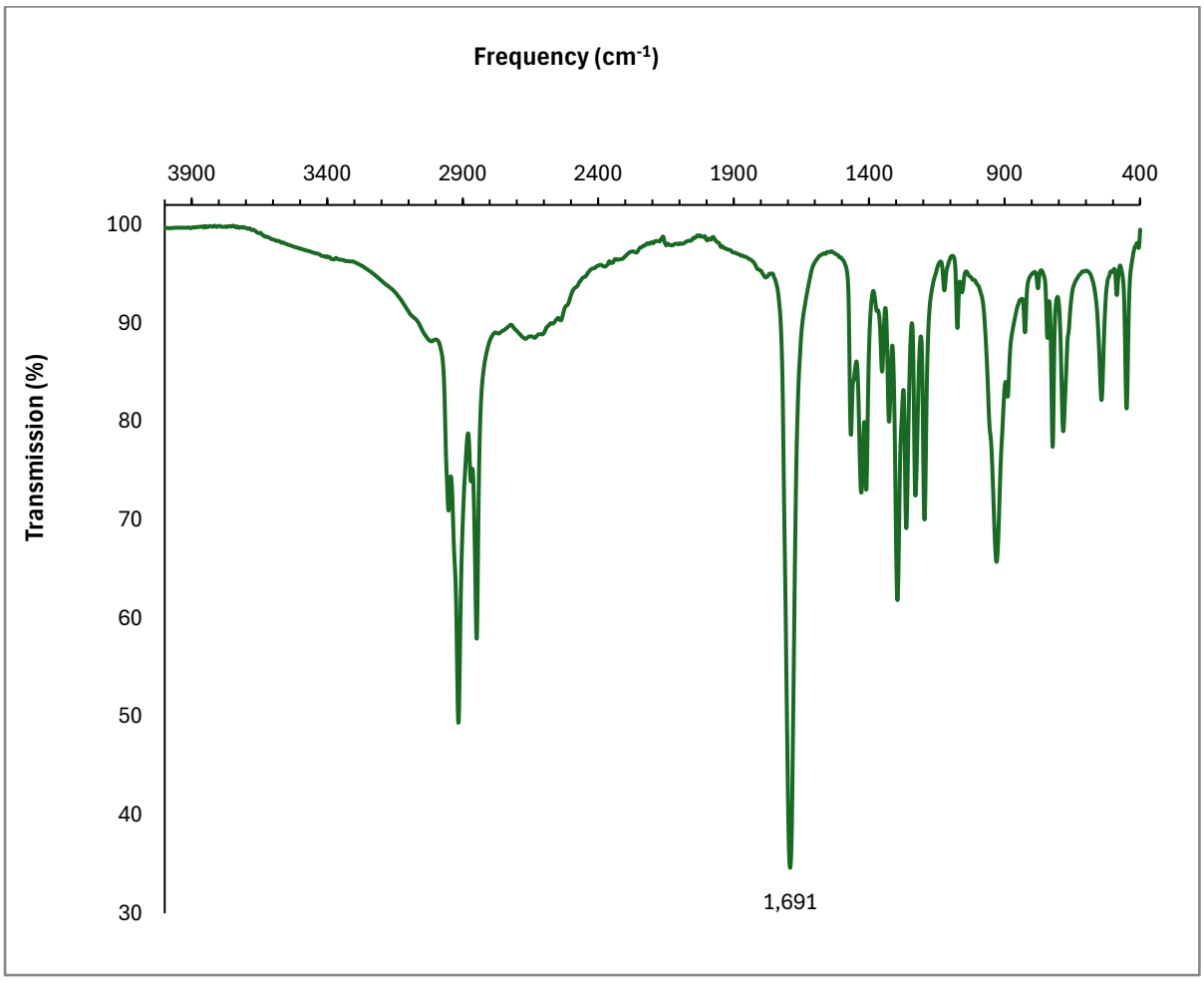

Figure S156. FTIR spectrum of fresh DA monomers. Indicative C=O stretching of the carboxylic acid is assigned at 1691cm^{-1}.

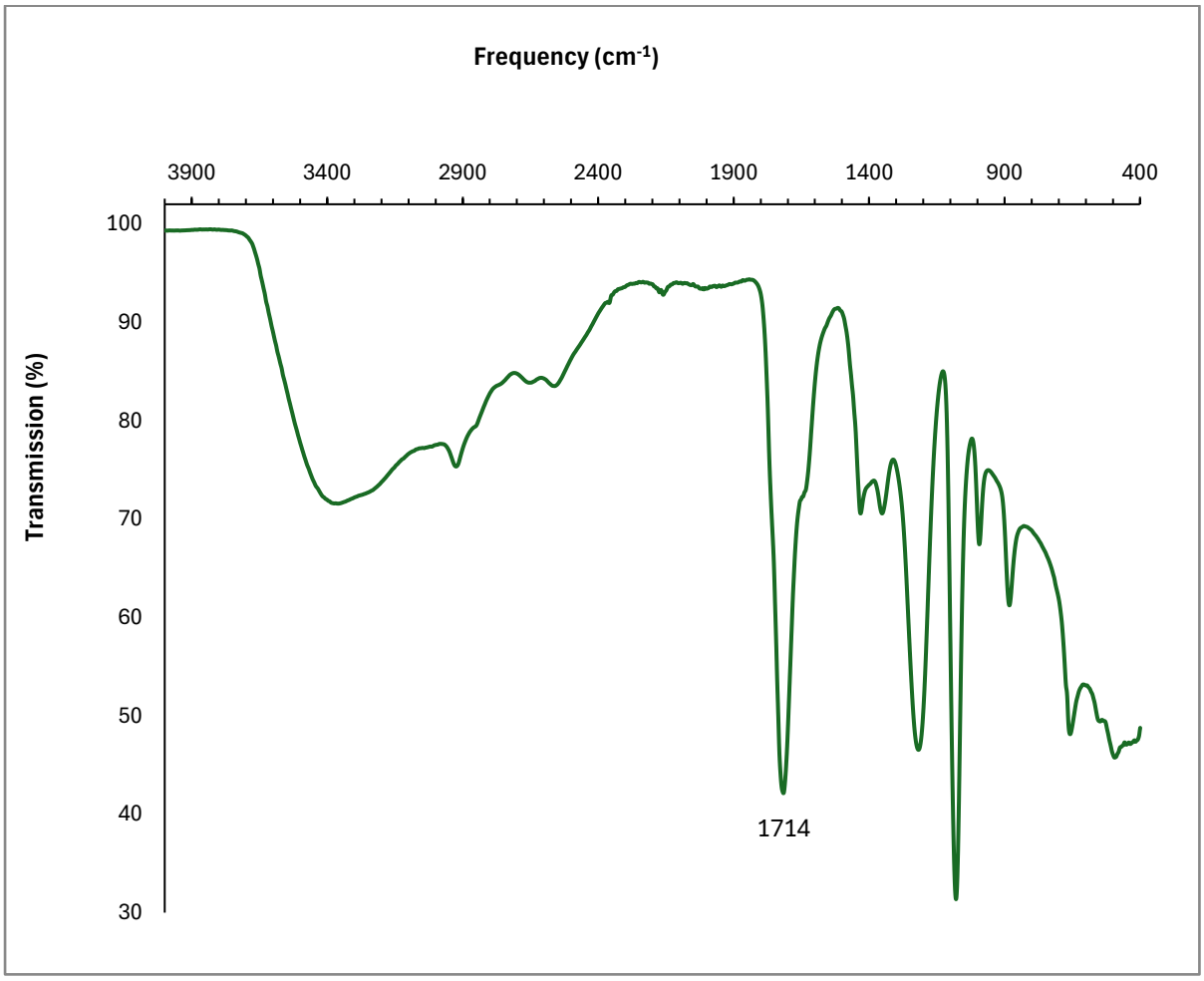

Figure S157. FTIR spectrum of fresh GA monomers. Indicative C=O stretching of the carboxylic acid is assigned at 1714cm^{-1}.

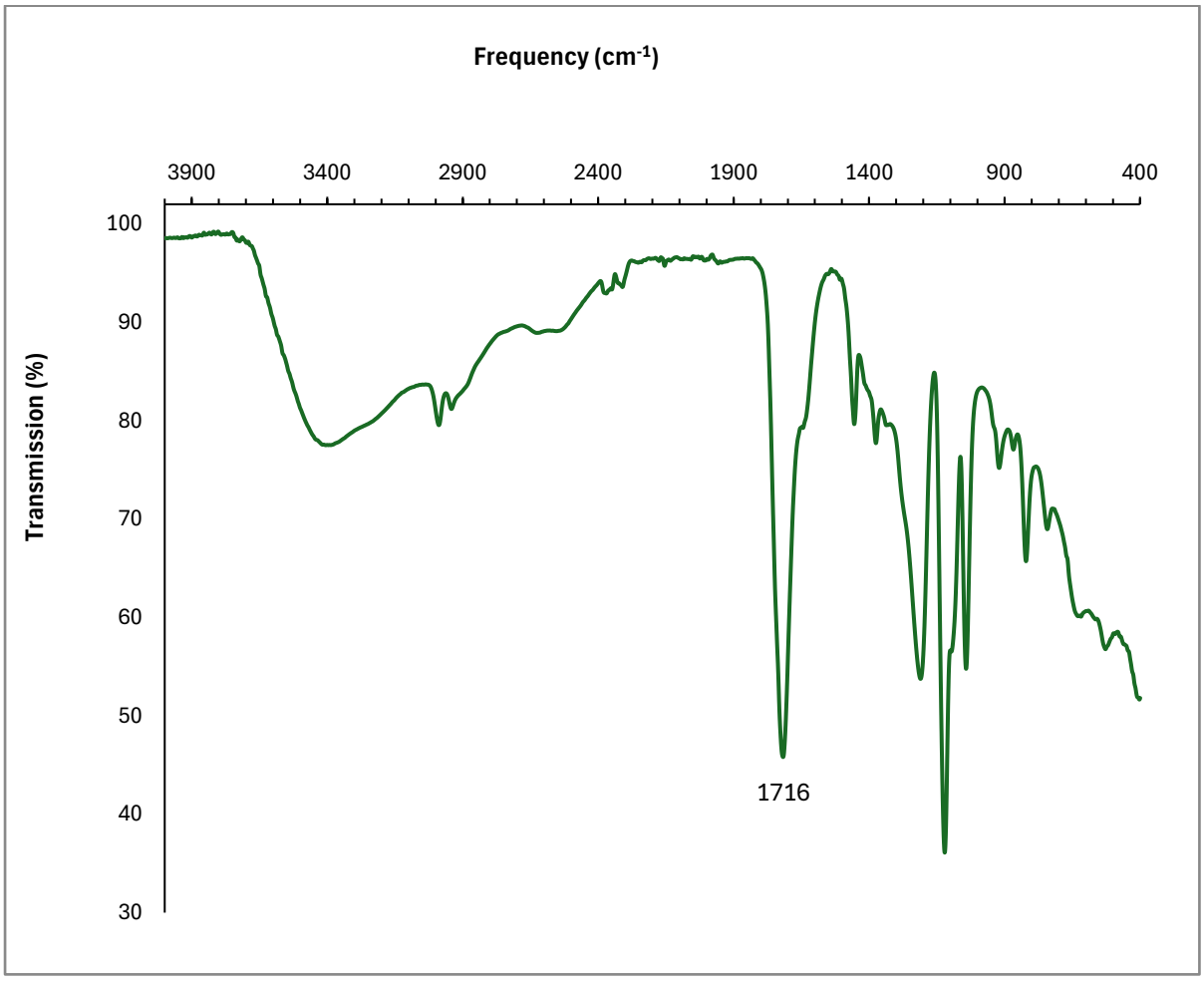

Figure S158. FTIR spectrum of fresh LA monomers. Indicative C=O stretching of the carboxylic acid is assigned at 1716cm^{-1}.

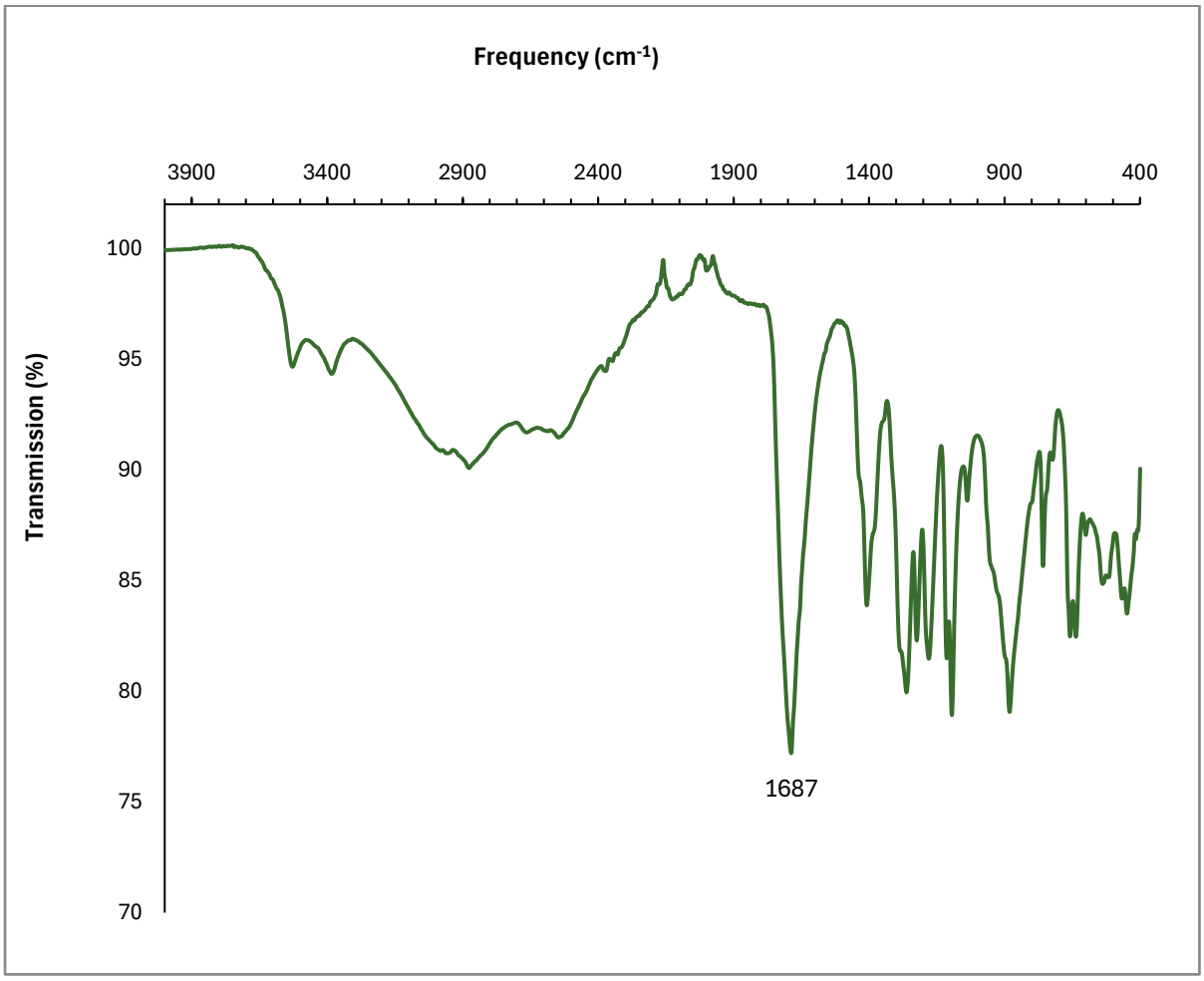

Figure S159. FTIR spectrum of fresh MA monomers. Indicative C=O stretching of the carboxylic acid is assigned at 16876cm^{-1}.

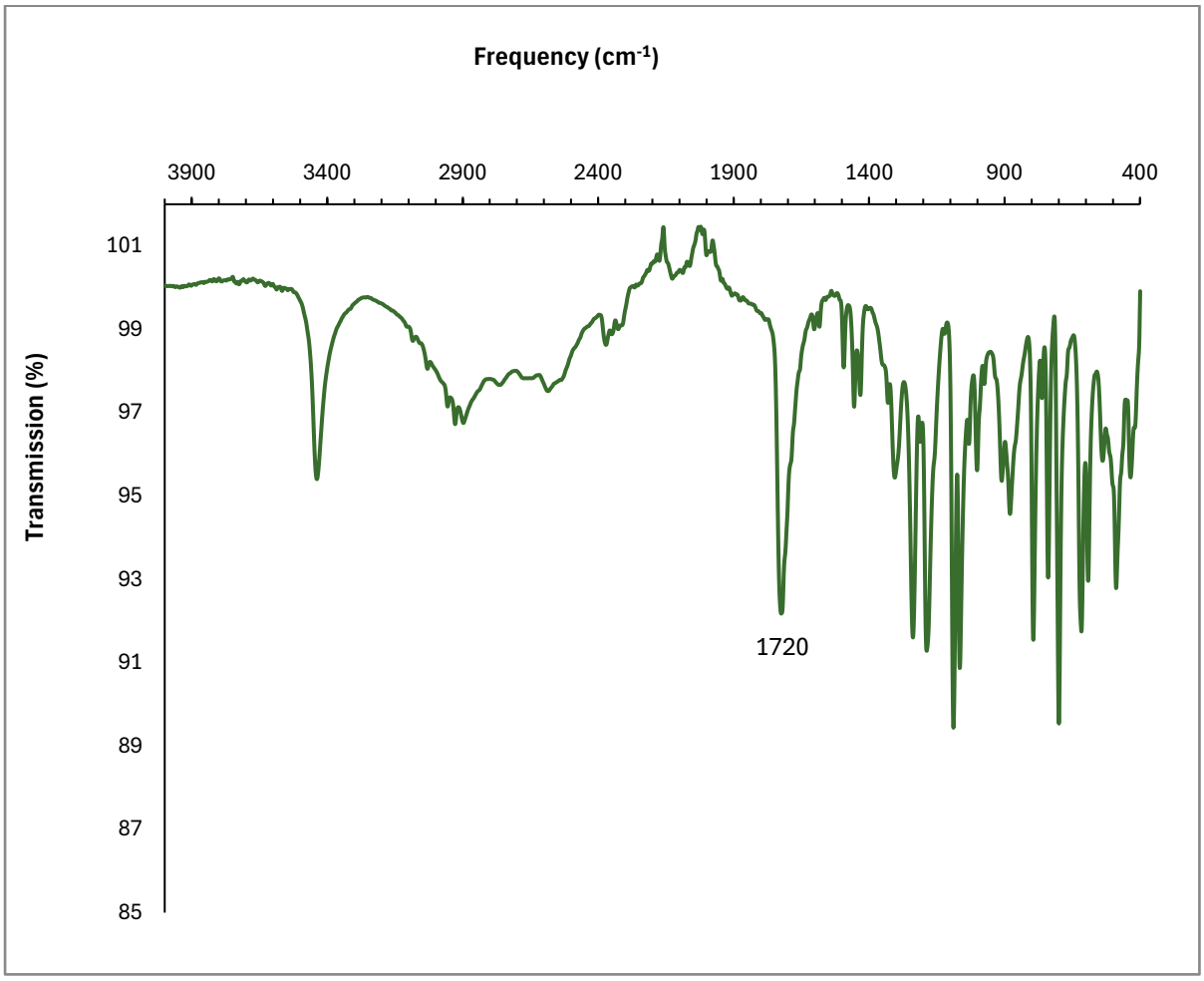

Figure S160. FTIR spectrum of fresh PLA monomers. Indicative C=O stretching of the carboxylic acid is assigned at 1720cm^{-1}.

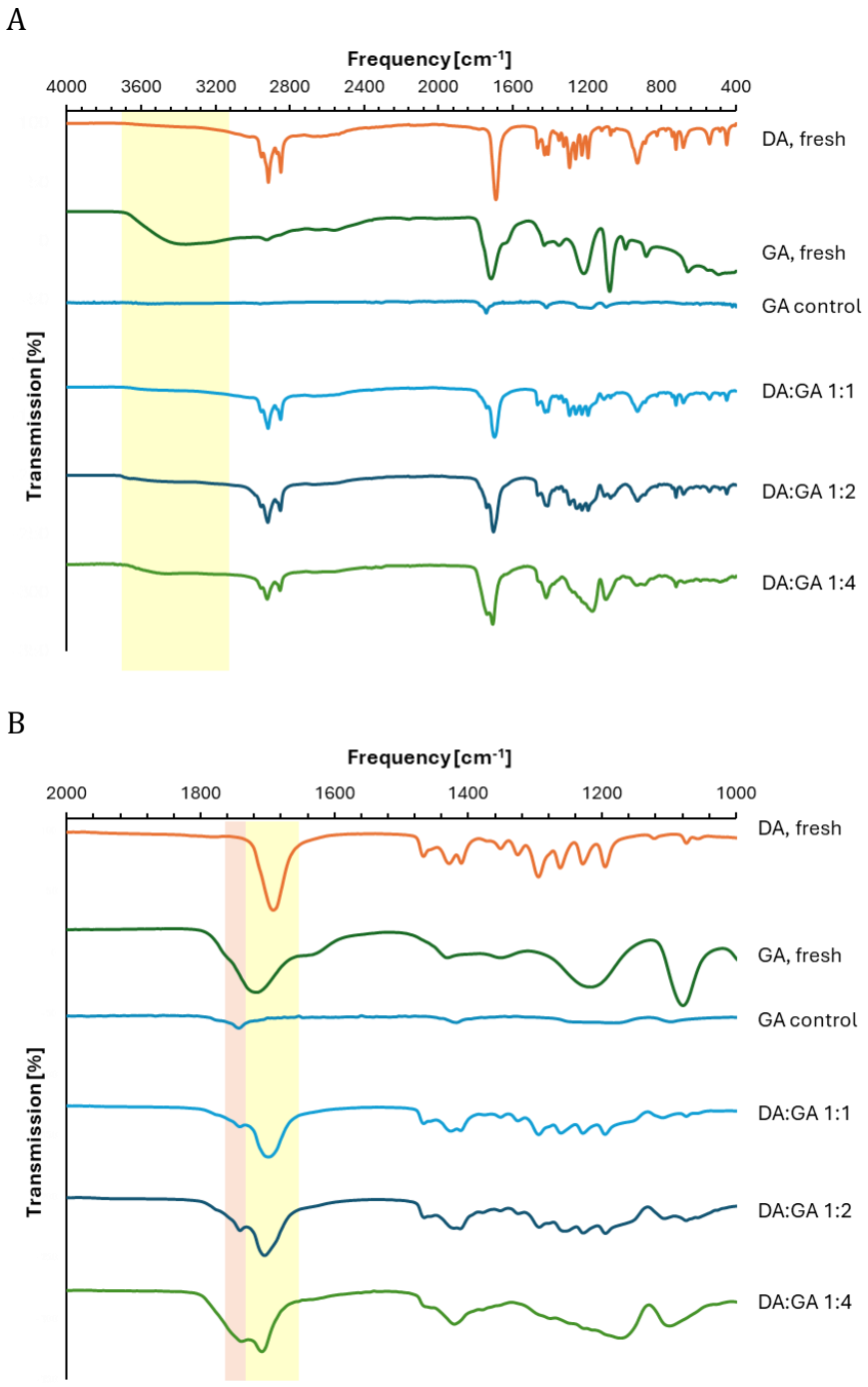

Figure S161. FTIR spectra of DA and GA fresh monomers and reaction products. Full-scale spectra within frequency range of 400-4000cm^{-1} (A) and zoom-in spectra of the frequency range indicative to the carboxylic acid to ester bonds shift (B). As indicated by the spectra, upon GA reaction, the O-H stretching signal of GA at about 3400cm^{-1} is lost. As GA and DA oligomerization proceeded, the intensity of the C=O stretching of ester bond at 1740cm^{-1} increased as highlighted in the red region in the spectra. The yellow region indicates the C=O stretching of the carboxylic group.

A

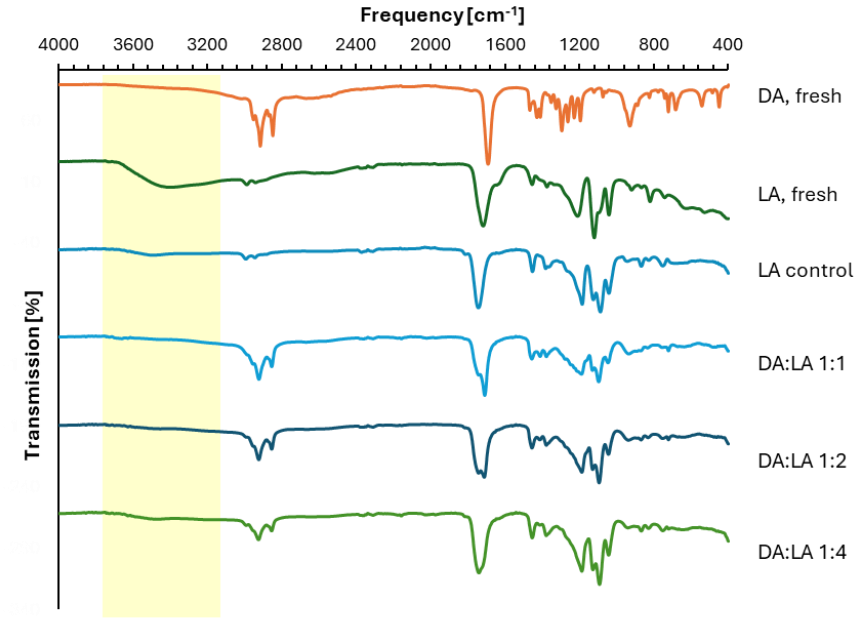

B

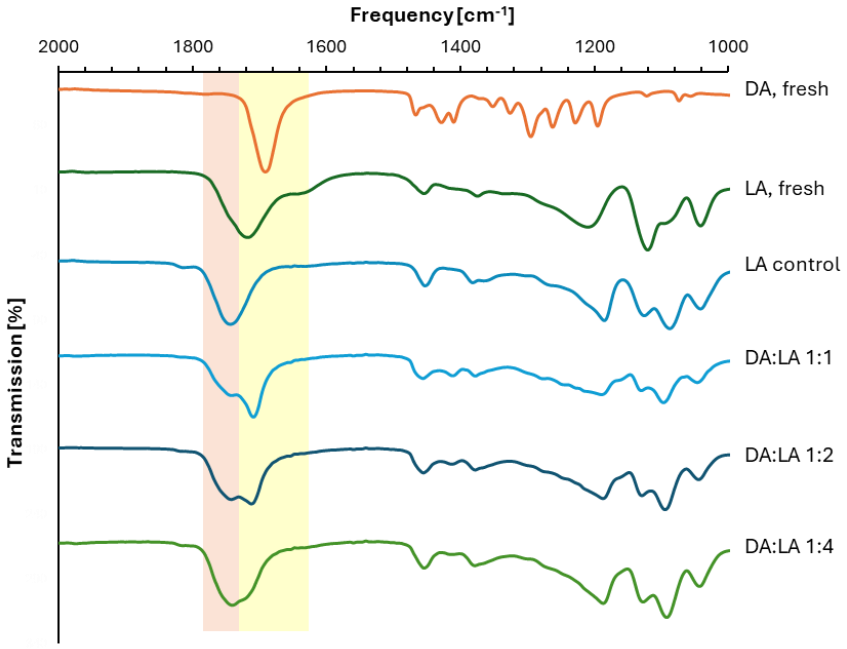

Figure S162. FTIR spectra of DA and LA fresh monomers and reaction products. Full-scale spectra within frequency range of 400-4000cm^{-1} (A) and zoom-in spectra of the frequency range indicative to the carboxylic acid to ester bonds shift (B). As indicated by the spectra, upon LA reaction, the O-H stretching signal of LA at about 3400cm^{-1} is lost. As LA and DA oligomerization proceeded, the intensity of C=O stretching of ester bond at about 1740-1745cm^{-1} increased as highlighted in the red region in the spectra. The Yellow region indicates the C=O stretching of the carboxylic group.

A

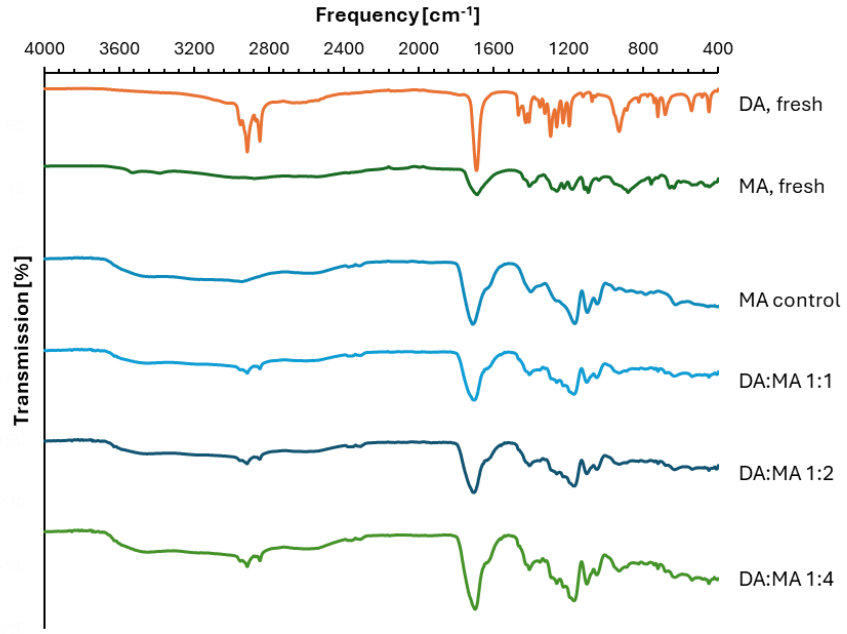

B

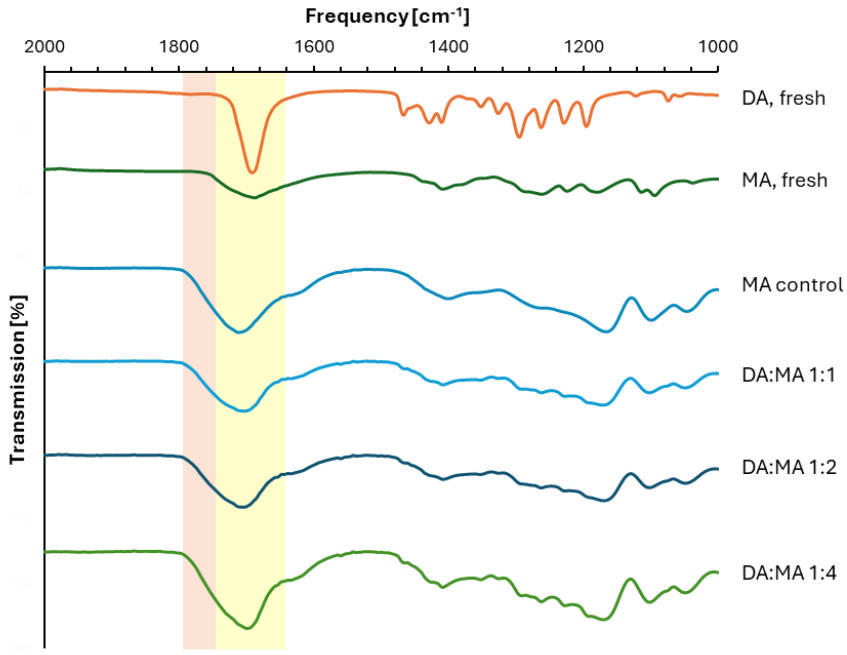

Figure S163. FTIR spectra of DA and MA fresh monomers and reaction products. Full-scale spectra within frequency range of 400-4000cm^{-1} (A) and zoom-in spectra of the frequency range indicative to the carboxylic acid to ester bonds shift (B). As indicated by the red region in the spectra, upon MA and DA oligomerization, the signal corresponding to C=O stretching becomes broaden with signal offsets shifted from ca 1730 cm^{-1} to about 1765-1770cm^{-1}.

A

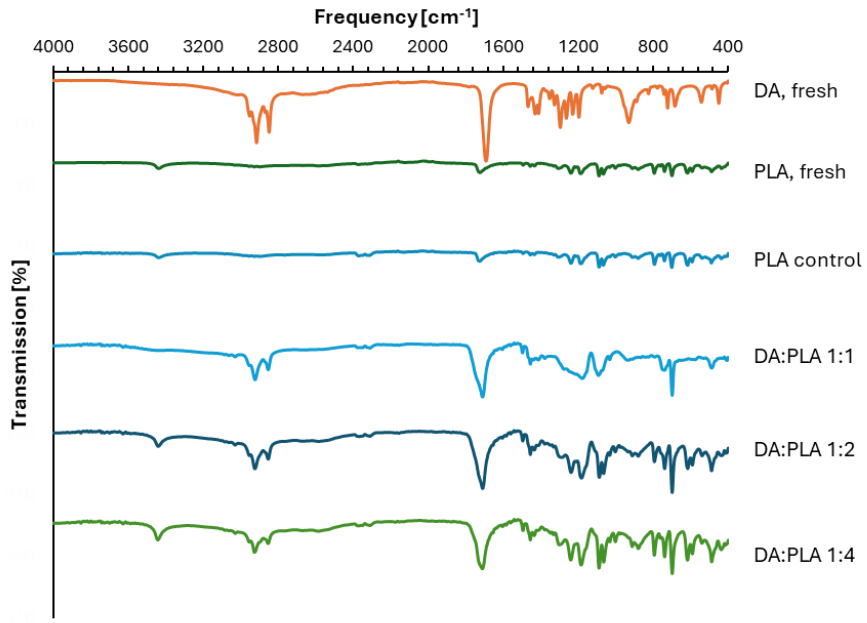

B

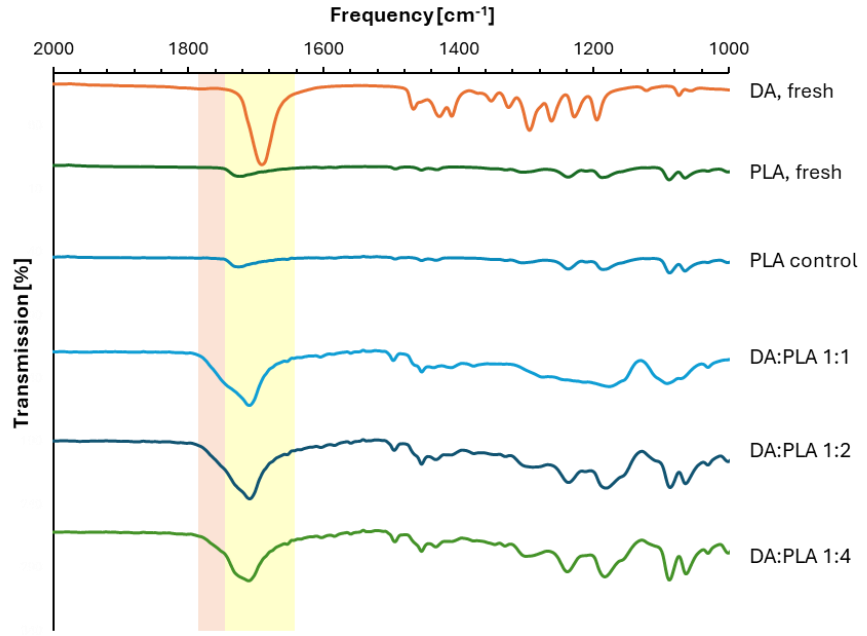

Figure S164. FTIR spectra of DA and PLA fresh monomers and reaction products. Full-scale spectra within frequency range of 400-4000cm^{-1} (A) and zoom-in spectra of the frequency range indicative to the carboxylic acid to ester bonds shift (B). As indicated by the red region in the spectra, upon PLA and DA oligomerization, a shoulder-like signal at around 1750-1760cm^{-1} is detected corresponding to C=O ester stretching.

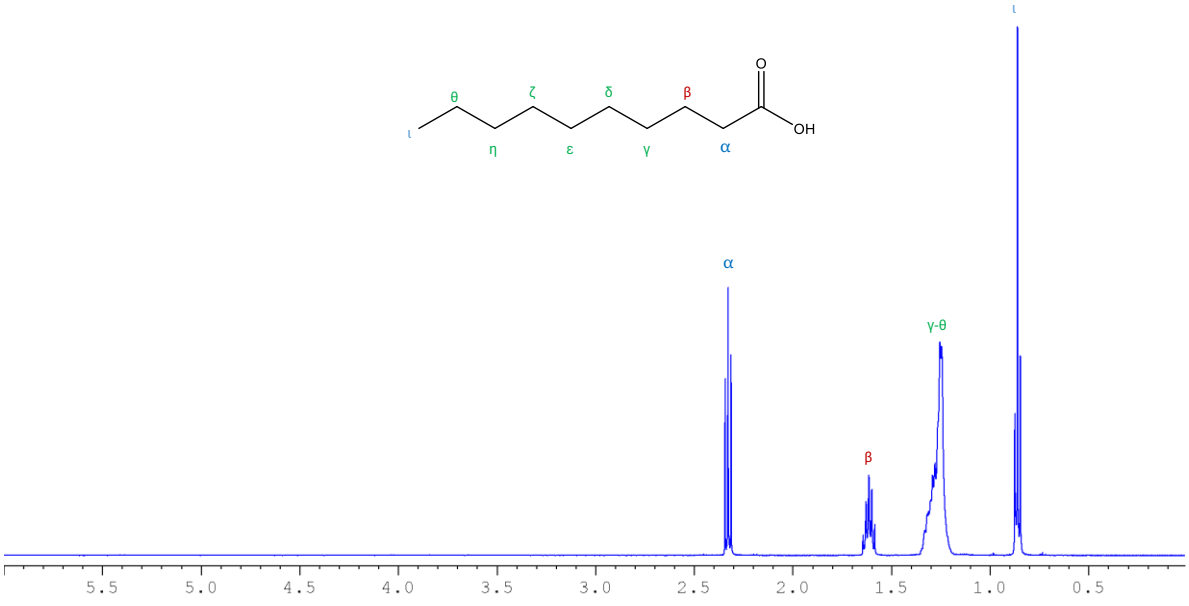

Figure S165. ^{1}H-NMR spectrum of DA fresh monomer in $CDCl_3$.

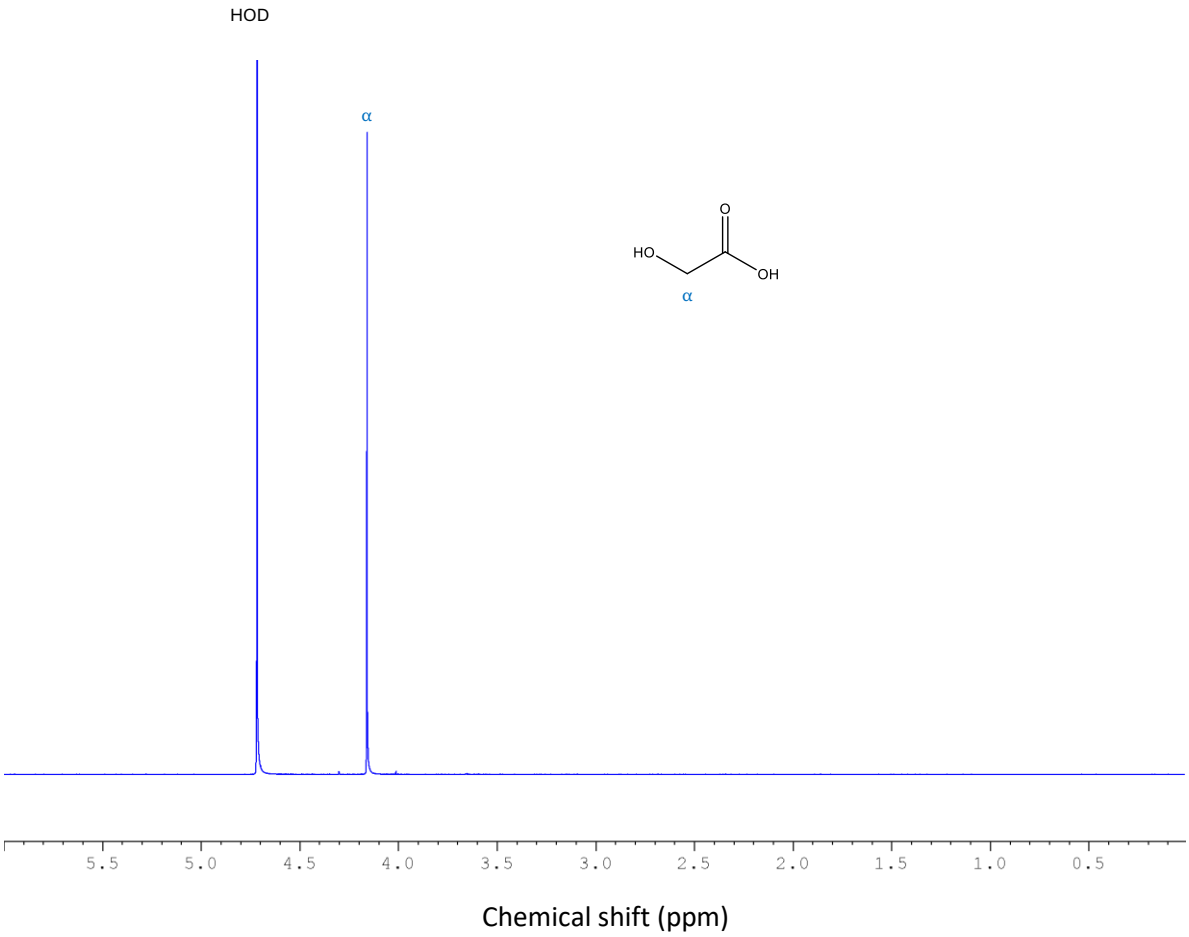

Figure S166. ^{1}H-NMR spectrum of GA fresh monomer in D_2O.

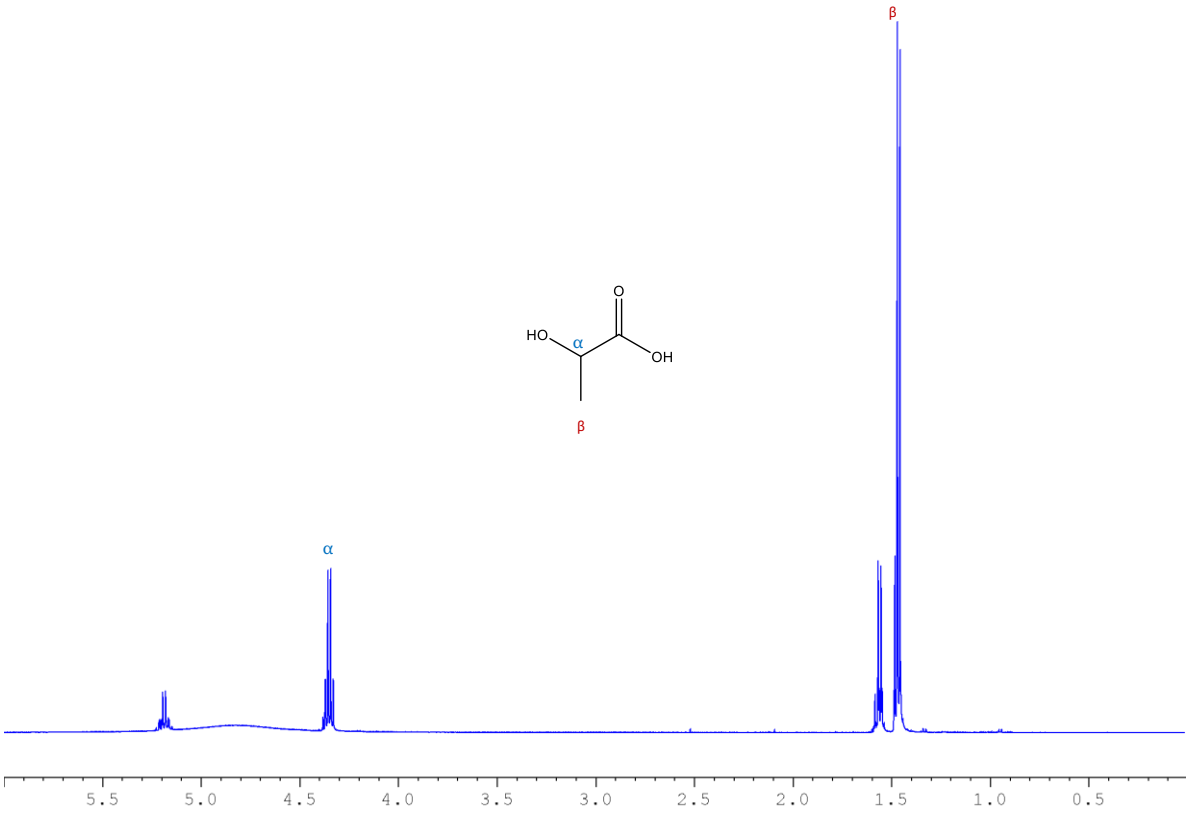

Figure S167. ^{1}H-NMR spectrum of LA fresh monomer in $CDCl_3$. The stock solution contains 2LA.

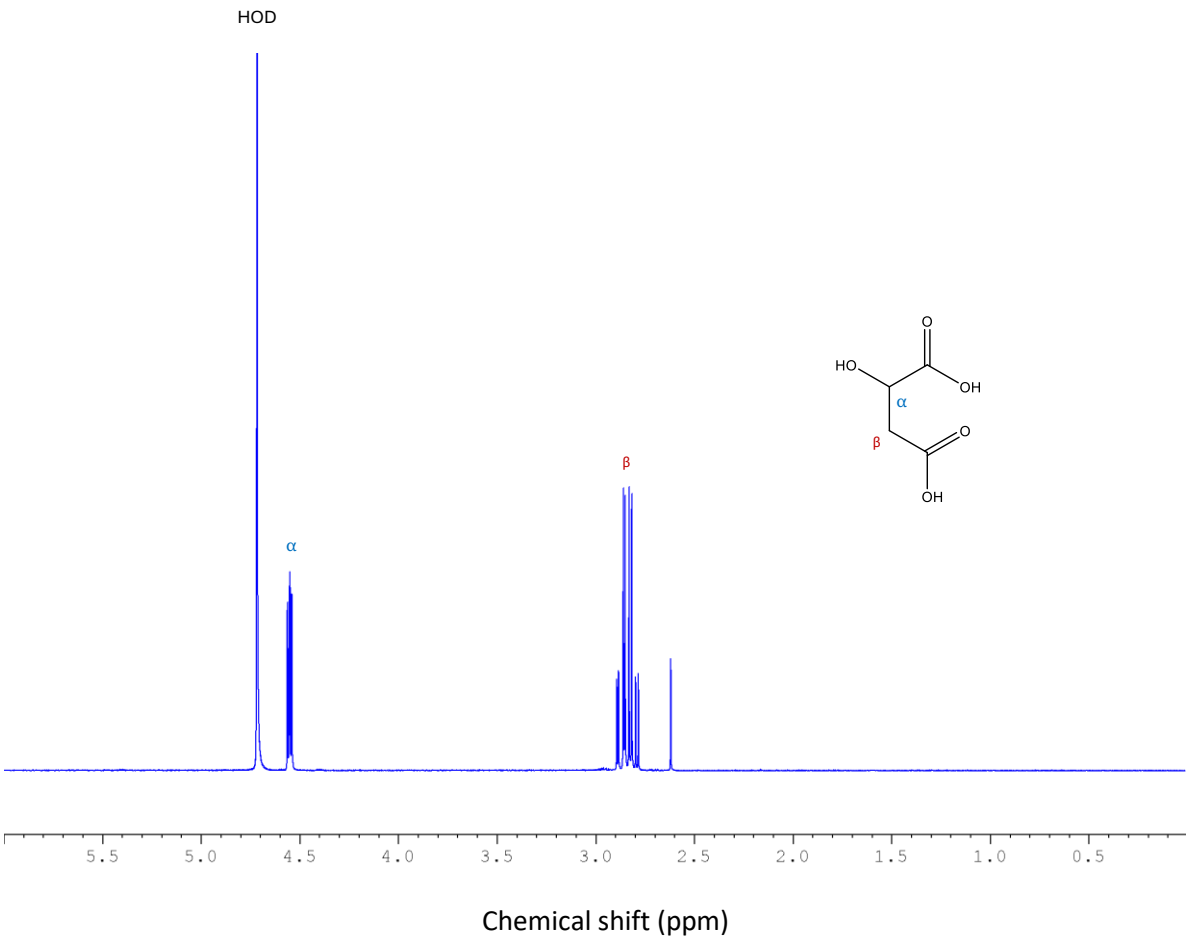

Figure S168. ^{1}H-NMR spectrum of MA fresh monomer in D_2O.

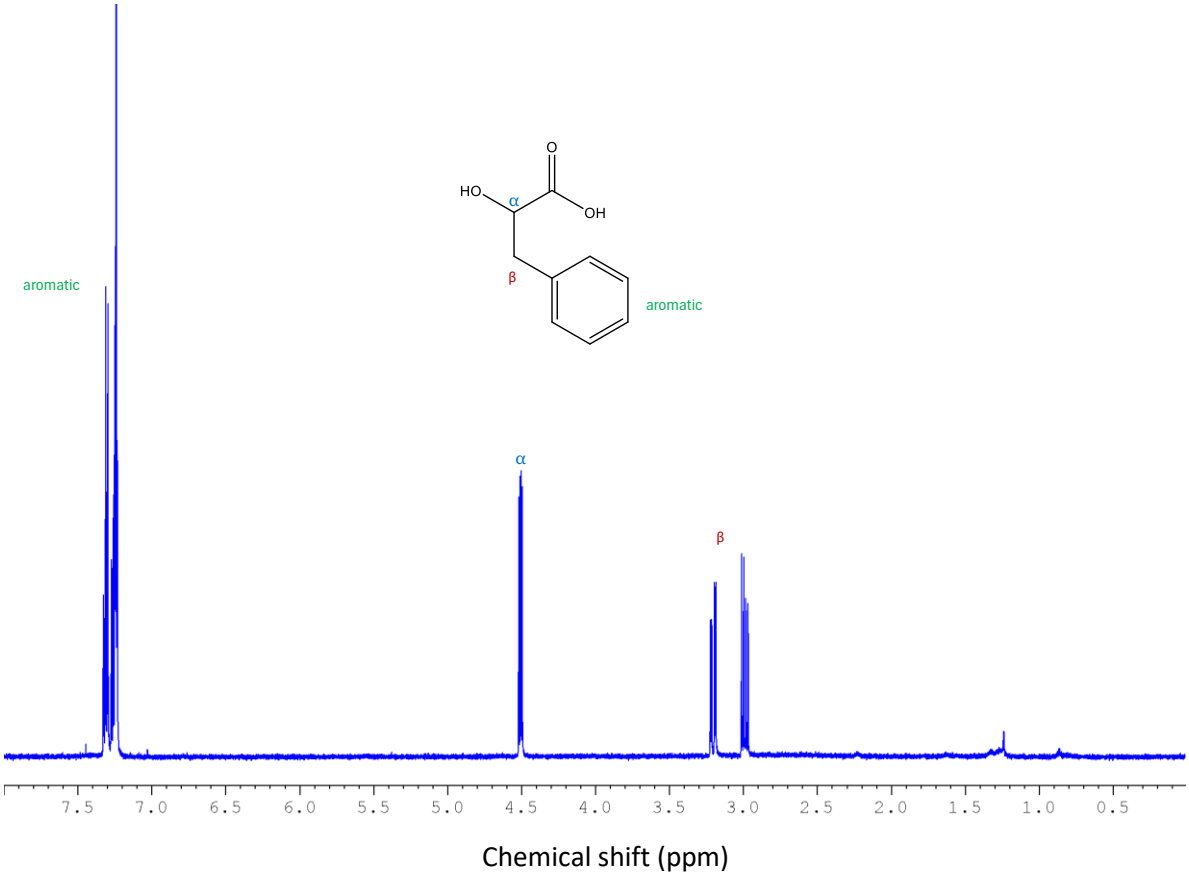

Figure S169. ^{1}H-NMR spectrum of PLA fresh monomer in $CDCl_3$.

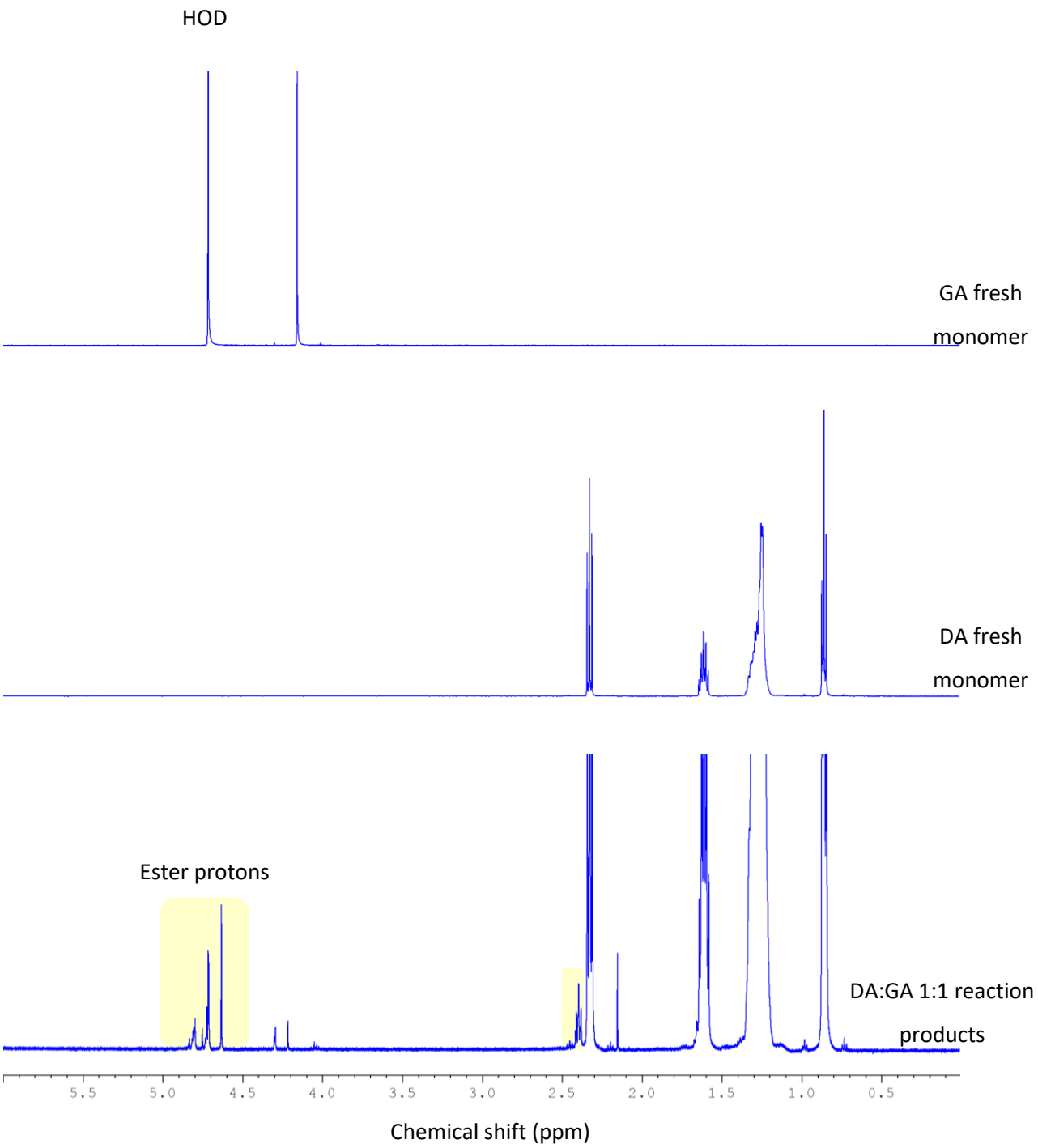

Figure S170. ^{1}H-NMR spectrum of DA:GA reaction product at 1:1 molar ratio. The dry reaction product was suspended in $CDCl_3$ and analyzed by ^{1}H-NMR. DA monomers in $CDCl_3$ and GA monomer in D_2O are presented for reference. Alpha protons shift downfield indicates the formation of ester bonds (highlighted in yellow).

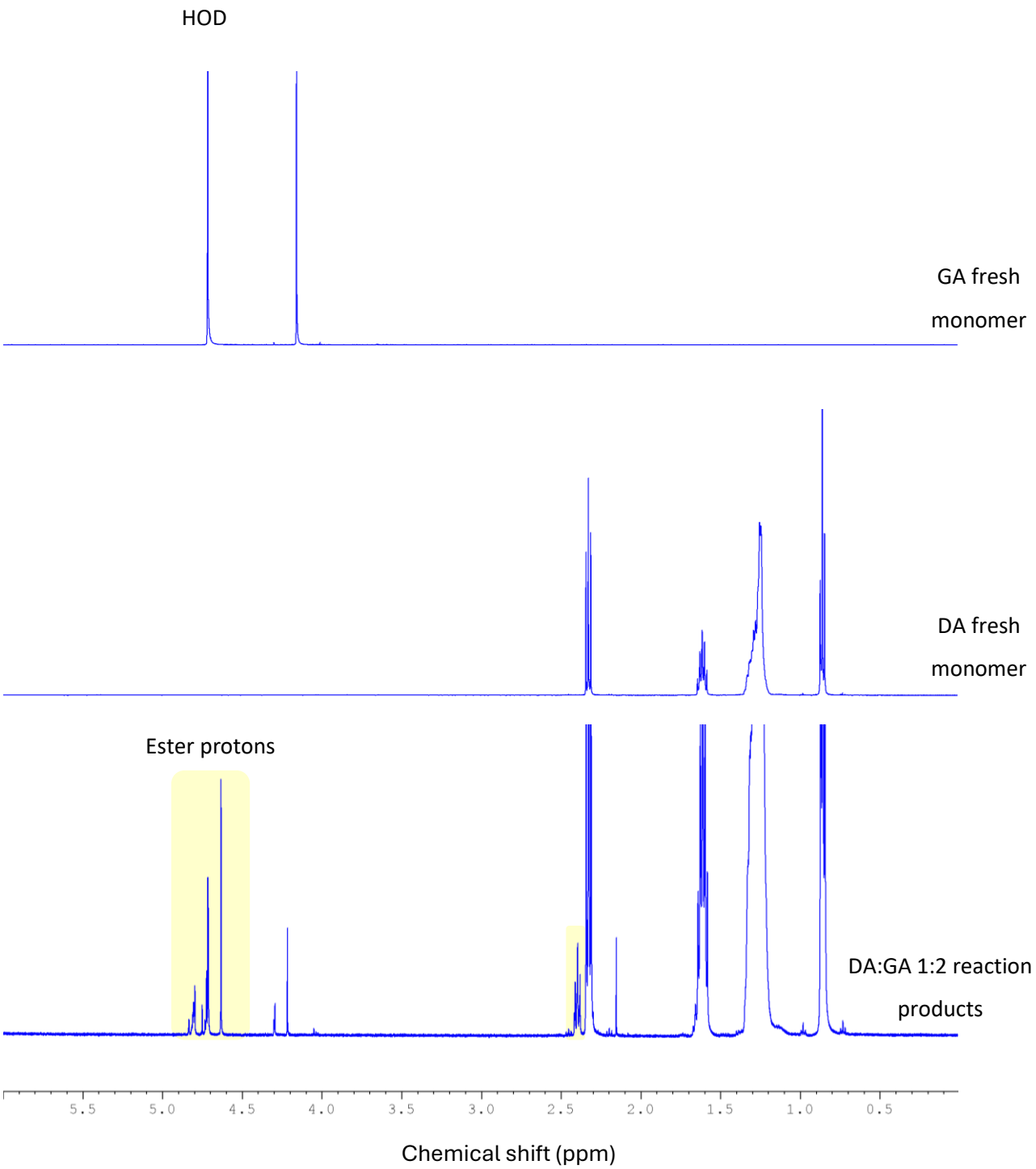

Figure S171. ^{1}H-NMR spectrum of DA:GA reaction product at 1:2 molar ratio. The dry reaction product was suspended in $CDCl_3$ and analyzed by ^{1}H-NMR. DA monomers in $CDCl_3$ and GA monomer in D_2O are presented for reference. Alpha protons shift downfield indicates the formation of ester bonds (highlighted in yellow).

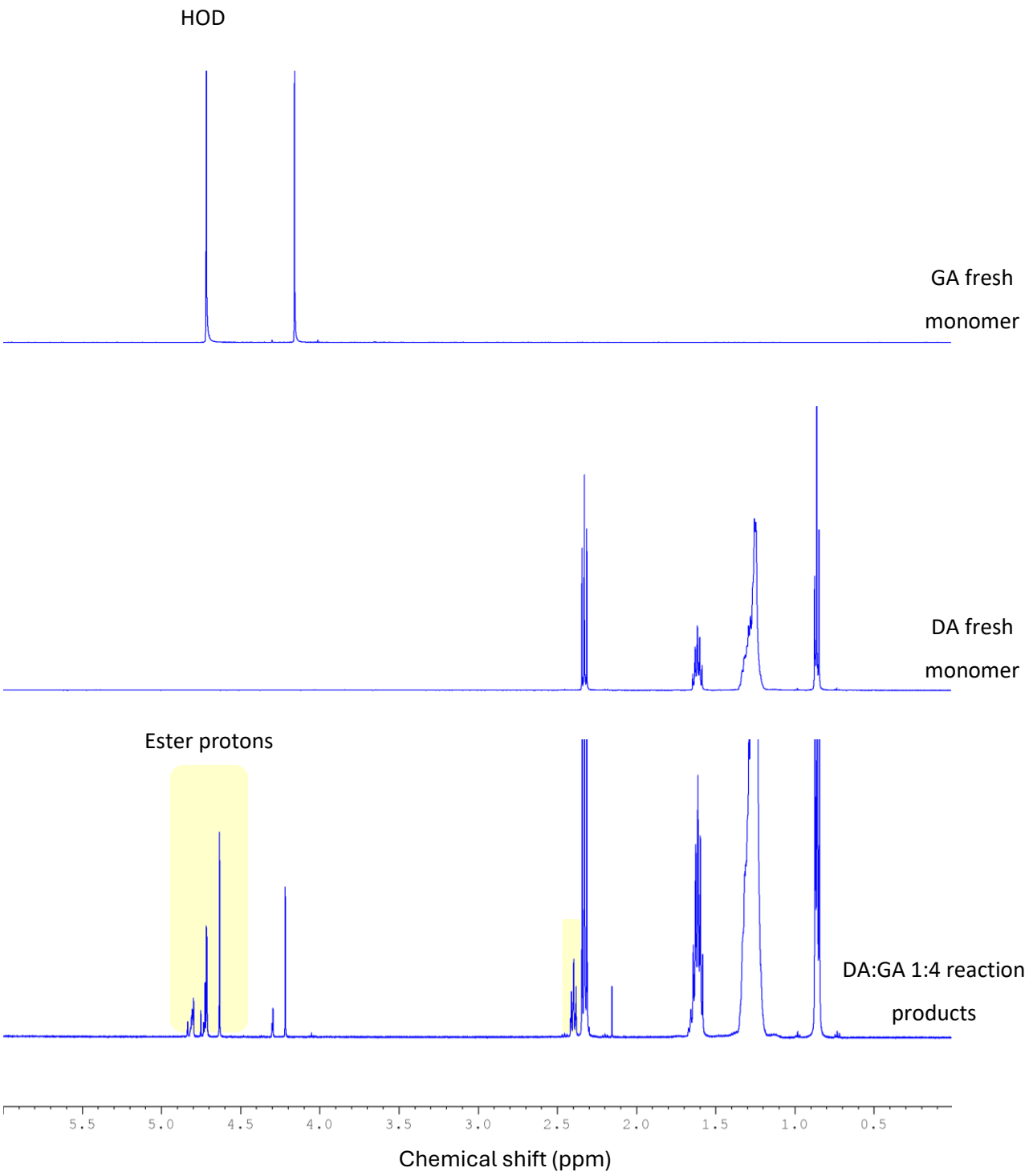

Figure S172. ^{1}H-NMR spectrum of DA:GA reaction product at 1:4 molar ratio. The dry reaction product was suspended in $CDCl_3$ and analyzed by ^{1}H-NMR. DA monomers in $CDCl_3$ and GA monomer in D_2O are presented for reference. Alpha protons shift downfield indicates the formation of ester bonds (highlighted in yellow).

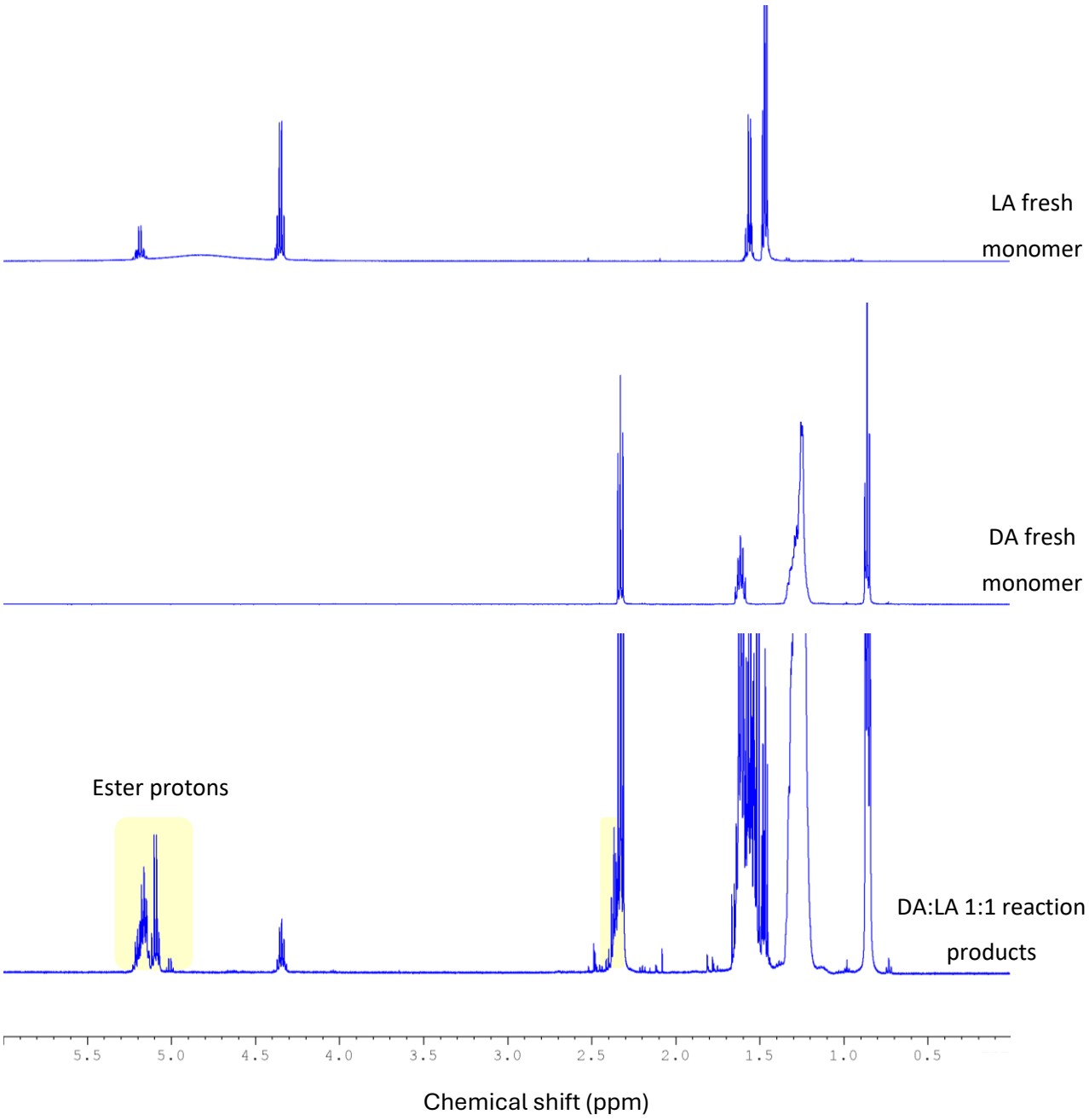

Figure S173. ^{1}H-NMR spectrum of DA:LA reaction product at 1:1 molar ratio. The dry reaction product was suspended in $CDCl_3$ and analyzed by ^{1}H-NMR. DA and LA monomers in $CDCl_3$ are presented for reference. Alpha protons shift downfield indicates the formation of ester bonds (highlighted in yellow).

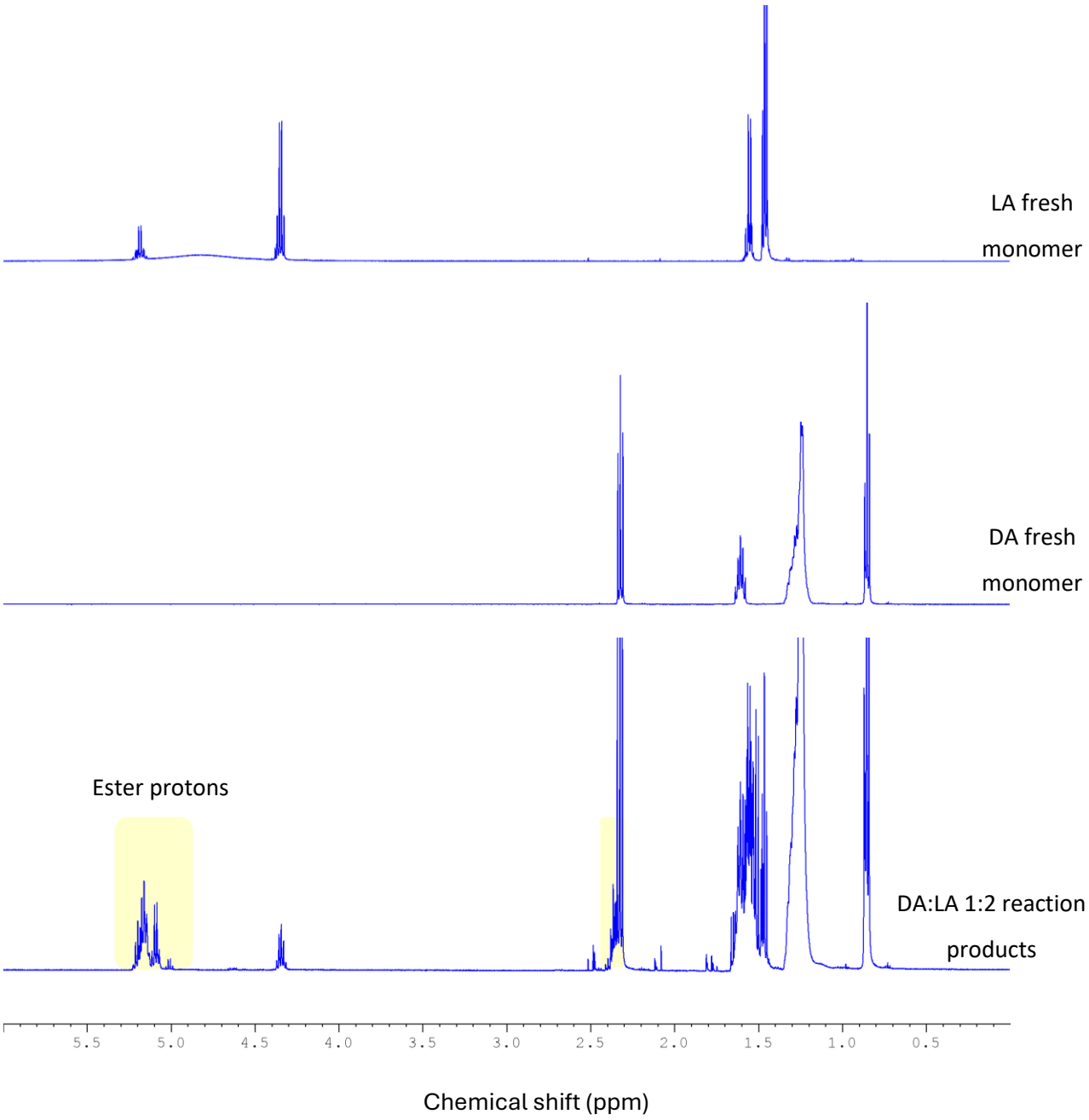

Figure S174. ^{1}H-NMR spectrum of DA:LA reaction product at 1:2 molar ratio. The dry reaction product was suspended in $CDCl_3$ and analyzed by ^{1}H-NMR. DA and LA monomers in $CDCl_3$ are presented for reference. Alpha protons shifts downfield indicates the formation of ester bonds (highlighted in yellow).

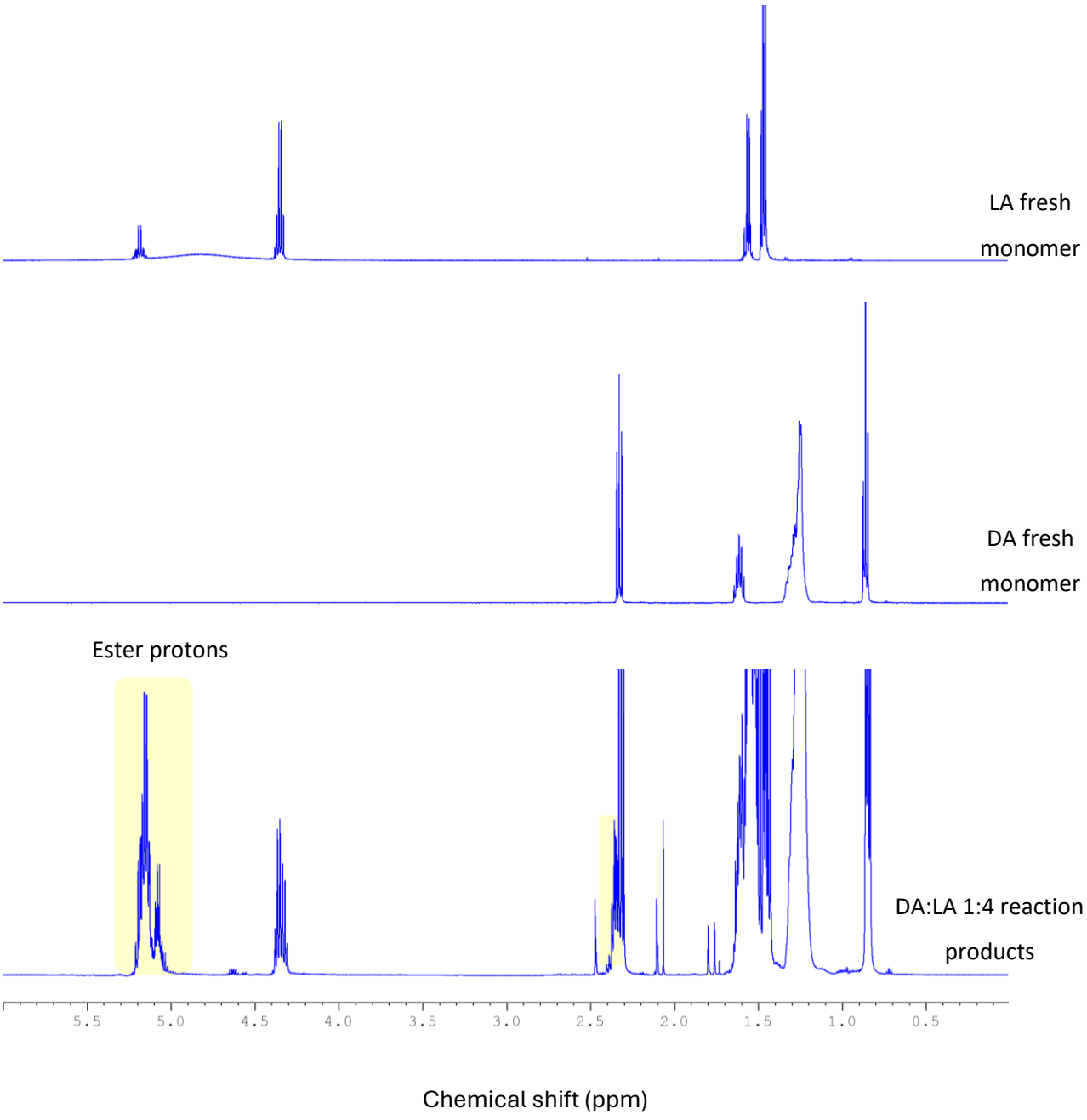

Figure S175. ^{1}H-NMR spectrum of DA:LA reaction product at 1:4 molar ratio. The dry reaction product was suspended in $CDCl_3$ and analyzed by ^{1}H-NMR. DA and LA monomers in $CDCl_3$ are presented for reference. Alpha protons shift downfield indicates the formation of ester bonds (highlighted in yellow).

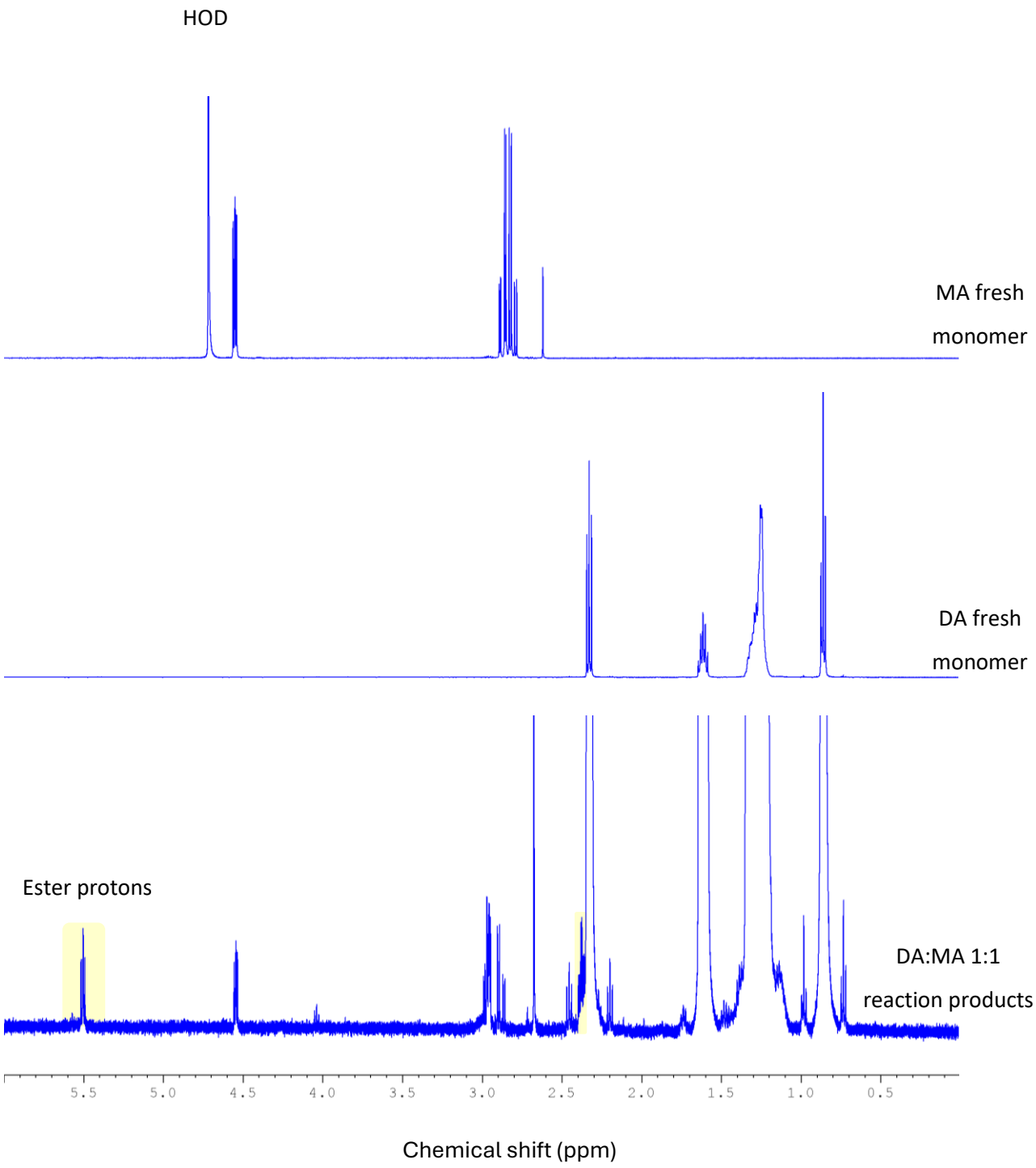

Figure S176. ^{1}H-NMR spectrum of DA:MA reaction product at 1:1 molar ratio. The dry reaction product was suspended in $CDCl_3$ and analyzed by ^{1}H-NMR. DA monomers in $CDCl_3$ and MA monomer in D_2O are presented for reference. Alpha protons shift downfield indicates the formation of ester bonds (highlighted in yellow).

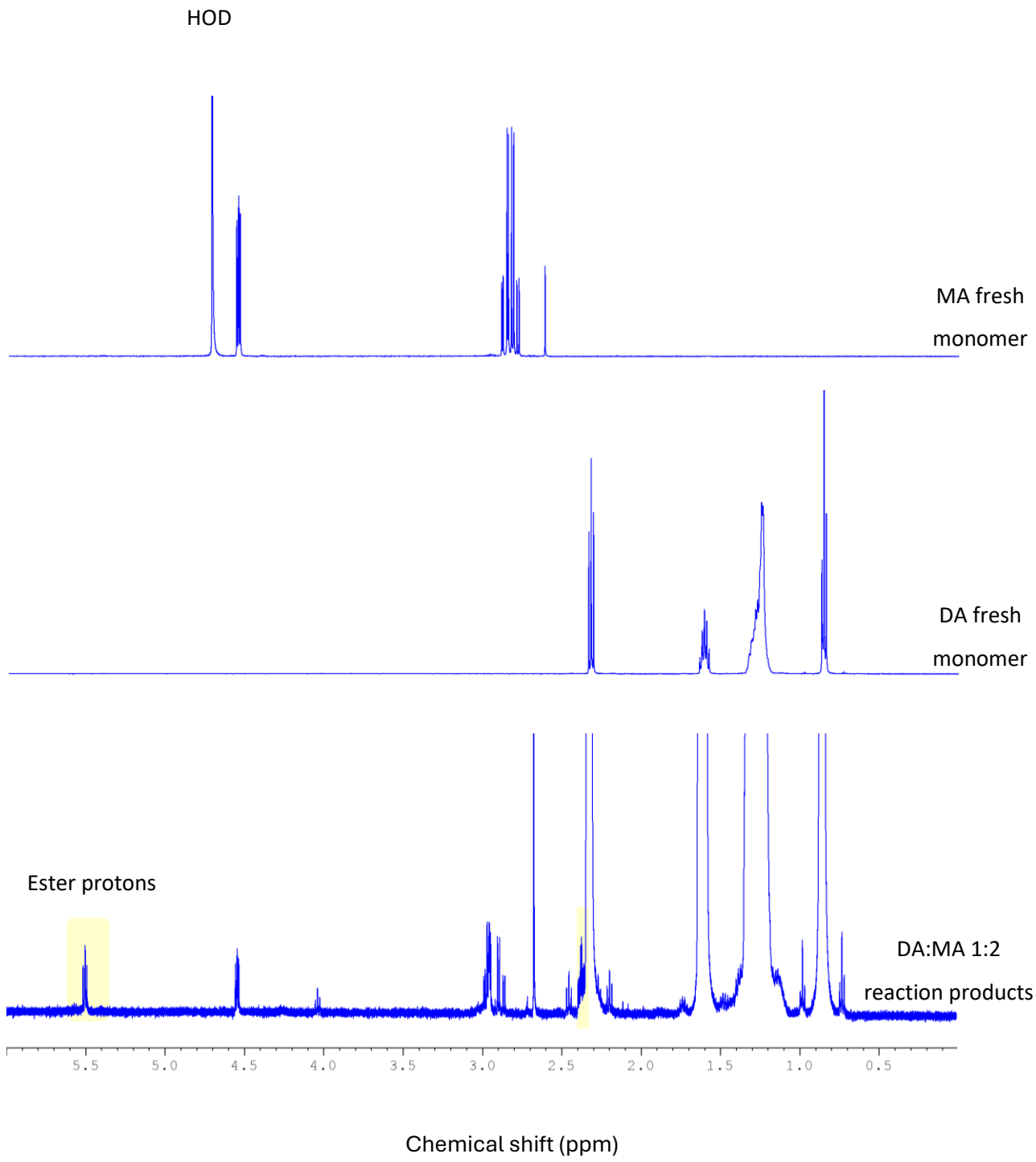

Figure S177. ^{1}H-NMR spectrum of DA:MA reaction product at 1:2 molar ratio. The dry reaction product was suspended in $CDCl_3$ and analyzed by ^{1}H-NMR. DA monomers in $CDCl_3$ and MA monomer in D_2O are presented for reference. Alpha protons shift downfield indicates the formation of ester bonds (highlighted in yellow).

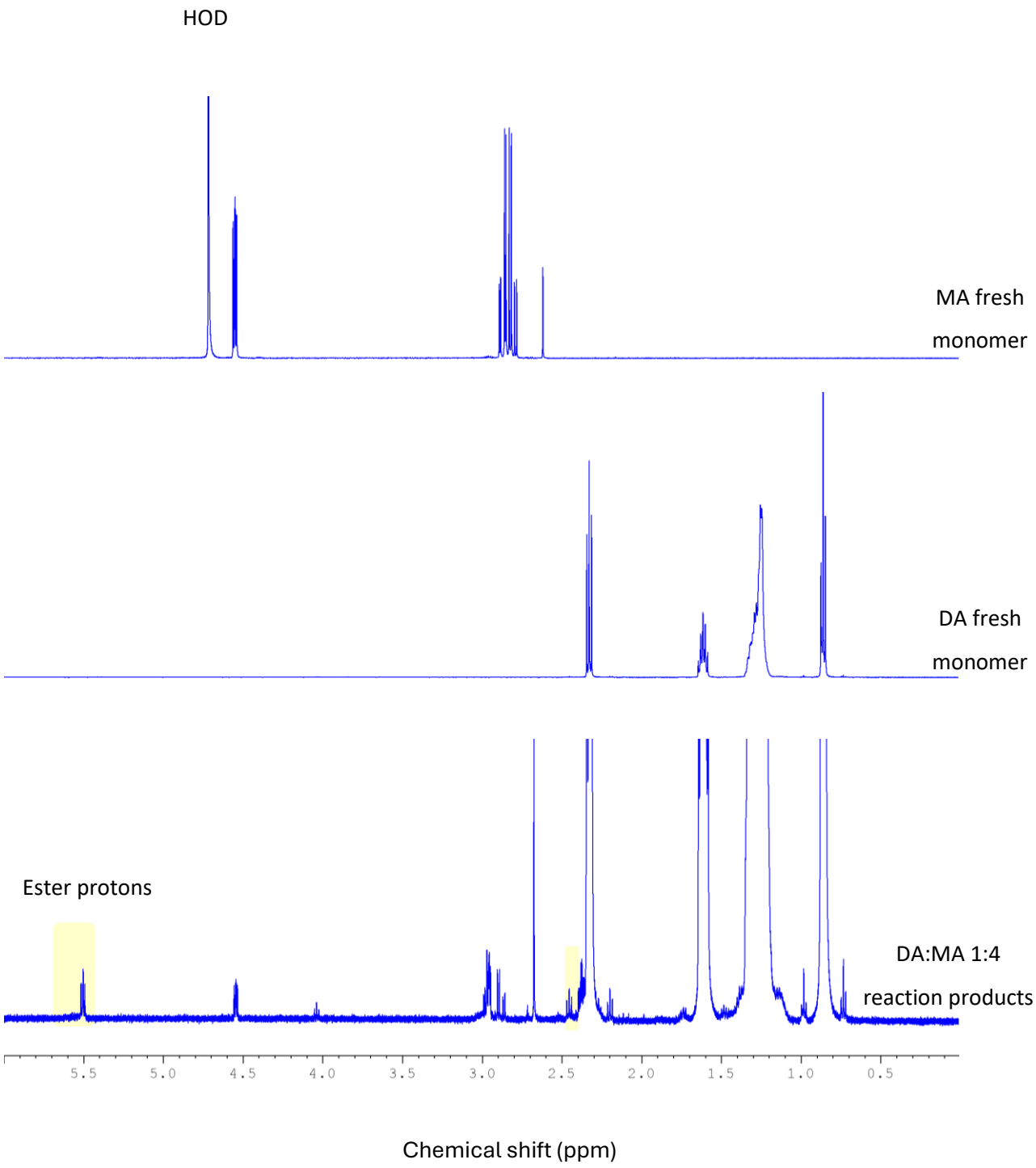

Figure S178. 1H-NMR spectrum of DA:MA reaction product at 1:4 molar ratio. The dry reaction product was suspended in $CDCl_3$ and analyzed by ^{1}H-NMR. DA monomers in $CDCl_3$ and MA monomer in D_2O are presented for reference. Alpha protons shift downfield indicates the formation of ester bonds (highlighted in yellow).

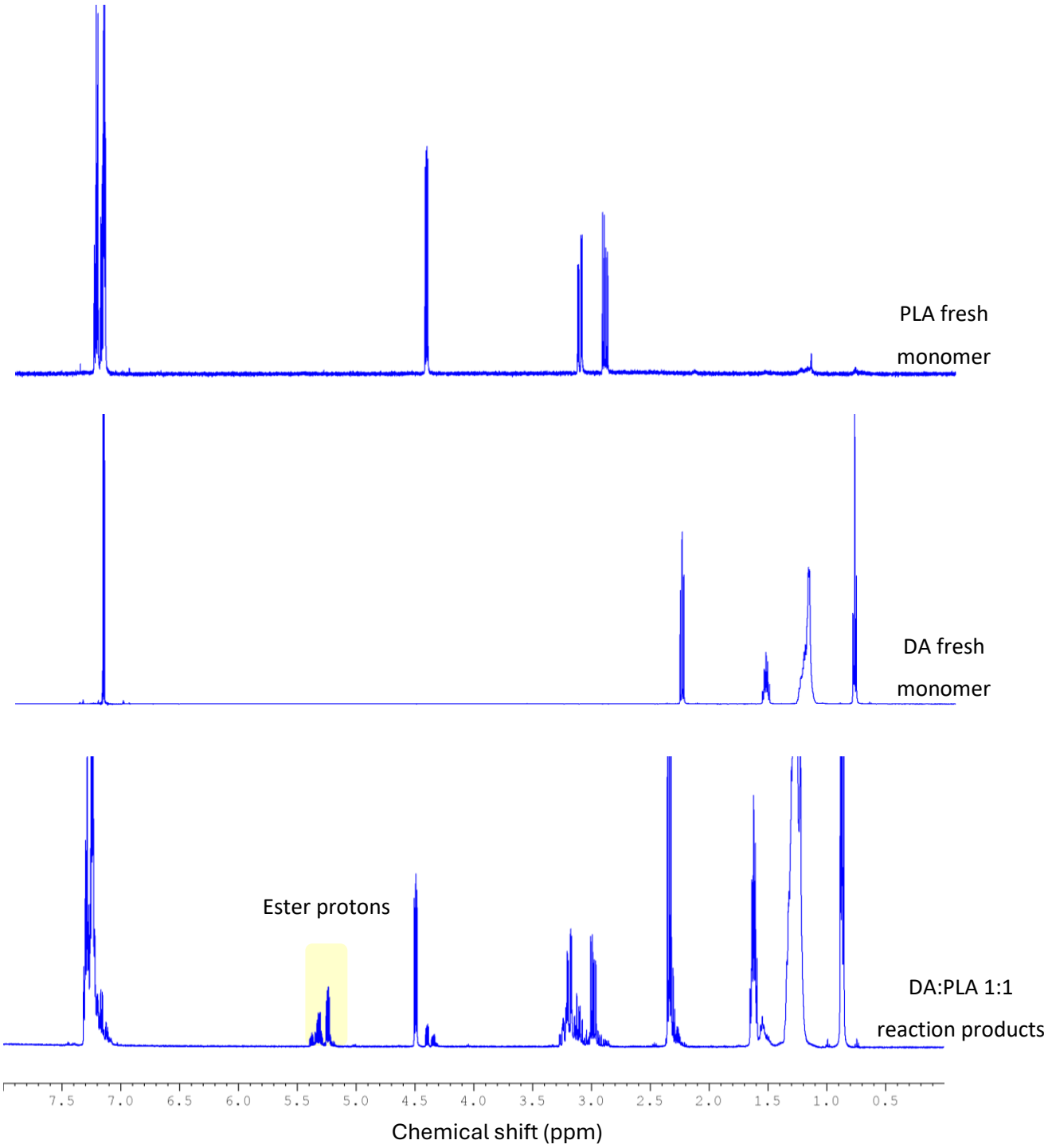

Figure S179. ^{1}H-NMR spectrum of DA:PLA reaction product at 1:1 molar ratio. The dry reaction product was suspended in $CDCl_3$ and analyzed by ^{1}H-NMR. DA and PLA monomers in $CDCl_3$ are presented for reference. Alpha protons shift downfield indicates the formation of ester bonds (highlighted in yellow).

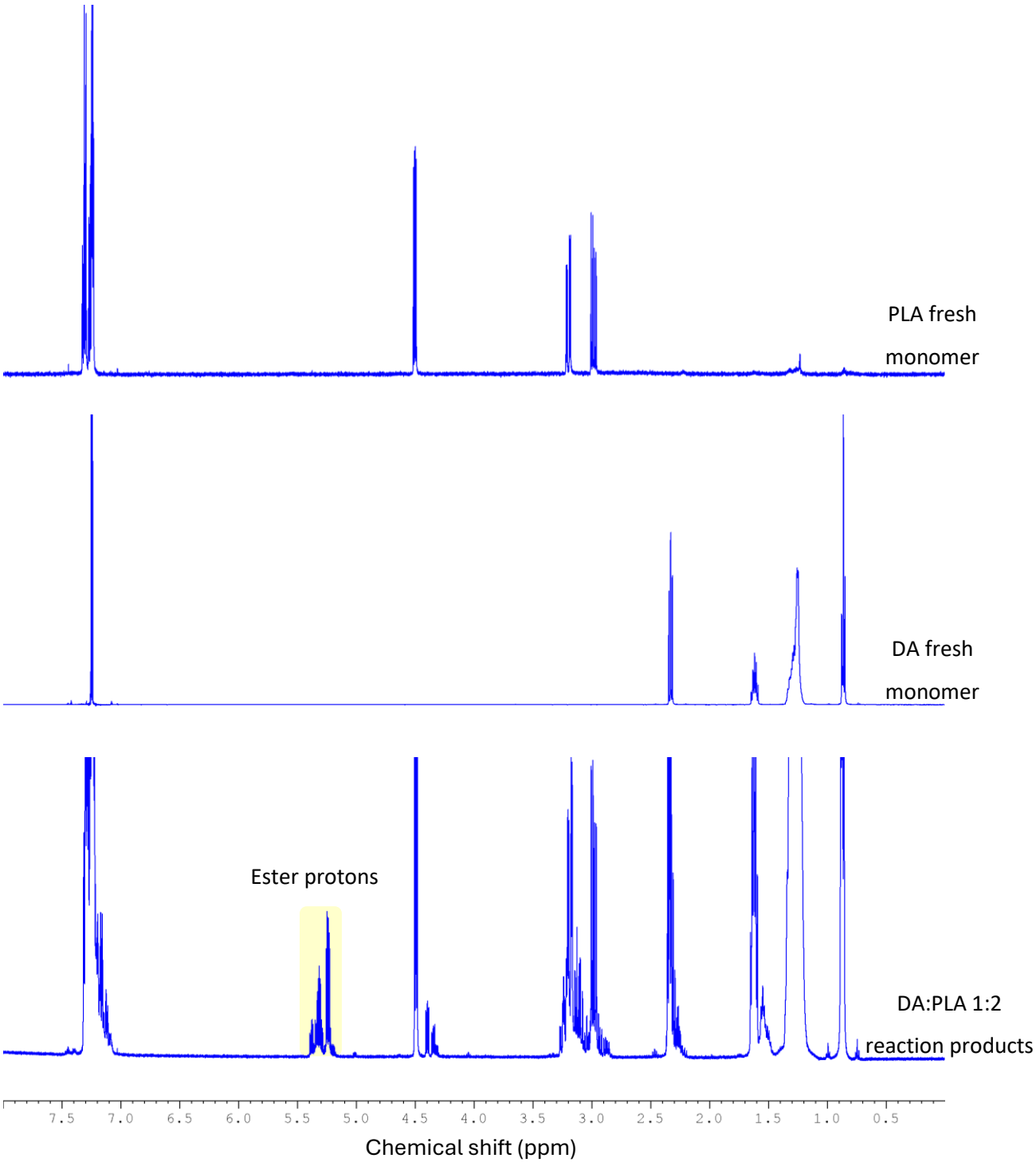

Figure S180. ^{1}H-NMR spectrum of DA:PLA reaction product at 1:2 molar ratio. The dry reaction product was suspended in $CDCl_3$ and analyzed by ^{1}H-NMR. DA and PLA monomers in $CDCl_3$ are presented for reference. Alpha protons shift downfield indicates the formation of ester bonds (highlighted in yellow).

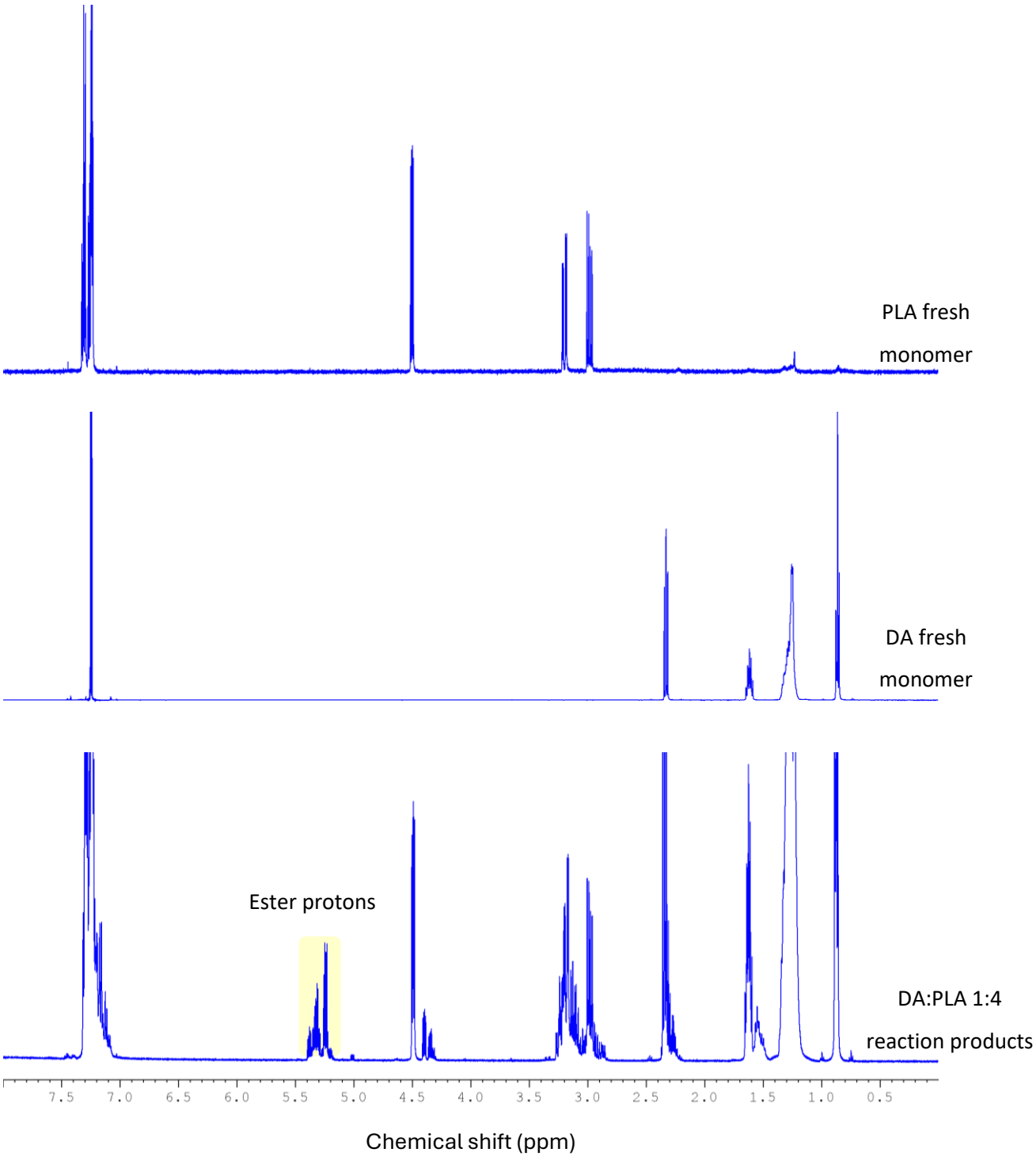

Figure S181. ^{1}H-NMR spectrum of DA:PLA reaction product at 1:4 molar ratio. The dry reaction product was suspended in $CDCl_3$ and analyzed by ^{1}H-NMR. DA and PLA monomers in $CDCl_3$ are presented for reference. Alpha protons shift downfield indicates the formation of ester bonds (highlighted in yellow).for reference.

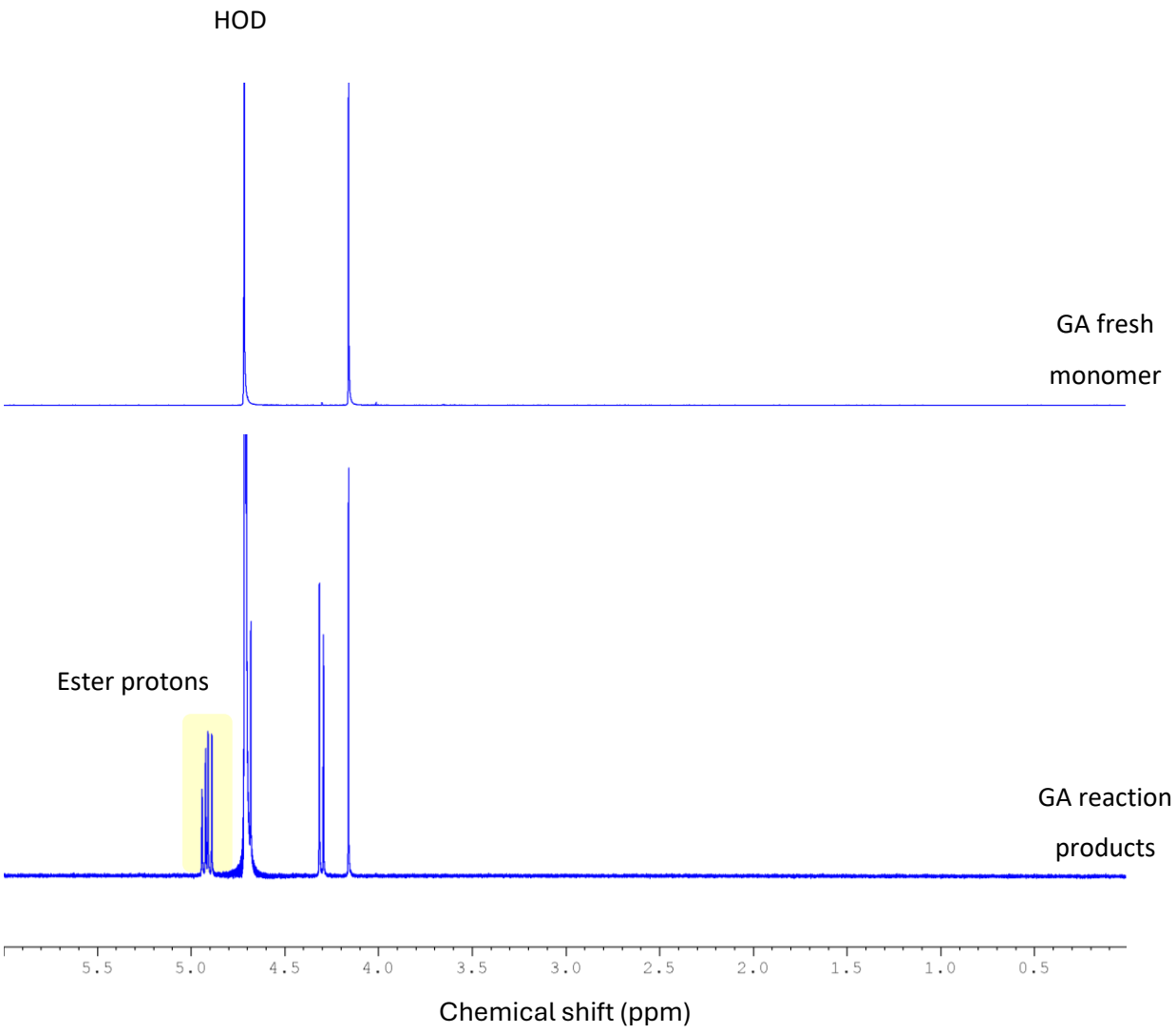

Figure S182. ^{1}H-NMR spectrum of GA control reaction products. The dry reaction product was suspended in D_2O and analyzed by ^{1}H-NMR. GA monomer in D_2O is presented for reference. Downfield shift of the alpha protons indicates the formation of ester bonds (highlighted in yellow).

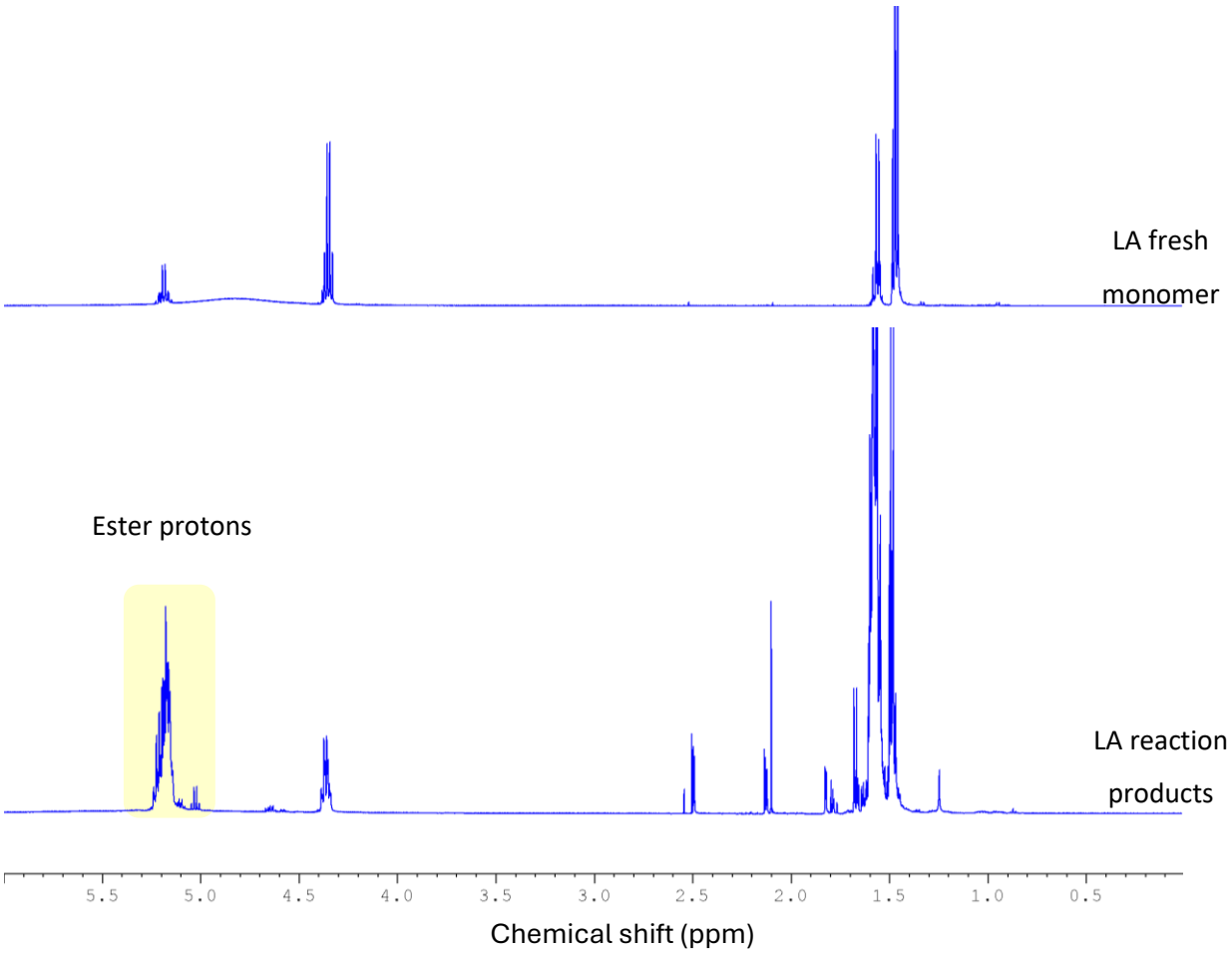

Figure S183. ^{1}H-NMR spectrum of LA control reaction product. The dry reaction product was suspended in $CDCl_3$ and analyzed by ^{1}H-NMR. LA monomer in $CDCl_3$ is presented for reference. Downfield shift of the alpha proton indicates the formation of ester bonds (highlighted in yellow).

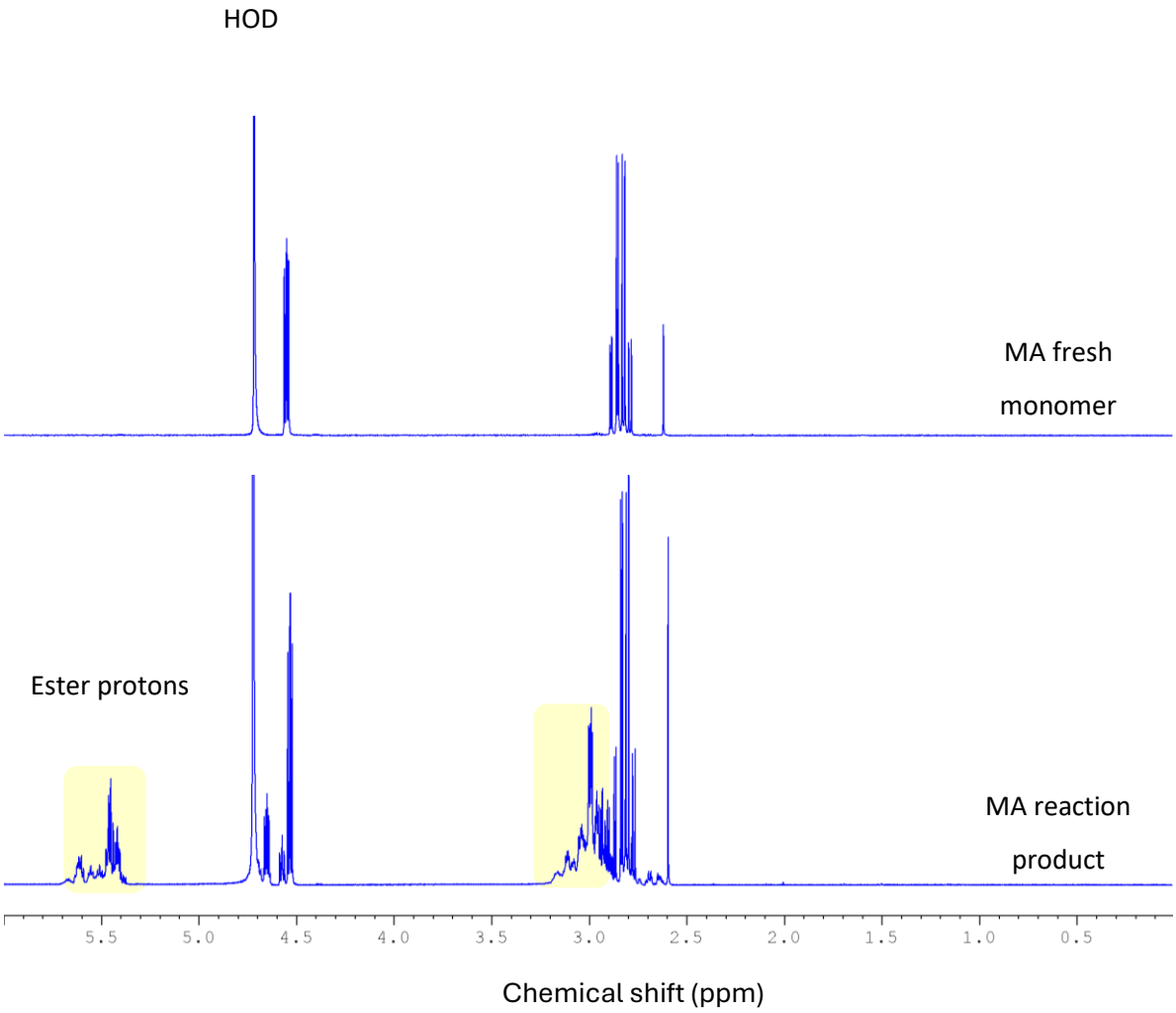

Figure S184. ^{1}H-NMR spectrum of MA control reaction product. The dry reaction product was suspended in D_2O and analyzed by ^{1}H-NMR. MA monomer in D_2O is presented for reference. Downfield shift of the alpha proton indicates the formation of ester bonds (highlighted in yellow).

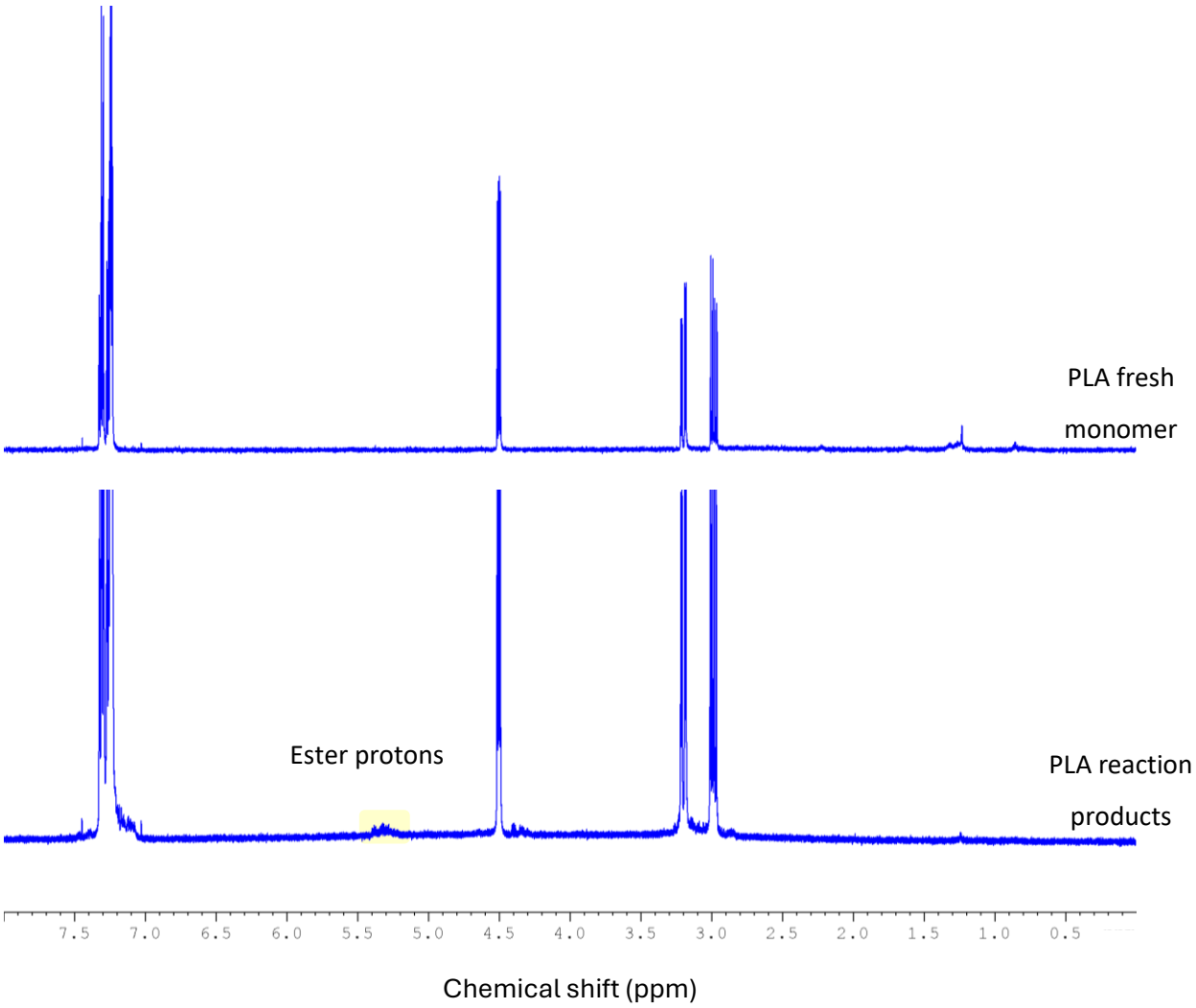

Figure S185. ^{1}H-NMR spectrum of PLA control reaction product. The dry reaction product was suspended in $CDCl_3$ and analyzed by ^{1}H-NMR. PLA monomer in $CDCl_3$ is presented for reference. Downfield shift of the alpha proton indicates the formation of ester bonds (highlighted in yellow).

A

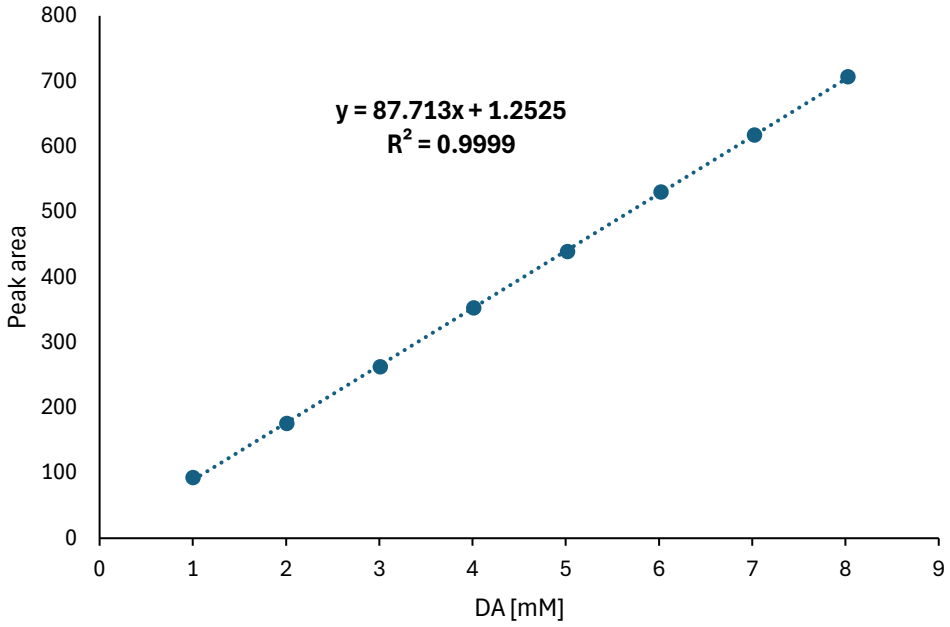

B

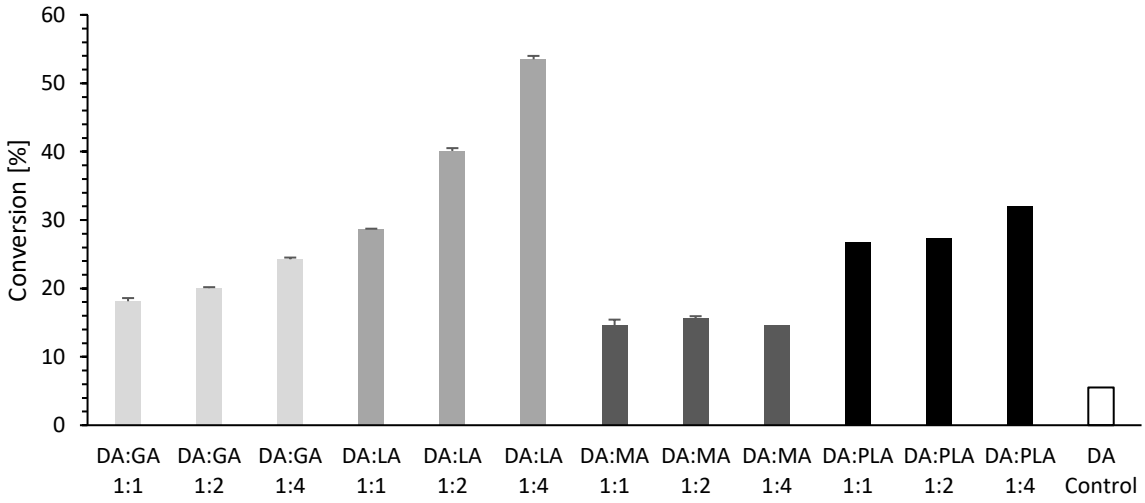

Figure S186. DA consumption under dry reaction at 85°C for 7 days determined by HPLC. Calibration curve was constructed at 210nm for the determination of DA conversion (A) .DA has been consumed when introduced to all HAs under the reaction conditions (B)

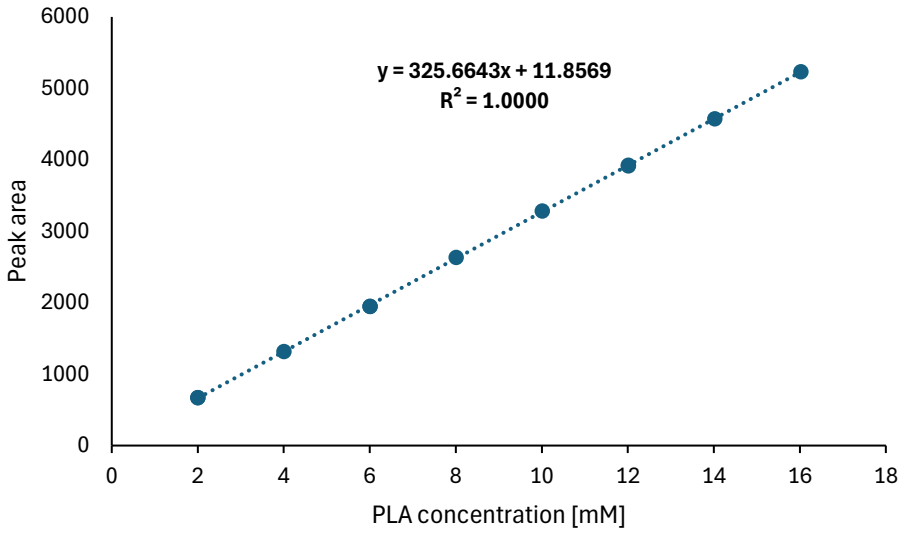

Figure S187. Calibration curve at 259nm constructed for the determination of PLA conversion.

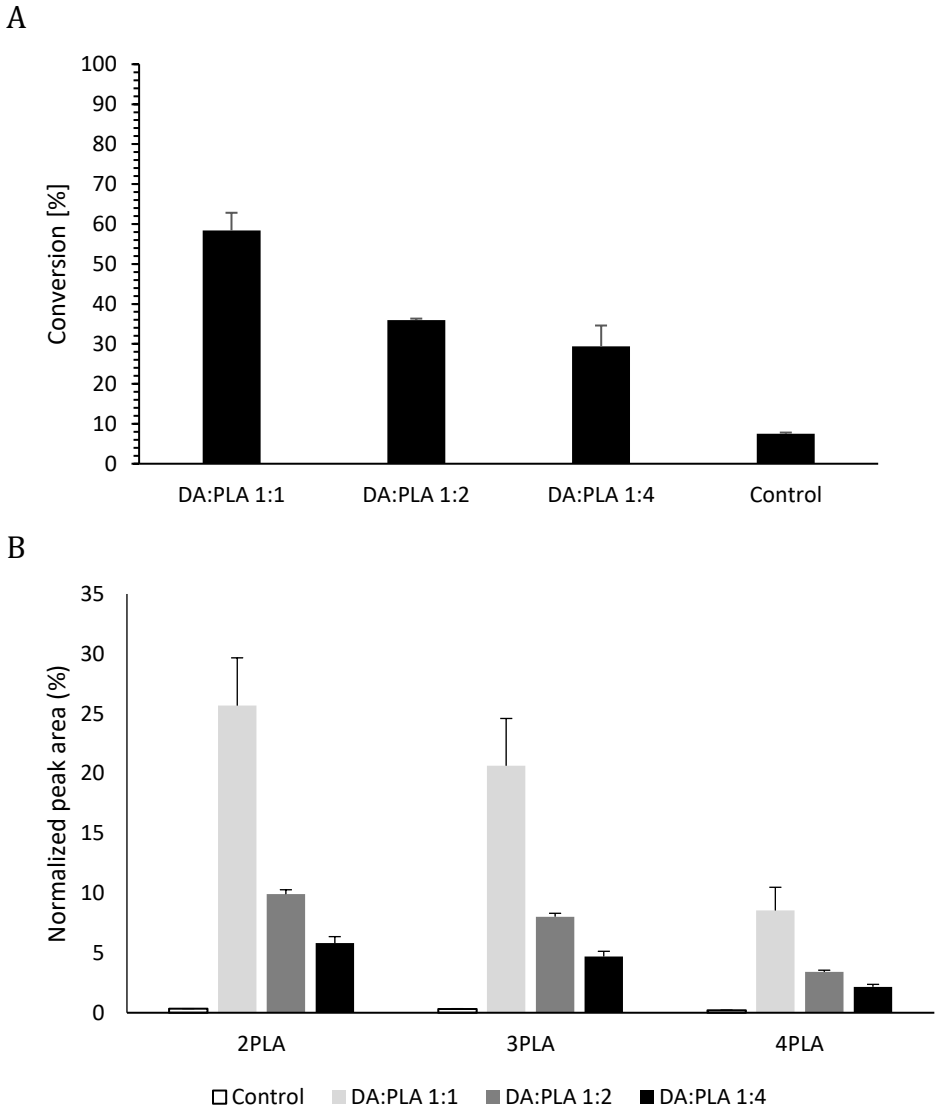

Figure S188. PLA consumption under dry reaction at 85°C for 7 days. The conversion of PLA following the reaction in the presence and absence ('control') of DA at PLA:DA 1:1, 1:2, and 1:4 molar ratios (A). The relative abundance of PLA dimer (2PLA), trimer (3PLA), and tetramer (4PLA) obtained by the reaction of PLA in the presence and absence of DA (B). The relative abundance was calculated as the ratio of homoesters peak area to PLA peak area at 259 nm. The presence of DA resulted in significant increase in the conversion of PLA into products. The formation of PLA homoesters in the presence of DA was also enhanced. The enhancement was inversely proportional to DA:PLA molar ratio exhibiting the highest PLA conversion and PLA homoesters formation at 1:1 molar ratio, following by 1:2 and 1:4 molar ratio. This effect is likely attributed to increased mobility of PLA molecules in the presence of DA molecules which are probably partially solubilizing PLA molecules.

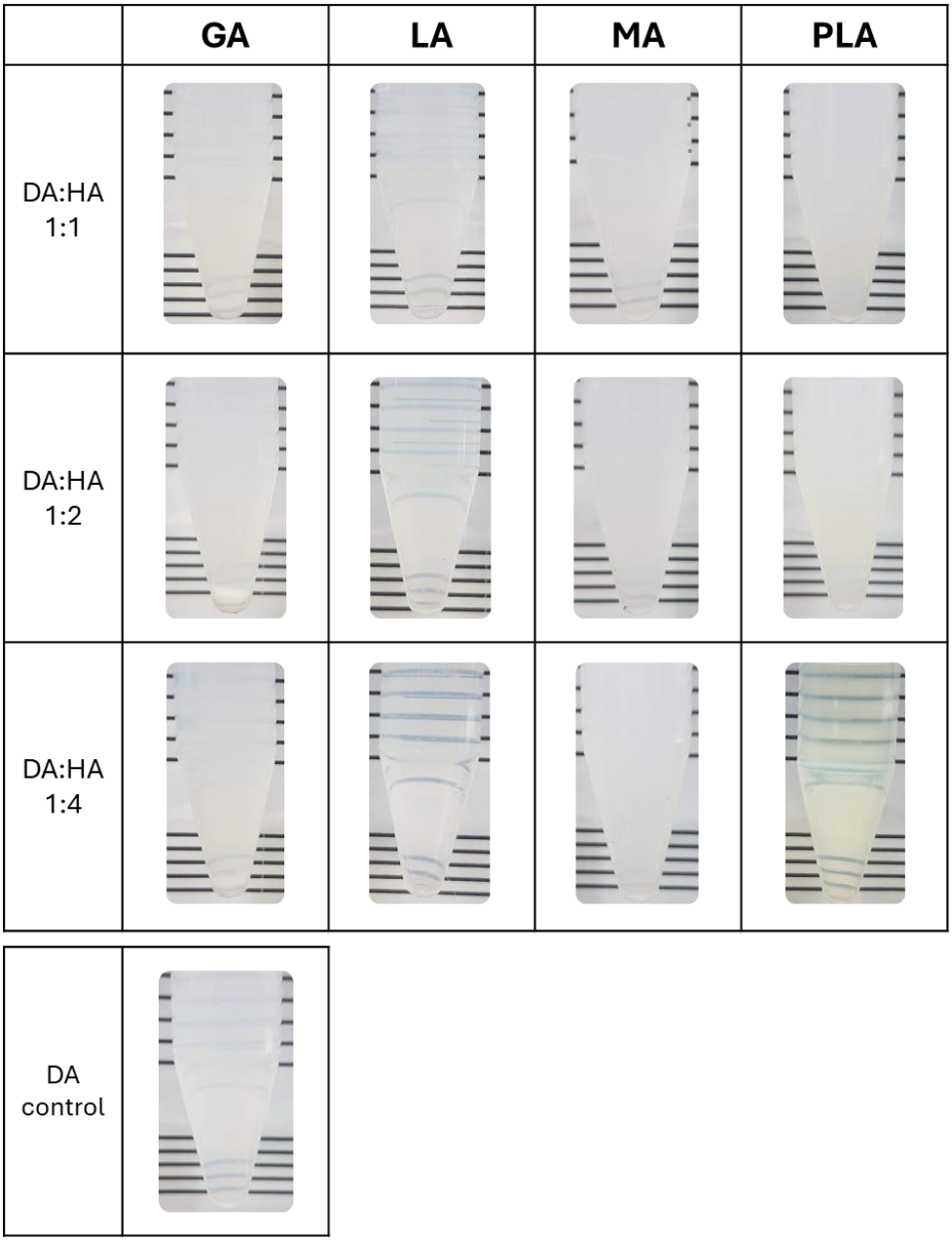

Figure S189. Visual appearance of rehydrated DA-HA reaction products at 1:1, 1:2, and 1:4 molar ratio. All samples were rehydrated in phosphate buffer (50mM) and their pH was adjusted to 6.8. The concentration of DA and the HAs were 50 mM and either 50, 100, or 200mM referring to initial amounts prior to the reaction. Reaction products of DA and GA contained insoluble GA oligomers as indicated in the figure. DA-LA reaction products exhibited increasing transparency as LA concentration was increased. DA-MA reaction products exhibited the opposite trend with increasing turbidity as MA concentration increased. DA-PLA products were turbid with one exception of DA:PLA at 1:4 molar ratio for which the rehydrated product was highly unstable and underwent phase separation into two liquid phases almost immediately.

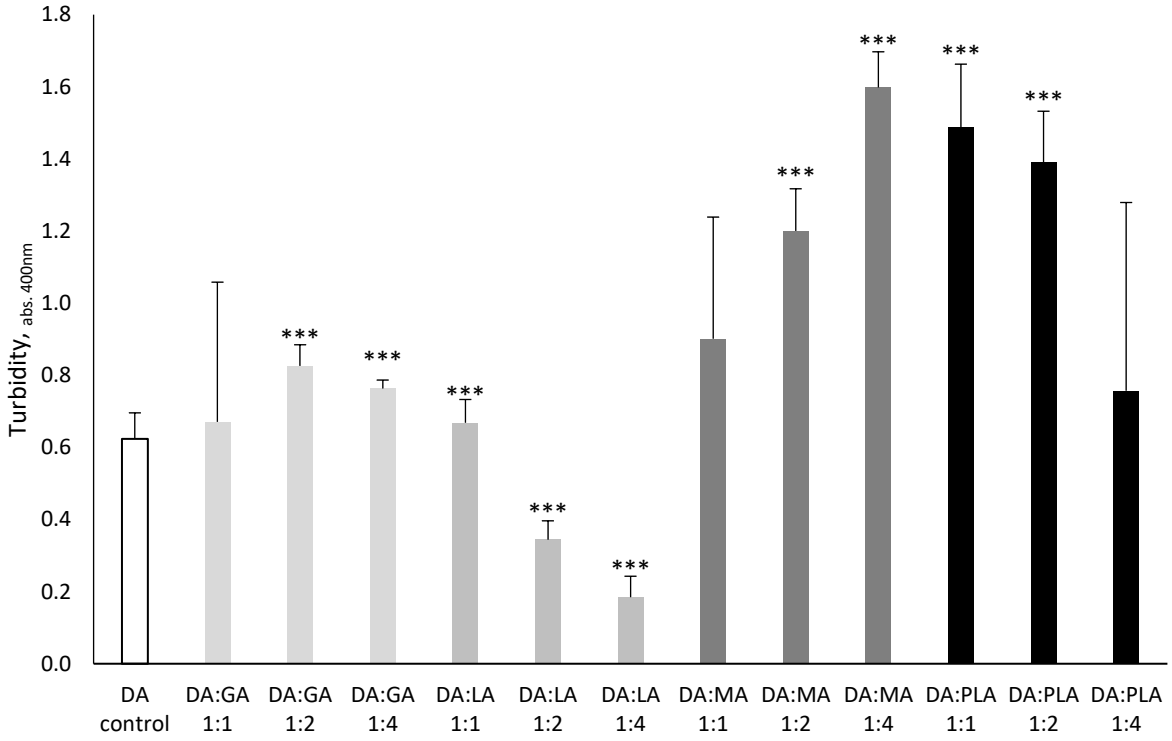

Figure S190. Turbidity meausrments of the rehydrated DA:HAs reaction products at 1:1, 1:2 and 1:4 molar ratio. All samples were rehydrated in phosphate buffer (50 mM) and their pH was adjusted to 6.8. The concentration of DA and the HAs were 50 mM and either 50, 100, or 200 mM, referring to initial amounts prior to the reaction. The turbidity (measured as the absorption at 400 nm) of the rehydrated reaction products is ratio-dependent. For GA and LA, the turbidity decreased as the DA:HA ratio increased. For MA the opposite trend was observed. In the case of PLA, a steep decrease in the turbidity was observed at DA:PLA 1:4 molar ratio, which is due to the rapid phase separation into two transparent liquids as also indicated in the visual assessment. Statisical significance was determined compared to DA control.

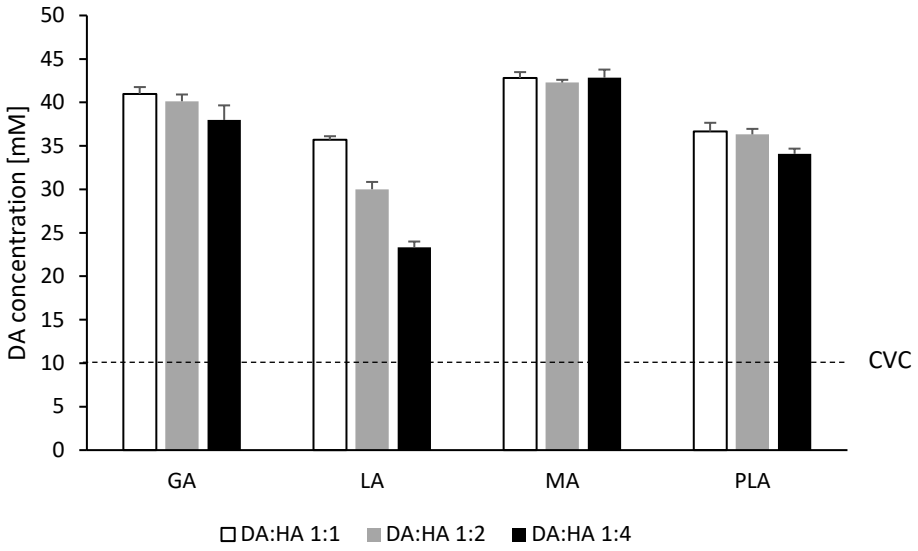

Figure S191. DA concentration in the resulting rehydrated products. All products were rehydrated in phosphate buffer (50 mM) and their pH was adjusted 6.8. The concentrations were calculated based on the measured conversion of DA in the reaction. The horizontal line at 10 mM represents the critical vesicular concentration of DA at the tested pH.

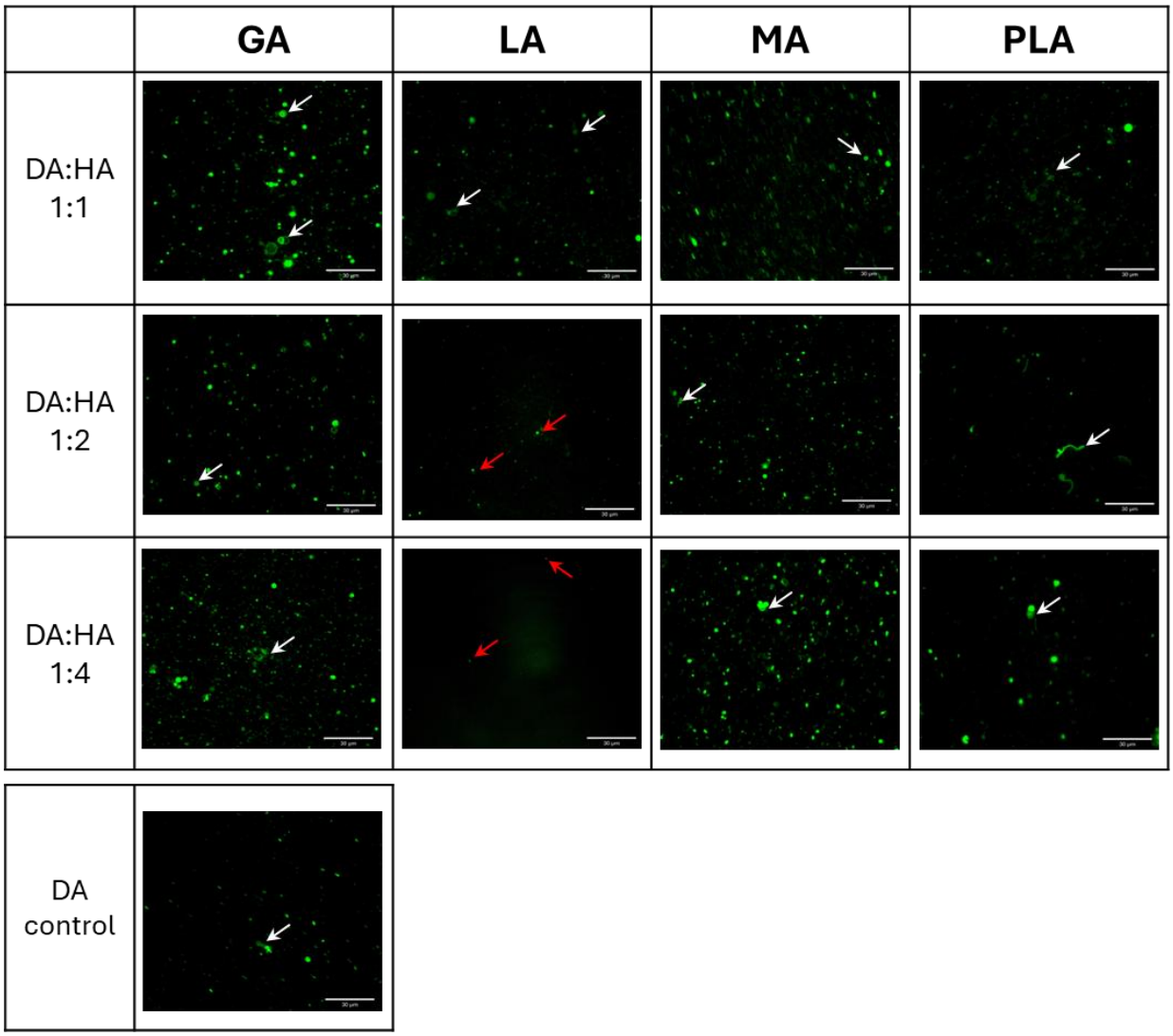

Figure S192. Fluorescent microscopy images of the rehydrated reaction products obtained by the reaction of DA and the tested HAs at different molar ratios. All samples were prepared in phosphate buffer (50 mM) at pH 6.8. The concentration of DA and the HAs were 50 mM and either 50, 100, or 200 mM, referring to the initial amounts prior to the reaction. Rhodamine 6G was used as a fluorescent probe. Structures were formed in all tested samples, as indicated by the images. Vesicles, indicated by the dying of the membrane (labeled with white arrows), were detected in all samples with the exceptions of DA:LA at 1:2 and 1:4 molar ratios, for which no clear membranous structures were detected. Nonetheless, small spherical structures were observed (labeled with red arrows). Scale bar is 30μm (x60 magnification).

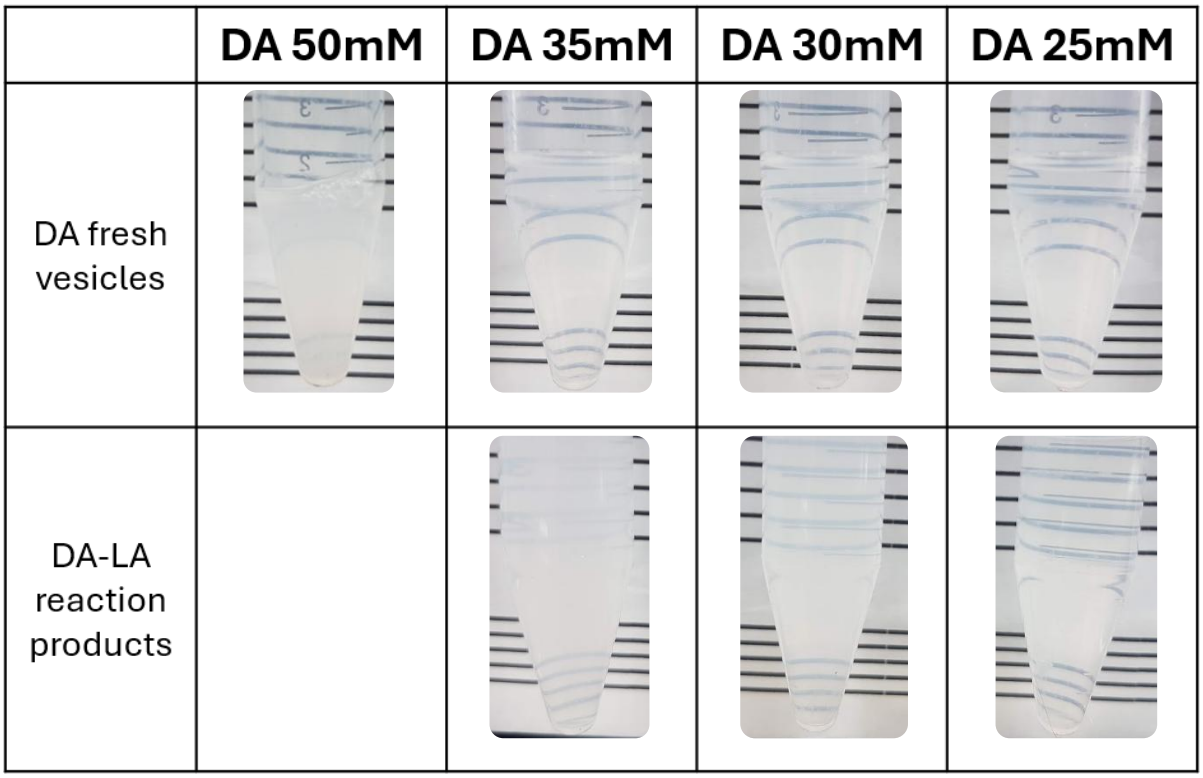

Figure S193. Visual appearance of DA fresh controls and DA:LA reaction products at 1:1, 1:2, and 1:4 molar ratios. DA fresh controls were prepared at either 50 mM, 35 mM, 30 mM, or 25 mM in phosphate buffer (50 mM) at pH 6.8. DA-LA reaction products were rehydrated in phosphate buffer (50 mM) at pH 6.8. DA final concentration in the resulting rehydrated products corresponds to 35 mM, 30 mM, and 25 mM on average for DA:LA at 1:1, 1:2, and 1:4 molar ratios, respectively. As indicated by the images, for DA fresh controls, the turbidity decreases as DA concentration decreases. For the reaction products, a similar trend was observed. While at 35 mM and 25 mM DA the reaction products appeared more turbid than the fresh controls, at 25 mM DA the turbidity of both fresh control and reaction products is comparable.

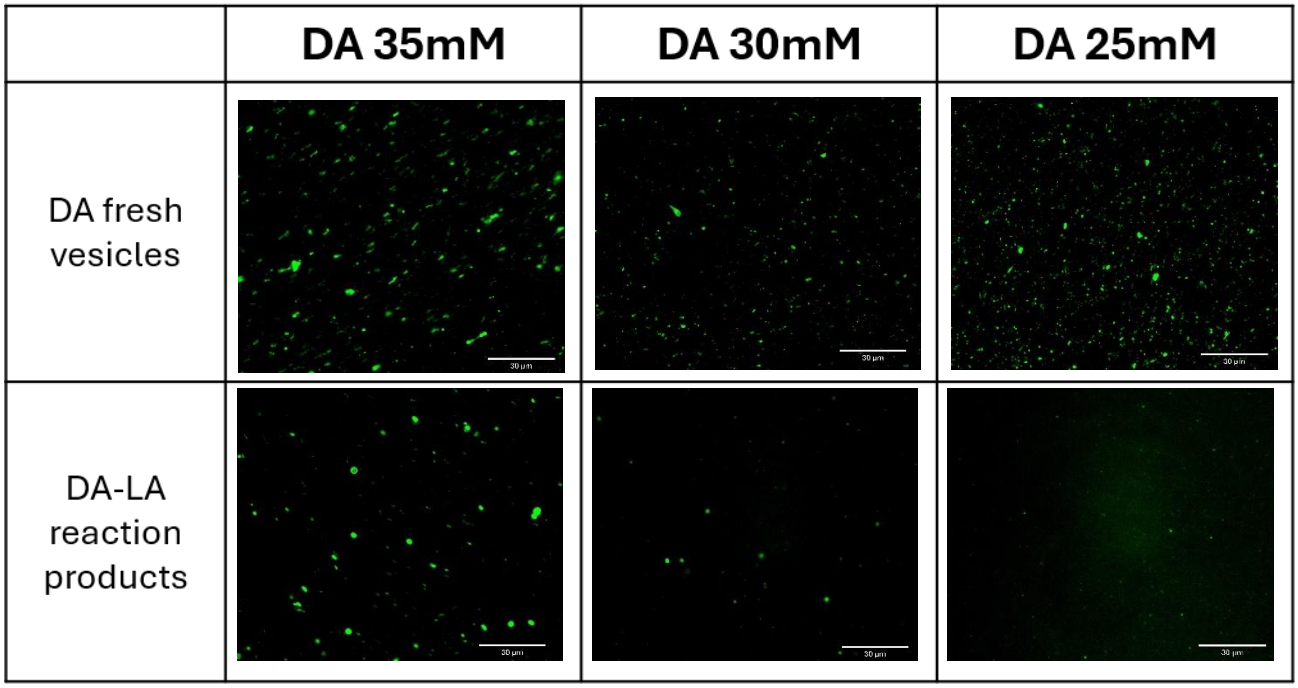

Figure S194. Fluorescent microscopy images of DA fresh controls at decreasing concentrations and DA:LA reaction products at 1:1, 1:2, and 1:4 molar ratios. DA fresh controls were prepared at either 35 mM, 30 mM, or 25mM in phosphate buffer (50 mM) at pH 6.8. DA-LA reaction products were rehydrated in phosphate buffer (50 mM) at pH 6.8. DA final concentration in the resulting rehydrated products corresponds to 35 mM, 30 mM, and 25 mM on average for DA:LA at 1:1, 1:2, and 1:4 molar ratios, respectively. Structures were observed in all samples. The extent of structures formation as indicated by the microscopy observation was relatively similar in the case of the samples of 35mM DA. However, at DA final concentrations of 30 mM and 25 mM, the distribution and number of structures was reduced in the reaction products compared to the fresh controls, suggesting that the aggregation properties of the DA-LA products mixture are different than those of DA. Scale bar is 30μm (x60 magnification).

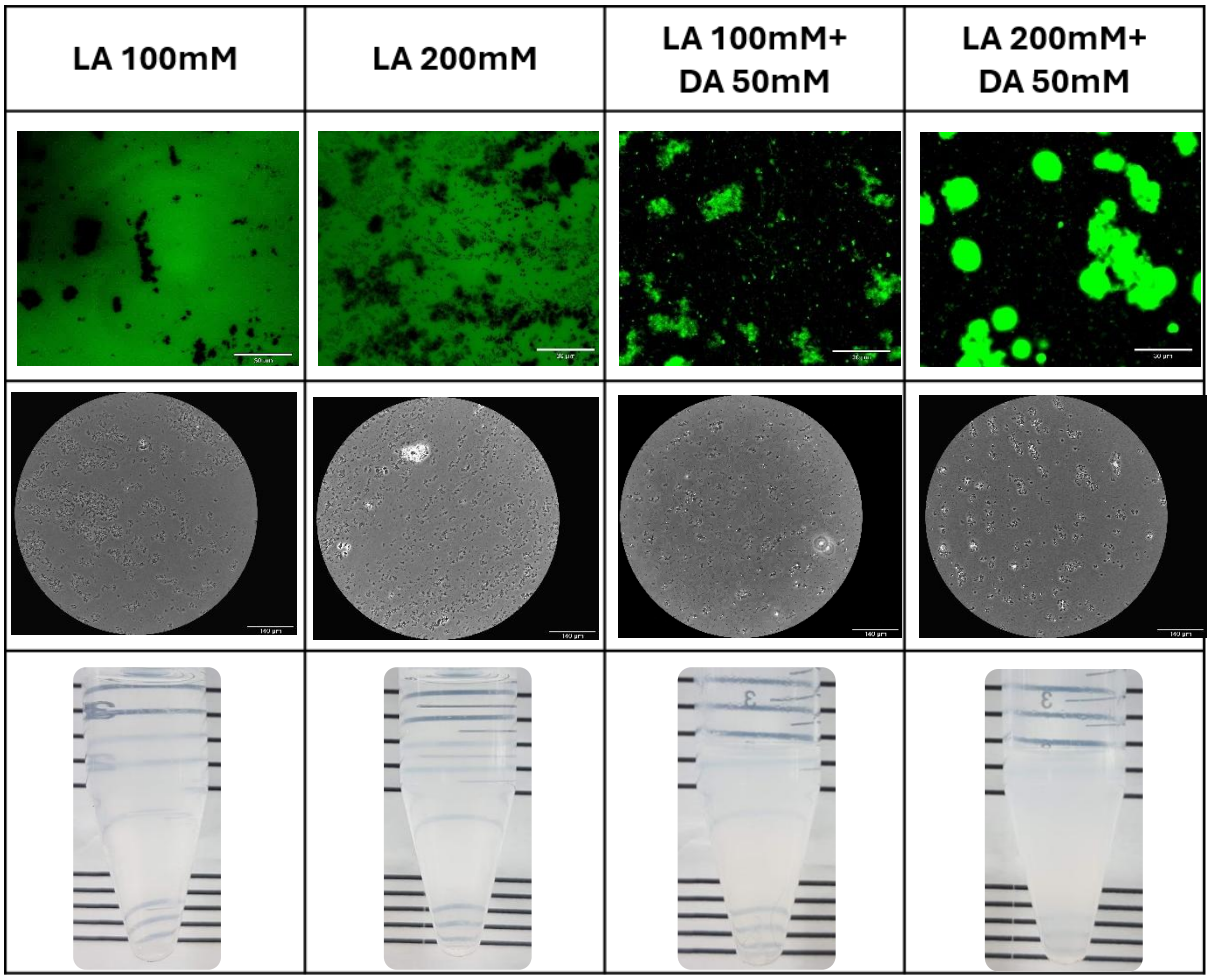

Figure S195. Fluorescent microscopy images , bright-field microscopy images, and visual appearance of LA reaction products at 100 mM and 200 mM in the presence and absence of 50 mM DA. For the samples in the absence of DA, LA reaction products were rehydrated in phosphate buffer (50 mM) at pH 6.8. In the presence of DA, LA reaction products were rehydrated in DA stock solution and phosphate buffer and pH was adjusted to 6.8. The concentration of LA was either 100 mM or 200 mM, referring to the initial amount prior to the reaction. When present, DA concentration was 50 mM. LA reaction products formed aggregates as indicated by the microscopy images. In the absence of DA, aggregates were not dyed by rhodamine 6G. When DA was added, vesicles were observed and aggregates formed by LA oligomers were dyed by the probe suggesting that DA adsorbed at the aggregates surface. Scale bar is 30μm (x60 magnification) for fluorescent microscopy images and is 140μm (x20 magnification) for brigh-field microscopy images.

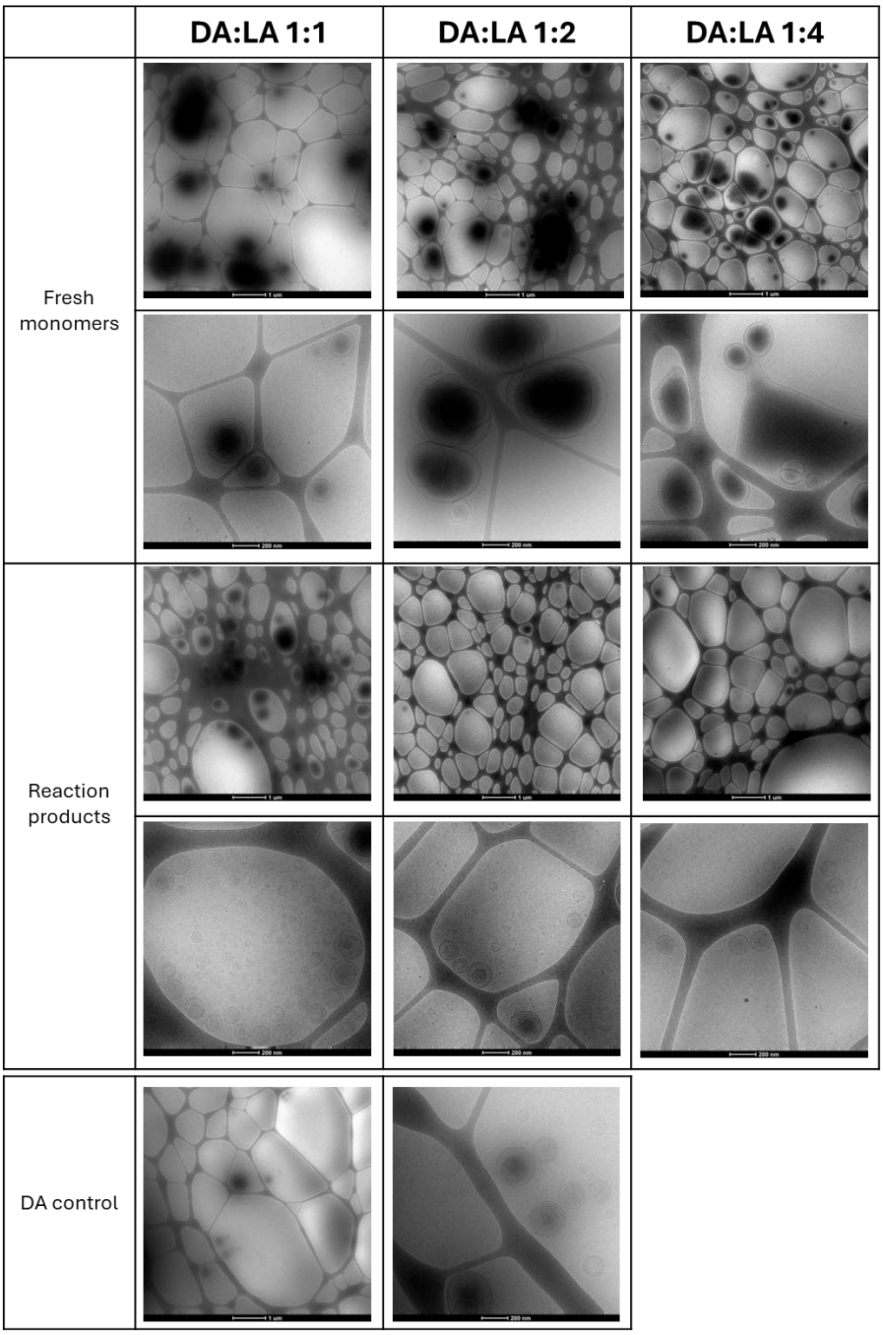

Figure S196. Cryo-TEM images of fresh monomers and reaction products of DA:LA at 1:1, 1:2, and 1:4 molar ratios. All samples were prepared in phosphate buffer (50 mM) at pH 6.8. The concentration of DA was 50mM, and the concentration of LA was either 50, 100, or 200 mM. In the case of the reaction products, DA and LA concentrations refer to the initial amounts prior to the reaction. The micrographs confirm the presence of vesicles in all samples. In the case of the fresh monomers, as the concentration of LA increased above 50mM, the average size of the observed vesicles increased, and the vesicles became less spherical and more deformed. In addition, the inner aqueous phase of the vesicles appears darker, possibly due to the presence of phosphate ions. In the case of the reaction products, at DA:LA molar ratios of 1:1 and 1:2 small vesicles of less than 100nm were abundant compared to vesicles of larger diameter. Remarkably, vesicles observed in DA:LA at 1:4 molar ratio were mostly unilamellar within 100-200nm. In general, the number of vesicles was signifcantly lower at DA:LA 1:4 molar ratio In this sample micelles of about 4-6nm were also observed. Note that the scale bar is the same (top raw is 1μm and bottom raw is 200nm) in images that are in the same row. For DA control sample the scale bars are 1μm and 200nm respectively.

A

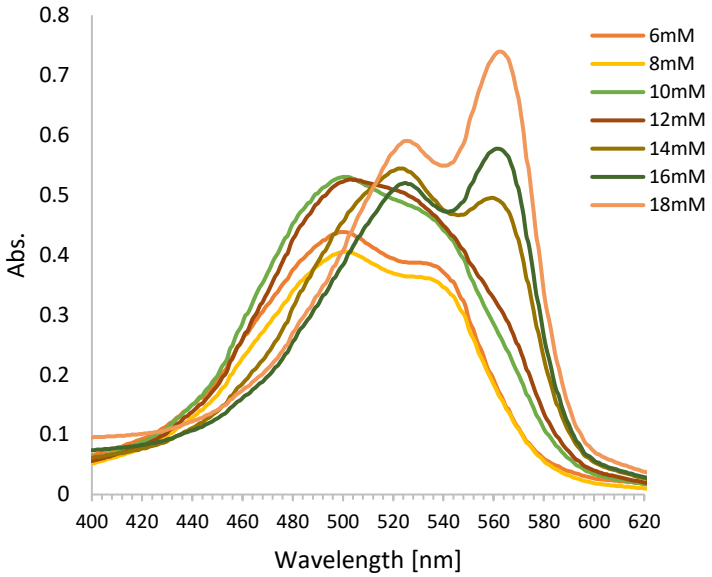

B

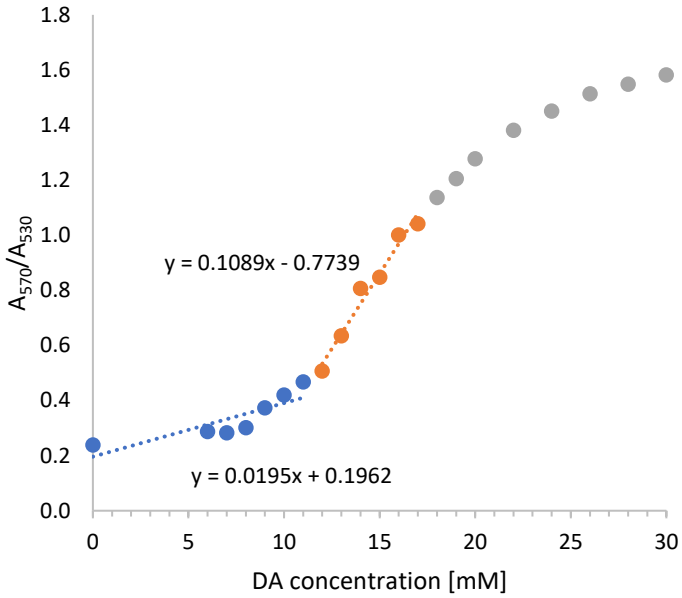

Figure S197. Determination of the critical aggregation concentration of DA for DA control sample. Absorption spectra of merocyanine 540 in the presence of increasing concentrations of DA obtained for DA control sample at pH 6.8 (A). Absorption ratio at 570 nm and 530 nm as a function of DA concentration. The intersection between the two fitting lines represents the CAC of DA – ca. 10 mM (B).

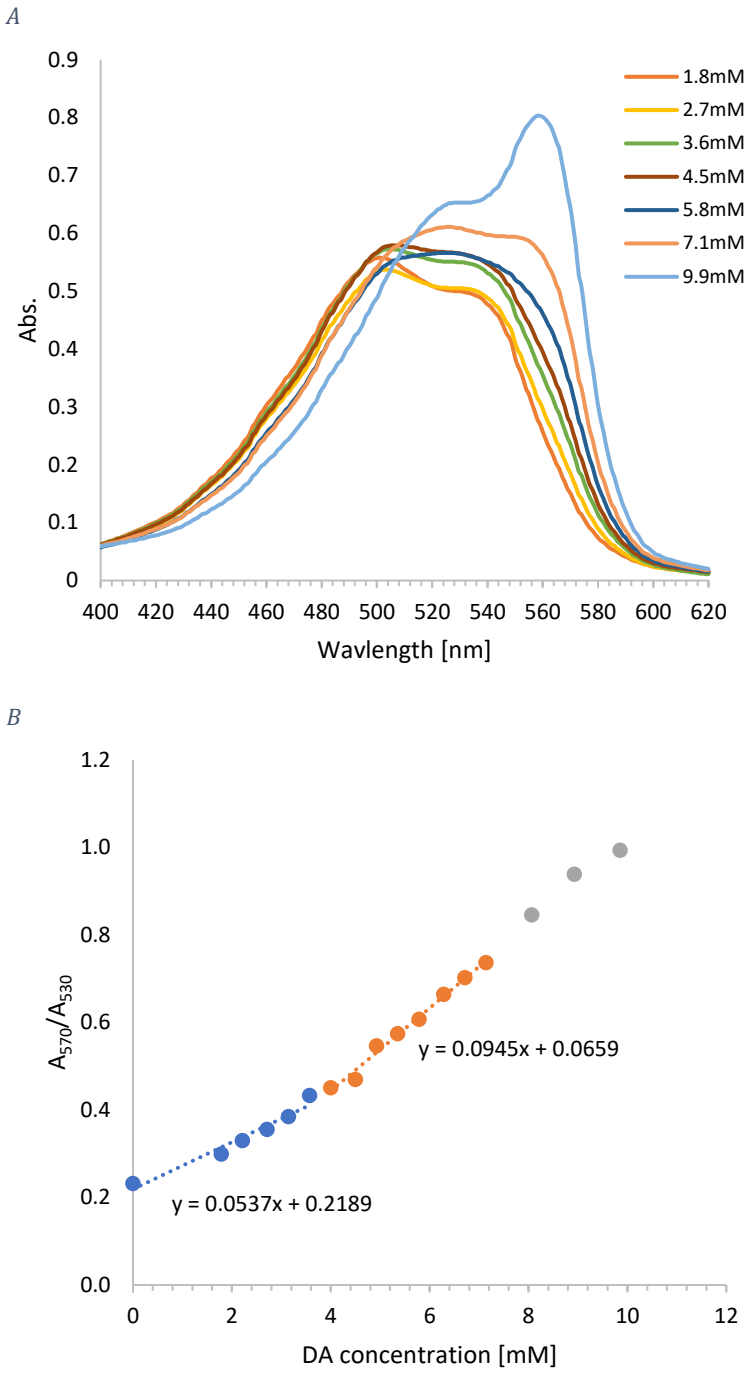

Figure S198. Determination of the critical aggregation concentration of DA for DA:LA reaction product at 1:1 molar ratio. Absorption spectra of merocyanine 540 in the presence of increasing concentrations of DA obtained for the reaction product of DA:LA at 1:1 molar ratio at pH 6.8 (A). Absorption ratio at 570 nm and 530 nm as a function of DA concentration. The intersection between the two fitting lines represents the CAC of DA – ca. 4 mM (B).

A

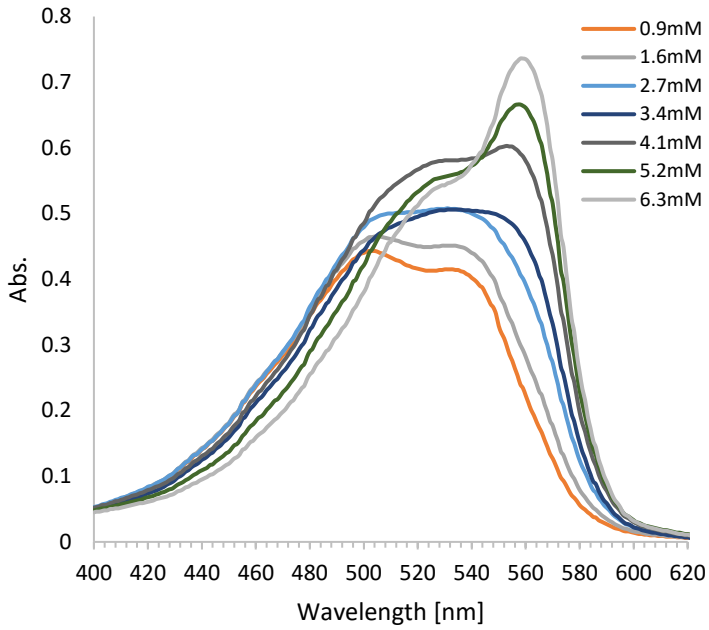

B

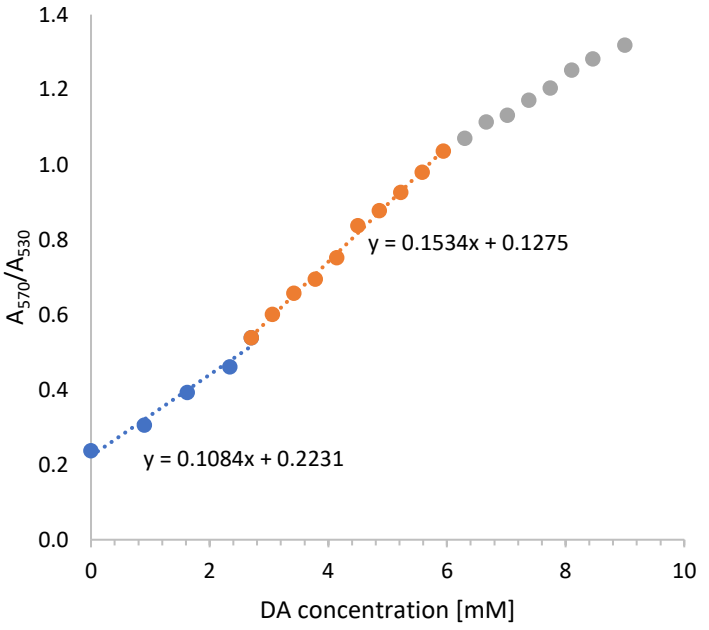

Figure S199. Determination of the critical aggregation concentration of DA for DA:LA reaction product at 1:2 molar ratio. Absorption spectra of merocyanine 540 in the presence of increasing concentrations of DA obtained for the reaction product of DA:LA at a 1:2 molar ratio at pH 6.8 (A). Absorption ratio at 570 nm and 530 nm as a function of DA concentration. The intersection between the two fitting lines represents the CAC of DA – ca. 2 mM (B).

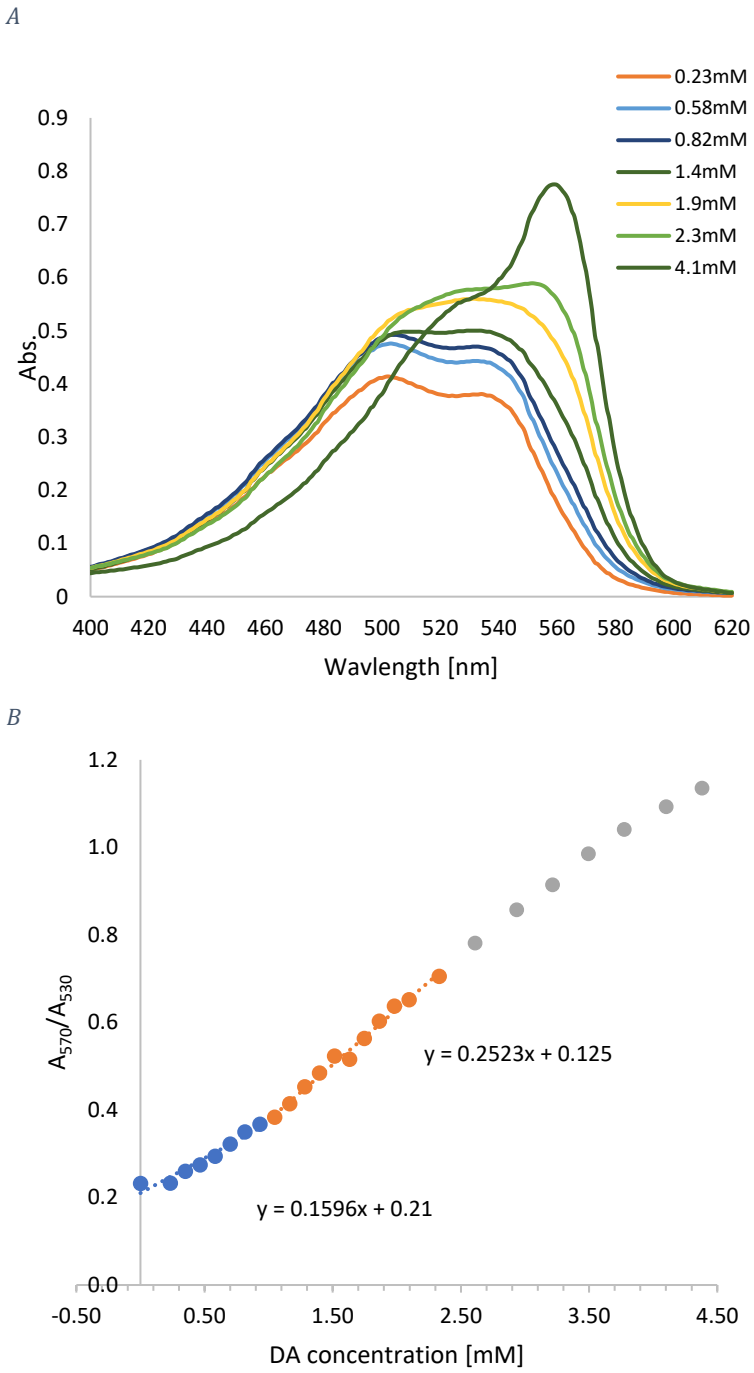

Figure S200. Determination of the critical aggregation concentration of DA for DA:LA reaction product at 1:4 molar ratio. Absorption spectra of merocyanine 540 in the presence of increasing concentrations of DA obtained for the reaction product of DA:LA at a 1:4 molar ratio at pH 6.8 (A). Absorption ratio at 570 nm and 530 nm as a function of DA concentration. The intersection between the two fitting lines represents the CAC of DA – ca 1 mM (B).

A

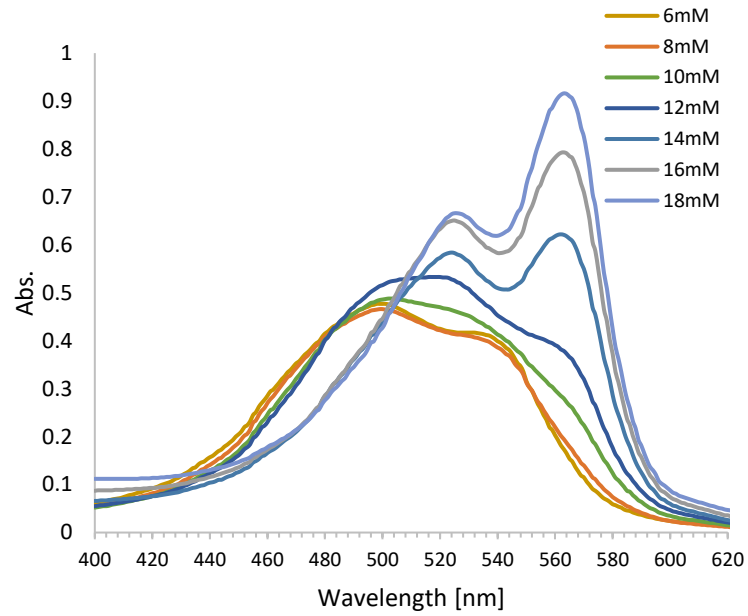

B

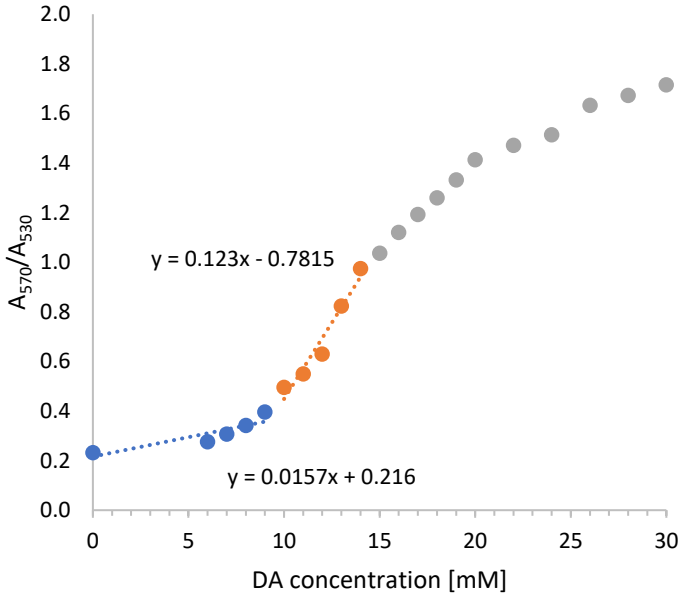

Figure S201. Determination of the critical aggregation concentration of DA for DA:LA fresh monomers at 1:2 molar ratio. Absorption spectra of merocyanine 540 in the presence of increasing concentrations of DA obtained for fresh monomers of DA:LA at 1:2 molar ratio at pH 6.8 (A). Absorption ratio at 570nm and 530nm as a function of DA concentration. The intersection between the two fitting lines represents the CAC of DA – ca. 10 mM (B).

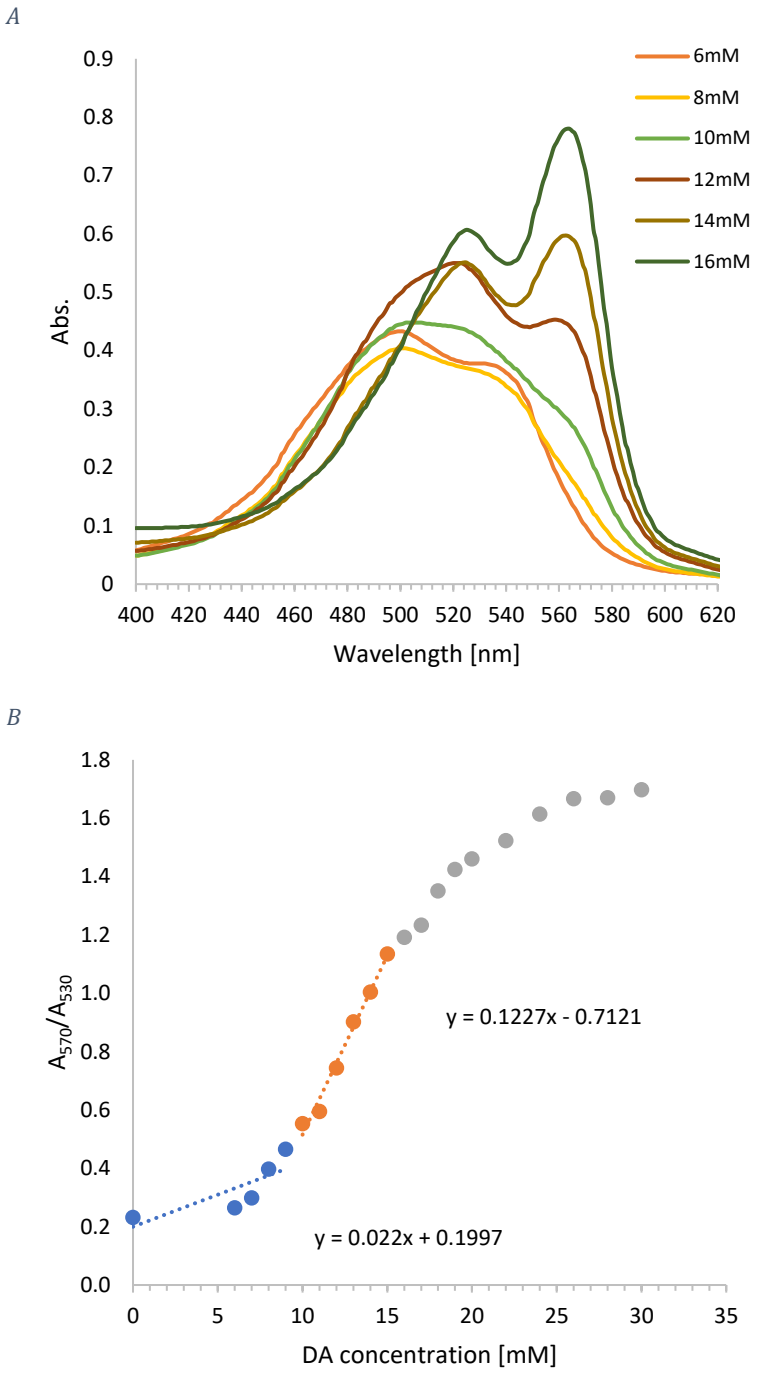

Figure S202. Determination of the critical aggregation concentration of DA for DA:LA fresh monomers at 1:4 molar ratio. Absorption spectra of merocyanine 540 in the presence of increasing concentrations of DA obtained for fresh monomers of DA:LA at 1:4 molar ratio at pH 6.8 (A). Absorption ratio at 570nm and 530nm as a function of DA concentration. The intersection between the two fitting lines represents the CAC of DA – ca. 9 mM (B).

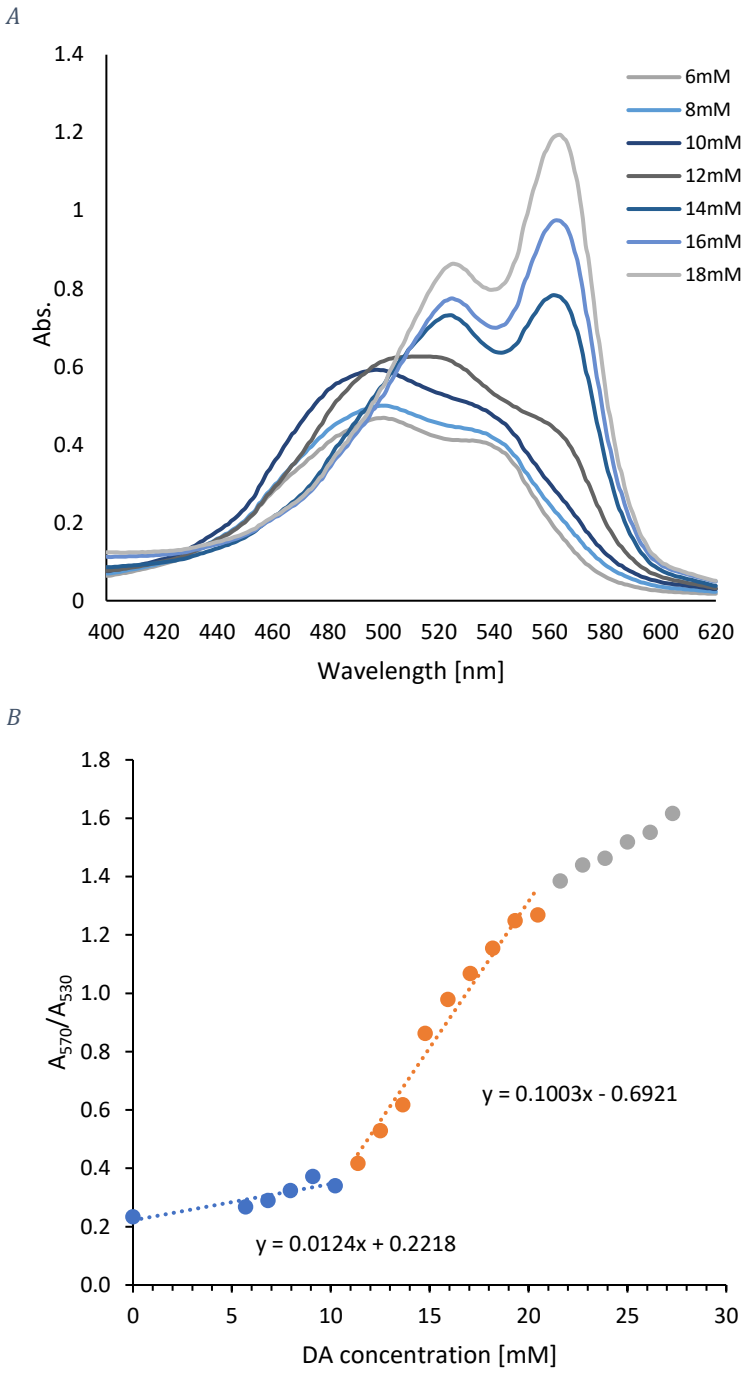

Figure S203. Determination of the critical aggregation concentration of DA for a mixture of DA and LA rection product at 1:2 molar ratio referring to initial amount of LA. Absorption spectra of merocyanine 540 in the presence of increasing concentrations of DA obtained for the reaction product LA into which DA was added at pH 6.8. The ratio between DA and LA was 1:2 referring to the initial amount of LA prior to the reaction (A). Absorption ratio at 570nm and 530nm as a function of DA concentration. The intersection between the two fitting lines represents the CAC of DA – ca. 10 mM (B).

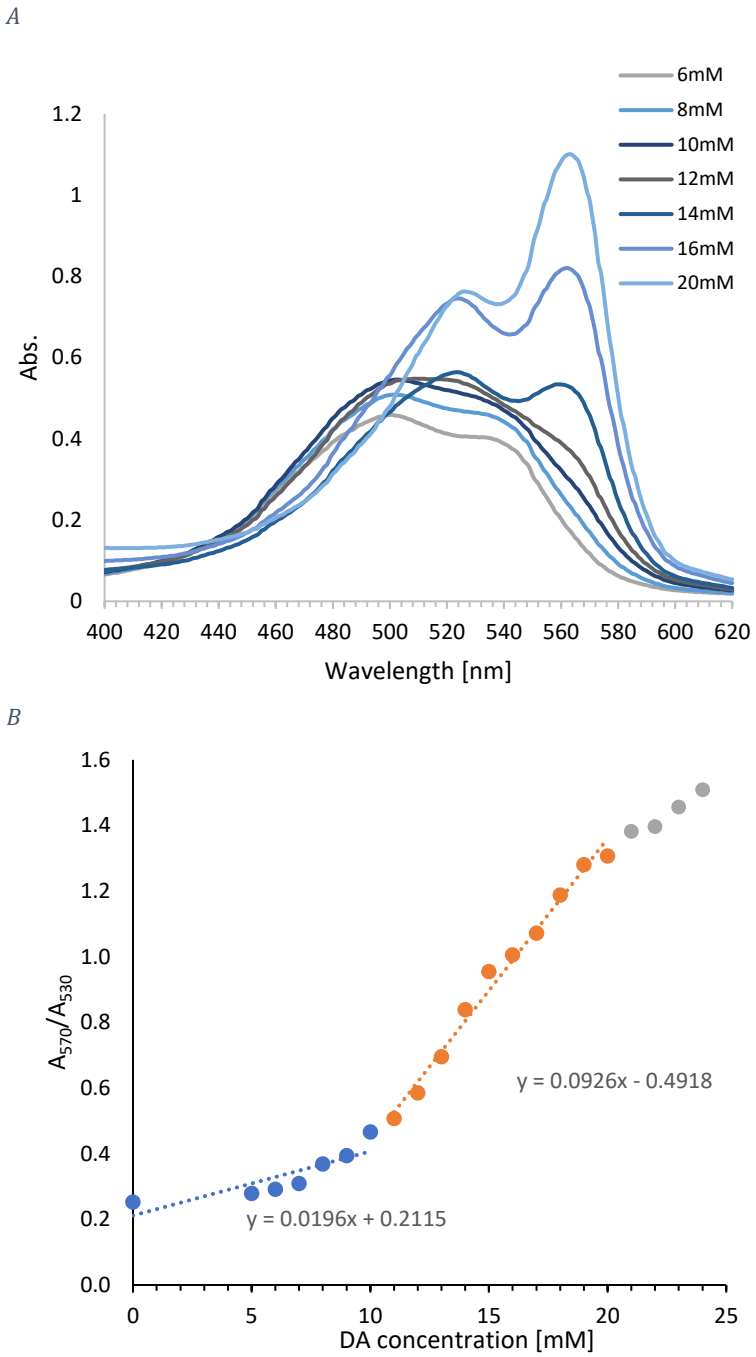

Figure S204. Determination of the critical aggregation concentration of DA for a mixture of DA and LA rection product at 1:4 molar ratio referring to initial amount of LA. Absorption spectra of merocyanine 540 in the presence of increasing concentrations of DA obtained for the reaction product LA into which DA was added at pH 6.8. The ratio between DA and LA was 1:4 referring to the initial amount of LA prior to the reaction (A). Absorption ratio at 570nm and 530nm as a function of DA concentration. The intersection between the two fitting lines represents the CAC of DA – ca. 10 mM (B).

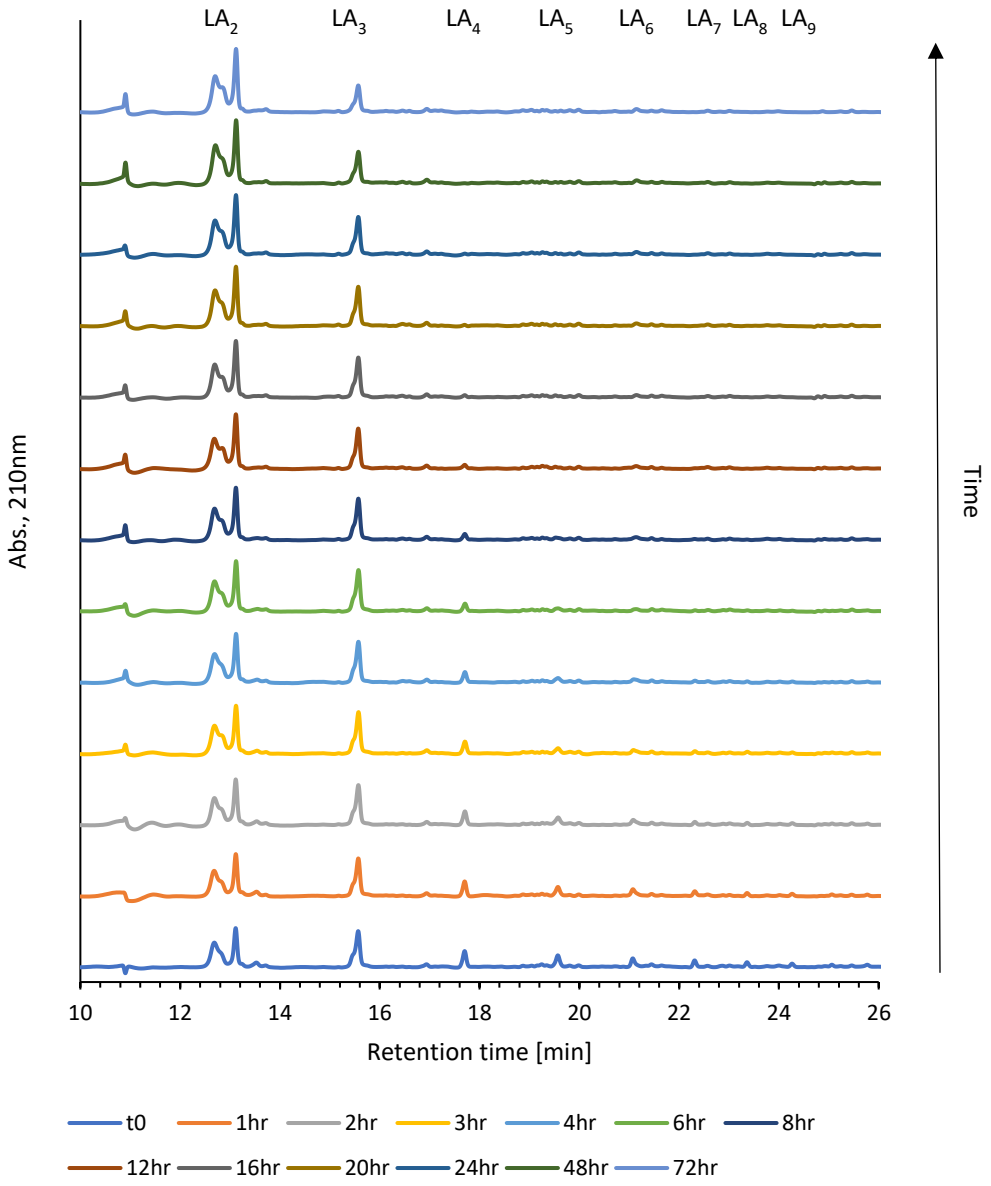

Figure S205. HPLC chromatograms obtained for LA homoesters of DA:LA reaction product at a 1:4 molar ratio at pH 6.8 and 40°C over the course of the degradation study. The region in the chromatograms that corresponds to the elution of LA homoesters is shown. As indicated by the chromatograms, the longer LA oligomers (LA5 to LA9) underwent degradation faster and to a greater extent compared to the shorter oligomers (LA2 to LA4). By the end of the incubation period (72 hours), only dimers and trimers were detected.

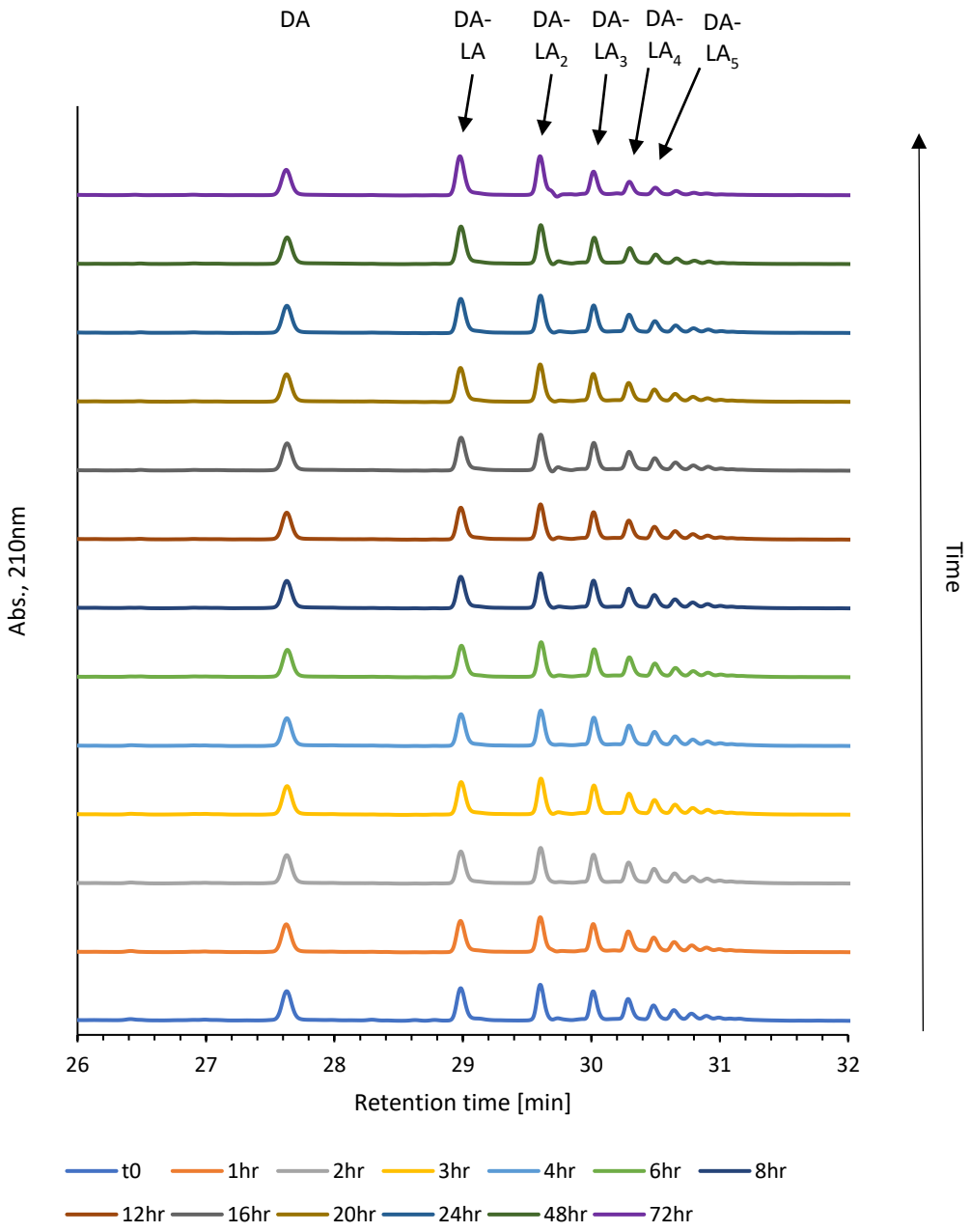

Figure S206. HPLC chromatograms obtained for DA-LA eteroesters of DA:LA reaction product at a 1:4 molar ratio at pH 6.8 and 40°C over the course of the degradation study. The region in the chromatograms that corresponds to the elution of DA-LA heteroesters is shown. As indicated by the chromatograms, during the course of the incubation period most of the products remained and were detected even after 72hr. Only the longest oligomers of more than 7-mers were significantly degraded.

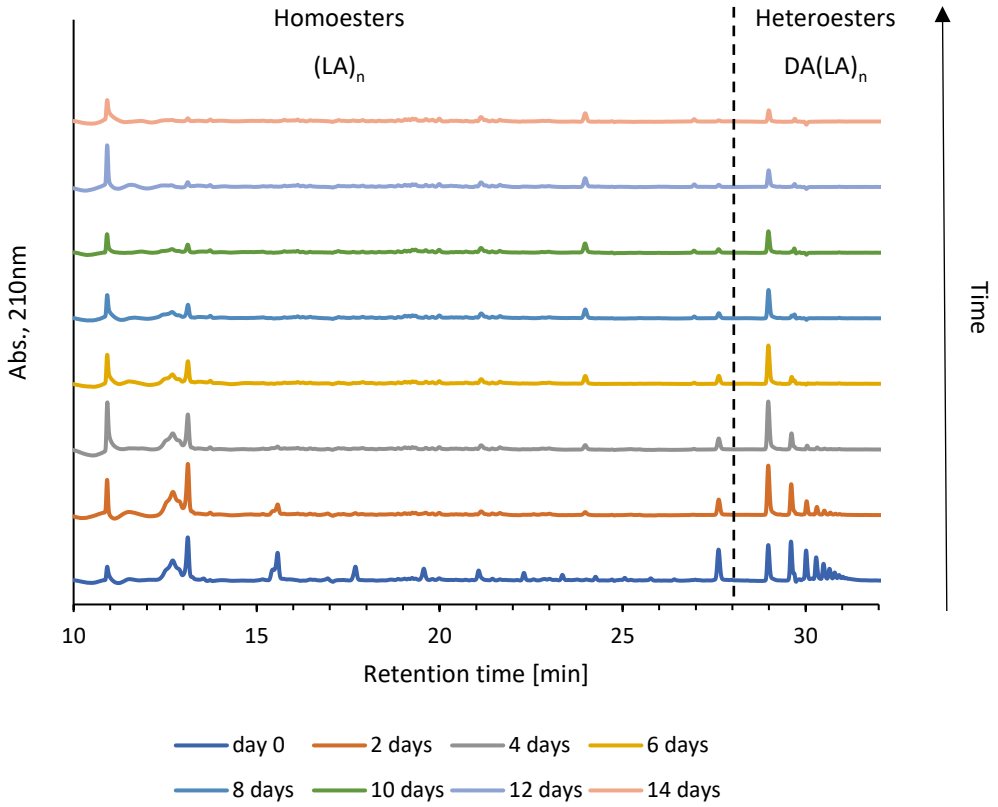

Figure S207. HPLC chromatograms obtained for DA:LA reaction product at a 1:4 molar ratio following incubation at 60°C and rehydration in citrate buffer at pH 5.5.

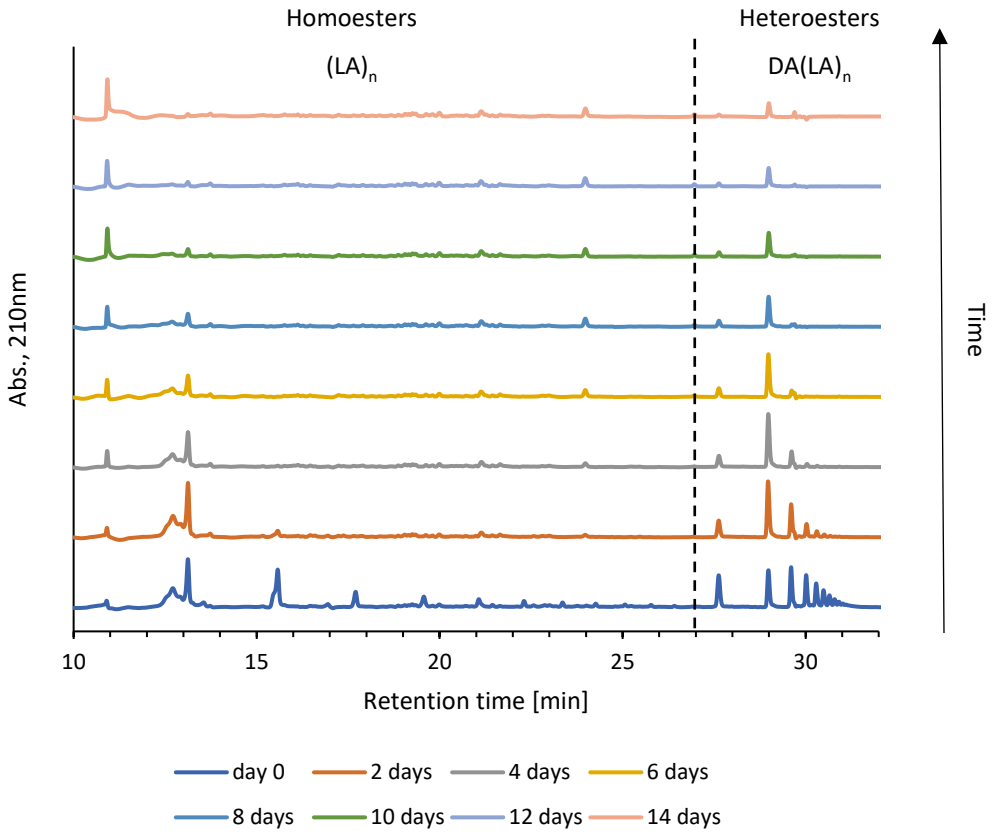

Figure S208. HPLC chromatograms obtained for DA:LA reaction product at a 1:4 molar ratio following incubation at 60°C and rehydration in phosphate buffer at pH 6.8.

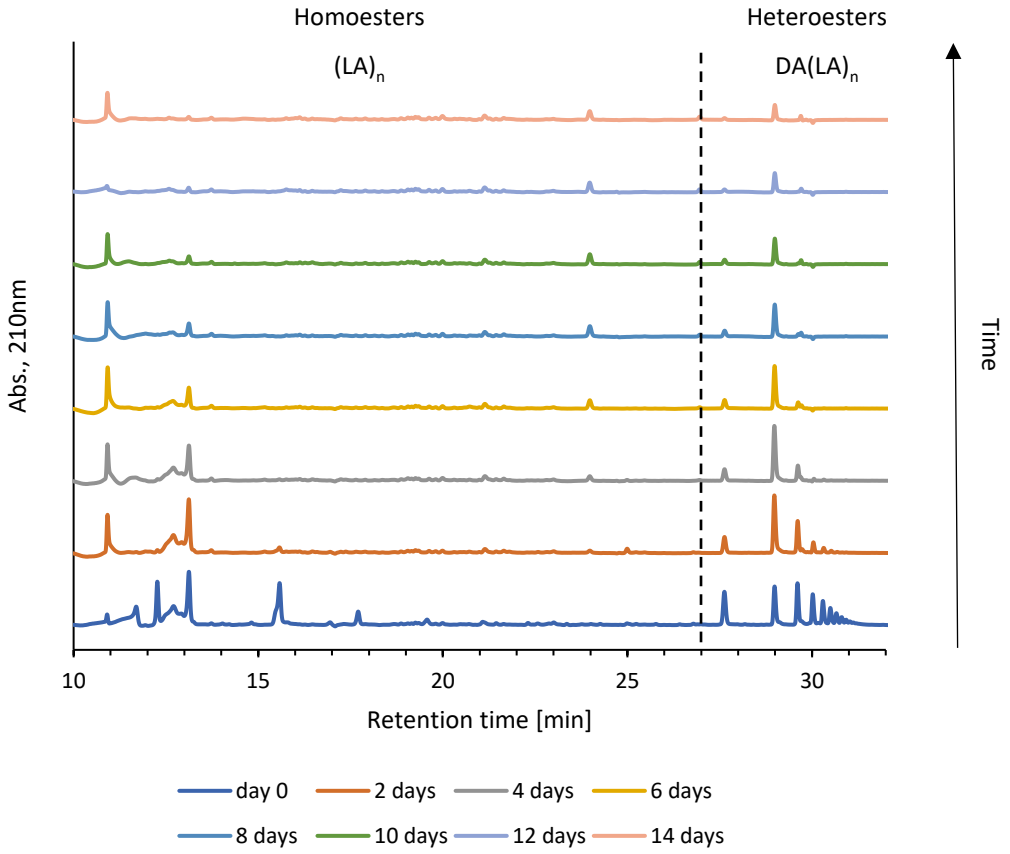

Figure S209. HPLC chromatograms obtained for DA:LA reaction product at a 1:4 molar ratio following incubation at 60°C and rehydration in tris buffer at pH 8.0.

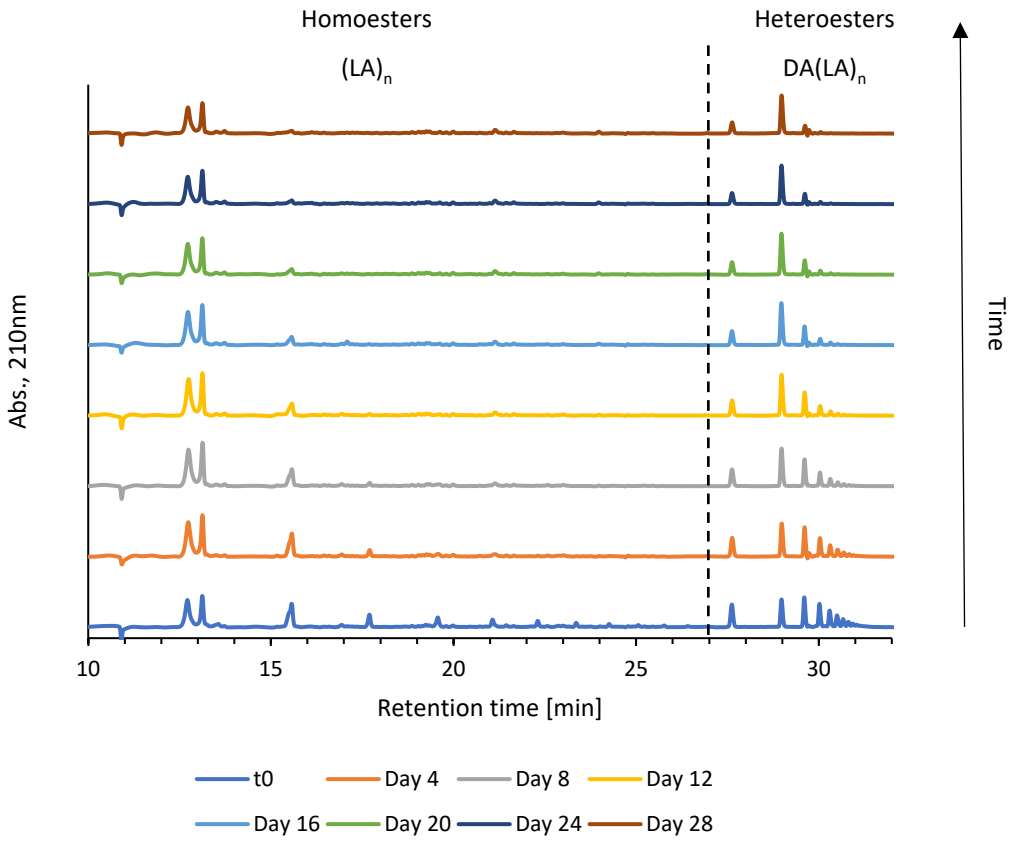

Figure S210. HPLC chromatograms obtained for DA:LA reaction product at a 1:4 molar ratio following incubation at 40°C and rehydration in citrate buffer at pH 5.5.

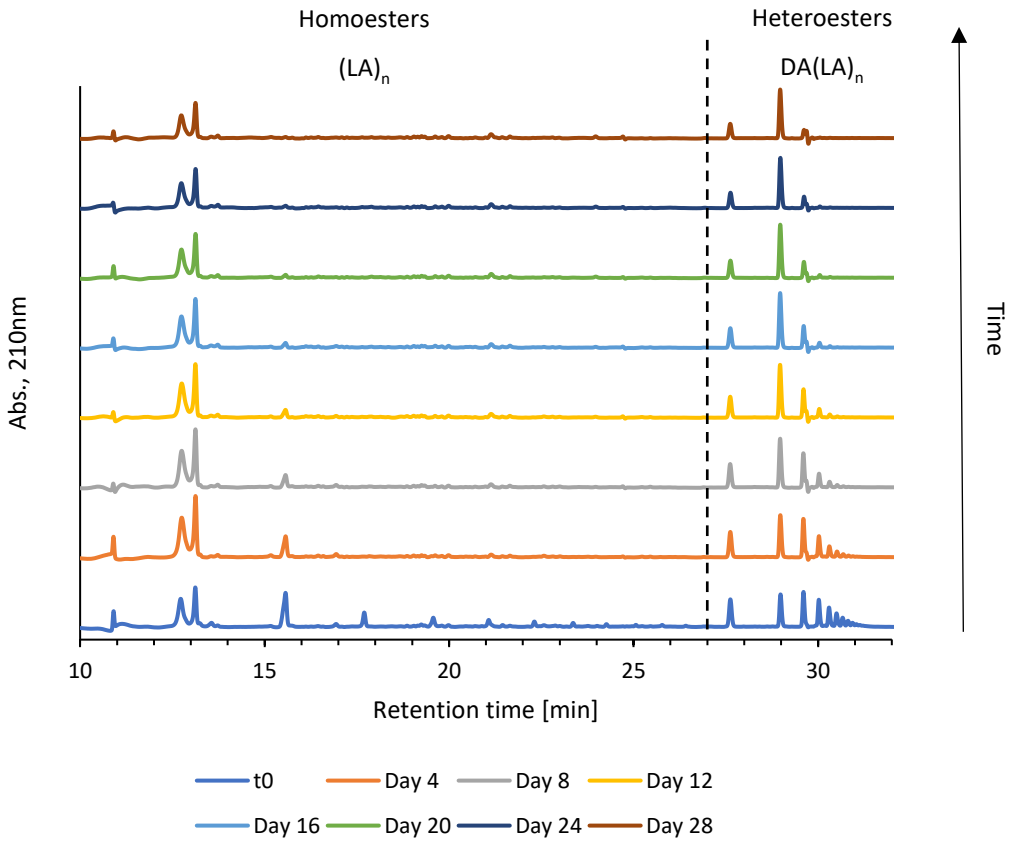

Figure S211. HPLC chromatograms obtained for DA:LA reaction product at 1:4 molar ratio following incubation at 40°C and rehydration in phosphate buffer at pH 6.8.

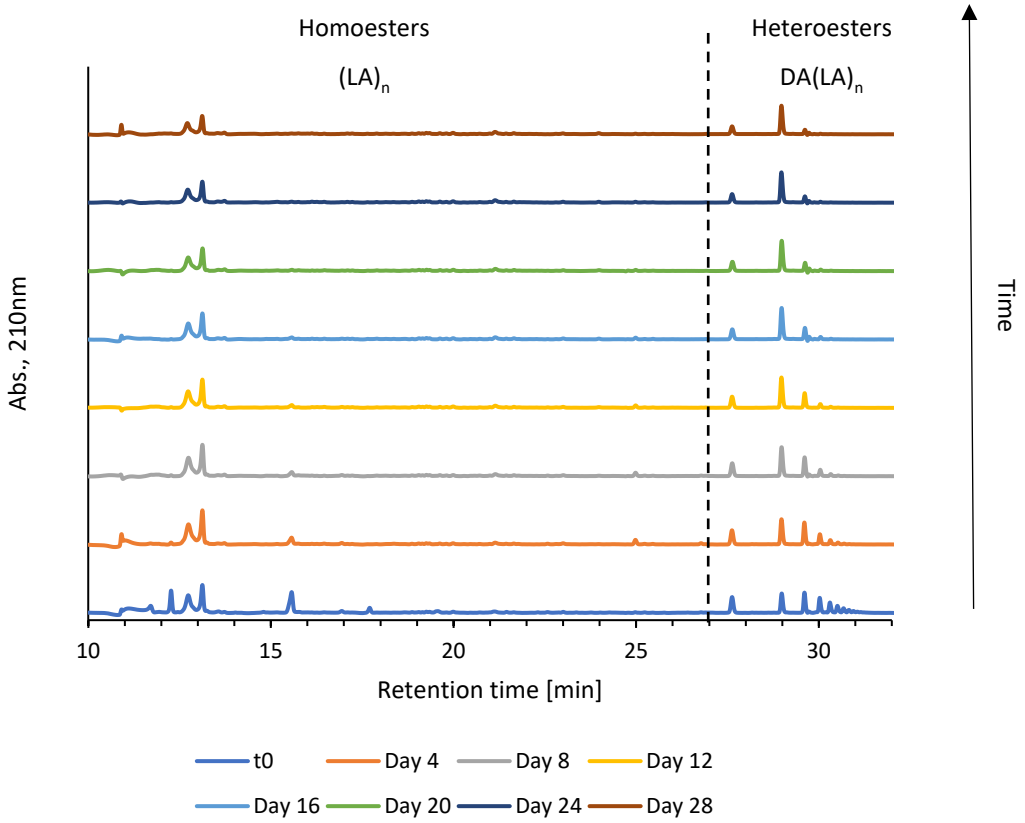

Figure S212. HPLC chromatograms obtained for DA:LA reaction product at 1:4 molar ratio following incubation at 40°C and rehydration in tris buffer at pH 8.0.

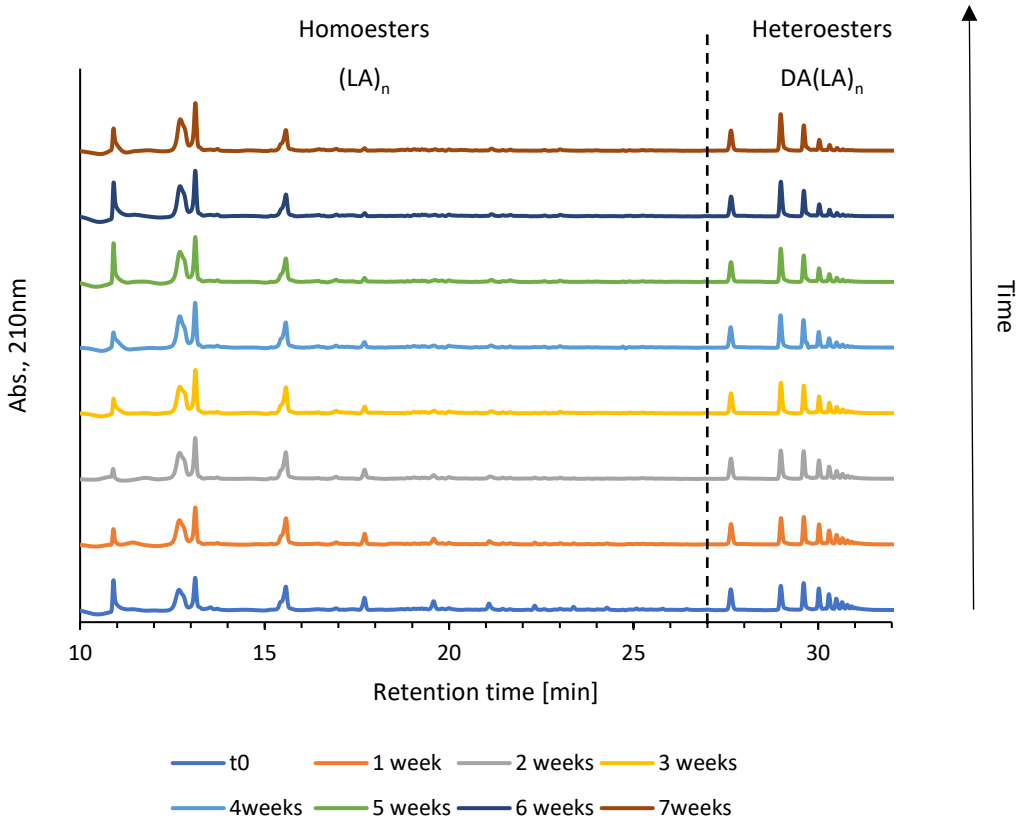

Figure S213. HPLC chromatograms obtained for DA:LA reaction product at 1:4 molar ratio following incubation at room temperature and rehydration in citrate buffer at pH 5.5.

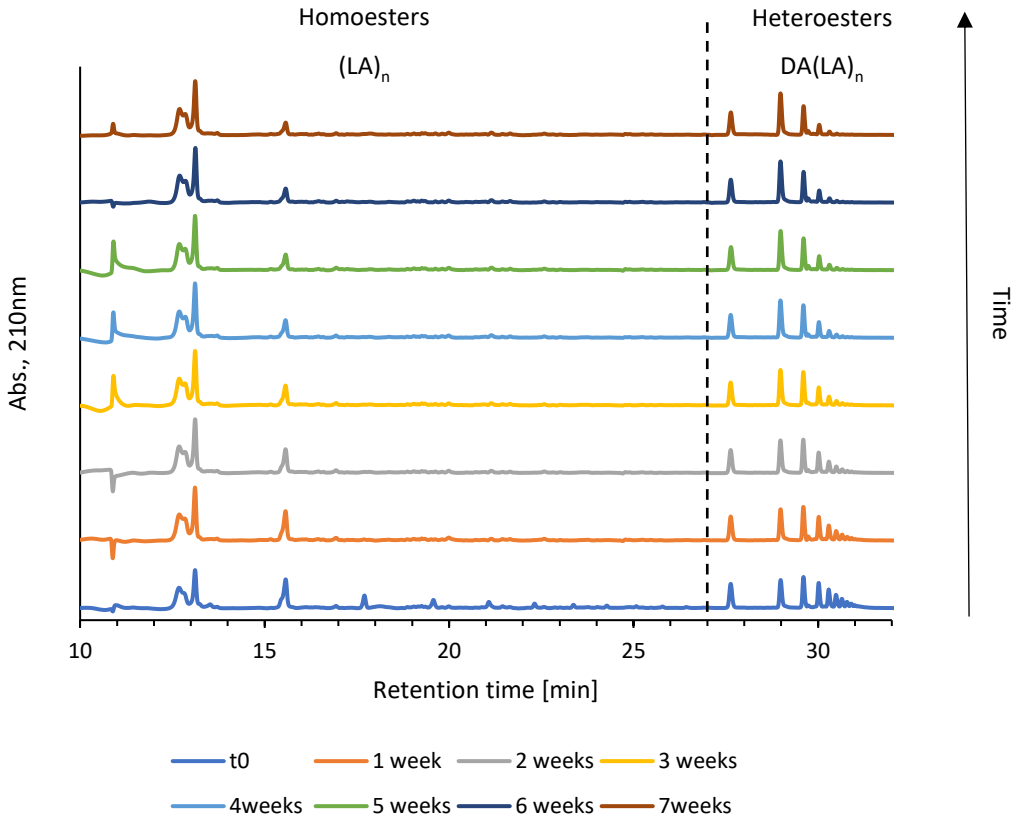

Figure S214. HPLC chromatograms obtained for DA:LA reaction product at 1:4 molar ratio following incubation at room temperature and rehydration in phosphate buffer at pH 6.8.

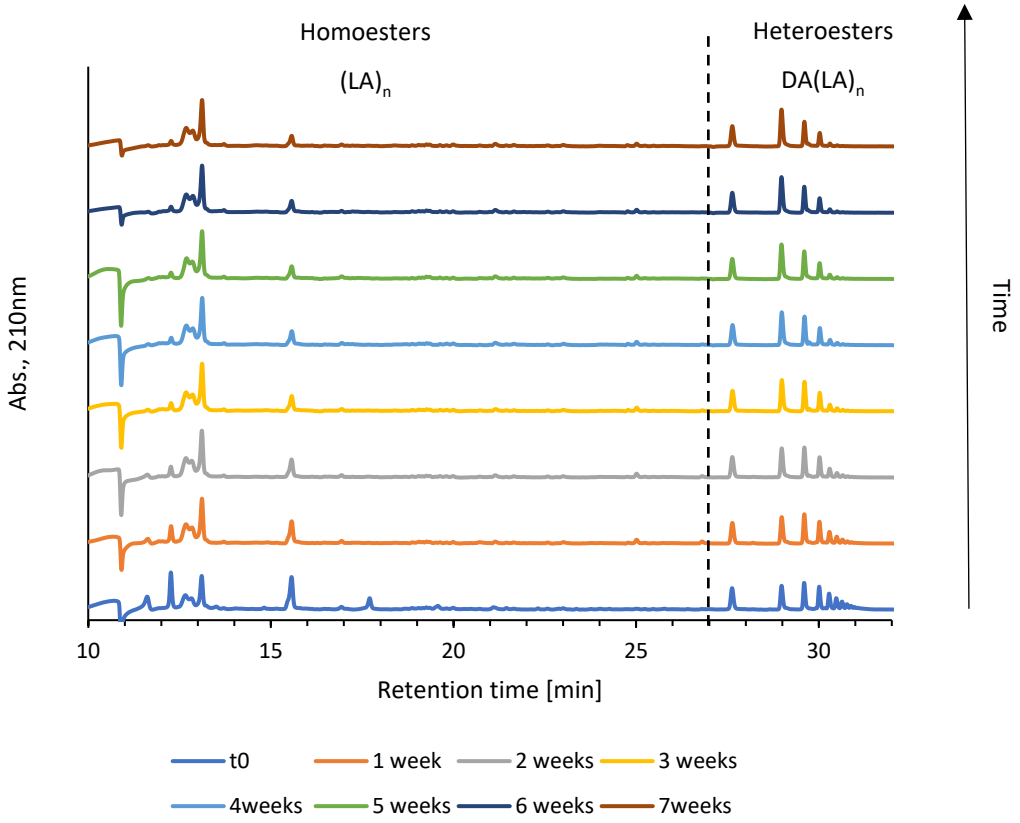

Figure S215. HPLC chromatograms obtained for DA:LA reaction product at 1:4 molar ratio following incubation at room temperature and rehydration in tris buffer at pH 8.0.

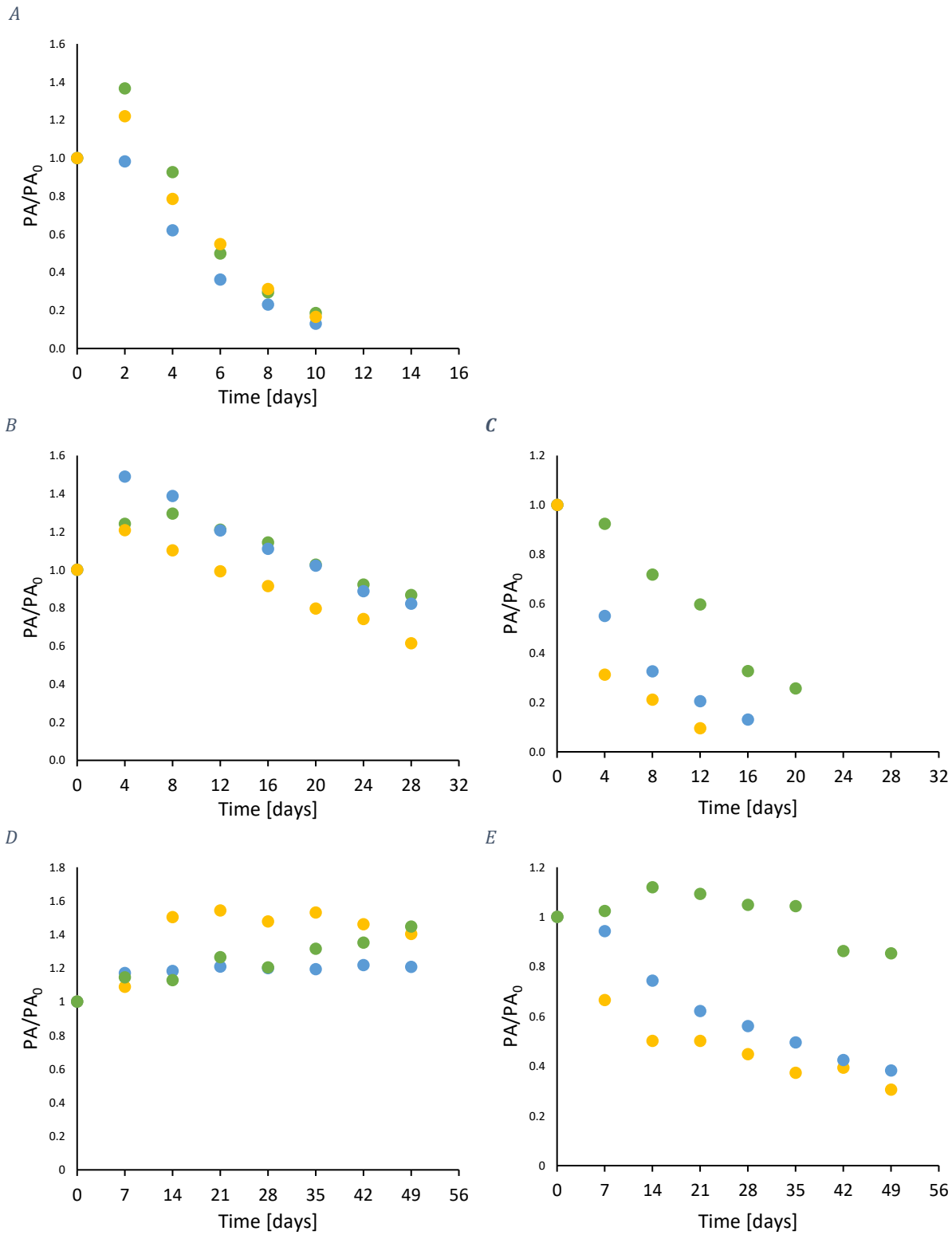

Figure S216. Relative peak area of LA dimer and trimer as a function of incubation period, pH, and temperature. Relative peak area of LA dimers obtained at 60°C and pH levels of 5.5 (green), 6.8 (blue), and 8.0 (yellow) (A). Relative peak area of LA dimers obtained at 40°C and pH levels of 5.5 (green), 6.8 (blue), and 8.0 (yellow) (B). Relative peak area of LA trimers obtained at 40°C and pH levels of 5.5 (green), 6.8 (blue), and 8.0 (yellow) (C). Relative peak area of LA dimers obtained at room temperature (RT) and pH levels of 5.5 (green), 6.8 (blue), and 8.0 (yellow) (D). Relative peak area of LA trimers obtained at room temperature and pH levels of 5.5 (green), 6.8 (blue), and 8.0 (yellow) (E). The effect of pH on the degradation rate of LA oligomers is pronounced at 40°C and at RT.

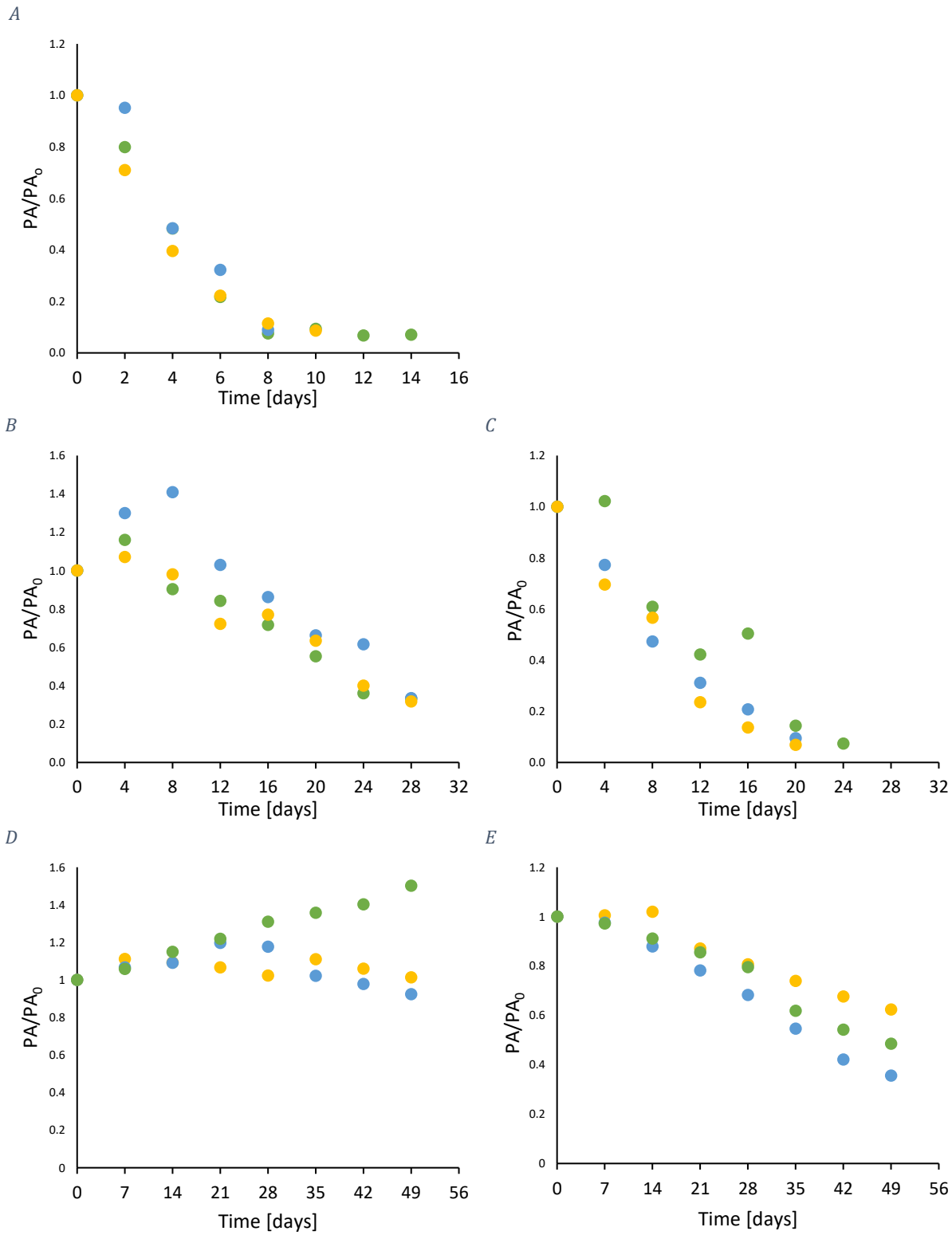

Figure S217. Relative peak area of DA-LA conjugates as a function of storage period, pH and temperature. Relative peak area of DA-LA2 obtained at 60°C and pH levels 5.5 (green), 6.8 (blue) and 8.0 (yellow) (A). Relative peak area of DA-LA2 obtained at 40°C and pH levels 5.5 (green), 6.8 (blue) and 8.0 (yellow) (B). Relative peak area of DA-LA3 obtained at 40°C and pH levels 5.5 (green), 6.8 (blue) and 8.0 (yellow) (C). Relative peak area of DA-LA2 obtained at room temperature (RT) and pH levels 5.5 (green), 6.8 (blue) and 8.0 (yellow) (D). Relative peak area of DA-LA3 obtained at room temperature and pH levels 5.5 (green), 6.8 (blue) and 8.0 (yellow) (E). The effect of pH on the degradation rate of DA-LA conjugates is relatively negligible, except for RT, at which degradation was only slightly faster at pH 6.8 and 8.0 in the case of DA-LA2.

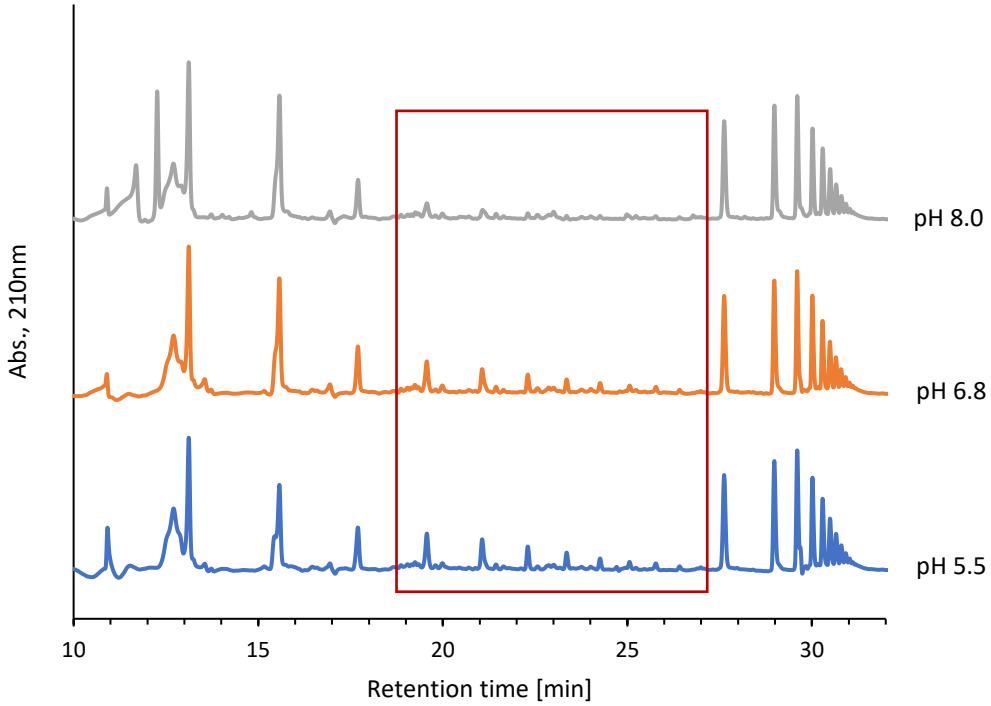

Figure S218. HPLC chromatograms obtained for DA:LA reaction product at a 1:4 molar ratio at t0 prior to incubation. Rection products were rehydrated in either citrate buffer, phosphate buffer, or tris buffer, at pH 5.5, 6.8, or 8.0, respectively. Already at t0, the peaks corresponding to LA oligomers are significantly reduced at pH 8.0 compared to lower pH levels.

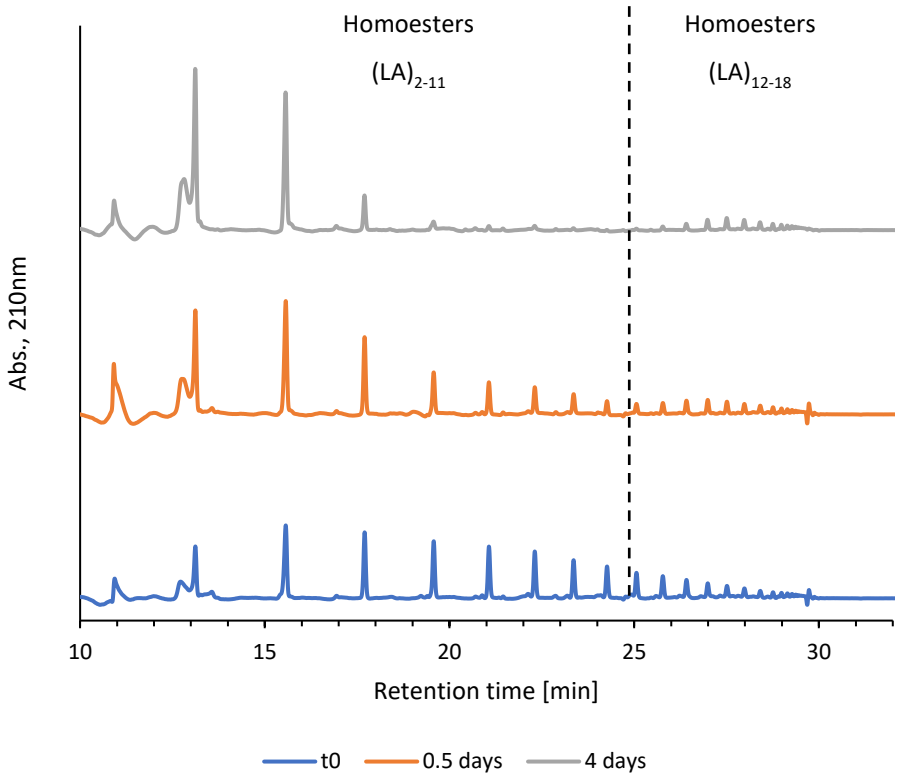

Figure S219. HPLC chromatograms obtained for 100mM LA reaction products following incubation at room temperature (RT). Reaction product was rehydrated in phosphate buffer (50 mM) at pH 6.8 and kept at RT. The initial amount of LA was 400 µmol, corresponding to LA monomer introduced at DA:LA 1:2 molar ratio. As indicated by the chromatograms, already after 4 days at RT, most of the medium-chain oligomers were hydrolyzed while the longer oligomers remained in the system.

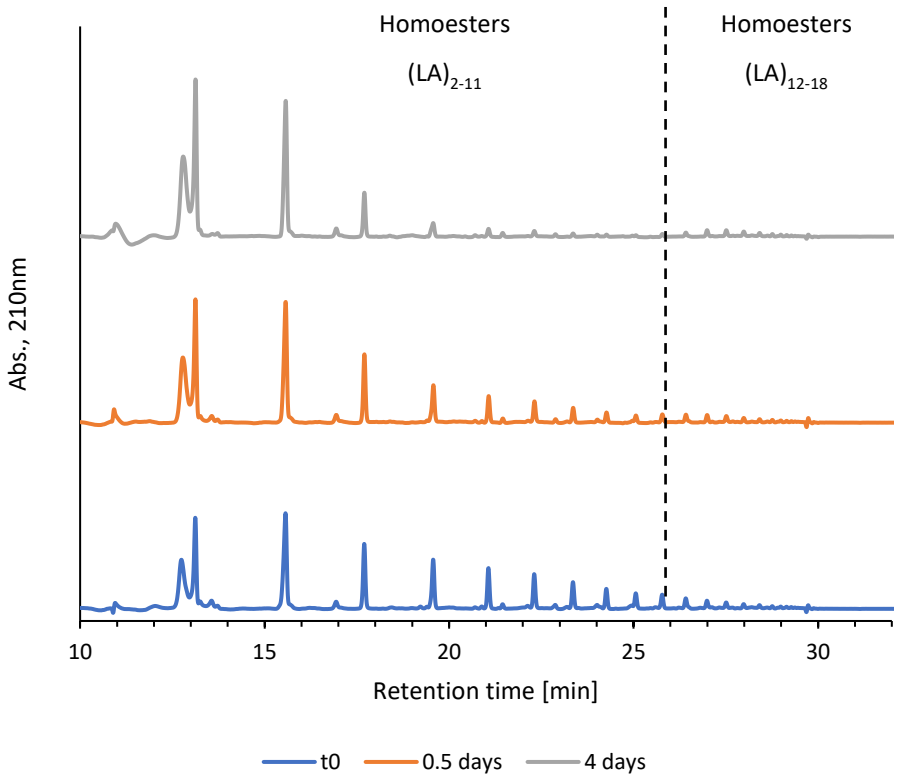

Figure S220. HPLC chromatograms obtained for 200mM LA reaction products following incubation at room temperature (RT). Reaction product was rehydrated in phosphate buffer (50mM) at pH 6.8 and kept at RT. The initial amount of LA was 800µmol, corresponding to LA amount introduced at DA:LA 1:4 molar ratio. As indicated by the chromatograms, already after 4 days at RT, most of the medium chain oligomers were hydrolyzed while the longer oligomers remained at the system.

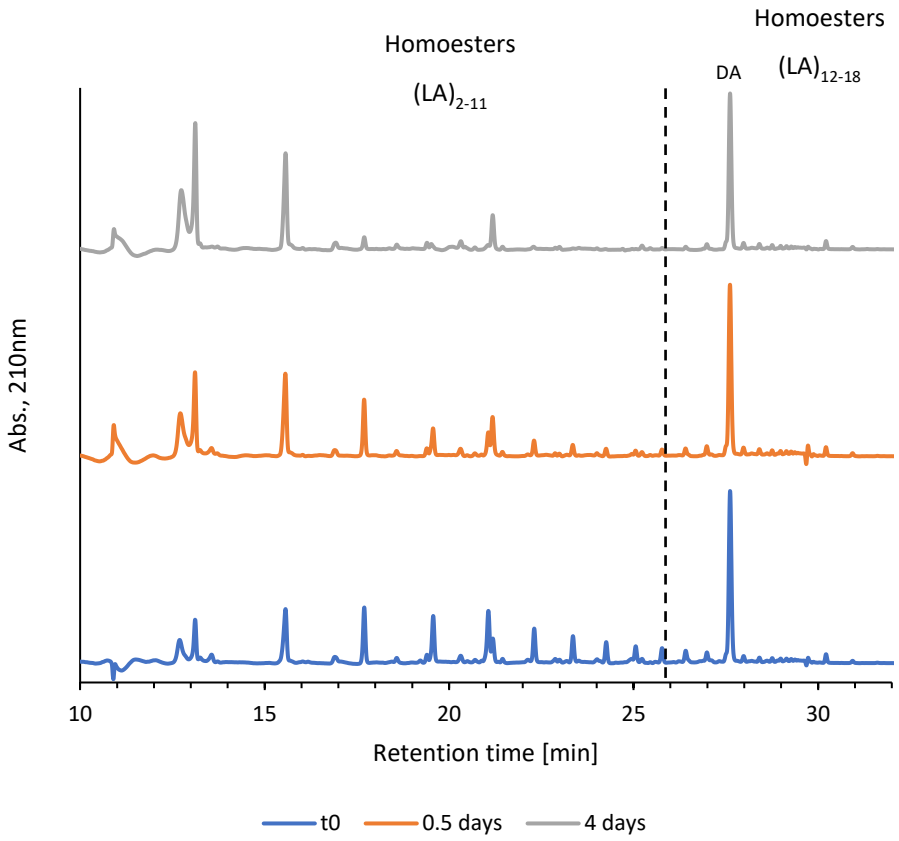

Figure S221. HPLC chromatograms obtained for 100mM LA reaction products in the presence of DA monomer following incubation at room temperature (RT). LA reaction product was rehydrated in DA monomers stock (50mM) and phosphate buffer (50mM) at pH 6.8 and kept at RT. The initial amount of LA was 400µmol, corresponding to LA amount introduced at DA:LA 1:2 molar ratio. As indicated by the chromatograms, already after 4 days at RT, most of the medium chain oligomers were hydrolyzed while the longer oligomers remained at the system.

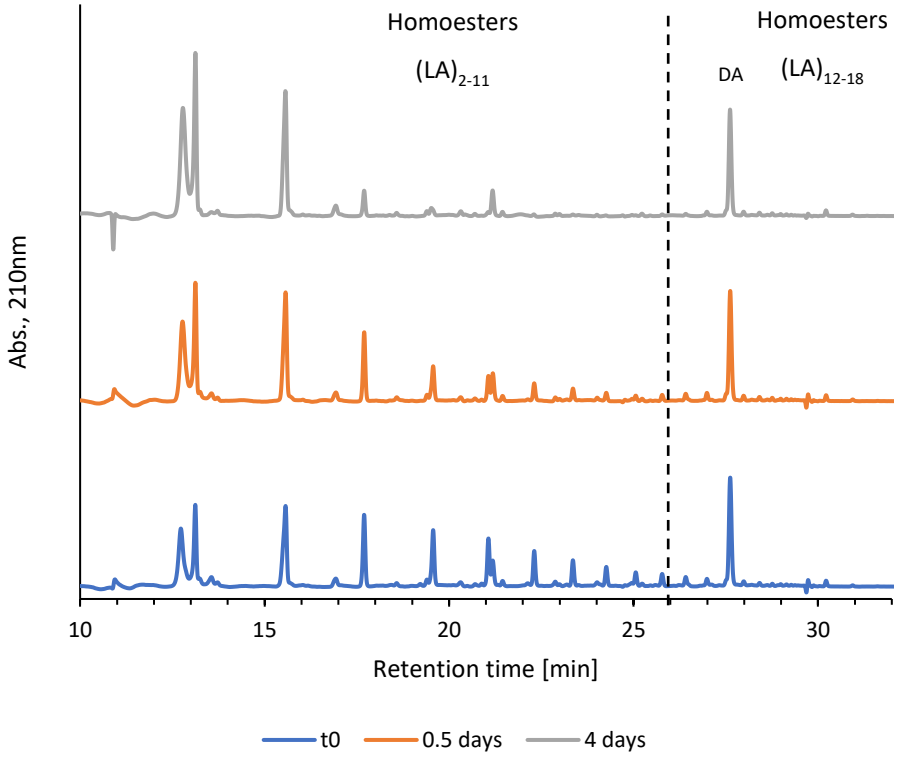

Figure S222. HPLC chromatograms obtained for 200mM LA reaction products in the presence of DA monomer following incubation at room temperature (RT). LA reaction product was rehydrated in DA monomers stock (50mM) and phosphate buffer (50mM) at pH 6.8 and kept at RT. The initial amount of LA was 800µmol, corresponding to LA amount introduced at DA:LA 1:4 molar ratio. As indicated by the chromatograms, already after 4 days at RT, most of the medium chain oligomers were hydrolyzed while the longer oligomers remained at the system.

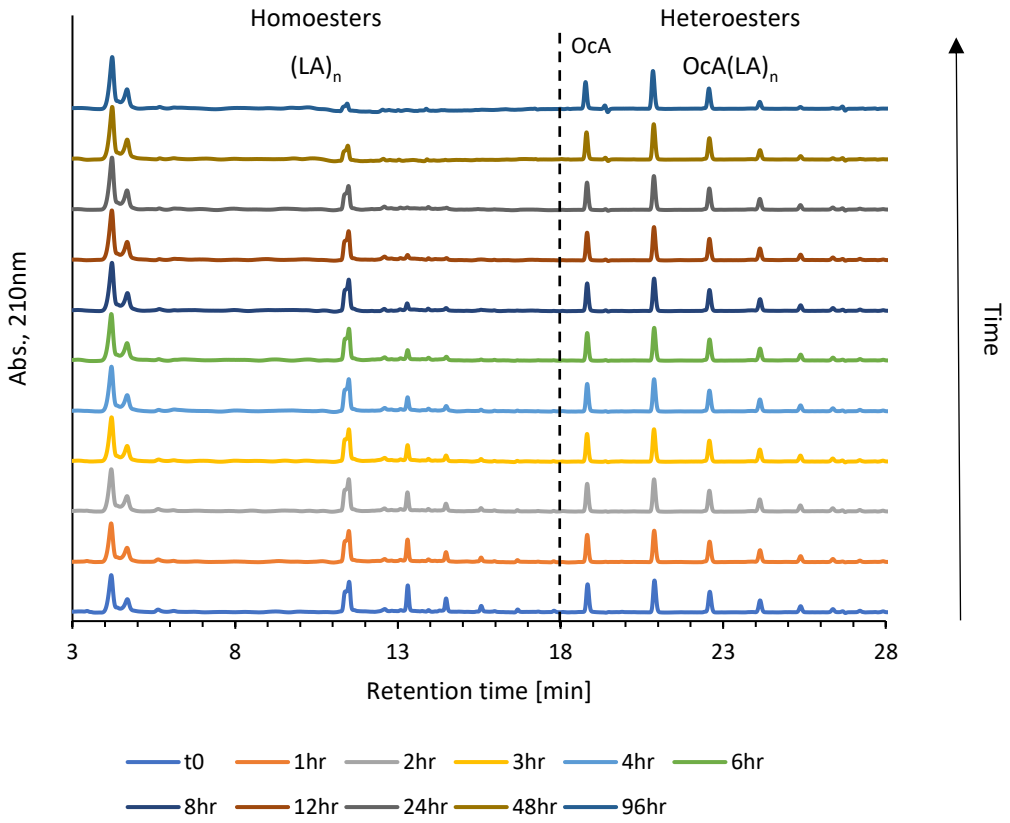

Figure S223. HPLC chromatograms obtained for OcA:LA reaction product at 1:4 molar ratio following incubation at 40°C and rehydration in phosphate buffer at pH 6.6. OcA:LA reaction product at 1:4 molar ratio was rehydrated in phosphate buffer (200mM) at pH 6.6 and stored at 40°C for up to 4 days. OcA and LA concentrations were 150mM and 600mM, respectively, referring to the initial amount prior to the reaction molar ratio. As indicated by the chromatograms, the hydrolysis of LA homoesters was significantly faster compared to the hydrolysis of the corresponding heteroesters.

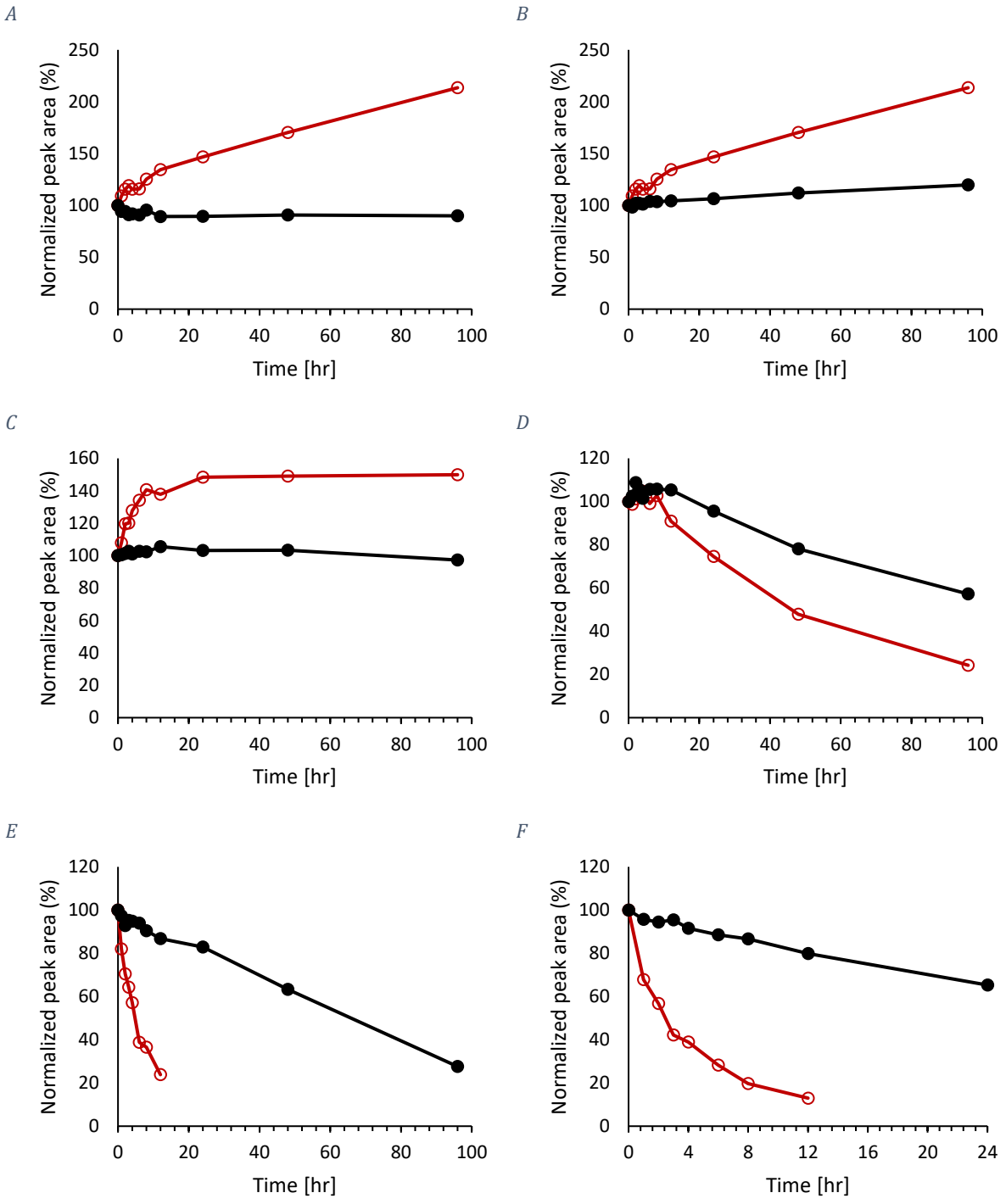

Figure S224. Relative peak area of LA and OcA-LA conjugates as a function of storage period. Relative peak area of OcA (black) and LA (red) monomers obtained at 40°C and pH 6.6. (A). Relative peak area of OcA-LA (black) and LA (red) obtained at 40°C and pH 6.6. (B). Relative peak area of OcA-2LA (black) and 2LA (red) obtained at 40°C and pH 6.6. (C). Relative peak area of OcA-3LA (black) and 3LA (red) obtained at 40°C and pH 6.6. (D). Relative peak area of OcA-4LA (black) and 4LA (red) obtained at 40°C and pH 6.6. (E). Relative peak area of OcA-5LA (black) and 5LA (red) obtained at 40°C and pH 6.6 (F). LA oligomers conjugated to OcA were hydrolyzed to a lesser extent compared to non-conjugated LA oligomers.

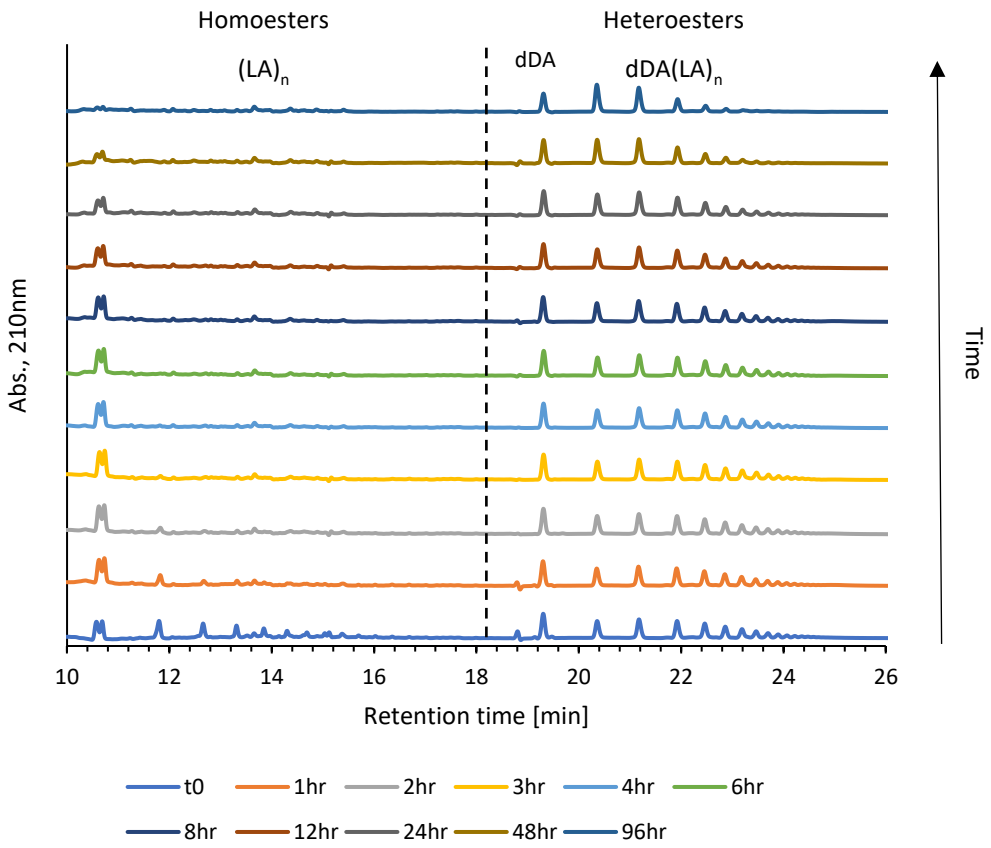

Figure S225. HPLC chromatograms obtained for dDA:LA reaction product at 1:4 molar ratio following incubation at 40°C and rehydration in phosphate buffer at pH 7.4. dDA:LA reaction product at 1:4 molar ratio was rehydrated in phosphate buffer (50mM) at pH 7.4 and stored at 40°C for up to 4 days. dDA and LA concentrations were 20mM and 80mM, respectively, referring to the initial amount prior to the reaction molar ratio. As indicated by the chromatograms, the hydrolysis of LA homoesters was significantly faster compared to the hydrolysis of the corresponding heteroesters.

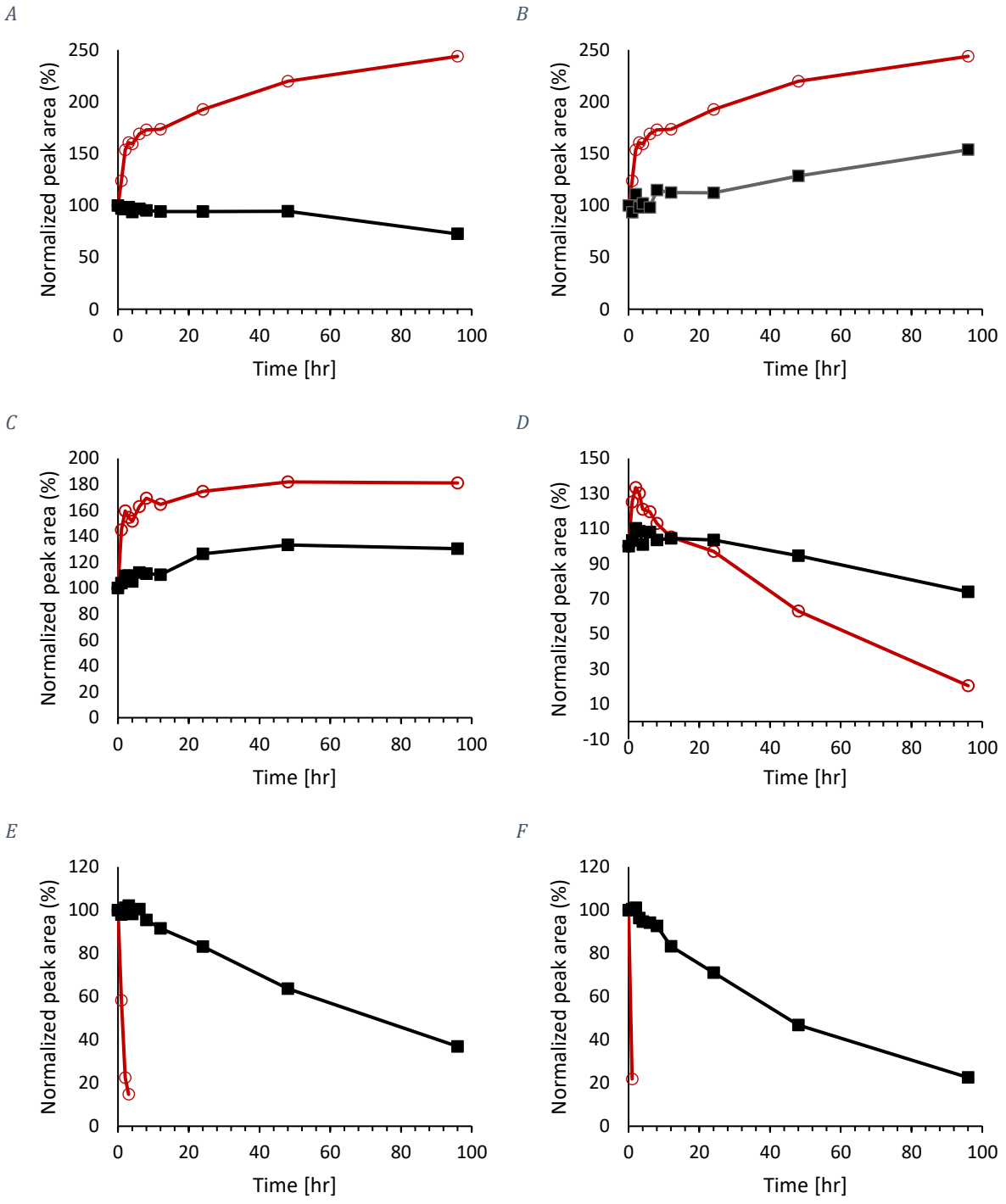

Figure S226. Relative peak area of LA and dDA-LA conjugates as a function of storage period. Relative peak area of dDA (black) and LA (red) monomers obtained at 40°C and pH 7.4. (A). Relative peak area of dDA-LA (black) and LA (red) obtained at 40°C and pH 7.4 (B). Relative peak area of dDA-2LA (black) and 2LA (red) obtained at 40°C and pH 7.4 (C). Relative peak area of dDA-3LA (black) and 3LA (red) obtained at 40°C and pH 7.4 (D). Relative peak area of dDA-4LA (black) and 4LA (red) obtained at 40°C and pH 7.4 (E). Relative peak area of dDA-5LA (black) and 5LA (red) obtained at 40°C and pH 7.4 (F). LA oligomers conjugated to dDA were hydrolyzed to a lesser extent compared to non-conjugated LA oligomers.

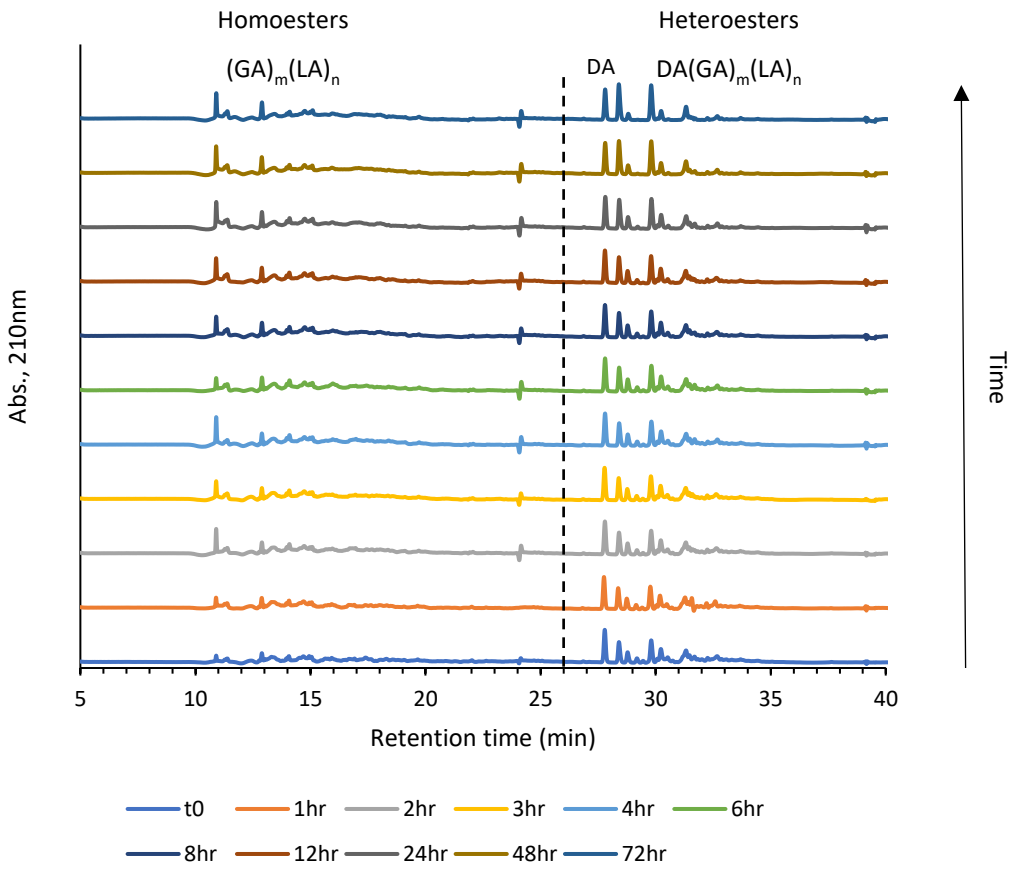

Figure S227. HPLC chromatograms obtained for DA:LA:GA reaction product at 1:2:2 molar ratio following incubation at 40°C and rehydration in phosphate buffer at pH 6.8. DA:LA:GA reaction product at 1:2:2 molar ratio was rehydrated in phosphate buffer (50mM) at pH 6.8 and stored at 40°C for up to 4 days. DA, LA and GA concentrations were 50mM, 100mM and 100mM, respectively, referring to the initial amount prior to the reaction molar ratio.

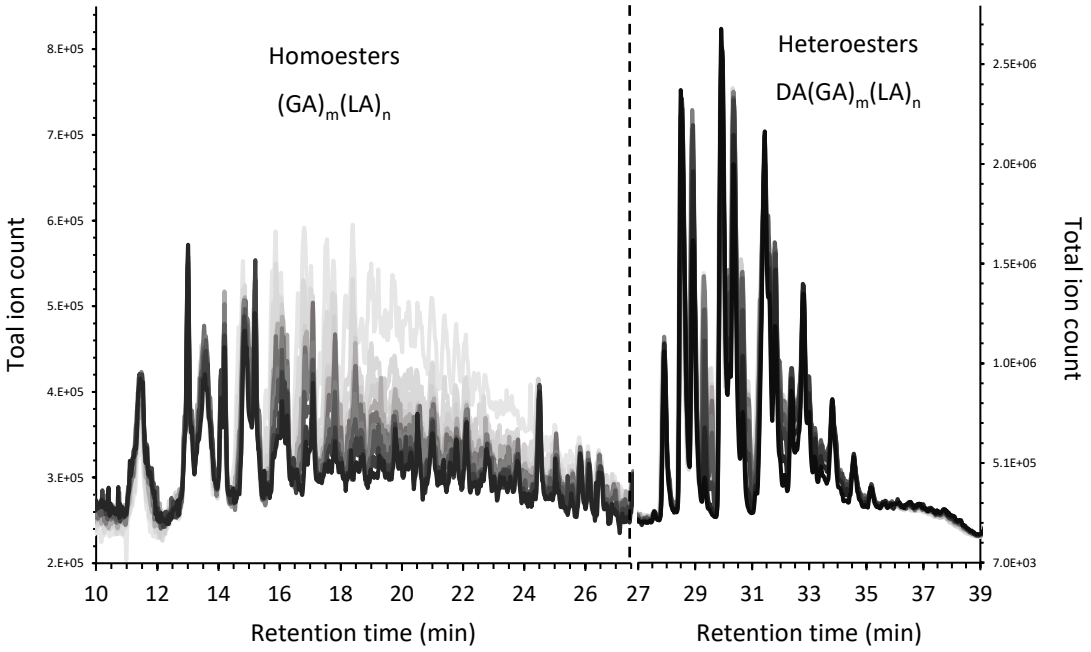

Figure S228. LC-MS chromatograms obtained for DA:LA:GA reaction product at 1:2:2 molar ratio following incubation at 40°C and rehydration in phosphate buffer at pH 6.8. DA:LA:GA reaction product at 1:2:2 molar ratio was rehydrated in phosphate buffer (50mM) at pH 6.8 and stored at 40°C for up to 4 days. DA, LA and GA concentrations were 50mM, 100mM and 100mM, respectively, referring to initial amount prior to the reaction. Time points are represented by color gradient. Light grey line represents t0 and the black line represents 72hr. As indicated in the chromatogram, GA-LA homoesters were hydrolyzed to a greater extent compared to DA-GA-LA heteroesters.

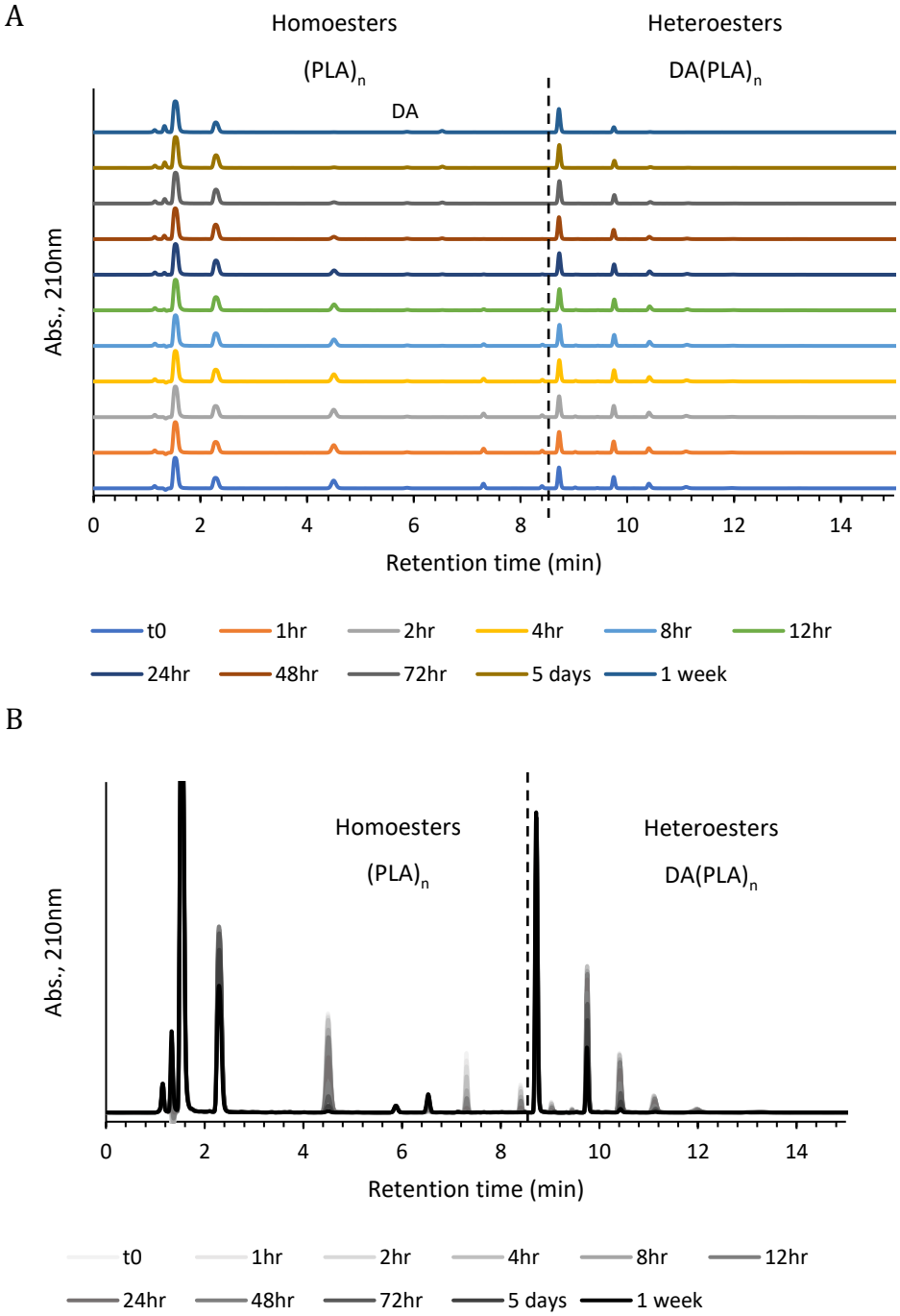

Figure S229. HPLC chromatograms obtained for DA:PLA reaction product at 1:1 molar ratio following incubation at 40°C and rehydration in tris buffer at pH 8.0. DA:PLA reaction product at 1:1 molar ratio was rehydrated in tris buffer (50mM) at pH 8.0 and stored at 40°C for up to 1 week. DA and PLA concentration was 50mM, referring to the initial amount prior to the reaction. Stack representation of the chromatograms obtained for the different time points (A) and overlay representation of the obtained chromatograms (B). Time points are represented by color gradient. The light grey line represents t0 and black line represents 72hr. Loger oligomers were hydrolyzed more slowly when conjugated to DA.

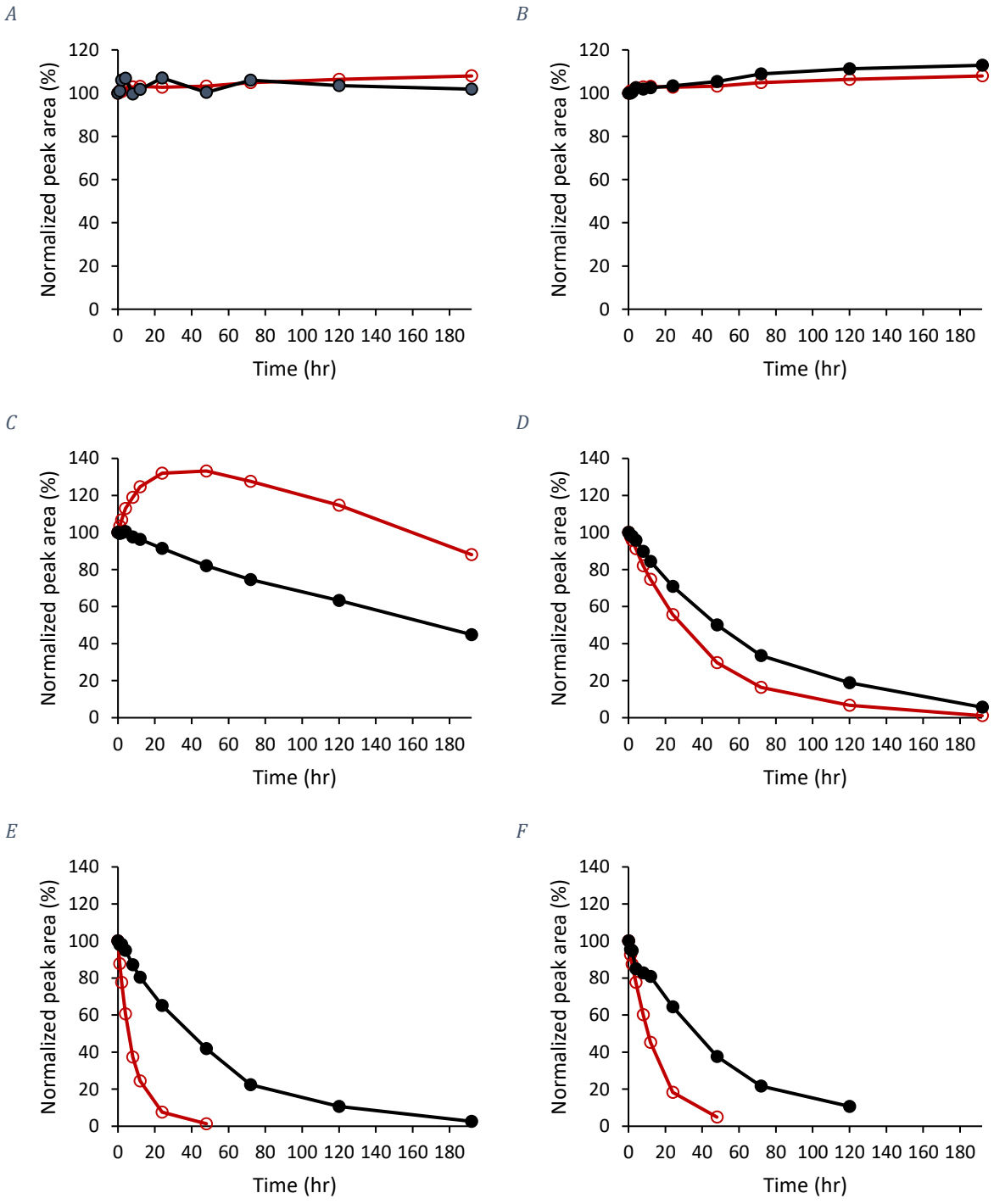

Figure S230. Relative peak area of PLA and DA-PLA conjugates as a function of storage period. Relative peak area of DA (black) and PLA (red) monomers obtained at 40°C and pH 8.0. (A). Relative peak area of DA-PLA (black) and PLA (red) obtained at 40°C and pH 8.0. (B). Relative peak area of DA-2PLA (black) and 2PLA (red) obtained at 40°C and pH 8.0. (C). Relative peak area of DA-3PLA (black) and 3PLA (red) obtained at 40°C and pH 8.0. (D). Relative peak area of DA-4PLA (black) and 4PLA (red) obtained at 40°C and pH 8.0. (E). Relative peak area of DA-5PLA (black) and 5PLA (red) obtained at 40°C and pH 8.0 (F). The longest PLA oligomers conjugated to DA were hydrolyzed to a lesser extent compared to non-conjugated PLA oligomers.

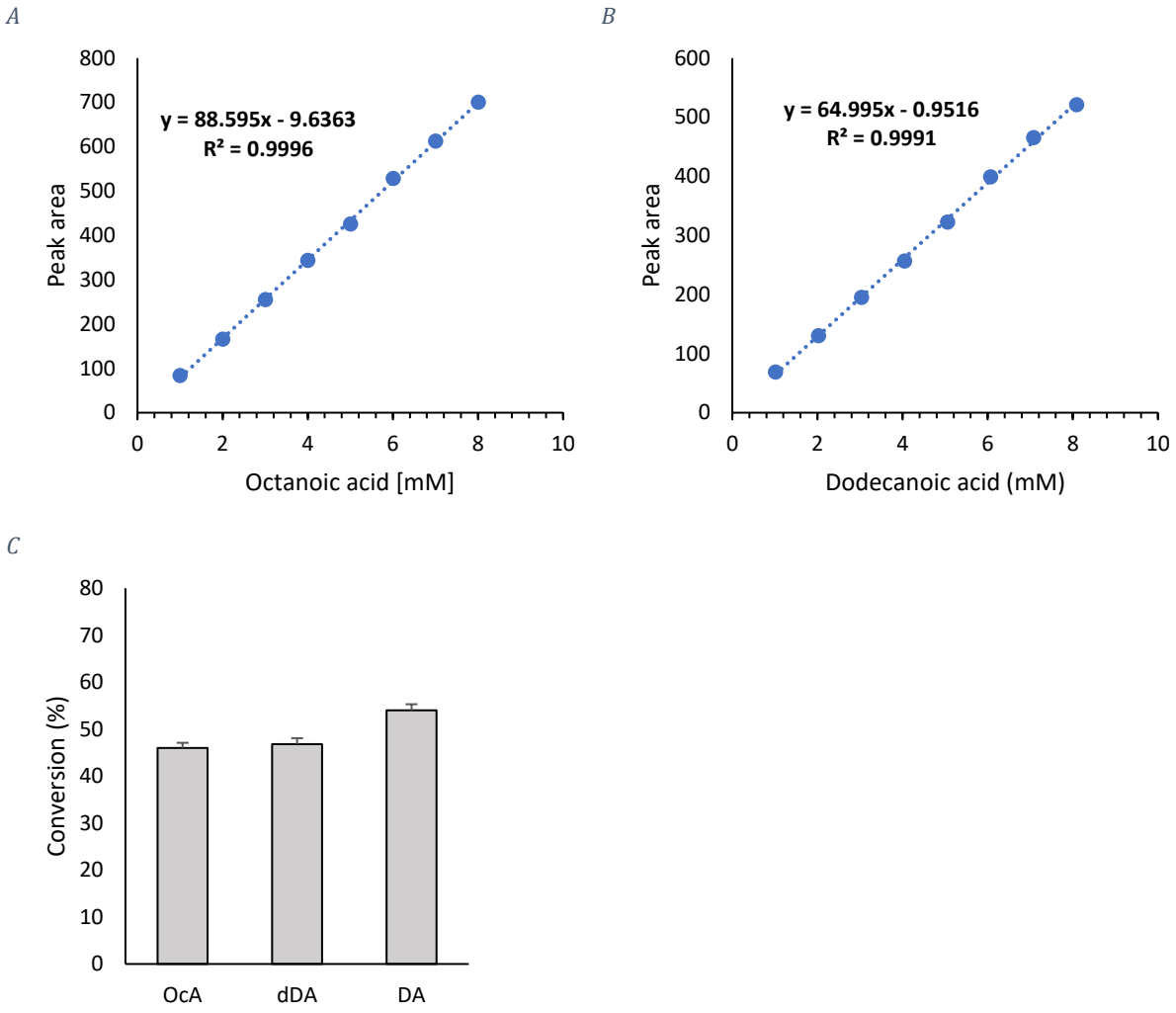

Figure S231. OcA and dDA consumption under dry reaction at 85°C for 7 days as determined by HPLC. A calibration curve was constructed at 210nm for the determination of the conversion of OcA when reacted with LA at 1:4 molar ratio in the favor of LA (A) . Calibration curve was constructed at 210nm for the determination the conversion of dDA when reacted with LA at 1:4 molar ratio in the favor of LA (B). Conversion of different fatty acids when reacted with LA at 1:4 molar ratio in the favor of LA (C). The measured conversion for OcA, dDA and DA was 46%, 47% and 54% respectively.

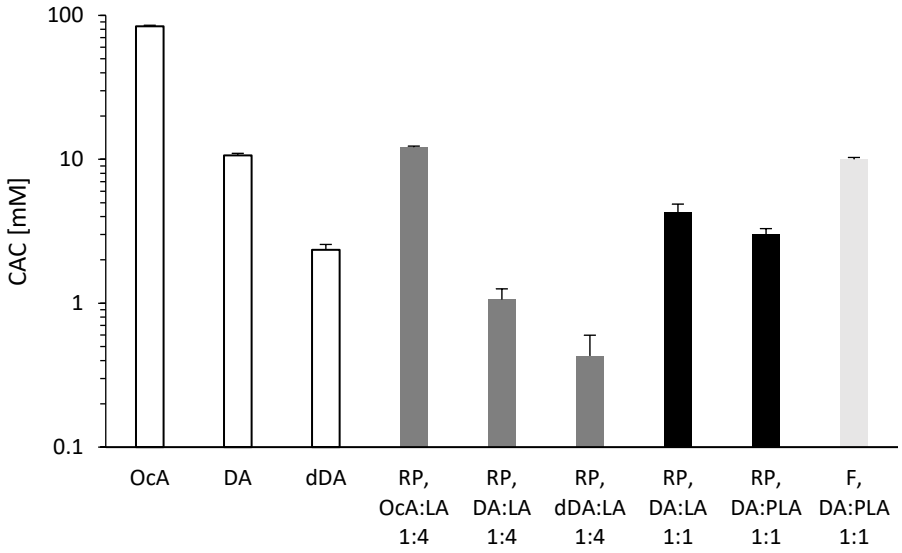

Figure S232. Determination of the critical aggregation concentration of fresh monomers and reaction products of different fatty acids. CAC of fresh OcA, DA and dDA at pH 6.6, 6.8 and 8.0 respectively (white columns), FA:LA reaction products (RP) at 1:4 molar ration (grey columns), DA:HA reaction products at 1:1 molar ratio (black columns) and fresh DA:PLA monomers at 1:1 molar ratio (light grey column). As indicated in the figure, the CAC of all tested fatty acids was significantly reduced by about one order of magnitude in the presence of FA-LA conjugates. DA:PLA reaction product at 1:1 molar ratio exhibited similar effect as the corresponding DA-LA mixture; a reduction of about 3-fold.

A

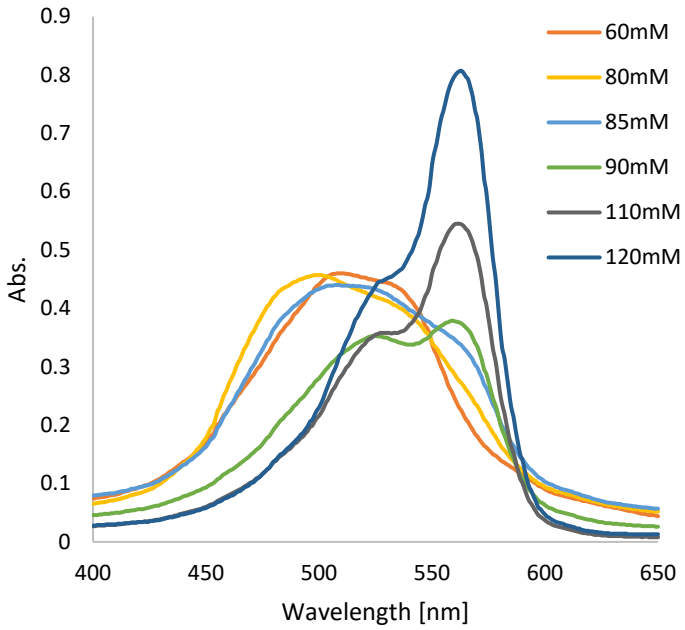

B

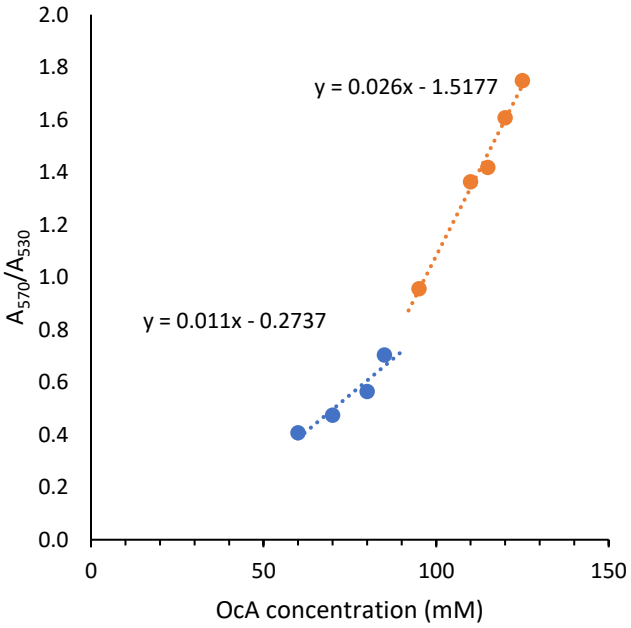

Figure S233. Determination of the critical aggregation concentration of OcA for OcA control sample. Absorption spectra of merocyanine 540 in the presence of increasing concentrations of OcA obtained for OcA control sample at pH 6.6 (A). Absorption ratio at 570 nm and 530 nm as a function of OcA concentration. The intersection between the two fitting lines represents the CAC of OcA – ca. 80 mM (B).

A

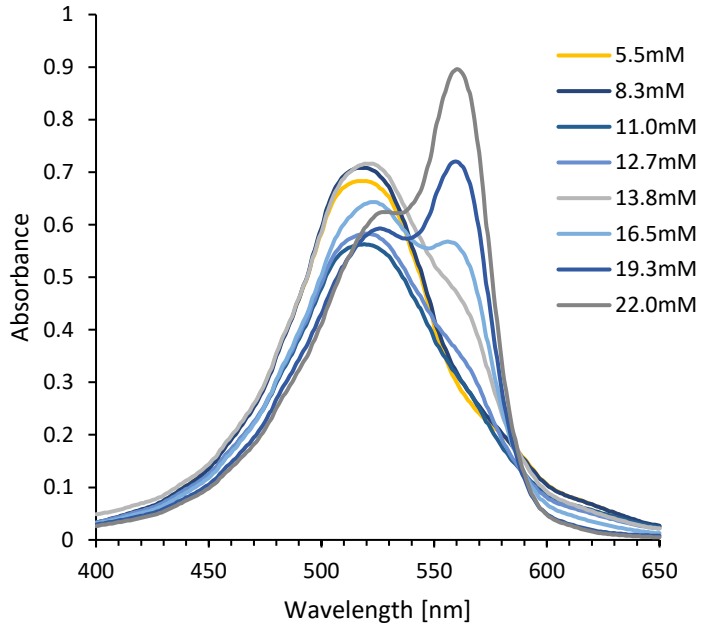

B

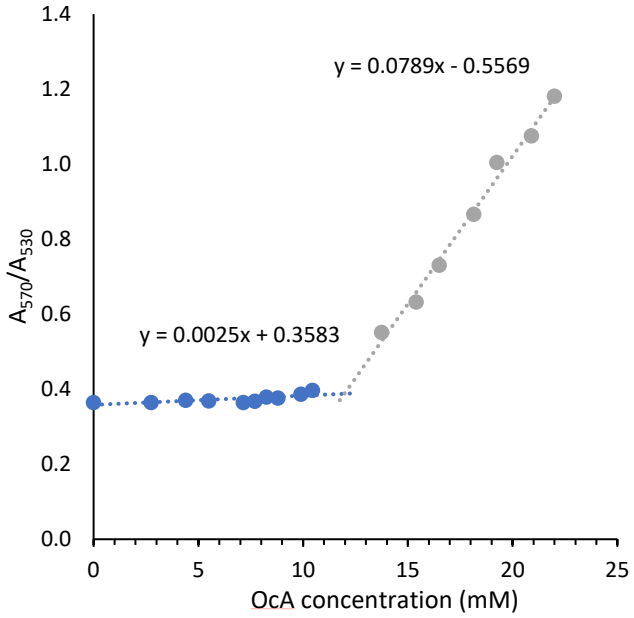

Figure S234. Determination of the critical aggregation concentration of OcA for OcA:LA reaction product at 1:4 molar ratio. Absorption spectra of merocyanine 540 in the presence of increasing concentrations of OcA obtained for the reaction product of OcA:LA at a 1:4 molar ratio at pH 6.6 (A). Absorption ratio at 570 nm and 530 nm as a function of OcA concentration. The intersection between the two fitting lines represents the CAC of OcA – ca 12 mM (B).

A

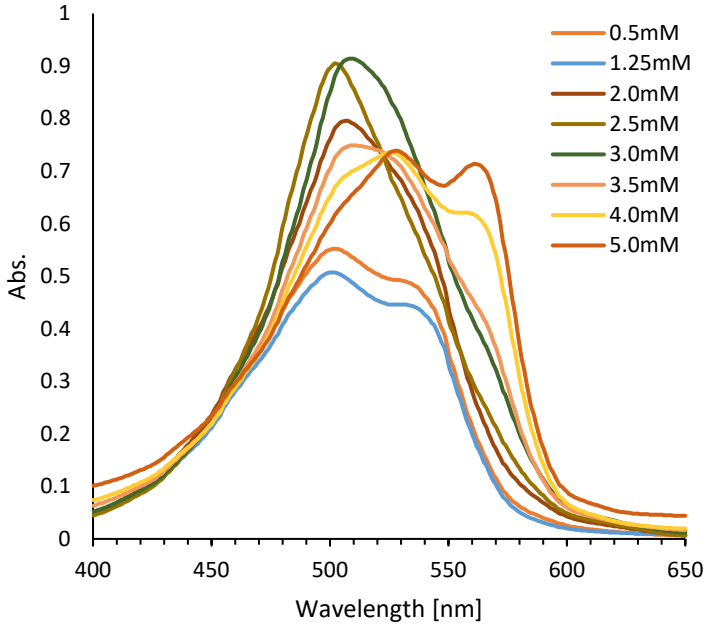

B

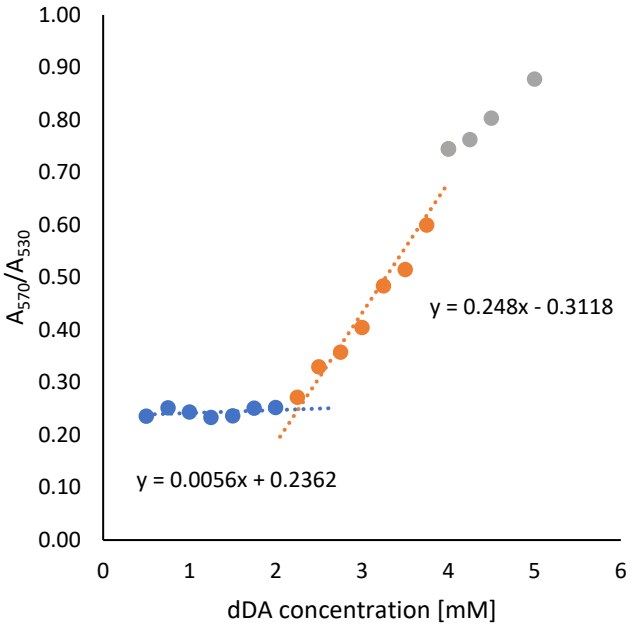

Figure S235. Determination of the critical aggregation concentration of dDA for dDA control sample. Absorption spectra of merocyanine 540 in the presence of increasing concentrations of dDA obtained for dDA control sample at pH 7.4 (A). Absorption ratio at 570 nm and 530 nm as a function of dDA concentration. The intersection between the two fitting lines represents the CAC of dDA – ca. 2.5 mM (B).

A

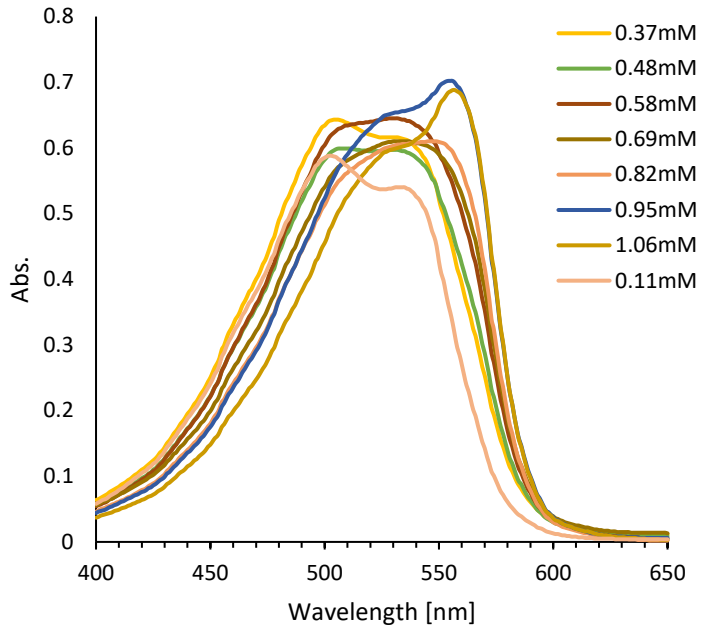

B

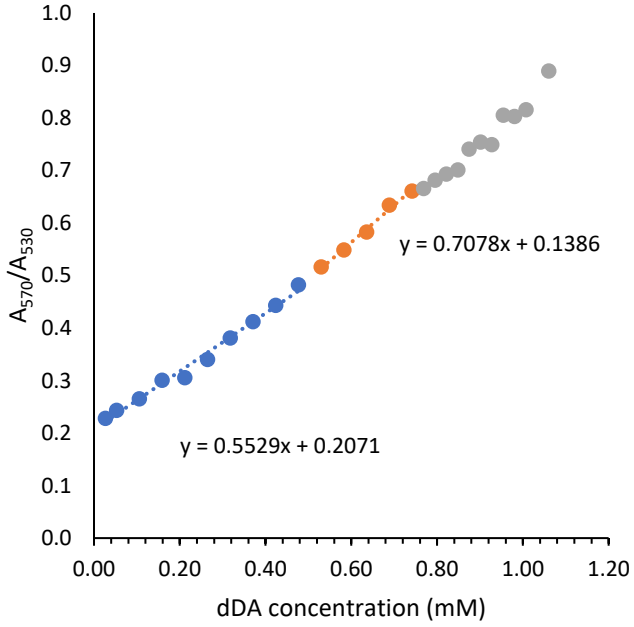

Figure S236. Determination of the critical aggregation concentration of dDA for dDA:LA reaction product at 1:4 molar ratio. Absorption spectra of merocyanine 540 in the presence of increasing concentrations of dDA obtained for the reaction product of dDA:LA at a 1:4 molar ratio at pH 7.4 (A). Absorption ratio at 570 nm and 530 nm as a function of dDA concentration. The intersection between the two fitting lines represents the CAC of dDA – ca 0.4 mM (B).

A

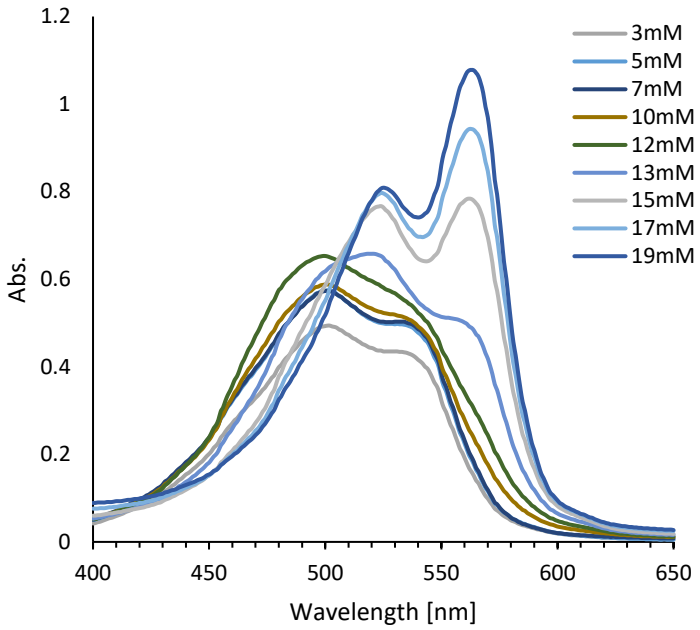

B

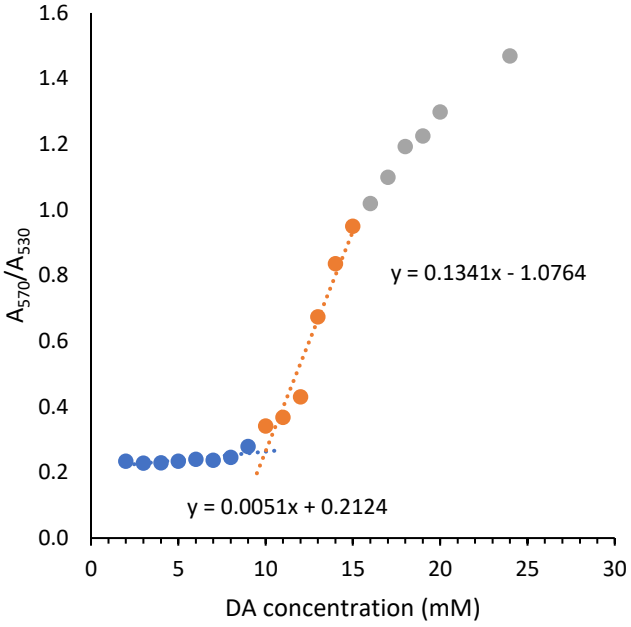

Figure S237. Determination of the critical aggregation concentration of DA for DA:PLA fresh monomers at 1:1 molar ratio. Absorption spectra of merocyanine 540 in the presence of increasing concentrations of DA obtained for DA:PLA fresh monomers at 1:1 molar ratio at pH 6.8 (A). Absorption ratio at 570 nm and 530 nm as a function of DA concentration. The intersection between the two fitting lines represents the CAC of DA – ca. 10 mM (B).

A

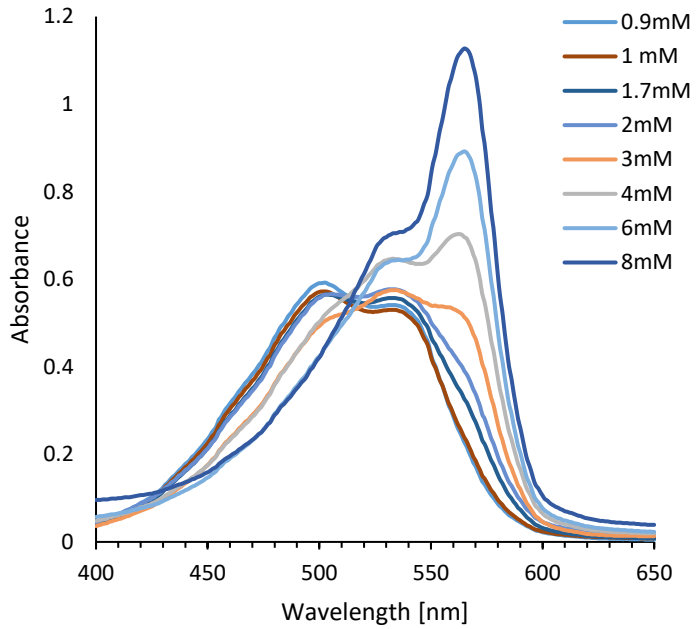

B

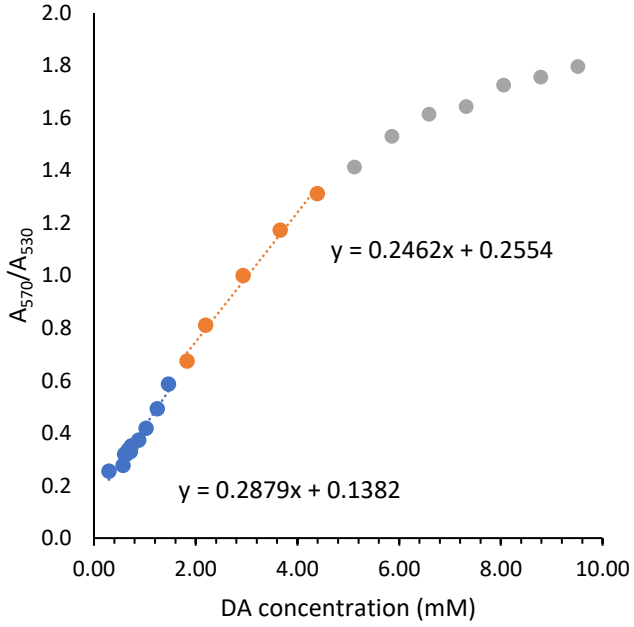

Figure S238. Determination of the critical aggregation concentration of DA for DA:PLA reaction product at 1:1 molar ratio. Absorption spectra of merocyanine 540 in the presence of increasing concentrations of DA obtained for the reaction product of DA:PLA at a 1:1 molar ratio at pH 6.8 (A). Absorption ratio at 570 nm and 530 nm as a function of DA concentration. The intersection between the two fitting lines represents the CAC of DA – ca 3 mM (B).